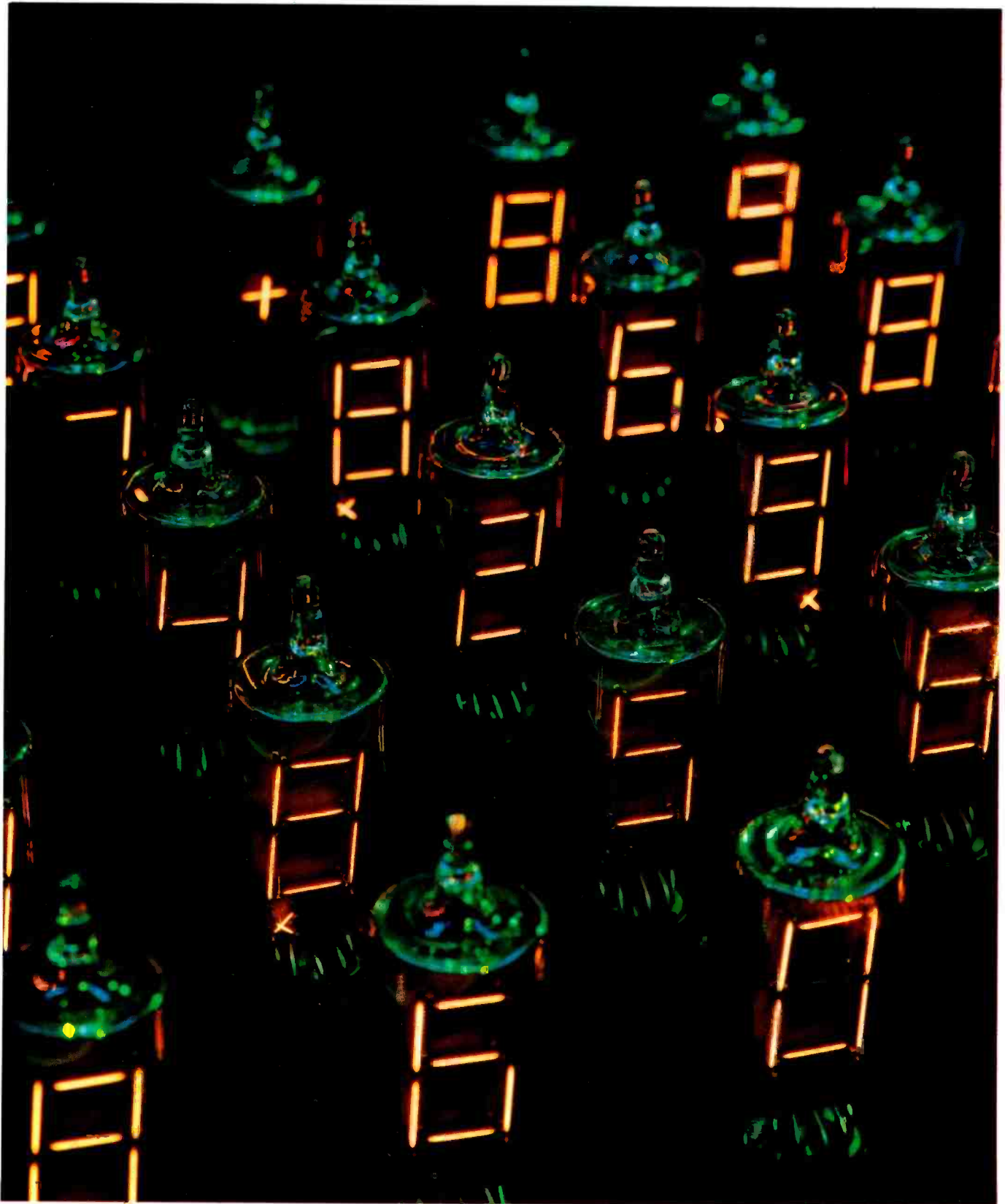


J&C

RCA Engineer

P/109

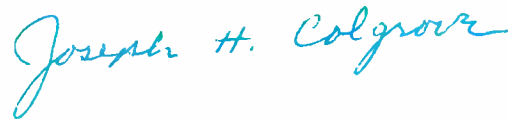
Vol 17 No 6
Apr|May
1972



Expanding business opportunities

Each of us must be ever aware that we live in a highly competitive world that is changing at an accelerating rate. These changes, which are reflected in growing domestic and foreign markets, offer great business opportunities for new applications of existing technologies and products and for the development of new products. Careful research of market trends and application of creative and innovative engineering skills and talents are major elements for providing the types of products and services that will meet these growing market needs.

In this issue are several articles dealing with NUMITRON digital display devices. This new product line offers several superior performance features over existing competitive products in selected areas of a rapidly growing digital display market. NUMITRON digital display devices, in their design and development stages, added creative engineering to existing technological knowledge that had already proven itself in small vacuum tubes. Similarly, in the manufacturing, marketing, and distribution areas, well proven skills and resources are being utilized. Like most new products, NUMITRON digital display devices have had their share of market entry and growing problems, but we continue to see an excellent opportunity for establishing another profitable, growth product line.



Joseph H. Colgrove
Division Vice President and
General Manager
Entertainment Tube Division
Harrison, N.J.



RCA Engineer Staff

W. O. Hadlock Editor
J. C. Phillips Associate Editor
J. P. Dunn Art Editor
Mrs. Diane Ahearn Editorial Secretary
Mrs. Julianne Clifton Subscriptions

Consulting Editors

C. A. Meyer Technical Publications Adm.,
Electronic Components
C. W. Sall Technical Publications Adm.,
Laboratories
F. J. Strobl Technical Publications Adm.,
Corporate Engineering Services

Editorial Advisory Board

R. M. Cohen Mgr., Quality and Reliability
Assurance, Solid State Div.
F. L. Flemming VP, Engineering, NBC
Television Network
C. C. Foster Mgr., Technical Information
Services, RCA Laboratories
M. G. Gander Manager, Consumer Products
Adm., RCA Service Co.
W. R. Isom Chief Engineer,
Record Division
L. R. Kirkwood Chief Technical Advisor,
Consumer Electronics
C. H. Lane Div. VP, Technical Planning
Electronic Components
P. Schneider VP, Engineering and
Leased Systems,
Global Communications, Inc.
A. R. Trudel Director, Corporate
Engineering Services
F. W. Widmann Manager, Engineering
Professional Development
Dr. H. J. Woll Division VP,
Government Engineering

Our cover

... features NUMITRON display devices. Several articles in this issue (Farina, Reichert, Feyder) discuss the design, applications, and potential market of these directly viewed, filament-type devices. Among the NUMITRON's advantages are low cost, high contrast, and compatibility with integrated circuitry. **Photo credit:** John Semonish, Commercial Engineering, Electronic Components, Clark, N.J.

A technical journal published by
RCA Corporate Engineering Services 2-8,
Camden, N.J.

• To disseminate to RCA engineers technical information of professional value • To publish in an appropriate manner important technical developments at RCA, and the role of the engineer • To serve as a medium of interchange of technical information between various groups at RCA • To create a community of engineering interest within the company by stressing the interrelated nature of all technical contributions • To help publicize engineering

achievements in a manner that will promote the interests and reputation of RCA in the engineering field • To provide a convenient means by which the RCA engineer may review his professional work before associates and engineering management • To announce outstanding and unusual achievements of RCA engineers in a manner most likely to enhance their prestige and professional status.

RCA Engineer articles are indexed annually in the April-May Issue and in the "Index to RCA Technical Papers."

Contents

Editorial input	Publish or Perish		2
Engineer and the corporation	The five hats of research	Dr. J. Hillier	3
Division profile	Cushman and Wakefield	F. J. Strobl	8
Survey papers	Digital readouts	P. Farina	12
	Visible-light-emitting diodes	Dr. C. J. Nuese Dr. H. Kressel I. Ladany	17
Numitrons	Numitron applications	F. Feyder	27
	Design and constructions of numitrons	R. Reichert	32
Liquid crystals	Application of liquid crystal dynamic scattering	Dr. H. C. Schindler	35
	Facsimile printing using liquid crystal arrays	J. Tults D. L. Matthies	40
Storage tubes	Storage tubes for computer displays	F. J. Marlowe	44
	Display system using the alphechon storage tube	F. J. Marlowe F. Wendt C. Wine	48
Display systems and techniques	Holographic audio/video storage & display	R. Norwalt P. Nelson	52
Special	David Sarnoff Outstanding Achievement Awards		56
Display systems and techniques (cont'd)	A technique for constant rate digital vector generation	L. W. Poppen J. Lyon	58
	Digital and optical techniques for image enhancement	Dr. P. C. Murray Dr. W. W. Lee	62
	Optical and mechanical limits of photomask resolution	H. Hook	67
Laser-beam displays	Third-generation laser beam image reproducer	S. Ravner	74
	High speed facsimile system using the LR 70 laser scanner	L. W. Dobbins	79
Cathode ray tubes	Hardware software tradeoffs for a CRT photo typesetting system	S. Raciti	83
	High resolution CRT	O. Choi C. J. Widder	86
	Precision CRT tester	E. D. Simshauser	91
Notes	Penetration-type cathode-ray tube for multicolor displays	D. D. Shaffer	94
	Circuit simulation of bipolar IC arrays	A. Feller	95
	Gigahertz-rate hundred-volt pulse generator	H. Kawamoto	96
	Binary light deflection system	Dr. J. A. Rajchman	97
	High power PIN diode RF switch	D. H. Hurlburt R. E. Cardinal	98
Departments	Pen and Podium		99
	Patents Granted		101
	Dates and Deadlines		103
	News and Highlights		105
	Index to Volume 17		110

editorial input

In basic research organizations, as in academic institutions, publishing is the primary vehicle of recognition. The researcher's reputation is measured to a large extent by the usefulness of what he reveals and by the quality and stature of his publications.

However, only part of RCA's activities are devoted to research, and essentially none to academia. A well-designed competitive product must always be the primary goal. Consequently, most engineering and development work is product and market oriented, and most engineers are *busy*—designing, developing, and manufacturing new products—moving rapidly from one assignment to the next—often taking little time to pause and consider the real need and value of documentation.

Therefore, the great practical benefit to be derived by the company and the individual engineer from a well-designed documentation program is frequently underestimated. This can be a grave omission; the best designed product is useless in the marketplace without the companion engineering article, the attendant product description, the instruction book, and the supporting sales materials so vitally needed to effectively launch the product into the marketplace.

But who will supply this much-needed help to RCA's planners and marketers? The obvious answer is the person possessing the basic information and know-how. *That person is the product engineer*; he must initiate the process.

Such a process, once initiated, generates a spinoff of benefits far beyond the original intent. For example, when an engineer publishes a professional technical paper, he may be aware that he enhances his professional prestige and adds to the technical stature of his company. Beyond that the benefits seem rather nebulous. However, it is beyond these acknowledged benefits that the published paper accrues unexpected rewards for the author and his company.

publish or perish

The most immediate but subtle reward comes during the writing effort itself. The conscientious author re-evaluates his work as he writes. The prospect of facing a broader, possibly more critical audience causes him to uncover new ideas and correct his original thinking.

The review-and-approval cycle adds further to this re-evaluation process. Comments fed back from legal, patent, technical, marketing, and policy sectors of the company solidify the paper and reinforce the engineer's confidence in his work. Yet even in this preliminary form, the information starts to become useful to others: to the patent department as a possible disclosure, to the marketing department as a description of a customer-oriented device, to the publications activity as a base for other documents, and to the author's management as a concise wrap-up of the work performed.

By publishing in a trade or professional journal, the author fulfills his original goal—enhancing his professional stature and that of his company. But the benefits do not stop there. The reprint can now be used to answer inquiries, to supplement technical proposals, and to train new employees. It can be bound together with other papers to form a brochure displaying RCA's unique skills in a particular technology.

Further, the first publication often prompts invitations to participate in other professional activities—the author is asked to present his paper at a technical conference, or the paper is re-published elsewhere. This is a particular advantage of publishing in the *RCA Engineer*. Because the *RCA Engineer* is distributed *only* to RCA engineers and scientists, these papers can be published again in the "open" literature without change.

Thus, most published professional papers benefit the authors and the company far beyond the initial appearance. The exact dollars-and-cents value of a published paper is impossible to estimate. However, because of its unobtrusive, authoritative, logical approach, the professional paper is far more valuable than most other forms of communication—and far more rewarding to the author.

Future issues

The next issue, the seventeenth anniversary of the *RCA Engineer*, will contain representative papers from most areas of RCA. Some of the topics to be covered are:

The AEGIS program

Integrated circuits for AM radios

Angle to sine/cosine digital conversion

Circuit failure analysis

Global Communications

Test automation

Holotape

Discussions of the following themes are planned for future issues:

Advanced Technology Laboratories

Mathematics in engineering

COS/MOS integrated circuits

Radar and antenna engineering

Transportation

Communication

Broadband information systems

Crime prevention systems

SelectaVision Systems

Five hats of R&D management

Dr. James Hillier

Editor's note: On September 29, 1971, Dr. James Hillier, Executive Vice President, Research and Engineering, delivered a keynote address at the National Conference on the Administration of Research at Wilmington, North Carolina.

Dr. Hillier prefaced his talk by stating that "no industrial manager can hope to present a complete synthesis of all the divergent ideas and attitudes that exist." However, his message treats a broad range of problems affecting research and development in the U.S. Among these problems are technical obsolescence, consumerism, a tight economy, reduced government support for R&D, and foreign competition. Since these problems are shared, to some extent, by each of us on the technical staff, Dr. Hillier's comments should be of considerable interest. The full text of Dr. Hillier's speech follows.

WHEN WE SPEAK OF UPDATING OUR VECTORS,* we must remember that a vector can be, and usually

is, the result of many components. Nowhere is this more true than in today's management of R&D. Some of these components are . . .

Tightening of the economy, particularly in the R&D-intensive industries.

Public emphasis on ecology, consumerism, product safety, etc.

Overreaction that blames technology for our problems and yet puts an unrealistic hope on technology to solve them.

Reduced rate of growth of government support of R&D, including the relatively greater impact on the government support of basic research.

Increasing foreign competition—particularly in high-technology industries.

Growth of the "future shock" problems; that is, problems introduced by the increasing discrepancy between the rate of accomplishing an R&D project and the rate of change of the technical and economic environment.

Increasing rate of technical obsolescence in our technical staffs.

Even this partial listing is staggering in its implications for industrial R&D management. Each of these components could be the topic of a full length talk at this meeting—in fact, of several talks, since I suspect that the treatment

of each would be quite different according to that specific part of the total R&D spectrum each speaker represented.

My remarks will have to be quite general. However, I shall try to give some perspectives that may be helpful.

Now, more than ever, the R&D manager of a company must be an active participant in all phases of the planning activity of his company. His responsibilities and problems have not really changed, but the risks of incomplete planning have greatly increased. In other words, the R&D manager is now faced with really doing all the things he has been talking about for the past decade or so.

The familiar dilemma of the R & D manager has been that while his organization must work for the future it must do so within the constraints and conditions of today. The tightened economy brings this dilemma into exquisite focus.

Reprint RE-17-6-18

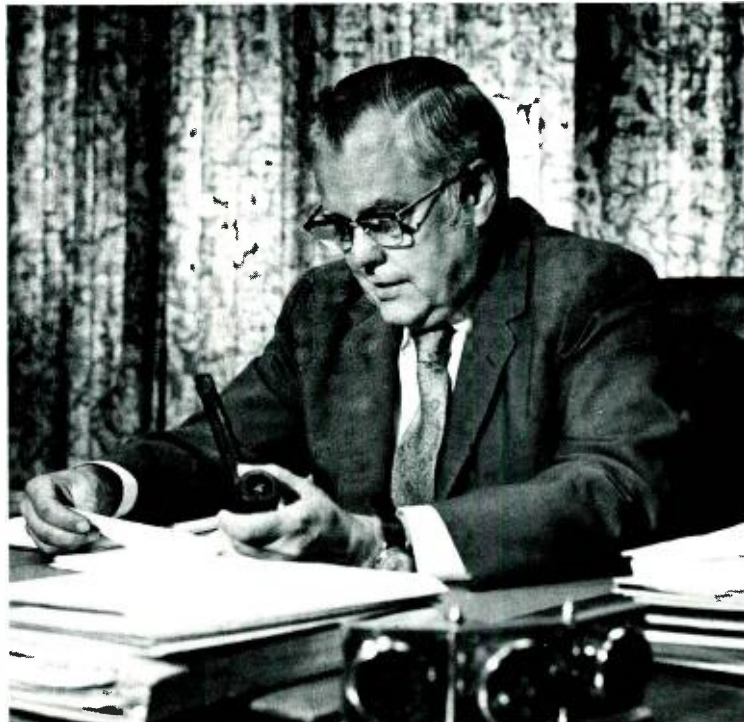
*The main theme of the conference was "catching the wave of re-adjustment" and the theme of the keynote speeches was "updating our vectors in moving co-ordinates."

Dr. James Hillier

Executive Vice President

Research and Engineering, RCA

studied at the University of Toronto, where he received a BA in Mathematics and Physics in 1937, MA in Physics in 1938, and PhD in Physics in 1941. Between 1937 and 1940, while Dr. Hillier was a research assistant at the University of Toronto, he and a colleague, Albert Prebus, designed and built the first successful high-resolution electron microscope in the Western Hemisphere. Following this achievement, Dr. Hillier joined RCA in 1940 as a research physicist at Camden, N.J. Working with a group under the direction of Dr. V. K. Zworykin, Dr. Hillier designed the first commercial electron microscope to be made available in the United States. In 1953, he was appointed Director of the Research Department of Melpar, Inc., returning to RCA a year later to become Administrative Engineer, Research and Engineering. In 1955, he was appointed Chief Engineer, RCA Industrial Electronic Products. In 1957, he returned to RCA Laboratories as General Manager and a year later was elected Vice President. He was named Vice President, RCA Research and Engineering, in 1968, and in January 1969 he was appointed to his present position. Dr. Hillier has written more than 100 technical papers and has been issued 40 U.S. patents. He is a Fellow of the American Physical Society, the AAAS, the IEEE, an Eminent Member of Eta Kappa Nu, a past president of the Electron Microscope Society of America, and a member of Sigma Xi. He served on the Governing Board of the American Institute of Physics during 1964-65. He has served on the New Jersey Higher Education Committee and as Chairman of the Advisory Council of the Department of Electrical Engineering of Princeton University. Dr. Hillier was a member of the Commerce Technical Advisory Board of the U.S. Department of Commerce for five years. He was elected a member of the National Academy of Engineering in 1967 and is presently a member of its Council.



The constraints and conditions of today force the R&D manager into a much more intimate relationship with his financial, marketing, administrative, and personnel counterparts in his company's organization. He is like the old-time vaudeville juggler who at some point in his act would pick up a number of top hats. Then, in a dazzling display of virtuosity, he would shift each hat in rapid succession to his head while keeping all of the others spinning through the air.

In current industrial R&D management, this is an act that we must perform almost every day. I may begin the day wearing my scientific hat, then as the day progresses, I find myself shifting—sometimes quite rapidly—into the marketing hat, the administrative hat, the financial hat, or the personnel hat. There are times when urgent necessity or the basic planning function for the R&D activity seems to require me to wear all five hats simultaneously.

This is not to say that R&D managers are going to exercise primary corporate responsibilities in non-scientific areas of competence. Quite obviously, such functions are performed by senior corporate officers, and divisional ones as well, who specialize in the fields of administration, finance, marketing, and personnel. But *they* cannot be expected to relate effectively to the peculiar problems of research and development without the informed counsel, recommendations, and active participation of the R&D management. Nor can R&D managers hope to operate efficiently unless they are both knowledgeable in, and responsive to, non-scientific business criteria.

With this caveat in mind, let me briefly touch on some of the basic considerations that must preoccupy the mind of any five-hatted industrial R&D manager. While I will treat each of them separately, and in so doing try to relate them to the relevant components of our vector, do not forget that each of the five hats is just part of an integrated whole.

The financial hat

First, because successful R&D management must stem from a sensible economic base, let's put on the financial hat. Here we must consider the company's financial resources and their

allocation to the total innovation process that carries the research and development through engineering and all the way to the marketplace. Fortunately in large diversified companies such as RCA, it is possible to develop certain rules of thumb with respect to financial considerations which, if not precisely accurate, are at least informative and provide some guidance.

We know, for example, that for every dollar spent for successful basic and exploratory research we can expect to invest another ten dollars for applied research, engineering development, and design. But that's just the beginning. Beyond this we must be prepared to lay out \$100 for all of those things it takes to create a new business or adapt an old one—new plants, new tools, new marketing and sales personnel, new training, etc.

Note that I have indicated that this one, ten, hundred-rule-of-thumb applies only to money spent on *successful* R&D. Since not all R&D projects are successful, the simple formula must be modified. In actuality, expenditures on the necessary basic and the unsuccessful exploratory research may very well total three or four dollars for every one dollar of successful and exploratory research obtained. In addition to this, one must realistically expect to budget for expenditures of perhaps eleven or twelve dollars at the applied research and engineering level to achieve ten dollars of useful output.

So you can see that one dollar's worth of successful basic and exploratory research involves a commitment to spend about fifteen dollars just to make it happen, and to bring it to the point where it *could* be introduced into the economy. And we're still committed to spend another one hundred dollars if the effects of the research are to have an impact upon the company's and the nation's economy.

It becomes obvious in this admittedly simplistic theory that it is the one hundred dollars that becomes a significant controlling factor in the R&D decision making process. In other words, if we can determine how much innovation investment money our growing, maturing and dying, and on-going businesses can generate, we would at least know roughly how much we could

afford to spend in the basic and exploratory research activities and in development, engineering, and design. Unfortunately, the problem is complicated by the fact that basic corporate accounting systems tend to reveal only a fraction of the innovation investment money available. The remainder—and probably the larger part—tends to be buried in a myriad of different operating accounts. It involves the cost of retraining salesmen, redistributing the sales force, retraining operators on the production line, retooling and rescheduling the production line, and a host of other items which are considered as part of the on-going business expenses but in reality are part of the investment in the total innovation process.

I am sure that all of you will recognize that, while there is no easy way of identifying the innovation investment money available for the total R&D process, in any company, or for that matter in the whole society, a multitude of self-correcting mechanisms ultimately do adjust the level of the company's research activities. It is my conviction that you have seen precisely this type of mechanism at work in the changing rate of growth of the government support of R & D.

The obvious difficulty with allowing the self-correcting mechanisms to operate, particularly in a company, is that they tend to do so on *historical* data whereas the research activity should be determined primarily by the anticipated needs of the future. In other words, if we do not take explicit action, it is easy to find our research spending out of phase with our true research needs.

On the national scene there is, of course, understandable concern in many quarters about the effect of the diminished spending for basic research. Fears are being expressed that we are in imminent danger of dismantling the academic base of all R&D. I do not share these fears. We are experiencing curtailment in this area, yes. But, more than that, what we are witnessing is a gradual shifting of responsibility for R&D from the public to the private sector of the economy—and a reordering of priorities towards an enlarging accent on applied rather than basic research—all in an effort to make our research activities more effective in improving our economy. This readjust-

ment—and I think that is the exact word that applies—is taking place in the wake of a period in which support for basic research had grown more rapidly than support for applied research or development. Between 1958 and 1968, funds for basic research multiplied six times; applied research, four times; and development, three times. Basic research was not short changed in this growth but note—all these rates of growth were unsustainable particularly that for basic research.

The number of people involved in R&D in this country has grown at a much more rapid rate than the population as a whole. The research output per man, is, in all likelihood, greater than it was a quarter of a century ago. One can only conclude that the output of our laboratories has also been increasing much more rapidly than our population—a situation which obviously could not be sustained indefinitely without outstripping our ability to generate enough innovation investment money to exploit it.

The nation seemed to be working on the philosophy that if research is good, more research is better, and without any consideration as to how much the nation could afford. Yet we seemed confounded when the inevitable self-correcting mechanisms began to take over. We did not seem to recognize the significance of the fact that twenty years of astronomical growth rates in our expenditures on research, including a decade of very high spending rates, had had no corresponding impact on the growth rate of our economy. Yet every R&D manager knows full well that if R&D is necessary for business success in his industry, it is definitely not sufficient. So I am really making two points—if research is good, more research is better *only* if the nation can afford it—and if the other segments of our society and economy are in place to exploit it.

Thus, while I still have my financial hat on, I must conclude that the R&D managers must wrest the control of the appropriate level of R&D spending in

our companies away from the self-correcting mechanisms in order to bring the expenditures into phase with future needs. The need to do this becomes more clear and urgent when we recognize that the pace of competitive developments must continue to quicken while the pace of our in-house research can only remain relatively steady. If our research spending is out of phase at the same time as it is being buffeted by competitive developments, I believe that we

and even for very short times, my administrative and personnel hats.

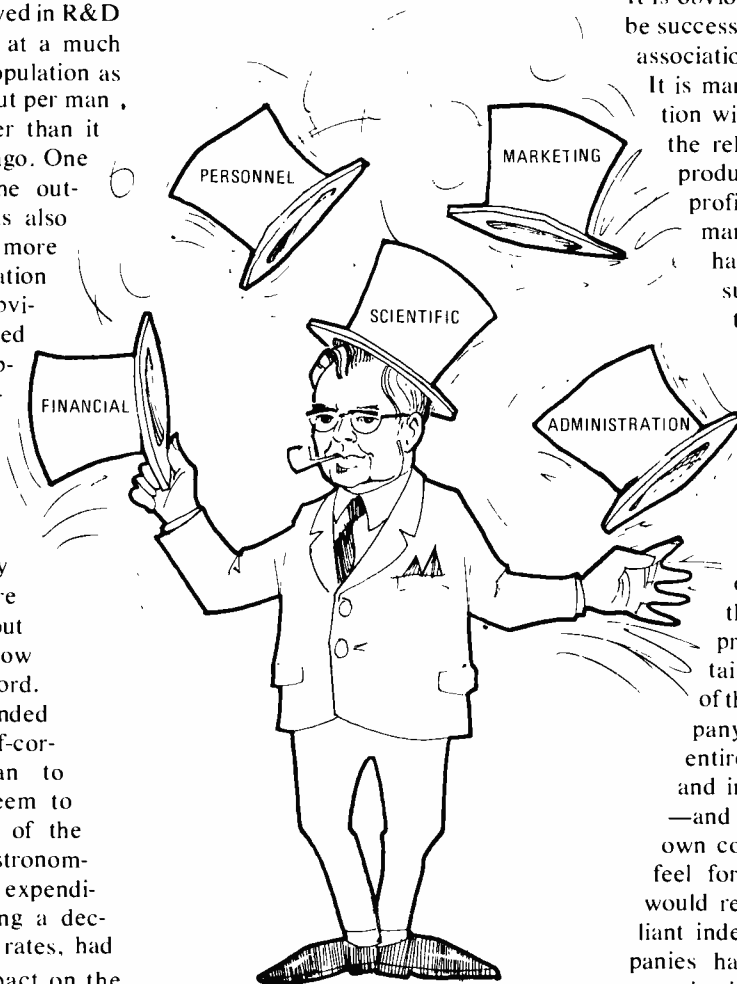
To make sure we are communicating, let me note that I am using the term *marketing* in its broad sense to make a basic distinction between selling and marketing. It has been said that selling tries to get the customer to *want* what the company has, while marketing tries to *have* what the customer wants. There's a world of difference in these two concepts.

It is obvious that, for the marketing to be successful, it must have a very tight association with the R&D planning.

It is marketing, working in conjunction with finance, that can appraise the relative impacts that different products will have on the future profits of the company. The R&D manager, with his marketing hat on, must comprehend such conclusions and use them, factored by probabilities of technical success, as part of his judgment in the process of allocating resources to his research projects.

This is basically no different than it has ever been; however, times have changed. In the past, the market-planning process was quite often contained entirely within the brain of the chief executive of the company who seemed to be working entirely on the basis of subjective and intuitive thinking. Sometimes—and certainly this is true in my own company's case—the intuitive feel for what product the market would respond to proved to be brilliant indeed. Unfortunately, as companies have grown larger and their organizations more complex, the inputs needed for that type of intuitive thinking have become dispersed among many staff and operating functions. Somehow these inputs must be transmitted to the chief executive since it is he and only he who can commit the company to a major change of direction. Such inputs can only come from the collaborative efforts of marketing, R&D, finance, etc.

Another change in our times is that technology has become plentiful. This is certainly true in electronics and possibly in several other industries. In elec-



have lost control and research management is merely participating in a game of chance.

The marketing hat

Determining the appropriate level of a company's R&D budget is obviously only a first step. I must now endeavor to make an appropriate allocation of the total funds among our research projects. To do this I must put on my marketing hat but juggle it rather quickly with my scientific hat, my financial hat,

tronics, we have a myriad of new products and services which have passed through the R&D labs at least to the stage where they have been demonstrated as technically feasible. You might ask the obvious question—why is it that these products have not reached the marketplace? It is my observation and belief that it is unwieldy corporate organization that is at fault.

The next step in R&D would be to develop a product prototype to demonstrate that it can also be a cost-effective product. However, this is an extremely expensive step and one that has considerable risk as to time of accomplishment. The decision to invest in this product and to accept the attendant risks usually has to be made by the top executive of the company. In earlier days, and even sometimes today, the chief executive would make such a decision rather quickly on the basis of his own intuition and conviction as to whether or not the market is ready for the proposed product. Today, he is more likely to base such a decision on a number of studies made by his staff and operating departments.

In the marketing department, for example, such a study will call for extensive market research to obtain answers to basic marketing questions: How big is the market? What is its composition? How intense is the level of demand? At what prices should our product be sold in order to achieve profitability? What share of the market must we aim for? and so on. Such market research is quite well developed for the easily understood modification of a simple and common product. However, it is also notoriously *unreliable* in predicting the market factors for the completely new and strange product or service. Yet, how often have you seen an executive hesitate when there is a disparity between his intuitively developed judgment and the results of a formal market study?

Another respect in which times have changed concerns the timing of marketing and, therefore, R&D decisions. In RCA, certain types of R&D projects take rather well-established lengths of time to accomplish. At one extreme is the completely new, complex system which appears to take about eight years from the original conception of the product to the time that it is actually de-

livered to customers. At the other extreme are simple transistors and integrated circuits for which the same process takes from a few months to a year. The remarkable fact is that the duration of this period has changed relatively little over the last several decades. As the process has been speeded up by our becoming increasingly adept in a given discipline, it has been comparably slowed by the increasing sophistication and complexity of the product. If this appears to contradict the general concept of an accelerating technology, I need only remind you of my earlier statements concerning the rapid growth of our national R&D which has certainly increased the frequency of *occurrence* of new developments but has not necessarily shortened the time required to attain any one of them. This leads to the concept of "future shock" to which I referred earlier. In the course of the total development sequence of a new product, there is, today, an ever-increasing probability that one or more competitive developments will appear that will threaten the integrity of the original plan. Extensive and continuing collaboration of the R&D management and the marketing activity is the only present defense against this problem.

In a commercial environment, marketing is the name of the game. No R&D manager can afford to ignore its implications nor does he dare abdicate his responsibility in this field.

The administrative hat

Then, there's that third hat to be put on, the administrative one. It's an old and familiar hat in corporate life, but when fitted for R&D managers it naturally tends to differ in shape and style from those worn by other executives. The whole thrust of R&D management is, after all, aimed at unleashing and guiding highly specialized forms of creativity in the directions of the corporation's perceived areas of growth. Given too tight a rein, such R&D creativity tends to languish; held in check too loosely, it rides off in all directions at once. This is a problem with which we are all familiar. However, in today's tight economy, it takes on a new significance and becomes even more difficult of solution. Today we are running our laboratories with less "fat" and less "cushion". As a result, our

laboratory programs are even more delicately balanced than they have been in the past. Any change in the allocation of our manpower resources represents a substantial change from the *status quo*.

Around our laboratory, we have fallen in the habit of calling this the "going from *A* to *B* problem." *A* is obviously the present situation and *B* is the desired situation that I assume can be worked out satisfactorily. More often than not, it turns out transition from *A* to *B* is the most difficult part of a problem. At this point I find that I am quickly juggling between my administrative and my personnel hats.

While I still have my administrative hat on I will, of course, be worrying about the normal problems of procedures control, information flow, and the functioning of the organization. These more or less familiar functions have changed in at least one fairly important aspect. The information flow that today's R&D manager requires in order to be able to function well under his five hats has become much more extensive and complicated than the straightforward technical reporting of a few years ago.

The personnel hat

Now I shall turn to consideration of the fourth hat worn by R&D management—the personnel hat.

I dislike that word, *personnel*. It sounds, somehow, too impersonal, too devoid of human values. The chronic problem we always have in any R&D organization is that of attracting and retaining outstanding people. This requires us to cultivate an attitude that is open, receptive, and flexible. Talent is where you find it. It is not necessarily clustered in a few prestigious academic institutions, but may be found even in those halls of learning that are not primarily noted for their emphasis on scientific training. The best talent is always in short supply in good times or bad. These are generalities with which I'm sure you are all familiar. In today's tight economy, however, we find many of our personnel trends substantially changed.

Economies have forced us to cut much of the fat and deadwood out of our organizations. So they are working considerably more efficiently than in the

past. At the same time, the voluntary attrition rates have almost vanished. Under these conditions, there is the possibility that the R&D manager may relax, comfortable in the fact that he has a reasonably stable organization for the first time in two decades. Personally, I consider such comfortable feelings an illusion and would propose that times of tight economy are precisely the time to do some upgrading in the R&D organization. This is a time when the competition for the best graduates is reduced though by no means negligible. Of course, the "new blood" must usually be balanced with some attrition. In bad times, such attrition has to be forced but by the same token it can be controlled and specific. This is in strong contrast to good times when the attrition may be high and allow substantial infusion of new blood, but the attrition is uncontrolled and may include some of your best people and the new blood may be of a considerably lower caliber.

There is another motive for upgrading the R&D organization during bad times. Particularly now. It is my conviction that there is going to be a very serious shortage of industrial R&D technologists and scientists in the middle-70's. I am aware that the demographers of science are predicting a surplus of scientists during the 70's with a shortage appearing only in the 80's. But such statistics include all scientists. Industrial scientists are a special breed, and there is primarily a negative motivation for today's high school graduates to aim their careers in our direction. Consumerism, the general disaffection with business, our association with the military and with pollution, taken in conjunction with the well-publicized unemployment among aerospace engineers—all have served to steer the students leaving high schools into other more fashionable careers. We have had little opportunity, and perhaps we have not known quite how, to counteract the negative image that many high school students have of industry and its R&D activities.

In great corporations, we have another problem that takes our personnel and other talents to try and solve. Year after year we face the possibility of losing some of our best and most productive talent who insist on leaving and setting up their own companies. Such individuals, who frequently possess an entrepreneurial flair, become absorbed in

projects that the corporation cannot economically justify supporting. The project may be a fascinating one. It may even be potentially profitable. But economic necessity dictates that large corporations refrain from frittering away their resources on high-risk ventures with relatively small profit potential.

As a result, the individuals associated with research on such projects, unwilling to abandon them, begin sooner or later to seek an environment in which they can continue to work toward their fulfillment. Often, they acquire a certain amount of financial backing and venture forth to form their own small company. Lacking adequate resources, characteristically undercapitalized, the majority of such ventures tend to fail. But, since they often involve our most talented people, enough of them do succeed to make the risk appear attractive to others.

One might expect that in a tight economy, this type of situation might tend to decrease primarily because venture capital may be more difficult to locate. While that may be true, it also tends to be balanced by the fact that companies tend to concentrate on mainstream projects in periods of tight economy. This tends to increase the number of good projects in our research programs that are candidates for spin-offs.

How do we deal with this problem? Can we do so in a way that does justice to the people involved and yet does not distract the corporation from concentrating on its most productive areas of growth? A number of solutions are being proposed. Almost all of them, in one way or another, attempt to create some kind of autonomous, or semi-autonomous, organization to provide an outlet for the best of the relatively small, high risk projects that intrigue some of our best people.

In essence, we are being challenged to recreate an artificial entrepreneurial environment in which outstanding people will be permitted to pursue projects to which they are totally committed. At best, this may open up new avenues of growth and profitability for our companies. At worst it will give us a means of reabsorbing into the corporate structure the kind of talents whose continued defection weakens our R&D capabilities. While I believe these

concepts are good or at least looking in the right direction, I do not know of any operating scheme that has proven itself to be successful. This is still a challenge for the future.

The science hat

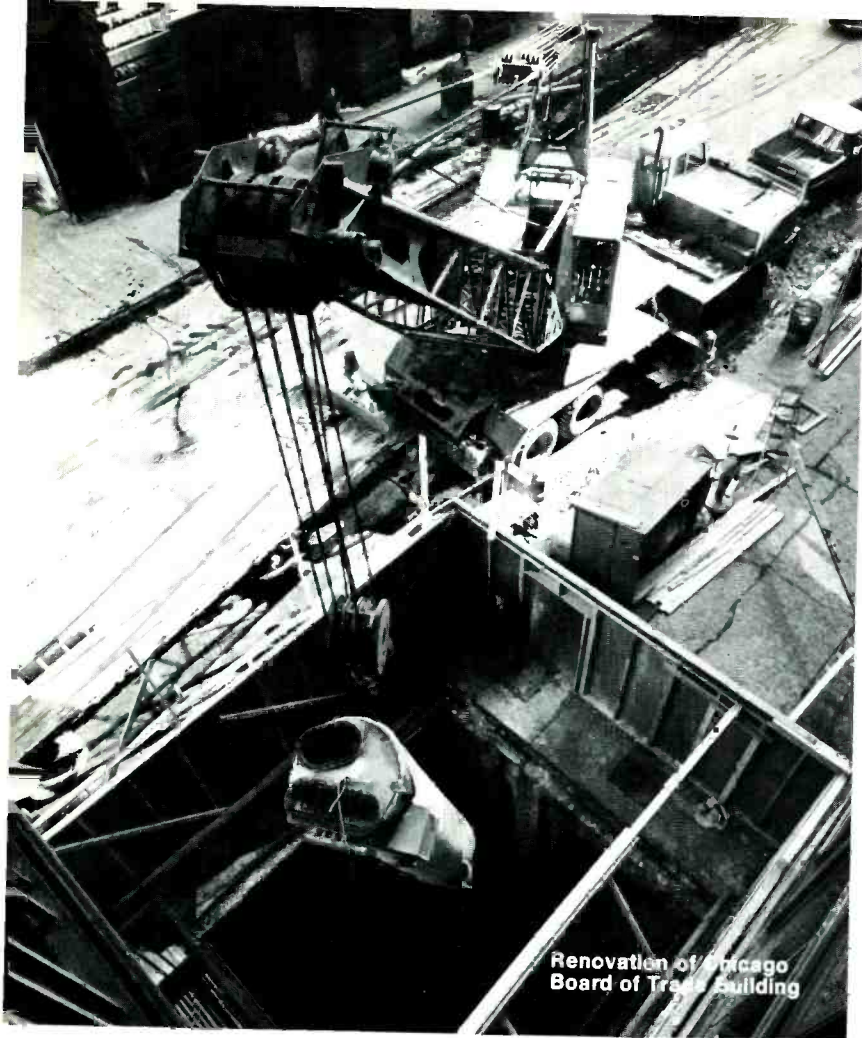
Now let me don the fifth, and in many ways the most comfortable, of all the R&D management hats; the one devoted to science.

This is, after all, the key responsibility of all R&D management. It is our over-riding function, our reason for being. But in the corporate environment, our devotion to this area of responsibility must be tempered by an ability to juggle our other four hats. Committed to corporate goals, we must direct our energy towards those avenues of exploration that will best serve to strengthen our company's economic base, and therefore, that of the nation.

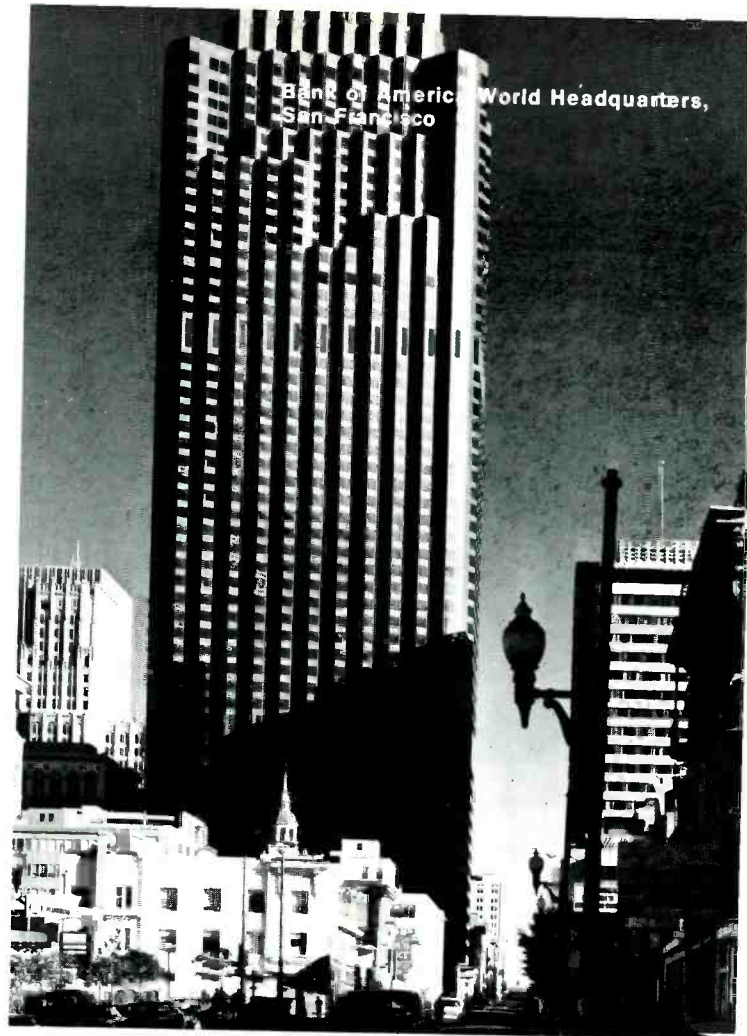
Such industrial R&D management has always required us to become scientific generalists. In the process of doing so we have all jokingly considered that we were learning less and less about more and more science and that we had to escape from the prison of our own specific education, experience, and expertise. Today I have made a strong point that we must add many non-scientific disciplines of management to our generalist's repertoire. Nevertheless, I still believe that our scientific hat is the most critical of all our hats. It is the sieve through which we must sift all of our non-scientific responsibilities. This is the vantage point that we alone possess. It is through the coupling of science to the other management disciplines that we are able to make the maximum contribution to the fortunes of our companies and to the economic well being of our country.

Conclusion

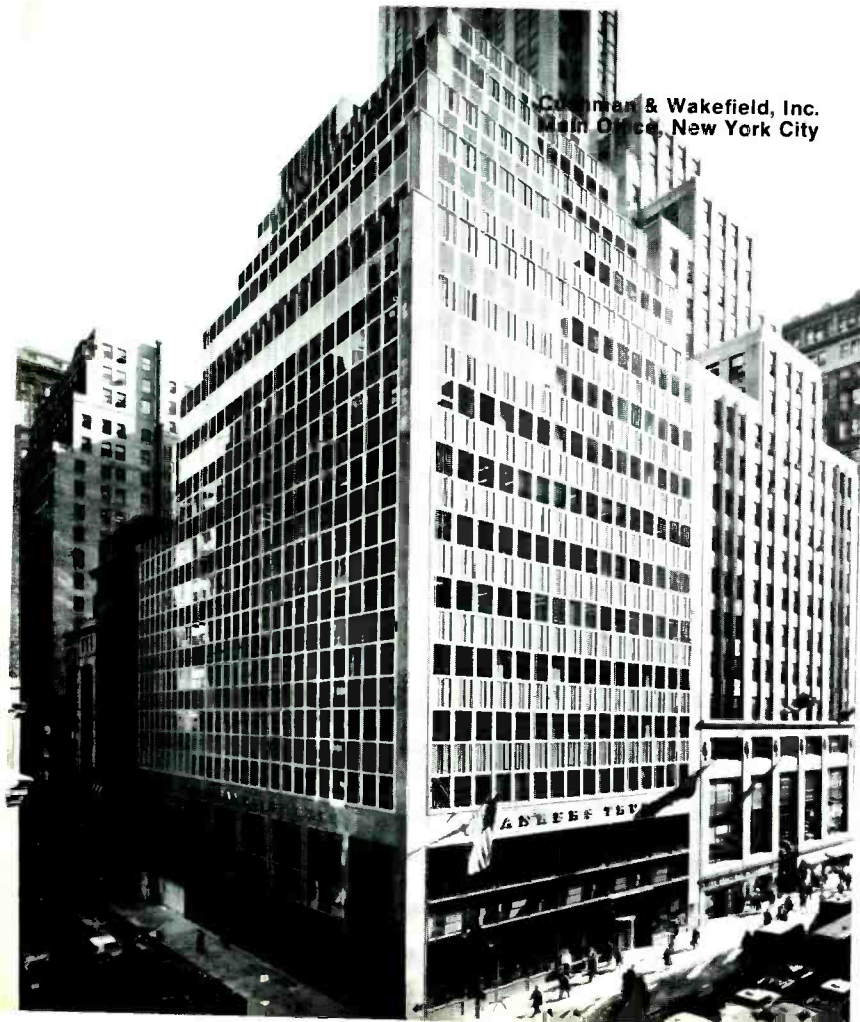
If it seems to you that I dwelled at some length on the five hats of commercial R&D management, please understand that it is not being done introspectively. If there's one thing that my brief and necessarily incomplete comments point up, it is the urgent necessity we have of learning more about how to master these different roles. Recognizing the increasing relevance and importance of these other disciplines in the R&D management function may be, by itself, a large step in the right direction.



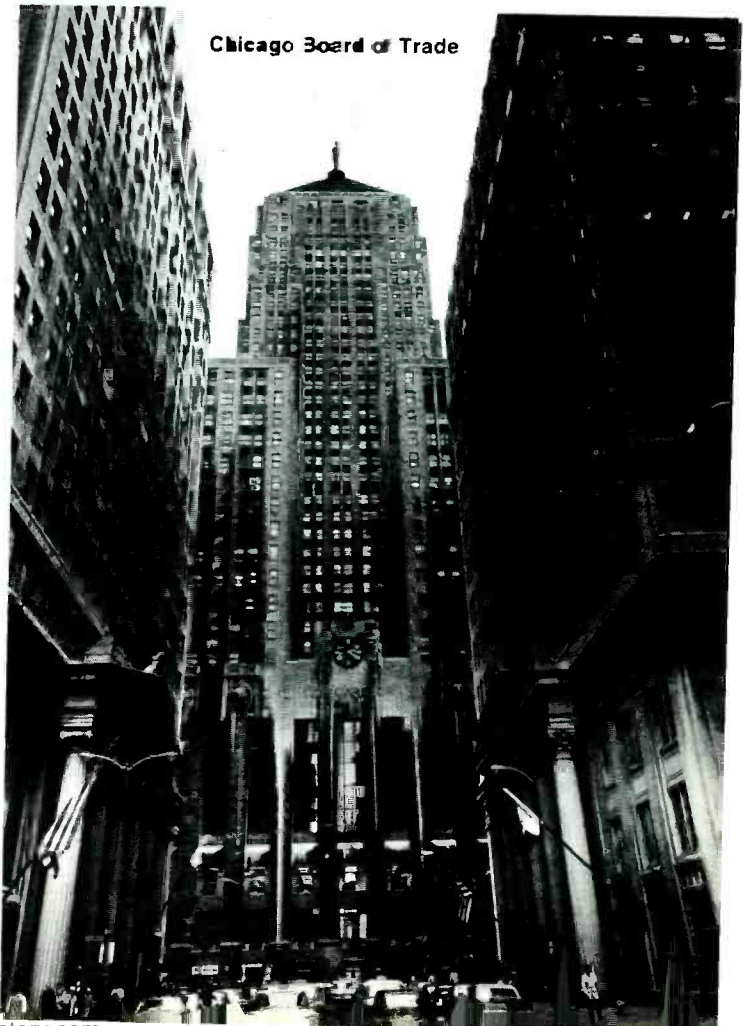
Renovation of Chicago Board of Trade Building



Bank of America World Headquarters, San Francisco

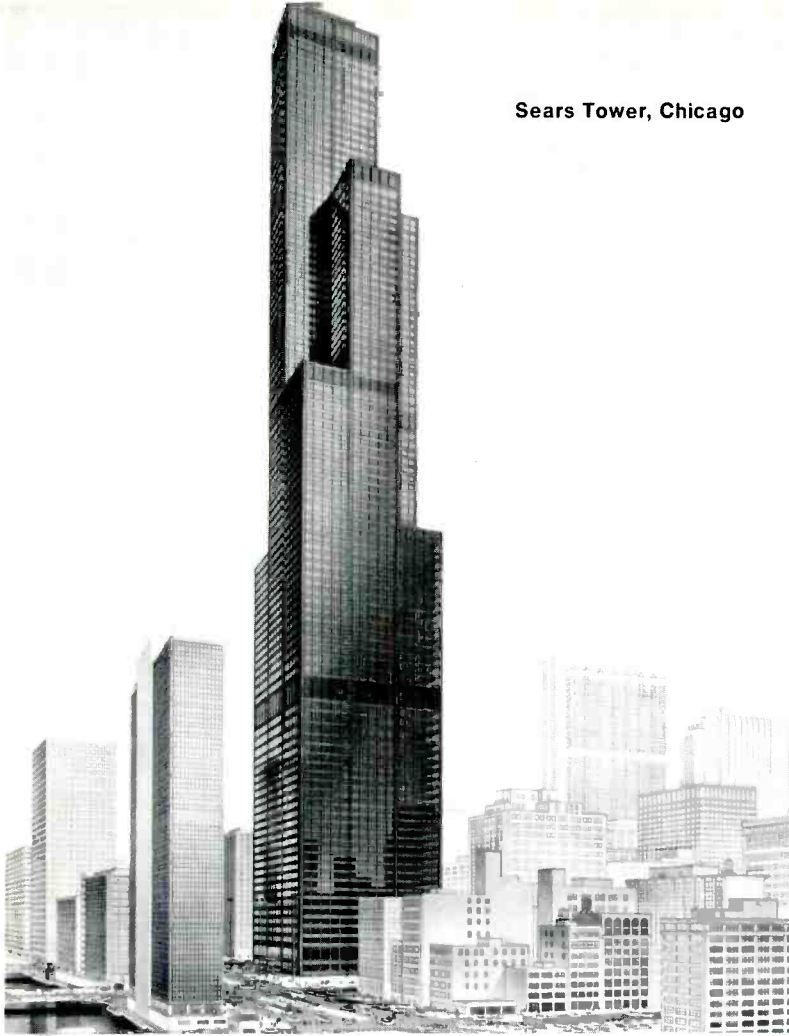


Cushman & Wakefield, Inc. Main Office, New York City



Chicago Board of Trade

Sears Tower, Chicago



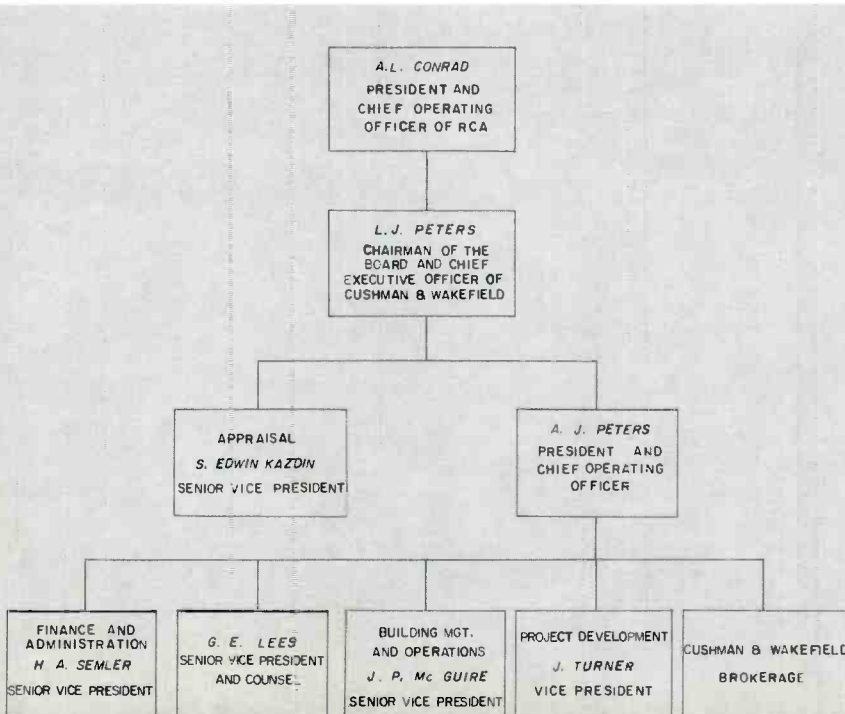
Cushman & Wakefield—a profile

Frank J. Strobl, Consulting Editor*

On October 14, 1970, Cushman & Wakefield, Inc. became a wholly owned subsidiary of RCA. As such, it functions as a separate entity under its own board of directors, personnel, and management. Today, the firm is leasing or management agent for more than 75 million square feet of office space in over a dozen U.S. cities and Puerto Rico, and it has an outstanding record in the commercial real estate industry.

FORMED OVER 50 years ago in New York City, Cushman & Wakefield, Inc. is now one of America's leading commercial real estate corporations. The firm is headquartered in New York City with four offices in the metropolitan area and offices in nine other cities from coast-to-coast, including San Juan, Puerto Rico.

From its initial business as a leasing broker and managing agent, Cushman & Wakefield has broadened its role considerably and is now applying its different expertises to the changing skylines of a number of American cities. Today, Cushman & Wakefield provides a multiplicity of commercial real estate services . . . these include brokerage functions, such as sales and leasing, building operation and management, project consultation, building modernization, insurance, and appraisal. Of all these services, the brokerage operation (sales



*Mr. Strobl is also Editor of *TREND*, The Research and Engineering News Digest
Reprint RE-17-6-6
Final manuscript received February 18, 1972

and leasing) provides the bulk of Cushman and Wakefield's income—over 75%. Table I shows how total income is derived.

Table I—Income by service line.

Service	Income (by percent)
Brokerage (sales and leasing)	75.1
Project consulting	10.7
Building modernization, operation & management	10.9
Appraisal	1.4
Insurance	1.9

Cushman & Wakefield as broker—sales and leasing

Cushman & Wakefield's brokerage activities involve the sale or lease of office space and industrial facilities, from complete manufacturing plants and office building complexes to partial floors in major structures. A partial listing of Cushman & Wakefield's industrial clients is shown in Table II.

The major capital investment called for in a long-term lease for office space involves many complex factors. Essentially, most companies make such decisions about acquisitions with respect to future growth. Because their decisions must be sound for many years, many companies turn to a professional broker for assistance in the selection of build-

Table II—Partial list of Cushman & Wakefield industrial clients.

Abbott Laboratories Inc.
Addressograph-Multigraph Corporation
AMBAC Corporation
Atlantic Gulf & Pacific Company
Atlantic Richfield Corporation
Baxter Laboratories, Inc.
The Borden Company
Burroughs Corporation
Diana Stores Corporation
Eastman Kodak Company
Fisher Scientific Company
General American Transportation Corporation
General Fireproofing
The Hertz Corporation
Honeywell, Inc.
International Flavors & Fragrances Inc.
JTT
Jaguar Cars, Inc.
Minnesota Mining & Manufacturing Company
The National Cash Register Company
Nestle Company
New York Telephone Company
Parke Davis Company
PepsiCo, Inc.
RCA Corporation
Raytheon Manufacturing Company
The Reuben H. Donnelley Corporation
Sears, Roebuck and Co.
Sperry Rand Corporation
Steelcase, Inc.
Union Bag-Camp Paper Corporation
Union Carbide Corporation
The Welch Scientific Company
Western Electric Company, Inc.
Western Union Telegraph Company
Westinghouse Electric Corporation
Zale Corporation

ings best suited for its immediate and long-range needs.

The task of selecting the best locations and buildings for a wide range of clients demands the evaluation of all available intelligence. This information is obtained from local chamber of commerce, development authorities, and city planning agencies, as well as from C&W's own resources. Comparative studies of tax structures, labor supply, transportation, land and construction costs, and housing accommodations for employees help the client select the area most suitable. Field studies then determine exactly which plants or plant sites are available.

The client may lease an existing facility or lease one built to his specifications by an investor-builder, freeing capital for other purposes.

Upon selection of the proper facility, the broker negotiates the most equitable lease for the tenant and owner. This process considers a combination of factors such as rental, term of lease, tenant standard and special installations and improvements, options for future expansion space, renewal options, cancellation privileges, extent of building services provided, disposition of the tenants existing lease obligations, and many other essential details. With each lease provision subject to negotiation, the application of a combination of the broker's skill, ability, and objectivity creates the most equitable lease agreement for both landlord and tenant.

As a leasing agent, C&W has negotiated five of the largest leases ever executed in America. Four of these transactions involved America's largest banking institutions—Chemical Bank of New York, Chase Manhattan Bank, Banker's Trust Company, and First National City Bank. A total of about 4,300,000 square feet of office space was contracted for in these leases.

Another of the firm's major accomplishments was leasing 1,300,000 square feet to the New York Telephone Company. Upon completion, this structure will be the largest telephone facility in the world.

A client may choose to buy an existing structure or to design and build to his own requirements. Cushman & Wakefield provides counsel on the most advantageous methods of acquiring a facility.

Building management

A corollary service of C&W is the operation and management of buildings. As building manager, Cushman & Wakefield performs a variety of services, from the complete management, operation, provision of services, and maintenance of a structure to the performance of a single function such as the collection of rents. Presently, C&W acts as manager for over 84 high-rise office buildings in the New York City area. Through a subsidiary in San Francisco, the firm acts as manager for a number of smaller apartment-type dwellings. On a national basis, C&W is managing agent for more than 300 properties.

Typical of the operation and management functions performed by C&W are the provision of building maintenance services, building attendants, and operation of other mechanical or electrical equipments. In the modern building, sophisticated electrical installations, automatic elevators, and computer-controlled air conditioning and heating systems require an experienced and skilled operations team.

Project consultation

As project consultant and developer, C&W represents the owner/investor or corporation in the intricate task of creating a new skyscraper complex, supplying the direction, supervision, and professional expertise required to ensure the success of the client's investment.

C&W's project consultation service may begin with site selection and advice in acquiring construction loans and permanent financing. The firm then provides assistance in the selection of architects, engineers, and contractors, working closely with each specialist and the structure's future occupants, to erect a modern and efficient building.

Another project consultation service can be the rental or sale of extra office/industrial space once a structure is completed. In many cases, project consultation clients of Cushman & Wakefield request the firm to operate and manage the new building once the tenants have moved in.

Buildings served by Cushman & Wakefield as project consultant include:

Sears Tower—a 110-story, 4,464,000-square-foot structure being erected in down-

town Chicago will serve as the headquarters building for Sears Roebuck and Co. Sears will occupy approximately 2-million square feet, with the remainder available to outside tenants. At 1,450 feet, it is destined to be the world's tallest building. This dramatic project will be served by 102 high-speed elevators, including 14 double-deck units, plus 16 escalators for serving lower levels, concourse, plaza, mezzanine levels, and "sky lobbies" at the 33-34th and 66-67th floors. Actually, the building will have the equivalent of seven main lobbies. Cushman & Wakefield assembled the site, is project developer, leasing, and managing agent.

The John Hancock Center—sponsored by John Hancock Insurance Company, is actually a second city within Chicago. This unique 100-story building contains office space, apartments, shopping, restaurants, indoor swimming pool, health club, observation deck, and parking, all under one roof. C&W was owner's representative for the project and is leasing agent for the office space.

Dresser Tower—will be the Third tallest building in Houston. The facility will house 6,000 people and contain an independent garage on an adjacent block for parking 1,600 cars.

Atlantic Richfield Plaza—in downtown Los Angeles is sponsored jointly by Atlantic Richfield Company, Bank of America, and Kaiser Industries. This \$175 million, 4.3-million-square-foot office complex has twin 52-story towers, the city's tallest.

Franklin Town development in Philadelphia—one of the more exciting ventures in which Cushman & Wakefield is participating is a planned new community sponsored by five leading Philadelphia corporations and The Girard Bank, with C&W acting as project consultant.

Urban development project

Historically, cities have been built for industrial and commercial purposes. In turn, residential areas have sprung up around the city core, with the more affluent population housed on the furthest perimeter. As a consequence, activity in the city dies at night; tax rates decrease; and the city slips further into economic decay and deterioration.

Franklin Town is an innovative attempt to revitalize an essentially dormant section of center-city Philadelphia. Franklin Town will be a \$400-million, 50-acre development covering 22 blocks. The development will consist of a major new in-town residential neighborhood built around a two-acre "Town Square." In addition there will be a commercial center with nearly 4 million square feet of space for offices, hotels, and convention and shopping facilities.

The entire development will be serviced by enclosed parking. The buildings will vary in style from "low rise" town houses to "high rise" apartments and office buildings. The more than 4,000 residential units will be priced for families with a wide range of income and will include both rentals and sales.

In addition, the sponsoring corporations also have plans for a separate non-profit program to lend financial and technical assistance to disadvantaged communities near the new neighborhood.

Insurance and appraisal services

Supplementing its capabilities in brokerage, building operation and management, and project consultation, C&W offers the services of insurance and appraisal. For insurance needs, the firm provides building owners with advice and counsel regarding the proper type and amount of insurance coverage needed for a particular property. Cushman & Wakefield also assists in obtaining such coverage at the most economical rates.

Appraisal activities center on providing valuation figures for property sale, acquisition, or condemnation purposes, as well as for *ad valorem* tax requirements.

Building modernization

Cushman & Wakefield is extensively involved in the supervision of building modernization projects. In such projects, older structures are completely renovated with remodeled lobby areas, new floor plans, and modern mechanical, electrical, and environmental systems to make them competitive with new office space. Building modernization services offered by the firm encompass a broad spectrum—from advance study, to project direction, contractor selection and supervision, and finally, but most importantly, leasing space at the most advantageous rental rates.

The firm has modernized several New York City landmarks and is presently completing the modernization of the Chicago Board of Trade building under a \$9.3-million program.

Business prospectus

Cushman & Wakefield is continuing to expand its realty activities. Receiving

particular attention are urban renewal and low-to-moderate income housing projects. In these areas, the firm is active through its ownership of a 50% interest in Construction for Progress, Inc., a joint venture with Celanese Corporation, to build moderate-income and low-income housing in New York City.

Construction for Progress (CFP), supported strictly by private capital, builds apartments under the "Turnkey" arrangement. Using this technique, CFP negotiates a building proposal with the New York City Housing Authority with the understanding that on completion, it will be purchased by that agency. CFP has constructed and sold five apartment buildings to the City of New York. The latest is a six-story, 90-unit structure in the South Bronx which sold for \$2.2 million. The CFP project has \$12 million still under construction.

Construction of moderate- and low-income housing is expected to experience a rapid and dramatic growth on a national basis. As a Cushman & Wakefield subsidiary, CFP will participate in this national activity as opportunities develop.

Another Cushman & Wakefield subsidiary, Buckbee Thorn in San Francisco, is engaged in the management of apartment buildings. An affiliate, Cushman & Wakefield of Puerto Rico, is involved in a similar venture.

Cushman & Wakefield management is also evaluating the area of shopping center and mall consultation and management.

Although acquired by RCA as a profit-making subsidiary, Cushman & Wakefield's expertise can also be of significant benefit to the needs of RCA with the Corporation's substantial real estate holdings and future requirements. For example, C&W was an agent in the sale of the Lewiston, Maine and Cincinnati, Ohio, plants and the firm is presently the agent for several other facilities including the plants at Dayton, N.J., and Marlboro, Mass.

Acknowledgment

Dana N. Nasuti, Manager, Advertising and Public Relations of Cushman & Wakefield, provided the background material for this article.

Digital readouts

P. L. Farina

The past few years have seen many changes in data presentation. In place of a meter scale or other analog indicator, the trend has been to digital readouts for applications ranging from voltmeters and desk calculators to medical instrumentation, clocks, and even wrist watches. This article describes the digital readout devices that are presently available, and surveys the market for these devices.

FIVE BASIC CHARACTERISTICS of digital readout devices should be considered when making a selection:

- 1) *Visibility*—The characters should be bright and well shaped and provide strong contrast with the background. The unlit segments should be invisible. The viewing angle should be adequate.
- 2) *Compatibility*—The device must be compatible with digital encoders, and should be screened from any RF-induced interferences.
- 3) *Reliability*—The average life should exceed 100,000 hours; replacement should be easy; and a failure should be readily detectable.
- 4) *Esthetics*—The appearance of the numerals must be good at normal brightness; a wide range of colors should be provided.
- 5) *Cost*—The device should help to minimize the system cost.

A dozen different digital readouts are discussed in this survey. They include electro-magnetic units, image projectors, cathode-ray tubes, and new solid-and liquid-state devices. Each has advantages and disadvantages that the engineer will weigh when selecting the display units for his particular system.

Reprint RE-17-6-3

Final manuscript received February 29, 1972.



Electromagnetic display systems (Ferranti-Packard)

This type of display, generally used in stock exchanges, accepts serial or parallel ASCII (American Standard Code for Information Interchange) input at speeds up to 250 characters/second. These displays have been interfaced with computers as well as keyboard and tape readers. The readout is an array of discs free to rotate to show either a colored or a dark side. Each disc is a permanent magnet, as shown in Fig. 1, and aligns itself with the field of an electromagnet that is controlled by two coils on a coincident-current basis. A 200- μ s current pulse sets the electromagnets, and their remanence provides the memory to bring the disc to the desired position and keep it there without any further power consumption. Reversing the current in the coils causes the other side of the disc to show. Viewing is by reflected light, so visibility increases with ambient light level. Because there are no mechanical linkages to wear or filaments to burn

Patrick L. Farina, Mgr.,
Special Products Engineering,
Receiving Tube Engineering,
Entertainment Tube Division,
Electronic Components
Somerville, New Jersey

graduated from the General Engineering course of RCA Institutes in 1941, received the BSEE from Polytechnic Institute of Brooklyn in 1952 and the MSME in Engineering Management from Newark College of Engineering in 1956. He joined RCA as a technician in 1941, enlisted in the Air Force as a Navigator in 1942, and returned to RCA in 1945. He advanced to electrical equipment designer and became Manager of Technical Services for Equipment Development, Receiving Tube Division in 1951 and Manager of Advanced Development in Equipment Development in 1959, where he was responsible for the design of equipment for the Nuvistor and Thermolectric programs. In 1962, he became Manager of Engineering Administration for Receiving Tube Product Engineering and in 1965 continued this responsibility for Commercial Receiving Tube and Semiconductor Product Engineering. In 1968, he became Manager of Special Products Engineering and Services for Receiving Tube Product Engineering. In this capacity he was responsible for the FD2201 receiver used in the APX-72 Transponder and is responsible for design and applications of Numitrons, future new product developments and service functions which include Measurement Standards and the Chemical and Physical Laboratory. He is a Senior Member of IEEE.

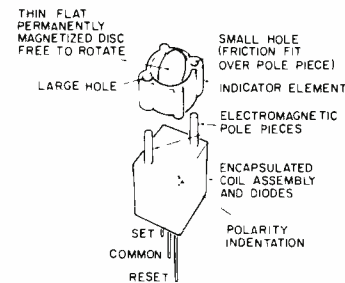


Fig. 1—Electromagnetic display unit.

out, life in the order of 20 million operations is possible. The change from one character to another occurs within a fraction of a second. There is redundancy of the dot matrix, so failure of a dot to operate will neither change a character nor make the character hard to read. Writing speeds vary with the application; the standard speed is 10 to 15 characters/second, and control units giving rates of 80 or 250 characters/second are available. Power is used only to change characters, so the average power consumption depends upon how often the data is changed; 200 watts is an approximate value. After a message is written, no power is consumed by the display; if power fails, the information will remain displayed. This type of presentation is best suited for airline arrival/departure boards, stock and commodity exchanges.

Edge-lighted displays

Edge-lighted readouts use miniature lamps arranged so that each one can edge-light one of a series of engraved, transparent acrylic plates stacked in depth behind a readout window. When a lamp is switched on, the character or message engraved on its plate glows through the other plates, which remain unlighted.

These displays are most suitable for laboratory bench instruments, small one-man consoles, vending machines, and other applications where the display is to be viewed head-on and close-up. Interference and parallax reduce the viewing angle, and the reliability of the display depends on the life expectancy of the bulbs. Today, this type of display enjoys little popularity.

Projected-image displays

Incandescent rear-projected displays use a lamp in a light-tight housing behind a printed transparent integer outlined on an opaque condensing lens.

When a lamp is lit, the character in front of it is projected onto a viewing screen. The film or mask can be altered to give any format or display required. The major advantages of this display are its versatility and wide viewing angle (up to 150 degrees). The disadvantages include limited brightness, higher cost than segmented displays, and wasted space. Brightness, a function of lamp wattage, is limited by the sensitivity of the module to heat. Character images can be distorted by a slight warping of the plastic lenses or by irregularities in the bulb filament. The cost of these displays is relatively high (\$14 to \$35).

Incandescent bar-segments

An incandescent bar-segment display consists of either seven or sixteen segments on a viewing block, each segment (bar) lighted by a separate incandescent lamp. Seven-segment displays can form numerals 0 through 9 and several letters of the alphabet. The sixteen-segment display can form all of the numerals and the complete alphabet. Each segment, with its own lamp source, is a separate unit. The segments are bonded to the molded viewing block to form a single display. Light is piped from each bulb to the surface of the block through a light pipe or chamber. Some advanced models provide for high contrast between lighted and unlighted segments by means of a 0.025-inch filter molecularly bonded to the surface of the viewing block. The filter reduces surface glare, and also virtually eliminates external lighting of the unlit segments. Incandescent bar-segment displays are fairly reliable because only the lamps are subject to wear and in a properly designed unit the lamps could last up to 100,000 hours. Maintenance varies with the supplier; some provide for direct lamp replacement, some require replacement of the lamp bank (sealed units), and others recommend replacing the whole display unit. The advantages of these devices are light weight, maximum reliability, and reasonably long life. The prime disadvantage is high initial cost. The lower cost units, however, have an average lamp life of 10,000 hours.

CRT displays

Cathode-ray tube (CRT) readouts are usually custom engineered for highly specialized applications such as military uses. However, shaped-beam CRT's and

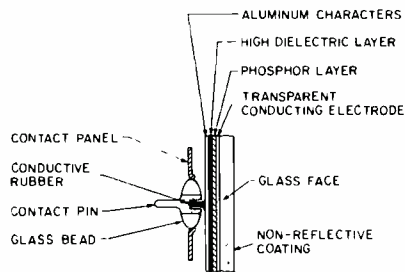


Fig. 2—Construction of an electroluminescent panel.

character generators that can write decimal information on conventional tubes are standard products. Some devices provide alphanumeric information, catalog formats, and page prints.

Digital character formation is generally accomplished either by extending an electron beam through individual "character cutters" pierced in a stencil-like mesh or by generating X- and Y-deflection voltages that cause the cathode ray to trace out a fixed character matrix. On command, selected segments are intensified to produce the required character.

Numerical CRT

Industrial Electronic Engineers, Inc. has built a low-cost miniature CRT, the "Nimo," that is capable of displaying four digits. This device combines CRT-display technique with the character-generation techniques of the rear-projection readout.

Fundamentally, the Nimo is a 10-gun cathode-ray tube. Each gun has a grid that controls the aperture of an electric lens in the gun structure. When any control grid is positive with reference to the cathode, the associated aperture is open; electrons are accelerated from the gun structure through the aperture. When the grid potential is sufficiently positive with respect to the cathode, the lens aperture is fully open, and the grid has no further effect. Under this condition, the character focus and position are determined only by the mechanical configuration of the gun structure.

The beam is picked up by the electrostatic field of the anode and accelerated. A metal mask with openings etched in the form of the desired characters, situated within the anode structure, shapes the cross section of the electron beam. The shaped beam is further accelerated by the anode field and finally collides with the P-31 phosphor screen

at the viewing end of the glass envelope, causing the phosphor to display a solid character. Because each gun is independent and is mechanically aimed at the screen, the only requirement for character selection and generation is the application of voltage to the proper control grid.

The Nimo tube has a diameter of 1.1 inches and a maximum length of 2.6 inches. The filament rating is 1.1 volts and 2 amperes, and the maximum anode requirement is 3 kV and 55 μ A. The normal brightness is 140 foot lamberts. The fluorescent color is green, with a persistence of 10 millisecond to 25 per cent brightness. This device displays four digits having a character height of 0.35 inch. The advantage of the Nimo tube is its relatively low cost per digit. The major disadvantage is the need for a high voltage (3 kilovolts DC) power supply, although the overall power consumption is low. Recently a new miniature CRT has been introduced by Industrial Electronic Engineers, Inc. that can display any of 64 messages or symbols in a custom-tailored character mask. The life expectancy of this device is 20,000 hours.

Electroluminescent numerals

Electroluminescence has been known for over 20 years, and has been used in lights for small areas (numerical and bargraph devices), but two difficulties have prevented widespread use: 1) the short lifetimes of materials when moderate-to-high light intensities are required; and 2) low output efficiency, which means that high input power is required and heat loss is high for large matrix applications.

As shown in Fig. 2, an electroluminescent panel is constructed by making a sandwich of a back-conductive plate; a phosphor; a dielectric, transparent-conductive layer; and a protective transparent cover. (The phosphor and dielectric may be combined in one layer.) The light output depends on the voltage and frequency of the electrical supply, the phosphor dielectric used, and the spacing of the electrodes.

The efficiency of a typical zinc sulphide electroluminescent device operated at 9 to 85 volts DC is 10^{-3} lumens/watt. This efficiency compares with 21 lumens/watt for a 500-watt tungsten light bulb and 50-70 lumens per watt for a fluorescent bulb. Brightness is

not very high; levels of 100 footlamberts can only be achieved at the expense of lifetime of the materials.

Operation with AC requires 100 to 600 volts. A typical 400-Hz device produces 8.5 footlamberts at 200 volts. Efficiency and brightness are low. Brightness varies linearly with frequency and not with a voltage. Luminance is directly proportional to the number of cycles applied, so half intensity (half-life) is obtained ten times faster at 600 Hz than 60 Hz; however, the panel may last only 1,000 hours instead of 40,000 hours.

New developments in phosphor technology give hope that better devices will be available shortly. Electroluminescent devices could have wider applications because they do have valuable assets. They are thin and light-weight; and because they fade at a known rate, preventive maintenance can be scheduled to avoid total loss of information at a crucial moment.

The major supplier has been Sylvania. More recently, Sigmatron introduced a light-emitting film (LEF) display. It has a sandwich of glass, a transparent tin oxide front electrode, a transparent zinc sulphide film, a light-absorbing dielectric, and opaque rear electrodes that form the segments.

The Nixie® Tube

The most popular numeric readout has been the bold-cathode gas-filled Nixie® tube made by Burroughs, and similar tubes made by Amperex, Raytheon, National, and Alco. Their cost is low and their IC decoder/drivers are also available at low cost.

The Nixie® has stacked elements in the form of metallic numerals with a common anode. When negative voltage is applied to a selected character, it glows like the cathode of a simple gas-discharge tube. However, only the selected numeral is visible in the viewing area because the visual glow discharge is larger than its metallic source. They can be adapted for binary-code decimal input by isolating the odd cathodes from the even ones and using two anodes. The operating voltage is 170 volts DC.

The major advantages of the Nixie® tube have been long life, high speed, relatively low power consumption, well-shaped characters, adequate brightness, and good reliability. In the

past, these qualities have made it the first choice for calculators, digital meters and other instruments. Its prime disadvantage is electronic complexity. The cathode current must be kept within tight limits. Moreover, if the ion current is excessive, the *off* cathodes will glow and produce background haze; but if the ion current is insufficient, there will be only partial presentation.

Vacuum fluorescent tubes

Vacuum fluorescent tubes made by Nippon Electric, Itron, Tung-Sol, Sylvania, and GE compete with the Nixie®. This type of tube uses fluorescent screens between the anode and cathode to enhance the light output. Their cost is low, and, requiring only 12 to 30 volts, they can be driven directly by MOS circuitry.

The readout is segmented into seven bars of phosphorescent material. The phosphor is treated P15 and is a green-blue color with low persistence. It is excited by electron bombardment from the cathode space-charge cloud when a segment is biased positive (as low as 4 volts). Because luminosity is generated on the surfaces of identical phosphor-coated segments, the characters are inherently of uniform brightness. All segmented characters are formed in the same viewing plane, providing wide-angle parallax-free viewing at distances up to 40 feet. The cathodes are almost invisible wires strung between the segments and the viewer. They draw 45 mA at 1.6 volts (AC or DC) and operate at 700°C, which is an unobjectionable dull red.

The Tung-Sol, Sylvania, and GE tubes are diodes, while the Nippon Electric and Itron tubes are triodes with fine-mesh grid between the anodes and cathodes. The grid serves to smooth out the brightness. The grid can be used to strobe the tube so that all the tubes in a display register can use the same driving logic. This feature is useful in desk calculator displays.

These tubes have some weaknesses. The long fine-wire filament will respond to external vibration and some of them are influenced by external electrostatic fields; moving one's hand close to an unshielded tube could cause momentary blackout of its segments, but pre-coating the tube with antistatic fluid eliminates this effect. The phosphor

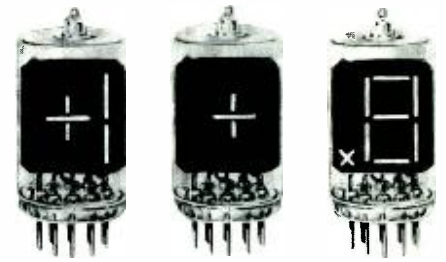


Fig. 3—RCA NUMITRON digital display devices.

light output decreases 30 per cent when temperature increases from 20°C to 70°C. When a diode device is operated at less than 15 volts, definite "hot spots" form on the three horizontal segments underneath the cathode. However, manufacturers claim that these devices will last for 100,000 hours. They ultimately fail because of phosphor poisoning by cathode sputtering throw-off, or because the glass envelope darkens.

Filamentary displays

The RCA NUMITRON devices discussed in companion papers in this issue are outstanding examples of directly viewed filamentary display devices. Fig. 3 shows the Numitron types. NUMITRON digital display devices have fully adjustable high brightness, low operating voltage (4.5V), high contrast, rugged construction, wide spectrum light emission, and a wide viewing angle that is free of "clutter." They are inexpensive, fit a low-cost socket, and are completely compatible with IC decoder/drivers.

Recently a new series has been introduced with a 68% power reduction (2.5V and 14 mA per segment) and a 40% reduction in brightness.

Liquid crystal display

Liquid crystals are an unusual class of organic materials that have certain properties of both liquid and solids. Liquid crystal compounds resemble liquids in that they pour, fill containers, and have a wide range of viscosities. However, their molecules are arranged in ordered structures such as those of crystalline solids. Liquid crystals are divided into three classes: smectic, nematic, and cholesteric phases. The liquid-crystal display developed by RCA, shown in Fig. 4, uses material of the nematic phase, where long slender molecules are randomly parallel to each other. In the display, the asymmetric nematic molecules rotate and realign

®Registered Trade Mark of Burroughs Corp.



Fig. 4—RCA liquid crystal display (reflection type).

under electrical or magnetic fields. Basically, this readout consists of a thin layer of liquid crystal placed between two glass layers having appropriate electrodes. In a reflective display one electrode is transparent, while the other is reflecting. With no field applied, the reflective liquid-crystal display appears to be an ordinary mirror. When voltage is applied, the liquid becomes turbulent, scatters light, and appears white. Increasing the field increases the brightness until saturation occurs. Depending upon the construction and material used, risetimes of 10 to 50 ms and decay times of 50 to 500 ms are obtainable. A contrast ratio of 15:1 is obtainable at a power level of one milliwatt/square inch. Typical operation requires 30 to 45 volts AC. Present devices operate over a temperature range from approximately 5°C to over 70°C, depending upon the specific liquid crystal material being used. Resolutions of more than 700 lines/inch can be attained.

Light scattering occurs due to variations in refractive index caused by the vibrating liquid-crystal molecules. The scattering centers are large compared to the wavelength of light, and the vibrations are caused by the disruptive effects of ions in transit through the ordered nematic medium.

Other companies like American Micro-Systems, General Electric, International Liquid Crystal, Motorola, North American Rockwell, Sperry, and Texas Instruments are active with liquid crystals. Optel Co. has a three-digit display for sale with 0.450-inch characters, it operates at 15 to 60 V and consumes 40 μ W/segment at 20 V. The cost is about \$15 each in 1000 quantity and a life of 13,000 hours is indicated at this time.

Although liquid-crystal displays may become a low-cost unit, there are problems associated with them. Speed is a problem below 15 V and at lower temperatures, the turn off time of 100 to 200 ms is noticeable making multi-

plexing very difficult. Operating with DC causes an electroplating action which reduces life substantially.

Multiple gas-discharge displays

Fig. 5 shows the Digivue electronic digital display panel, a plasma-discharge device fabricated by Owens-Illinois, consisting of an all-glass sandwich incorporating orthogonal electrode lines that are isolated from a selected gas mixture by glass dielectric sheets. Each intersection of two electrode lines defines an individual cell location. The isolation of the discharges at individual cell locations is accomplished by control of device parameters rather than by physical separation using a perforated center sheet. During operation, the memory is maintained by the storage of charge on the dielectric sheets covering the respective electrode patterns.

In operation the Digivue panel has an AC-sustaining signal of approximately 100 to 150 V peak normally applied to all X and Y electrodes. If a sinewave sustainer is used, 150 V peak at 50 kHz is satisfactory. Any cell within the panel can be addressed by selecting the desired pair of X and Y conductors, as in a core memory. A 4-inch by 4-inch panel with 33 $\frac{1}{3}$ cells per inch has been demonstrated, and development of 8-inch-square and 10-inch-square panels is now underway. Manufacture of a 17-inch-by-17-inch panel, providing a 1024 \times 1024 dot matrix, is considered possible.

Another contender in the multiple numerical readout field comes from Burroughs in the form of a miniature plasma panel specifically designed to eliminate 90 per cent of the addressing and drive circuitry usually needed for gas-discharge arrays. This design uses a self-scanning technique whereby a row of dots is sequentially scanned by a crossed array of backface wire anodes and cathode conductors. Neon gas-filled pinholes in the cathode, which are nearly invisible, serve as sources for spreading the glow discharge to a larger

Fig. 5—The DIGIVUE gas plasma display. [DIGIVUE is a trademark of Owens-Illinois, Inc.]



cell in an insulator sheet between the cathode and front-face, wire-addressing, anodes. The sequential firing technique makes the device useful for large flat displays; its brightness is 200 foot-lamberts. Initial applications were a 16-digit electronic calculator display and a similar 16-digit, dot-matrix display for other instruments. A 256-character communications terminal is also available.

More recently, Burroughs has introduced their Panaplex I and Panaplex II multiple, single-plane panels. They are available in 8 to 16 digits per display. The Panaplex I has a numeral height of 0.4 inch and Panaplex II is 0.255 inch. The cathode segments, as well as anodes and the screen, in Panaplex I are made of stamped and formed metal strips, positioned in a glass form. In Panaplex II, common cathode segments and interconnections are screened onto a glass substrate.

Although a 170 V DC supply is still required for the Panaplex, the voltage swing needed to illuminate a segment is as low as 25 V making it compatible with MOS devices for the first time.

In March, 1971, Sperry introduced a 0.33 inch and 0.5 inch, seven bar numeric readout having two digits in one flat package and a three-digit version. This product shares the same advantages and disadvantages of other gas-discharge devices.

Solid state displays

The solid-state light emitting diode (LED) has attracted a great deal of interest, and there are many suppliers. Light-emitting diodes can be obtained from Bowmar, Dialight, Fairchild, General Electric, Hewlett-Packard, Litronix, Monsanto, Opcoa, Texas Instrument, and Hitachi.

The emission from the LED is produced by the recombination of injected holes and electrons. As these excess carriers recombine, they give up energy in the form of photons. In theory, the total photon output should equal the electrical input into an LED, but ohmic losses, losses by recombination at the crystal defects, and absorption of the emitted photons cause low efficiencies.

Because the most commonly used material, gallium arsenide phosphide (GaAs-P), is opaque, the light-emitting junction must be located very

close to the surface to minimize absorption. Also, this material permits the generated light to escape over a relatively narrow angle. In contrast, gallium phosphide (*GaP*) is translucent and has higher efficiencies. Red *GaP* diodes show efficiencies of 7% in the laboratory and usually 2% in production.

Readouts using LED's are available today with either segment or dot-matrix character elements, and in either monolithic or hybrid construction. They operate from low voltages used for bipolar logic circuits. If operated from a 5-V supply, a series resistor is required so that the seven segments will consume 200 mW or more. The choice of color is red and the brightness varies from 100 to 500 footlamberts.

In mid-1969 Monsanto introduced the hybrid MAN-1 in which individual diode chips are bonded to a substrate and interconnected with thin-film metallization. By March, 1970, Monsanto introduced the MAN 3, the first monolithic LED display in which all diodes are on a single chip. Although this development suggests a lower cost unit, the lowest prices today are for hybrid and not monolithic LED displays.

In February, 1971, GE announced developmental *GaAs* readouts for green or for red through yellow. The *GaAs* segments are coated with a phosphor that emits visible light when excited by infrared emission. By November, 1971, Monsanto announced a green and a yellow LED. Both of these devices should be commercially available in the near future. However, the light-output efficiency of green *GaP* is only 10% of the red *GaP* efficiency. Studies also continue on a blue-emitting silicon carbide diode. The LED readouts are solid-state and should enjoy long life; however, wire bonds do break and leaks in packages can allow humidity to reduce life. The cost of LED's over the past four years has dropped from \$60 per digit to less than \$5 today. Prices are expected to drop further but not below \$2.50 per digit in high volume.

Digital readout market

The numeric display market was \$25 million in 1968 and was approximately \$30 million in 1969. In 1969, Nixie[®], segmented incandescent, and rear projection devices constituted 95% of all digital readouts, with the Nixie by far the most popular.

The Nixie[®] dominated the market, with sales of about \$15 million in 1968 and \$17 million in 1969. This market is increasing rapidly, primarily because of reduced cost of digital readouts and associated circuitry (IC's). The position of the Nixie is threatened, however, by lower voltage devices such as vacuum fluorescent tubes, the RCA NUMITRON device, solid-state displays, liquid crystals, and gas-discharge multiple readouts. The IEE "Nimo" CRT display has good numerical formation, good brightness and relatively low cost per digit and, therefore, should be able to share in a limited segment of the market.

Electroluminescent panels have been studied longer than other matrix arrays. They require higher voltage and have low energy-conversion efficiency and short lifetime when made to give moderate light intensities. These properties, along with complex fabrication, make them unattractive unless new phosphors are discovered. It is not clear today that they will beat the intensity and lifetime problems. Electroluminescent displays will find some use as low-level area illuminators and, because of their mechanical stability, as numerical readouts in military applications and in the Apollo program. Otherwise, they are not expected to be a significant factor in the numerical readout market.

Recent developments in the liquid crystal field have made possible a new type of information display offering extremely low power dissipation, good contrast under high ambient lighting conditions, and a new dimension of flexibility in both size and information content of displays. RCA has pioneered these developments and is now beginning to offer liquid crystal displays for commercial use along with several other manufacturers. If problems associated with liquid crystal displays are solved, they will make a significant impact in the digital readout market.

Vacuum fluorescent tubes have become very popular in calculator applications because they are compatible with MOS, large-scale integrated circuits and are lower cost than Nixie. But the trend of the calculator market is toward lower selling prices, approaching \$100 /calculator. This trend, in turn, requires lower cost digital readouts (\$1/digit) which precludes the use of multiple-type displays such as the Sperry or Burroughs Panaplex gas-discharge devices.

A multiple vacuum fluorescent readout would be necessary to share in this future market.

The technology of LED's is sufficiently perfected to permit their effective penetration in the numerical readout market. Their lower voltage requirements, extended lifetime, and complete compatibility with solid state IC's make them attractive, providing the price is right. But when compared to the cost of vacuum fluorescent, gas-discharge, and incandescent types, it does not appear that they can get below a \$2.50/digit cost in the near future. Although they do have extended life, the popular low-cost devices last longer than most equipment. The speed of LED's is three orders of magnitude greater than that of the competitive devices, but most customers don't care since competitive devices are fast enough. Sales of LED displays were \$1.8 million in 1969, \$2.0 million in 1970, \$5.0 million in 1971, and are expected to be about \$25 million in 1975.

Digital readouts in the industrial and commercial markets are growing at a rate in excess of 20%/year. This rate of increase is supported by forecasts. For example, digital panel meter sales were \$9 million in 1970 and will grow to \$17 million in 1975; digital voltmeters \$37 million in 1970 to \$42 million in 1975; and calculators from \$119 million in 1970 to \$490 million in 1975. Added to these markets are applications such as digital clocks, digital scales, medical monitoring systems, cash registers, marine depth finders and compasses, police Vascar, gas pumps, and automotive, to list only a few.

Summary

There is no display device that is well suited to all applications. Every type of display device has its advantages and disadvantages, and the design engineer must sift through such characteristics as performance, cost, form factor, and reliability to make a suitable choice.

It is generally agreed that there is a need for better visual presentation of information at lower costs. Because of this need, there is a real opportunity and challenge to engineers and scientists in the industry to come up with technical breakthroughs and manufacturing skills to produce the display of the future. The potential market exists, is growing, and will represent very substantial sales.

Visible-light-emitting diodes

Dr. C. J. Nuese | Dr. H. Kressel | I. Ladany

This paper reviews the operation and characteristics of electroluminescent p-n junctions which are specifically designed for incoherent emission in the visible portion of the optical spectrum. We hope to describe those parameters and phenomena which limit the performance of present light-emitting diodes (LEDs), and to indicate material and technological trends which could provide future advances. Throughout this paper, each aspect of electroluminescence is covered only in sufficient depth to clarify its role in the performance of electroluminescent diodes. For further details, the reader is referred to several recent review articles which more strongly emphasize luminescent materials,^{1, 2} recombination mechanisms^{3, 4} and electroluminescent junction properties.^{5, 6} Introductory treatments of electroluminescence also can be found in recent texts.^{7, 8}

H. Kressel, Head, Semiconductor Devices Research Group, Materials Research Laboratory, RCA Laboratories, Princeton, N. J., received BA in 1955 from Yeshiva University the MS in 1956 from Harvard University the MBA in Industrial Management and the PhD degree in Materials Science and Metallurgy from the University of Pennsylvania in 1959 and 1965, respectively. From 1959 to 1963 and from 1965 to 1966, he was with the Solid State Division where he worked initially on the development of high frequency silicon transistors and later supervised a group responsible for the development of high power microwave diodes subsequently used for the Lunar Excursion Module communication system. From 1963 to 1965 he was a David Sarnoff Fellow at the University of Pennsylvania. He transferred to the RCA Laboratories, Princeton, N. J. in 1966 and became Head of the Semiconductor Optical Devices Research group in 1969. He pioneered in the field of (AlGa)As-GaAs heterojunction devices and has been actively engaged in the study of luminescent processes in various III-V compound materials. He is the recipient of three RCA Achievement Awards two of which were for contributions to the microwave diode field including the high power avalanche diodes. Dr. Kressel is a member of the IEEE, the American Physical Society and Sigma Xi.

C. J. Nuese, Semiconductor Materials Research Group, Materials Research Laboratory, RCA Laboratories, Princeton, N. J., received the BSEE with distinction from the University of Connecticut, Storrs, in 1961 and the MS and PhD in electrical engineering from the University of Illinois, Urbana, in 1962 and 1966, respectively. Since joining the technical staff of RCA Laboratories in 1966, he has carried out studies of electroluminescent p-n junctions in a variety of III-V semiconductor compounds, including GaAs, GaAs_{1-x}P_x, AlAs, In_{1-x}Ga_xAs, and In_{1-x}Ga_xP. He has also devised improved techniques for etching and contacting compound semiconductors. Recently, he has become involved in the development of vapor-grown GaAs bipolar transistors and Shockley diodes. For his efforts in the fields of III-V electroluminescent diodes and bipolar transistors, Dr. Nuese received an RCA Laboratories Achievement Award in 1970. He has published about 25 technical papers on semiconductor devices and materials. Dr. Nuese is a member of Eta Kappa Nu, Tau Beta Pi, and Sigma Xi.

I. Ladany, Semiconductor Devices Research Group, Materials Research Laboratory, RCA Laboratories, Princeton, N. J., received the BS and MS from Northwestern University. In 1953, he joined the Naval Research Laboratory in Washington, D.C., where he worked briefly in the field of underwater sound, spending most of his time in semiconductor device research. Since joining the staff of RCA Laboratories in 1966, he has worked on GaP, GaAlP, and GaAs luminescent diode research. In 1969, he was awarded an RCA Laboratories Achievement Award for his contributions to GaP electroluminescence. He is the author or coauthor of some twenty published papers. Mr. Ladany is a member of the American Physical Society, the IEEE, and Sigma Xi.

Authors Ladany, Kressel, Nuese (left to right).

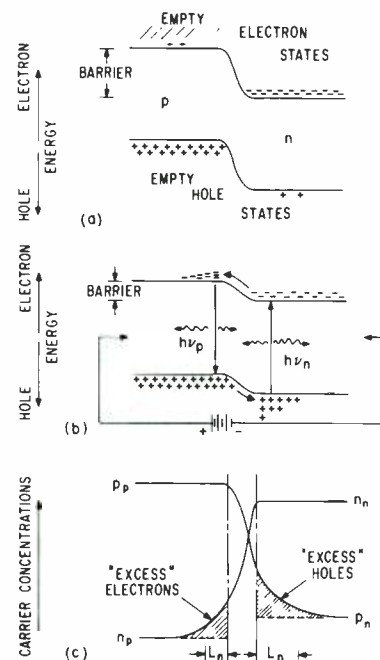


Fig. 1—Electroluminescent p-n junction operation. (a) Zero bias. Built-in potential across the p-n junction represents a large barrier for motion of electrons and holes. (b) Forward-bias. Potential barrier is significantly reduced by the external voltage. (c) Majority and minority carrier concentrations on the n- and p-side of a forward-biased p-n junction.

LUMINESCENCE is the emission of optical radiation (ultraviolet, visible or infrared) which results directly from the energy released during electronic transitions within a material. The luminescence arises from a two-step process in which 1) electrons and holes are generated in concentrations greater than those statistically permitted at thermal equilibrium, and 2) a significant fraction of these carriers recombine via mechanisms whereby the energy of the recombining holes and electrons is used to generate photons. The recombination process itself is nearly independent of the source of the excess carriers, but is very strongly characteristic of the physical and electrical properties of the material.

The manner in which the excess carriers are generated in an electroluminescent diode is the same used to inject minority carriers from the emitter into the base region of a bipolar transistor. For a zero-biased p-n junction in thermal equilibrium (Fig. 1a), a built-in potential barrier prevents the large concentration of mobile conduction-band electrons on the n-side of the junction from diffusing into the p-side, and similarly prevents the holes in the valence band from diffusing from the p- to the n-side of the junction. Under forward-bias (Fig. 1b), the magnitude of the potential barrier is reduced, which allows some of the conduction-band electrons on the n-side and some of the valence-band holes on the p-side to diffuse across the

junction. Once across, these carriers significantly increase the minority carrier concentrations (Fig. 1c). [For example, a p-n junction passing 10 A/cm² injects minority carriers at a rate of about 10²⁴ carriers/cm²-sec within a narrow region typically 1 to 2 μm wide adjoining the junction. Assuming a minority carrier lifetime of 10⁻⁹ sec, this generation rate yields a net excess carrier concentration of 10²⁴ × 10⁻⁹ = 10¹⁵ carriers/cm³, which is much in excess of typical equilibrium minority carrier concentrations at room temperature.] The "excess" carriers then recombine with some of the many oppositely charged majority carriers, thereby tending to return the minority carrier concentrations to their equilibrium values. The recombination of these excess minority carriers within a diffusion length, *L*, of the junction is the mechanism by which the optical radiation (electroluminescence) is generated.

Radiative recombination

The desire for semiconductor materials with an energy-band structure that can support laser operation has enhanced the exploration of direct bandgap semiconductors since 1962. In fact, prior to about 1964, a direct bandgap was assumed to be a prerequisite for efficient LEDs. Although direct recombination of electrons and holes from the conduction and valence band, respectively (or from "tails" of these bands into impurity states) can indeed be highly efficient, the indirect-bandgap material *GaP* can also provide reasonably efficient electroluminescence, as first illustrated in 1964 by Grimmeiss and Scholz.⁹ For this reason, both direct and indirect recombination processes will be considered in this section. Intrinsic (band-to-band) recombination will be treated first; then the more realistic case of "extrinsic" recombination via impurity states will be considered.

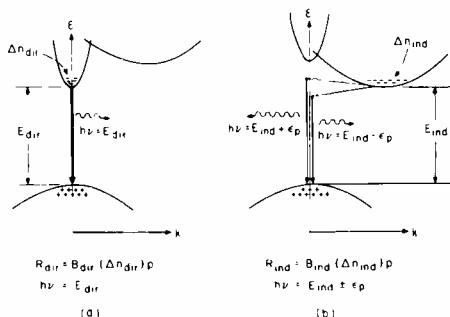


Fig. 2—Electron energy, *E*, vs. wave number, *k*, for energy states near the valence-band maximum and the conduction-band minimum or (a) direct, and for (b) indirect semiconductors. *k* is directly proportional to carrier momentum. ϵ_p is the phonon energy.

Intrinsic (band-to-band) recombination

When an excess minority electron concentration, Δn , is injected into the p-side of an electroluminescent junction, the probability of an excess electron in the conduction band recombining with one of the many available holes, *p*, in the valence band is proportional to the concentration of both Δn and *p*. The radiative recombination rate, *R*, for such a process can be written

$$R = K(\Delta n)p, \quad (1)$$

where the proportionality factor, *K*, is called the recombination coefficient. For an electron and hole to recombine and emit a photon, both energy and momentum must be conserved. Although a photon can have considerable energy, its momentum ($h\nu/c$) is very small. Therefore, the most simple (and most probable) recombination process will be that where the electron and hole have the same value of momentum. Such a situation actually occurs in many III-V compounds when the conduction-band minimum and the valence-band maximum both lie at the zero momentum position, as shown in Fig. 2a. A semiconductor energy-band structure such as this is said to be *direct*.

In contrast, Fig. 2b illustrates an *indirect* band structure, where the conduction-band minimum and the valence-band maximum occur at different values of momentum. For an indirect semiconductor, the band-to-band recombination necessarily must involve a third particle to conserve momentum. Phonons (i.e., lattice vibrations) serve this purpose, however, the probability of electron-hole recombination in this three-particle process is drastically reduced relative to the simpler two-particle direct recombination process. This difference is clearly reflected in significantly larger values of *K* for direct- than for indirect-bandgap semiconductors, as illustrated in Table I¹⁰ for several III-V compounds and for *Si* and *Ge*.

Impurity effects in direct-bandgap materials

In the III-V compounds, the introduction of donor and acceptor impurities

Table I—Recombination coefficient for representative direct- and indirect-bandgap semiconductors.¹⁰

Material	Energy-bandgap	Recombination coefficient, <i>K</i> (cm ³ /sec)
Si	Indirect	1.79 × 10 ⁻¹³
Ge	Indirect	5.25 × 10 ⁻¹⁴
GaP	Indirect	5.37 × 10 ⁻¹⁴
GaAs	Direct	7.21 × 10 ⁻¹⁰
GaSb	Direct	2.39 × 10 ⁻¹⁰
InAs	Direct	8.5 × 10 ⁻¹¹
InSb	Direct	4.58 × 10 ⁻¹¹

plays a major role in determining not only the conductivity type and resistivity of the material, but also the dominant recombination processes for light generation. The choice of a particular impurity is usually made from the group-VI donors—*Te*, *Se*, and *S*—and from the group-II acceptors—*Zn*, *Cd*, and *Mg*. In some cases, *amphoteric* dopants such as *Ge*, *Si*, and *Sn* from group IV of the periodic table can be used as either donors or acceptors, depending on which of the two available types of lattice sites (group III or V) they occupy.

For each dopant and semiconductor combination, an optimum impurity concentration is usually determined empirically for most efficient electroluminescence. In general, the following limits can be placed on such concentrations: they cannot be too *small* because 1) the recombination probability for an injected minority carrier is directly proportional to the concentration of majority carriers with which it will recombine, and 2) the higher series resistance which results from low carrier concentrations can cause excessive heating and large voltage drops at high currents. On the other hand, the concentration cannot be too *large* because metallurgical imperfections such as precipitates and metal complexes are introduced at concentrations near the solubility limit of the semiconductor. Such imperfections are known to introduce competing nonradiative recombination centers which drastically reduce the electroluminescence efficiency. For these reasons, impurity concentrations in the range of 10¹⁷ to 10¹⁸ cm⁻³ for donors and 10¹⁷ to 10¹⁹ cm⁻³ for acceptors generally have been found to be best for high electroluminescence efficiency.

Concerning the relative efficiency of the radiative recombination from n- and p-type material, it was originally thought that the radiative processes in p-type material were the more efficient, perhaps due to the involvement of acceptor states. This idea was based largely on the fact that the dominant emission from most LEDs was found to originate from the p-side of the electroluminescent junction. Detailed cathodoluminescence measurements revealed, however, that the luminescence intensities of n- and p-type *GaAs* at optimum doping concentrations are almost identical.¹¹ The fact that the observed emission from many LEDs originates on the p-side of the junction stems from several impurity effects.⁷

First, the injection of electrons into the p-region is usually favored over the injection of holes into the n-region by the large ratio of electron-to-hole mobility for most III-V compounds. In addition, since the Fermi level is slightly higher than the intrinsic energy gap in n-type material but slightly less than the energy gap for p-type material, a heterojunction is created which reduces the injection of minority holes into the n-side of the junction. Finally, since the emission energy is usually slightly higher in n-type than in p-type material, any radiation which does originate from the n-side of the junction is very strongly absorbed in the p-type material, where strong band tailing has effectively shrunk the energy gap. Conversely, the radiation originating in a heavily doped p-type layer will pass through n+ material with reduced absorption losses due to the reduced emission energy for p-type material. This consideration is usually used to good advantage in designing efficient LEDs.

Impurity effects in indirect bandgap materials

As previously mentioned, electron-hole recombination without the intermediary of impurity centers is a very inefficient way of obtaining light from indirect bandgap semiconductors because the participation of a phonon is needed to conserve crystal momentum. This requirement can be removed however by first localizing one of the charge carriers at an impurity center, and by then attracting the oppositely charged carrier. By being trapped on a *neutral* impurity center, a carrier is very highly *localized* in space, and it then follows from the Heisenberg Uncertainty Principle that the crystal momentum extends over a large range, thereby allowing it to take up the momentum difference in an indirect transition with an oppositely charged carrier. In this fashion, efficient radiative recombination can be obtained in an indirect bandgap semiconductor. However, only a rather limited number of impurities have been found to be suitable for this purpose. In *GaP*, nitrogen¹² has been found to so enhance the efficiency of the near-bandgap green emission, while *Zn* and *O* centers are used to obtain efficient red emission.^{13,14}

The nitrogen substitution for phosphorus in the *GaP* lattice is said to be *isoelectronic* because both *N* and *P* are in the same column of the periodic table. As a result, nitrogen introduces only a short range, non-Coulombic attractive potential with a binding

energy of about 8 meV for electrons. After the capture of an electron, the center becomes negatively charged and the long-range Coulombic potential now allows it to capture a free hole, thus forming a bound exciton. The annihilation of this exciton by radiative recombination gives rise to the relatively efficient green diode luminescence at room temperature.¹⁵ Unfortunately, the exciton may dissociate by thermal activation prior to radiative recombination, and many competing processes exist for the nonradiative recombination of electrons and holes. As a result, the internal quantum efficiency for the green luminescence in *GaP* is on the order of 1%, which is significantly lower than that for direct bandgap radiative recombination processes.

The efficient red emission is obtained from p-type *GaP* by a related but not identical method. Here the shallow acceptor *Zn* ($E_a = 60$ meV) and deep donor oxygen ($E_d = 800$ meV) are believed to be situated on nearest neighbor gallium and phosphorus sites. This complex, which is effectively neutral with regard to long range Coulombic forces when both impurities are ionized, behaves as an isoelectronic complex with a binding energy of 300 meV for electrons. At room temperature, the red emission results mainly from recombination of an electron and a hole captured by the *Zn-O* complex, and is centered at 1.79 eV.^{16,17} The internal red emission quantum efficiency (10 to 15%) is considerably higher at this time than the green emission, and is limited both by competing nonradiative centers and by Auger recombination in which the electron-hole recombination energy is transferred to a third particle in the form of kinetic energy. A drawback of the *GaP:Zn,O* system is that the intensity of the red emission saturates at relatively low current densities (≤ 10 A/cm²) because the effective density of *Zn-O* centers is limited to the low 10¹⁷ cm⁻³ range. In *GaP:N*, on the other hand, the nitrogen concentration can reach 10¹⁹ cm⁻³, and the green luminescence does not readily saturate.¹⁵

Upconversion phosphors

As an alternative to the use of high-energy-gap semiconducting compounds to obtain visible emission, one can employ a suitably doped "upconverting" phosphor, in which two or three infrared photons are converted into a single higher-energy photon in the visible portion of the spectrum.¹⁸

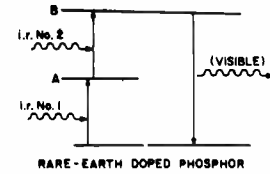


Fig. 3—Simplified upconversion process for rare-earth-doped phosphors.

For this technique, a highly efficient diode which emits in the proper infrared wavelength range (e.g., *GaAs:Si* with $\eta_{ext} \approx 10\%$ at 9300 to 9700 Å) is coated with a layer of phosphor doped with rare-earth impurities.¹⁹ The combination of phosphor host and impurity is chosen for the particular excitation wavelength desired.

The basic upconversion process is illustrated schematically in Fig. 3. Here, the absorption of one infrared photon excites an impurity ion to level A, after which a second absorbed infrared photon can excite it to level B. The subsequent decay of the excited state to its original level is then accompanied by the emission of one high-energy visible photon. In this way, upconversion to the red, green, and blue has been achieved. Because the upconversion is a two-step process (or even a three-step process for blue emission), the intensity of the emitted visible radiation is approximately proportional to the second or third power of the infrared excitation intensity. Hence, for high-efficiency operation of the diode-phosphor system, the *GaAs* diode must be driven to very high current densities.

A fundamental limitation of the upconversion scheme lies in the difficulty of adequately coupling the infrared diode emission to the phosphor. Although the conversion efficiency of the phosphor itself is quite reasonable (30 to 55%)²⁰, only a small fraction of the diode emission is absorbed by the phosphor, which must be kept quite thin in order to reduce self-absorption of the visible radiation. This also means that the diode-phosphor system produces a large amount of undesired *GaAs* infrared radiation as well as the visible emission.

Efficiency and brightness

The response of the human eye is limited to a wavelength range between about 4000 Å (violet-ultraviolet) and 7200 Å (red-infrared), as illustrated in Fig. 4. Because of the immense variation in the visual sensitivity over this spectral range, the performance of a visible-light-emitting diode must be appraised

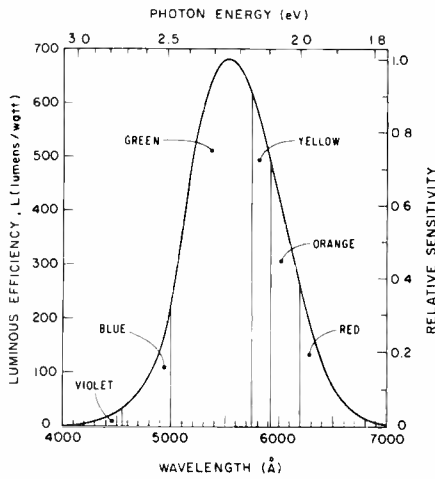


Fig. 4—Luminous efficiency, L , of "standard" (photopic) eye vs. wavelength of incident light. Maximum response of 680 lumens/watt occurs for green light at 5550 Å.

not only by the absolute intensity of the emitted radiation, but also by the relative response (i.e., the luminous efficiency) of the eye at the wavelength of interest. Hence, two important figures of merit have evolved for LEDs. The first is the *quantum efficiency*, which is simply the ratio of the number of photons produced to the number of electrons passing through the diode, i.e., the conversion efficiency of the device independent of the eye's response to it. The *internal quantum efficiency*, η_{int} , is evaluated at the p-n junction, while the *external quantum efficiency*, η_{ext} , is evaluated at the exterior of the diode. The external quantum efficiency is always less than the internal quantum efficiency due to optical losses which occur in extracting the emitted radiation from the semiconductor. Representative values of η_{ext} for visible LEDs fall between 0.1 and 7% at room-temperature, while values of η_{int} can exceed 50% under optimum conditions.

The second figure of merit for an LED is the *brightness*, which is a measure of the *visual* response to the radiation emitted from the diode surface. The brightness, B , in foot-Lamberts (fL), is proportional to the external quantum efficiency of the diode and to the sensitivity of the eye, and can be calculated from the equation

$$B = 1150 \frac{\eta_{ext} L J}{\lambda} \frac{A_j}{A_s} \quad (2)$$

Here, λ is the emission wavelength (μm); J is the current density through the junction (A/cm^2); and L is the luminous efficiency of the eye (see Fig. 4), which has a maximum value of 680 lumens/watt for green emission at 5550

Å. A_j and A_s are the areas of the p-n junction and of the observed emitting surface, respectively. The ratio (A_j/A_s) is unity for the simplest case of a flat, unencapsulated, surface-emitting LED, but can be much less than unity in some cases (e.g., phosphor-coated dome-shaped diodes, edge- and surface-emitting structures, diodes with encapsulated plastic lens, etc.). Since the brightness of a diode can be varied by changing its size or the junction current, B is often normalized with respect to the current density, J , so as to more fairly compare the relative performance of different electroluminescent materials. Values of brightness in excess of 1000 fL are readily available in commercial LEDs at normal current densities of 10 A/cm^2 . By comparison, the brightness of the frosted surface of a 40 W incandescence bulb is about 7000 fL.

From the considerations discussed above, it is apparent that efficient LEDs which emit near the peak of the eye sensitivity are required. Since the upper limit for the emission energy is approximately equal to the semiconductor energy gap, values of E_g greater than 1.72 eV (7200 Å) and as close as possible to 2.23 eV (5550 Å) are needed. The selection of semiconductors which have appropriate energy-gap values and which can be amphoterically doped is shown in Table II.

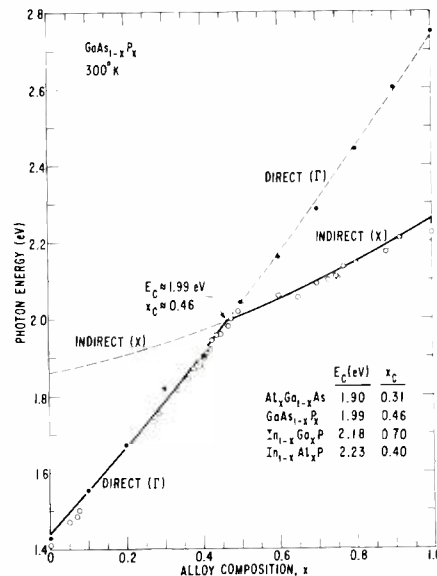


Fig. 5—Direct (Γ) and indirect (X) conduction band minima for $\text{GaAs}_{1-x}\text{P}_x$ as a function of alloy composition, x . The closed data points are from electroreflectance measurements⁵⁵, while the open points are from electroluminescence spectra^{45,56}. The values of E_c and x_c for $\text{Al}_x\text{Ga}_{1-x}$ and $\text{In}_{1-x}\text{Al}_x\text{P}$ are from Ref. 2.

Quest for higher-energy-bandgap semiconductors

Most of the direct-bandgap *III-V* binary compounds (e.g., GaAs , InP , GaSb , etc.) have energy-gap values much less than 1.72 eV, and therefore, are not capable of providing visible emission. One approach which is widely used to obtain materials with somewhat larger direct energy gaps is to form ternary alloy systems between a binary compound with a small direct energy gap and a second binary compound with a larger indirect energy gap (e.g., $\text{GaAs}_{1-x}\text{P}_x$ from GaAs and GaP). In this way, the direct band structure of the smaller-energy-gap-material is increased monotonically in the alloy as the content of the second compound is increased, as shown in Fig. 5 for a representative ternary alloy, $\text{GaAs}_{1-x}\text{P}_x$. For this alloy, as well as for the other materials listed in Fig. 5, the direct (Γ) conduction band minimum lies below the indirect (X) conduction band minima over a significant fraction of the alloy system. For values of x somewhat less than the crossover value, x_c , each of the semiconductors in Fig. 5 is direct and of sufficiently high energy to provide visible emission. Herein lies the real value of such alloys. However, at alloy compositions close to x_c , some of the electrons that would otherwise occupy the direct conduction band minimum at $k=0$ transfer to the indirect minima ($k \neq 0$) as a result of their small but finite thermal energy. This effect is particularly dramatic since there are typically 50 to 100 times more available energy states in the heavy-mass indirect minima than there are in the direct minimum. It has been found experimentally for $\text{Al}_x\text{Ga}_{1-x}\text{As}$,²¹ $\text{GaAs}_{1-x}\text{P}_x$,²² and $\text{In}_{1-x}\text{Ga}_x\text{P}$ ²³ that such a transfer results in a severe reduction in the luminescence intensity, because the non-radiative processes associated with the indirect minima are more efficient than the radiative processes there.

Recently, Archer²⁴ has used estimated positions of the conduction band minima to calculate the dependence of the electroluminescence efficiency and brightness on alloy composition (or equally, their dependence on the photon emission energy for these near-bandgap processes). For these calculations, equal radiative (direct) and nonradiative lifetimes were assumed, which is equivalent to the assumption of a 50% internal quantum efficiency for the direct-bandgap recombination. The calculated curves for the external quantum efficiency are shown in Fig.

Table II—Materials for visible electroluminescence.

Material	Energy gap (eV)	Band structure	State-of-development	Major limitations
GaN	3.5	Direct	Exploratory	p-type doping
SiC	2.8 to 3.2	Indirect	Moderate	High-temperature processing
$Al_xGa_{1-x}P$	2.26 to 2.45	Indirect	Exploratory	High reactivity of Al; instability
GaP	2.26	Indirect	Advanced	
AlAs	2.16	Indirect	Exploratory	High reactivity of Al; instability
$In_{1-x}Ga_xP$	1.34 to 2.26	Direct-Indirect	Moderate	Strain; lattice mismatch
$In_{1-x}Al_xP$	1.34 to 2.45	Direct-Indirect	Exploratory	Strain; lattice mismatch
$GaAs_{1-x}P_x$	1.44 to 2.26	Direct-Indirect	Advanced	
$Al_xGa_{1-x}As$	1.44 to 2.16	Direct-Indirect	Advanced	

Table III—III-V ternary alloys for electroluminescence.

Material	Direct-indirect transition				Maximum Brightness			
	x_c	E_c (eV)	x_m	E_m (eV)	a_m (Å)	Substrate	a_s (Å)	$\left[\frac{a_m - a_s}{a_m} \right]$ (%)
$Al_xGa_{1-x}As$	0.31	1.90	0.27	1.82	5.6556	GaAs	5.6532	0.04
$GaAs_{1-x}P_x$	0.46	1.99	0.39	1.88	5.5744	GaAs	5.6532	1.4
						GaP	5.4512	2.2
$In_{1-x}Ga_xP$	0.70	2.18	0.61	2.03	5.6140	InP	5.8687	4.5
						GaP	5.4512	2.9
$In_{1-x}Al_xP$	0.40	2.23	0.34	2.06	5.7267	InP	5.8687	2.5
						GaP	5.4512	4.8

6a. Also superimposed on the efficiency curves are data points obtained for the respective alloys by electroluminescence or by cathodoluminescence emission. Fig. 6a illustrates that $GaAs_{1-x}P_x$ has potential for slightly higher efficiencies than $Al_xGa_{1-x}As$ for red-light emission, but the $In_{1-x}Ga_xP$ and $In_{1-x}Al_xP$ have clearly higher potential efficiency than either $GaAs_{1-x}P_x$ or $Al_xGa_{1-x}As$ for red, yellow, or orange emission.

The potential brightness (per unit current density) can be calculated for these alloys from Fig. 6a and from Eq. 2. From these calculations, plotted in Fig. 6b, it is clear that the potential brightness of $In_{1-x}Ga_xP$ and $In_{1-x}Al_xP$ is about 20 times higher than that for $GaAs_{1-x}P_x$. Equally important, the maximum in brightness for $In_{1-x}Ga_xP$ occurs at about 2.03 eV, which is in the orange portion of the optical spectrum. It is important to note that the curves in Fig. 6 are based solely on the energy band structure of these alloys and the assumption of equal radiative and non-radiative lifetimes. These calculations do not take into consideration such important problems as the stability of the compound, the extent of lattice mismatch for the alloy, or the relative ease of crystal preparation. Such considerations are treated further in ensuing sections.

Material synthesis

Light-emitting diodes are generally fabricated from material which is epitaxially deposited on single crystal $GaAs$ or GaP substrates cut from melt-grown ingots. Both $GaAs$ and GaP substrates

are commercially available with ingot cross sections of 2 to 3 cm. However, the GaP technology is relatively young, and GaP crystals are still costlier than $GaAs$ ones and contain more dislocations and other imperfections.

The choice of substrate depends on the lattice constant of the desired epitaxial layer and the thermal coefficient of expansion. Table III shows the lattice constants at room temperature of the III-V compounds of interest for visible LEDs. In the case of mixed alloys, the lattice constant is a function of composition. The best alloy material from the point of view of lattice constant match is $Al_xGa_{1-x}As$ since $AlAs$ and $GaAs$ have almost identical lattice constants. The worst systems are $Al_xIn_{1-x}P$ and $In_{1-x}Ga_xP$ with $GaAs_{1-x}P_x$ being intermediate.

Both vapor-phase epitaxy (VPE) and liquid-phase epitaxy (LPE) are used to prepare materials for LEDs. Each technique has unique advantages in some cases. Vapor-phase epitaxy is used exclusively for $GaAs_{1-x}P_x$ synthesis while liquid-phase epitaxy yields the best GaP and $Al_xGa_{1-x}As$ devices at this time.

The p-n junction can be formed by epitaxially growing the p- and n-type regions or by Zn diffusion into an n-type layer. Diffusion, which is commonly used in the fabrication of $GaAs_{1-x}P_x$ diodes, allows the definition of selected diode areas by masking, which is a simple way of forming monolithic diode displays. However, efficient diodes are not always obtainable by diffusion, particularly in GaP where the best red-emitting and green-emitting

diodes are formed by double epitaxy. An attractive alternative in GaP is to epitaxially deposit a p-type layer on an n-type bulk grown substrate. Unfortunately, the present quality of GaP substrates is too poor to permit the reproducible fabrication of diodes by this simple technique, and two epitaxial layers are therefore grown to ensure that the radiative recombination occurs in the higher quality epitaxial layer.

Liquid-phase epitaxy (LPE)

Liquid-phase epitaxy was originally developed by Nelson²⁵ for the growth of epitaxial films for tunnel diodes and for $GaAs$ homojunction laser diodes. In the commonly-used "tipping" technique, GaP is grown from melt consisting of Ga , GaP (polycrystalline) and a dopant such as Zn (for p-type) or Te (for n-type). The melt is positioned at one end of a graphite boat (Fig. 7) while a polished substrate is placed at the other end. The graphite boat is heated to 1060°C in a pure hydrogen atmosphere in a quartz furnace tube. The furnace, mounted on a hinge at its center, is tipped at the desired tem-

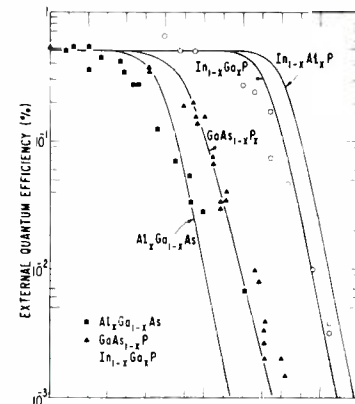


Fig. 6a—Calculated external quantum efficiency² for $Al_xGa_{1-x}As$, $GaAs_{1-x}P_x$, $In_{1-x}Ga_xP$, and $In_{1-x}Al_xP$ LEDs as a function of photon emission energy. The data points for $Al_xGa_{1-x}As$ ^{21, 57} and for $GaAs_{1-x}P_x$ ⁵⁶ are relative electroluminescence efficiencies. The $In_{1-x}Ga_xP$ data²³ are relative cathodoluminescence efficiency values.

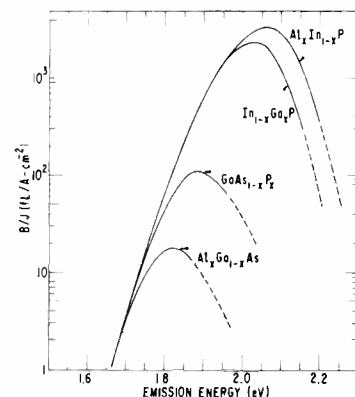


Fig. 6b—Calculated² brightness values (per unit current density) for the same alloys in (a).

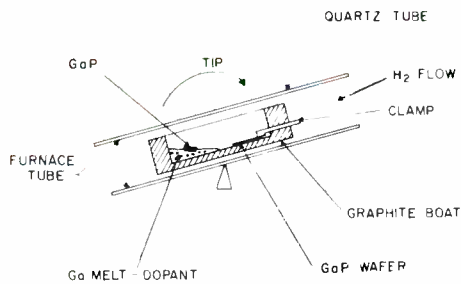


Fig. 7—Schematic diagram of typical liquid-phase epitaxy (LPE) "tipping" apparatus used for the deposition of GaP single-crystal layers on a GaP substrate

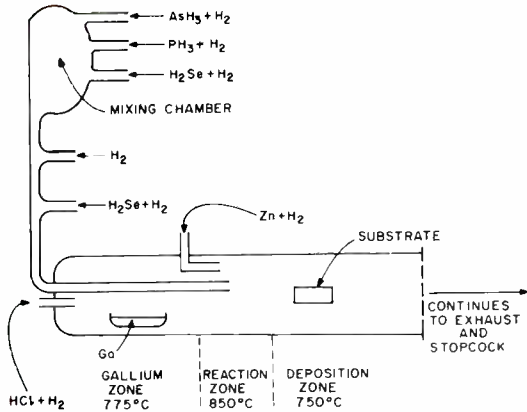


Fig. 8—Schematic diagram of typical vapor-phase epitaxy (VPE) growth apparatus used for the deposition of single-crystal GaAs_{1-x}P_x layers on a GaAs substrate

perature and the melt than covers the substrate. Some dissolution of the substrate may occur on contact, depending on the initial GaP content of the melt, but as the furnace is slowly cooled, GaP precipitates from the melt in the form of an epitaxial deposition on the substrate.

The growth of two layers is now required for efficient red emission from GaP.²⁶ In this case, an n-type layer doped with Te or S is grown first, followed by a p-type layer doped with Zn and O from a Ga melt containing elemental Zn and GaO. A similar technique with varied temperatures and melt constituents is used for several other compounds. While liquid phase epitaxy requires simple equipment for small-volume production, large-scale manufacturing calls for a multiple wafer

processing capability which is now under development.

Vapor-phase epitaxy (VPE)

The epitaxial vapor-phase growth technique is widely used in the preparation of red-light emitting diodes of GaAs_{1-x}P_x, which have been commercially available for several years. With this technique, the primary source chemicals are predominantly gaseous, which provides a high degree of flexibility for controlling doping concentrations and alloy composition. In addition, since the reactant concentrations can be accurately established with precision flow meters and valves, the growth parameters can be regulated over relatively wide ranges with good accuracy. An important feature of this control is the ability to slowly grade the alloy composition of the growing layer from the substrate composition ($x=0$ for a GaAs substrate) to that of the p-n junction (typically, $x \approx 0.4$) so as to minimize strain due to lattice mismatch. Such grading has been found to lead to improved p-n junction performance. In vapor-grown epitaxial layers, the p-n junction can be incorporated during growth by the sequential introduction of gaseous donor and acceptor impurities, or after growth by Zn diffusion. For GaAs_{1-x}P_x red-light-emitting diodes, highest efficiencies to date have been prepared by the post-growth diffusion process.

A typical vapor-phase growth system for GaAs_{1-x}P_x²⁷ is illustrated in Fig. 8. Here, Ga is transported as its subchloride by passing HCl gas over the molten metal. Arsenic and phosphorus are formed by the thermal decomposition of arsine and phosphine, respectively, while hydrogen is usually used as the carrier gas. As the gases pass over the substrate, they react with its surface to form a single-crystal epitaxial deposit of GaAs_{1-x}P_x, the composition and electrical properties of which are determined by the vapor constitution. The donor impurity in vapor-grown GaAs_{1-x}P_x is usually Se, which is intro-

duced as H₂Se, although Te and Si have occasionally been employed. The Zn inlet illustrated in Fig. 8 is not used for p-n junctions formed by Zn diffusion after growth.

There are several reasons why GaAs_{1-x}P_x LEDs have received widespread commercial attention. Most importantly, the system shown in Fig. 8 can be scaled up to hold many GaAs substrates simultaneously, thereby reducing the manufacturing cost per wafer. Secondly, the surface of the epitaxial layers following vapor growth is usually smooth and free of surface imperfections, eliminating the need for additional lapping or polishing steps. Finally, the ready-availability of large, high-quality, single-crystal GaAs substrates adds to the commercial viability of this process.

Besides GaAs_{1-x}P_x, GaN²⁸ and In_{1-x}Ga_xP²⁹ are also frequently prepared by vapor-phase epitaxy. However, AlGa_{1-x}As is difficult to grow by this technique, primarily due to the reactivity of the Al-containing gases needed here.

Loss mechanisms

The external efficiency and brightness of an LED are determined by the generation of light at the junction and by the extraction of light from the crystal. For each of these processes, there are several loss mechanisms which limit the overall performance of an LED.

At the p-n junction, the internal quantum efficiency is highly dependent on the perfection of the material in the vicinity of the p-n junction where the radiative recombination occurs. Defects (and contaminants such as copper) give rise to deep recombination centers with consequent infrared emission or nonradiative recombination. Relatively little is known about the details of the nonradiative recombination processes via defect centers, but dislocations with their associated impurity clusters, and complexes of vacancies with impurities are known to be harmful.

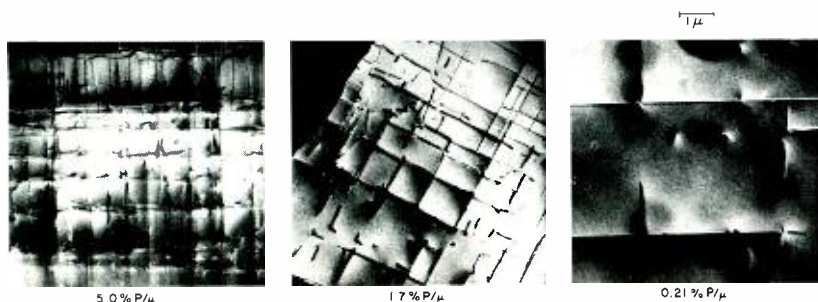


Fig. 9—Lattice misfit dislocation networks³⁰ in GaAs_{1-x}P_x layers which were vapor-deposited with different compositional grading rates on GaAs substrates. The density of misfit dislocations decreases with decreasing compositional gradient. The gradients in each illustration are given in units of mole fraction GaP per micron of growth

Table IV—Internal loss mechanisms in electroluminescent junctions.

Loss mechanism	Typical cause
Point Imperfections:	
Vacancies	Deviation from stoichiometry during growth
Metal complexes, precipitates	Impurity concentrations approaching solubility in material
Frenkel defects	Generated by external electron bombardment; possibly formed during forward-bias operation
Dislocations	Lattice mismatch between substrate and epitaxy
Auger recombination	High carrier concentrations
Deep-level recombination	Contamination (e.g., Cu, O)
Surface or contact recombination	Location of surface or ohmic contact too close to p-n junction
Surface leakage	Work damage; surface contamination during device fabrication

Table V—Methods for increasing external diode efficiency.

Objectives	Techniques
Minimize absorption coefficient, α	<ol style="list-style-type: none"> 1) Keep absorbing layers thin 2) Provide optical "window" with higher-energy-gap material 3) Reduce carrier concentrations 4) Generate below-bandgap radiation
Maximize surface transmissivity, T	<ol style="list-style-type: none"> 1) Shape semiconductor for normal incidence 2) Encapsulate diode with transparent material with high refractive index 3) Apply antireflection coating

Imperfections can be introduced into the materials during epitaxial growth if the lattice constants for the substrate and the epitaxial film differ. Since the density of lattice misfit dislocations is directly related to the compositional gradient, one technique which is frequently used in ternary alloys to reduce these dislocations is to slowly grade the composition from that at the substrate to that desired at the p-n junction. In this way, epitaxial layers with acceptably low dislocation densities can be grown routinely. Fig. 9 illustrates the dependence of dislocation density on compositional gradient for $GaAs_{1-x}P_x$ epitaxial layers deposited on $GaAs$ substrates.³⁰

Poor quality substrates also adversely affect the crystalline perfection, and hence the electroluminescence performance, of epitaxial layers. Even with "perfect" layers, however, imperfections may be introduced during the diffusion process used to form a p-n junction. A summary of the types of nonradiative recombination mechanisms and their typical causes is presented in Table IV.

Independent of the light generation processes at the p-n junction, the extraction of the emitted radiation from the semiconductor crystal is also a very major problem. Since the refractive index for a III-V semiconductor is typically about 3.5, the internal critical angle for light incident at the crystal-air boundary is only 16°, and a major fraction of the light (i.e., all rays striking the surface at angles exceeding 16°) suffer total internal reflection. The total optical path inside the diode therefore exceeds the diode dimension with the result that severe internal reabsorption of the emitted light occurs. A simple expression relating the external quantum efficiency, η_{ext} , and the internal quantum efficiency, η_{int} , is³¹

$$\eta_{ext} = \frac{\eta_{int}}{1 + (\alpha V / T_{av} A)} \quad (3)$$

Here, α is the average absorption coefficient in the diode, V is the diode volume, A is the area of the emitting surface and T_{av} is the average surface transmissivity.

To improve the external efficiency, a number of techniques can be used to decrease the absorption coefficient, α , or to increase the transmissivity of the surface, as listed in Table V. Dome shaping is effective,³² but also is the most expensive of these techniques, since it involves machining the semiconductor and uses a significant volume of material. Hemispherical domes and lenses cast from epoxy or acrylic-polyester resin (with a refractive index of about 1.5) simplify device construction, and are quite effective in increasing the external efficiency by a factor of typically 2 to 3, depending on the material.

The average internal absorption coefficient is appreciably higher in diodes which rely on the near-bandgap emission of direct-bandgap materials than in diodes from indirect-bandgap materials where the emission is much below the bandgap energy. Table VI illustrates these observations for epoxy-coated $GaAs$ diodes doped with Zn , which is a shallow acceptor ($E_a = 0.03$ eV), and

those doped with Si , in which the radiative processes involve a deeper center ($E_a = 0.1$ eV)³³. For the $GaAs:Zn$ diodes, α is about 10^3 cm⁻¹, while for $GaAs:Si$, it is only about 200 cm⁻¹,³⁴ and the external quantum efficiency is correspondingly higher. In both types of diodes, the internal quantum efficiency is about 50%. For the $GaP:Zn,O$ diodes, α is very small, but since the internal quantum efficiency is only 10 to 15%,^{26,35} the external quantum efficiency is still limited to a few percent.

Diode reliability

The quantum efficiency and brightness of LEDs may decrease without evidence of mechanical damage in the course of forward bias operation.³⁶ Several mechanisms are factors in such degradation: 1) increased surface leakage, 2) in-diffusion of contaminants such as Cu ,³⁷ and 3) formation of nonradiative recombination centers in the junction vicinity.^{38,39}

Surface leakage and contamination problems are the simplest to eliminate with proper passivation, encapsulation, and cleaning techniques. The formation of nonradiative centers, however, is a far more difficult problem, and the causes are still not well understood. It is known that the degradation rate depends on the current density, and that a high concentration of imperfections such as dislocations increases the degradation rate for a given current density.³⁸ It is therefore essential that the defect density in LEDs be as low as possible. Although data on LED reliability are somewhat limited, it has been established that properly fabricated diodes of GaP , $GaAs_{1-x}P_x$, and $Al_xGa_{1-x}As$ can be operated for many thousands of hours at moderate current densities (a few tens of A/cm²). In fact, accelerated life tests on GaP ⁴⁰ indicate extrapolated half-lives of many years. Clearly a long operating life is one of the features of LEDs, as compared to miniature incandescent sources. It is also clear, however, that careful life tests should be included in

Table VI—Internal and external quantum efficiency of selected LEDs.

Material	Emission wavelength (Å)	$E_g - h\nu$ (eV)	Band structure	η_{int} (%)	Abs. Coef.* (cm ⁻¹)	η_{ext} ** (%)
$GaAs:Zn$	9000	0.03	Direct	50 to 60	1000	0.5 to 2
$GaAs:Si$	9500	0.12	Direct	50 to 60	200	10 to 30
$GaP:Zn,O$	6950	0.48	Indirect	10 to 15	2 to 10	3 to 7

*Absorption coefficient of the most absorbing portion of the diode.
**Efficiencies for encapsulated diodes.

Table VII—State-of-the-art performance of p-n junction LEDs.

Material	Commercially available?	Color	Peak wavelength (Å)	Lum. eff. (lumens/watt)	η_{ext} (%)	BJJ^{**} (fL/A-cm ²)	Ref.
GaP:Zn,O	Yes	red	6900	20 ^a	3 to 7 ^b	350 ^c	41
Al _{0.3} Ga _{0.7} As	No	red	6750	16	1.3	140	50
GaAs _{0.9} P _{0.1}	Yes	red	6600	42	0.5	145	44
GaAs:Si with YOC:Yb,Er	No	red	6600	30 ^a	1.0 ^d	18 ^e	53
In _{0.42} Ga _{0.58} P	No	amber	6170	284	0.1	310 ^f	48
GaAs _{0.5} P _{0.5}	Yes	amber	6100	342	0.013	35	45
GaAs _{0.25} P _{0.75}	No	amber	6100	342	0.04	40 to 100 ^g	45
SiC	Yes	yellow	5900	515	0.003	10	58
In _{0.4} Ga _{0.6} P	No	yellow-green	5700	648	0.02	115	46
GaP:N	Yes	green	5500	677	0.05 to 0.6 ^b	470 ^b	15
GaAs:Si with YF ₃ :Yb,Er	No	green	5500	660 ^a	0.1 ^d	23 ^e	53
GaAs:Si with YF ₃ :Yb,Tm	No	blue	4700	60 ^a	0.01 ^d	0.2 ^e	53

Notes

- *Except where noted, efficiencies for diodes with plastic encapsulants.
- **Except where noted, BJJ calculated from Eq. 2 using efficiency for unencapsulated diode with $(A_p/A_s)=1$. Diode efficiencies assumed to be 2.5 times less without encapsulation.
- ^aMean value for non-monochromatic emission spectrum.
- ^bRange between commercially practical and best laboratory results.
- ^cAssumed 3% unencapsulated diode efficiency; (A_p/A_s) assumed to be $1/3$ to compensate for significant edge emission.
- ^dEfficiency at $J=300$ A/cm². Efficiency drops off by at least the square of the current at lower current densities.
- ^e $(A_p/A_s)=0.016$ for these dome-shaped phosphor-coated structures.
- ^f BJJ calculated from measured efficiency value of 5.9×10^{-4} for unencapsulated diode.
- ^gTypical values of BJJ reported as 40 to 60 fL/A-cm² in Ref. 45. Value of 100 fL/A-cm² calculated from Eq. 1 using efficiency value found in Ref. 45.^b
- ^hCalculated for representative DC efficiency of 0.1% for unencapsulated diode. (A_p/A_s) assumed to be $1/3$.

the evaluation of new materials and alloys, where high defect densities are likely, before reaching a conclusion on the utility of such materials.

State-of-the-art

Because of the wide variety of structures used for LEDs, and the importance of internal absorption and surface reflectivity, the external efficiency for identical material can vary greatly from diode to diode, depending in many cases on the ingenuity of the investigator in fabricating the device. We attempt in this section to summarize the state-of-the-art for a variety of electroluminescent materials by comparing their reported efficiency and brightness values. The reader must keep in mind, however, the limitation of such numbers, particularly since reproducibility does not enter this picture, yet determines in most cases the economic significance of a particular result. The most important parameters in our comparison are summarized in Table VII. A description of the advantages and disadvantages of each of the electroluminescent materials is described briefly below.

GaP

The most efficient GaP LEDs are presently prepared by liquid-phase epitaxy. Red-emitting diodes of GaP are commercially available with external quantum efficiencies as high as 3%,

but large-volume production on the scale used for GaAs_{1-x}P_x diodes has not yet been attempted. Laboratory efficiency values as high as 7% have been reported.⁴¹ However, these diodes were prepared with low-Zn-doping concentrations, which enhance the external efficiency by reducing the internal absorption coefficient, but lead to an efficiency saturation at current densities as low as 1 A/cm². By comparison, GaP LEDs with 3% efficiency values saturate at current densities of about 10 A/cm². The brightness value of 350 fL/A-cm² entered in Table VII was obtained by multiplying Eq. 2 by the ratio of the primary surface area to the total (primary surface + edge) area, since a large portion of the red emission escapes from the edges of GaP diodes. This brightness value appears to be more than adequate for standard display applications. At the moment, it does not appear likely that significant efficiency increases will be made for the GaP red emission, but we can expect refinements in the manufacturing technology which will reduce the cost of these devices.

Because of the small internal absorption in Zn-O-doped GaP, the fabrication of monolithic displays requires a different approach than that used for GaAs_{1-x}P_x. Using a combination of etching and masking, monolithic GaP displays have been made.⁴² However, in view of the cost of the GaP wafer

needed for a large monolithic display, it is not clear whether these will be economically more attractive than individual segment displays.

Green-emitting diodes of GaP are still in an early developmental stage. The efficiency of routinely fabricated diodes is below 0.1%, while the best laboratory results have reached 0.6% when small, high-quality platelets were used as the substrate material.¹⁵

With large-area GaP substrates prepared by liquid-encapsulated crystal pulling, the best efficiency is lower (0.3%),¹⁵ probably because of the higher defect density in these diodes. Since the limits of the GaP:N system have not yet been fully explored, higher performance can be expected in the future. It is already clear, however, that the technology is substantially more difficult for reproducibly fabricating high-efficiency GaP green-emitting diodes than red-emitting ones.

It is also possible to obtain orange- or yellow-appearing emission from GaP diodes by introducing N and O into the n- and p-sides of the junction, respectively. Since green emission arises predominantly from the n-side, and red emission from the p-side of the junction, one and the same diode can simultaneously emit both colors, whose integration by the eye gives an orange or yellow appearance to the device. Because of the saturation of the red emission at relatively low current densities, the hue of such diodes shifts toward green with increasing current.⁴³ Although potentially attractive, further research is required before such devices can become practical.

GaAs_{1-x}P_x

For maximum brightness in GaAs_{1-x}P_x LEDs, the alloy composition is selected to provide emission at about 1.88 eV or 6600 Å. At this wavelength, external quantum efficiencies as high as 0.5% (encapsulated) have been obtained,⁴⁴ although values on the order of 0.2% are more typical and are commercially available. An efficiency of 0.5% for an encapsulated diode corresponds to about 0.2% for an unencapsulated one, which yields a calculated brightness value of about 150 fL/A-cm² for the red GaAs_{0.6}P_{0.4} emission. By increasing the GaP content, electroluminescence can be attained at shorter wavelengths, thereby providing orange emission, but at reduced efficiency and brightness values (see Fig. 6). Discrete amber-colored GaAs_{0.3}P_{0.5} LEDs are available commercially with bright-

ness values of about 10 fL/A-cm² for emission at 6100 Å. Because the recombination processes are approximately band-to-band, impurity saturation is not a problem in $GaAs_{1-x}P_x$, and intense light pulses can be generated under high-current excitation.

With SiO_2 masking and Zn diffusion, $GaAs_{0.6}P_{0.4}$ monolithic arrays can be fabricated into alphanumeric displays. Reasonably good resolution of individual segments is obtained in such displays due to the confinement of the generated light by the severe optical absorption which occurs in direct-bandgap semiconductors. Individual display figures are typically about 6-mm tall; however, a line of $GaAs_{1-x}P_x$ displays with 1.5-cm figures has now been introduced.

Recently, electroluminescent junctions of $GaAs_{1-x}P_x$ have been prepared with nitrogen doping on the n-side of the junction.¹⁵ For $GaAs_{1-x}P_x$ with $x \geq 0.4$, efficiencies have been significantly enhanced, presumably due to an excitonic recombination process similar to that which occurs in green-light-emitting GaP . Brightness values of 40 to 60 fL/A-cm² have been reported for yellow emission with the $GaAs_{1-x}P_x:N$, which are not too much lower than values for the commercially-available red $GaAs_{1-x}P_x$ LEDs, and which represent a significant advancement over the performance of presently-available $GaAs_{1-x}P_x$ amber LEDs.

Future trends in $GaAs_{1-x}P_x$ are expected to lie primarily in the area of more sophisticated and more economical monolithic displays, which are beginning to gain widespread acceptance.

$In_{1-x}Ga_xP$

Clearly, the electroluminescence potential of $In_{1-x}Ga_xP$ is very high (see Fig. 6). Only the difficulty in material preparation has thus far prevented its full-scale exploration and exploitation for electroluminescence applications. To date, most $In_{1-x}Ga_xP$ has been prepared either by variations of the Bridgeman technique for growth from a melt, or via liquid-phase epitaxy from a saturated metal solution.

Electroluminescent junctions in $In_{1-x}Ga_xP$ prepared by both growth techniques have been formed by Zn diffusion. From liquid-phase-epitaxy material deposited on $GaAs$ substrates, a room-temperature efficiency of 0.02% (encapsulated) was obtained¹⁶ for yellow-green emission at 2.17 eV (5700 Å). From polycrystalline melt-

grown material, an efficiency of 0.04% (unencapsulated) was reported¹⁷ at 2.06 eV (6020 Å) for orange emission, which yields a calculated brightness value of 320 fL/A-cm². However, the polycrystalline nature of the material prepared to date, as well as the difficulty in preparing single-crystal ingots is a severe limitation of the melt-grown $In_{1-x}Ga_xP$.

Recently, vapor-grown p-n junctions of $In_{1-x}Ga_xP$ have been prepared¹⁸ which yield external quantum efficiencies in excess of 0.1% (encapsulated) for emission between 1.86 and 2.01 eV. For the red-orange emission at 2.01 eV a brightness value of 315 fL/A-cm² has been attained. The fact that the vapor-growth of these $In_{1-x}Ga_xP$ junctions is very similar to that used routinely for the commercial preparation of $GaAs_{1-x}P_x$ LEDs is particularly attractive. At present, the electroluminescence in the vapor-grown diodes is thought to be limited by dislocations which arise at least in part by the large lattice mismatch between the epitaxy and the substrate. As epitaxial growth techniques are developed to reduce the introduction of such dislocations, the performance of these diodes should improve.

$Al_xGa_{1-x}As$

The highest brightness diodes of $Al_xGa_{1-x}As$ have been fabricated from alloys with $x \approx 0.3$ for emission at 6750 Å. With diodes having both the n-type and p-type regions grown by liquid-phase epitaxy,⁴⁹ efficiency values as high as 1.3% (encapsulated) have been obtained at this wavelength,⁵⁰ yielding a brightness value of about 140 fL/A-cm². The fact that such a brightness value is well above that predicted²⁴ in Fig. 6b is attributed to a reduced defect concentration in $Al_xGa_{1-x}As$ due to the excellent substrate-epitaxy lattice match. Using a single epitaxial layer with a planar Zn diffusion process to define the emitting area, efficiency values of 0.25% have been attained at 6750 Å.⁵⁰ The diffusion process is suitable for the convenient fabrication of red-emitting diode arrays, but such devices are not yet commercially available.

$Al_xGa_{1-x}As$ is also receiving increasing interest for diodes emitting at about 8000 Å, the wavelength needed to pump $Nd:YAG$ laser rods. The substitution of the present short-lived lamps used to pump these lasers with efficient (12%)⁵¹ long-lived diodes will represent a significant advance in the utility

of $Nd:YAG$ lasers. This application requires, however, that the diodes be operated at current densities on the order of several hundred amperes/cm² to increase their power output.

GaN

Gallium nitride is a relatively unexplored semiconductor with a direct energy bandgap of 3.5 eV. In 1969, single-crystal layers of GaN were prepared²⁸ by epitaxial deposition on sapphire substrates. To date, low-conductivity GaN is obtainable only for n-type material; attempts to dope GaN p-type (e.g., with Zn) have thus far resulted in the formation of high-resistivity material. Electroluminescence has been obtained³² from the Zn-doped insulating GaN by the application of an electric field between two point contacts. From such preliminary devices, green and blue emission have been observed at 2.4 eV (5200 Å) and 2.8 eV (4400 Å), respectively. More recently, avalanche breakdown at intentional i-n transitions has also produced green and blue luminescence.³² Room-temperature external quantum efficiencies as high as 1% have been observed for the green emission, but power efficiencies are much lower (0.01% for the green, and 0.005% for the blue) due to the large voltage drop across the high-resistivity GaN . Values of BJJ as high as 4000 fL/A-cm² are calculated for the green GaN electroluminescence, however, brightness normalized with respect to current density is not a good figure of merit for these devices due to their large voltage drop and low power conversion efficiency. If low-resistivity p-type GaN can be achieved with further research, this material could become a single source of efficient light emission across the entire visible spectrum. The possibility also exists, however, that GaN is limited to n-type or compensated high-resistivity material by a vacancy formation mechanism of the type which has prevented p-n junction formation in most III-VI compounds.

Upconversion phosphors

Because of the strong dependence of the phosphor conversion efficiency on the infrared diode excitation, best performance is achieved at high current densities. For example, with a 10% efficient $GaAs:Si$ electroluminescent diode operated at 300 A/cm², efficiencies of about 1%, 0.1%, and 0.01% are obtained for the red, green, and blue upconversion phosphors listed in Table VII.⁵³ However at a current density of

10 A/cm² the efficiencies are much lower. Note that the blue emission is still somewhat unique in that only a few semiconductors (namely GaN and SiC) have energy gaps sufficiently large to generate this color directly.

Other materials

There has been a great deal of discussion over the years concerning SiC diodes which are capable in principle of yielding luminescence throughout the visible spectrum. Unfortunately, the technology involves very high temperature processing ($\approx 2000^\circ\text{C}$), and the results to date have not been attractive enough to justify extensive development aimed at commercial products, particularly in view of the rapid progress made in the GaP and GaAs_{1-x}P_x technologies.

With regard to In_{1-x}Al_xP, cathodoluminescence measurements⁵⁴ on melt-grown material suggest a high-brightness potential for this alloy system; however, no report of electroluminescent diodes has been made. In view of the difficulty in synthesizing this compound, progress will most likely be slow.

The use of Al_xGa_{1-x}P alloys also has been considered to produce diodes which emit at higher photon energies than GaP. However, since the band-gap energy of AlP is only 2.4 eV, the available bandgap range for device applications is limited. The only Al_xGa_{1-x}P diodes reported to date⁵⁹ had a quantum efficiency of about 10⁻⁵ at a wavelength of $\sim 5500 \text{ \AA}$.

Conclusions

The past decade has seen a dramatic improvement in the efficiency and reliability of visible-light-emitting diodes. Due to a mastery of the major problems limiting the performance of these devices, large-scale manufacturing of diodes suitable for a variety of applications has become possible. LEDs should increasingly replace other types of small display elements in the coming years as costs further decrease. In addition, LEDs will be used in areas where other types of light-emitting elements are impractical because of excessive power dissipation, bulkiness, or inadequate life. At this time, GaAs_{1-x}P_x diodes, which emit red light, are the most widely used. Newer materials such as GaP for green emission, InGa_{1-x}P_x for amber, and GaN for blue are being developed, and will become increasingly important as the materials problems limiting their reproducibility are overcome.

References

1. Casey, H. C., and Trumbore, F. A., "Single Crystal Electroluminescent Materials," *Materials Science and*

Engineering, vol. 6 (1970) pp. 69-109.

2. Archer, R. J., "Materials for Light Emitting Diodes," *J. Electr. Materials*, no. 1 (1972) pp. 128-154.

3. Landsberg, P. T., "Radiative Decay in Compound Semiconductors," *Solid-State Electronics*, vol. 10 (June 1967) pp. 513-537.

4. Dean, P. J., "Recombination Processes Associated with Deep States in Gallium Phosphide," *Journal of Luminescence*, vol. 1, 2 (1970) pp. 398-419.

5. Dean, P. J., "Junction Electroluminescence," in Wolfe, R., and Kreissman, C. J. (eds.), *Applied Solid-State Science* (Academic Press; N.Y.; vol. 1; 1969) pp. 1-151.

6. Lorenz, M. R., "The Generation of Visible Light from p-n Junctions in Semiconductors," *Trans. Met. Soc. AIME*, vol. 245 (March 1969) pp. 539-549.

7. Pankove, J. I., *Optical Processes in Semiconductors* (Prentice-Hall Inc.; Englewood Cliffs, N.J.; 1971).

8. Sze, S. M., *Physics of Semiconductor Devices* (Wiley-Interscience; New York; 1969).

9. Grimmeiss, H. G., and Scholz, H., "Efficiency of Recombination Radiation in GaP," *Physics Letters*, vol. 8 (Feb 1964) pp. 233-235.

10. Varshni, Y. P., "Band-to-band Radiative Recombination in Groups IV, VI, and III-V Semiconductors (I)," *Phys. Stat. Sol.*, vol. 19 (Feb 1967) pp. 459-514.

11. Cusano, D. A., "Radiative Recombination from GaAs Directly Excited by Electron Beams," *Solid State Communications*, vol. 2 (Nov 1964) pp. 353-358.

12. Dean, P. J., Gershenzon, M., and Kaminsky, G., "Green Electroluminescence from Gallium Phosphide Diodes near Room Temperature," *J. Appl. Phys.*, vol. 38 (Dec. 1967) pp. 5332-5342.

13. Starkiewicz, J., and Allen, J. W., "Injection Electroluminescence at p-n Junctions in Zinc-doped Gallium Phosphide," *J. Phys. Chem. Solids*, vol. 23 (Nov. 1961) pp. 881-884.

14. Lorenz, M. R., and Pilkuhn, M., "Preparation and Properties of Solution-Grown Epitaxial p-n Junctions in GaP," *J. Appl. Phys.*, vol. 37 (Oct 1966) pp. 4094-4102.

15. Logan, R. A., White, H. G., and Wiegman, W., "Efficient Green Electroluminescent Junctions in GaP," *Solid-State Electronics*, vol. 14 (Jan. 1971) pp. 55-70.

16. Cuthbert, J. O., Henry, C. H., and Dean, P. J., "Temperature-Dependent Radiative Recombination Mechanisms in GaPt(Zn,O) and GaPtCd(O)," *Phys. Rev.*, vol. 170 (June 1968) pp. 739-748.

17. Morgan, T. N., Walker, B., and Bhargava, R. N., "Optical Properties of Cd-O and Zn-O Complexes in GaP," *Phys. Rev.*, vol. 166 (Feb. 15, 1968) pp. 751-753.

18. Auzel, F., "Compteur Quantique par Transfert d'Énergie entre deux Ions de Terres Rares dans un Tungstate Mixte et dans un Verre," *Compt. Rend.*, vol. 262 (1966) p. 1016.

19. Galiginatis, S. V., and Fenner, G. E., "A Visible Light Source Utilizing a GaAs Electroluminescent Diode and a Stepwise Excitable Phosphor," *Proc. 2nd Internat. Conf. on Gallium Arsenide* (Dallas, Texas, October 1968). Inst. of Phys. and Phys. Soc. Conf. Ser. 7, p. 131.

20. Wittke, J. P., Yocom, P. N., and Ladany, I., "Y₂O₃:Yb-Er—A New Red-emitting, Infrared-excited Phosphor," *J. Appl. Phys.*, to be published.

21. Kressel, H., Hawrylo, F. Z., and Almeleh, N., "Properties of Efficient Silicon-Compensated Al_xGa_{1-x}P_x Electroluminescent Diodes," *J. Appl. Phys.*, vol. 40 (April 1969) pp. 2248-2253.

22. Maruska, H. P., and Pankove, J. I., "Efficiency of GaAs_{1-x}P_x Electroluminescent Diodes," *Solid-State Electronics*, vol. 10 (Sep. 1967) pp. 917-925.

23. Onton, A., Lorenz, M. R., and Reuter, W., "Electronic Structure and Luminescence Processes in In_{1-x}Ga_xP Alloys," *J. Appl. Phys.*, vol. 42, (Aug. 1971) pp. 3420-3432.

24. Archer, R. J., "Light-Emitting Diodes in III-V Alloys," *Electrochem. Soc. Meeting*, Los Angeles, Calif., Spring 1970, paper 66; see also Ref. 2.

25. Nelson, H., "Epitaxial Growth from the Liquid State and Its Application to the Fabrication of Tunnel and Laser Diodes," *RC 4 Review*, vol. 24 (Dec. 1963) pp. 603-615.

26. Ladany, I., "Gallium Phosphide Double-Epitaxial Diodes," *J. Electrochem. Soc.*, vol. 116 (July 1969) pp. 993-996.

27. Tietjen, J. J., and Amick, J. A., "The Preparation and Properties of Vapor-Deposited Epitaxial GaAs_{1-x}P_x," *J. Electrochem. Soc.*, vol. 113, (July 1966) pp. 724-729.

28. Maruska, H. P., and Tietjen, J. J., "The Preparation and Properties of Vapor-Deposited Single-Crystalline GaN," *Appl. Phys. Letters*, vol. 15 (Nov. 1969) pp. 327-329.

29. Nuese, C. J., Richman, D., and Clough, R. B., "The Preparation and Properties of Vapor-Grown In_{1-x}Ga_xP," *Metallurgical Trans.*, vol. 2, (March 1971) pp. 789-794.

30. Abrahams, M. S., Weisberg, J. R., Buiochi, C. J., and Blanc, J., "Dislocation Morphology in Graded Heterojunctions: GaAs_{1-x}P_x," *J. Materials Science*, vol. 4 (March 1969) pp. 223-235.

31. Stern, F., "Transmission of Isotropic Radiation Across an Interface Between Two Dielectrics," *Appl. Optics*, vol. 3 (Jan. 1964) pp. 111-113.

32. Carr, W. N., and Pittman, G. E., "One Watt GaAs p-n Junction Infrared Source," *Appl. Phys. Letters*, vol.

3 (Nov. 15, 1963) pp. 173-175.

33. Kressel, H., Dunse, J. U., Nelson, H., and Hawrylo, F. Z., "Luminescence in Silicon-Doped GaAs Grown by Liquid-Phase Epitaxy," *J. Appl. Phys.*, vol. 39 (March 1968) pp. 2006-2011.

34. Ladany, I., *unpublished data*.

35. Dishman, J. M., DiDomenico, M., Jr., and Caruso, R., "Luminescence and Minority Carrier Recombination in p-Type GaP(Zn,O)," *Phys. Rev.*, vol. 2 (Sep. 15, 1970) pp. 1988-2009.

36. Lanza, C., Konnerth, K. L., and Kelly, C. E., "Aging Effects in GaAs Electroluminescent Diodes," *Solid-State Electronics*, vol. 10 (Jan. 1967) pp. 21-31.

37. Bergh, A. A., "Bulk Degradation of GaP Red LEDs," *IEEE Trans. Electron Devices*, vol. ED-18 (March 1971) pp. 166-170.

38. Kressel, H., Byer, N. F., Lockwood, H., Hawrylo, F. Z., Nelson, H., Abrahams, M. S., and McFarlane, S. H., "Evidence for the Role of Certain Metallurgical Flaws in Accelerating Electroluminescent Diode Degradation," *Met. Trans.*, vol. 1 (March 1970) pp. 635-638.

39. Schade, H., Nuese, C. J., and Gannon, J. J., "Direct Evidence for the Generation of Defect Centers During Forward-Bias Degradation of GaAs_{1-x}P_x Electroluminescent Diodes," *J. Appl. Phys.*, vol. 42, (Nov. 1971) pp. 5102-5108.

40. Hartman, R. L., Schwartz, B., and Kuhn, M., "Degradation and Passivation of GaP Light-Emitting Diodes," *Appl. Phys. Letters*, vol. 18, (April 1971) pp. 304-307.

41. Saul, R. H., Armstrong, J., and Hackett, W. H. Jr., "GaP Red Electroluminescent Diodes with an External Quantum Efficiency of 7%," *Appl. Phys. Letters*, vol. 15 (Oct. 1, 1969) p. 229.

42. Kasami, A., Naito, M., and Toyama, M., "GaP Monolithic Display with Low Drive Power," *IEEE International Electron Devices Meeting*, Washington, D.C. (Oct. 1971) paper 10.5.

43. Rosenzweig, W., Logan, R. A., and Wiegman, W., "Variable Hue GaP Diodes," *Solid-State Electron.*, vol. 14 (Oct. 1971) pp. 655-660.

44. Lawley, K., Monsanto Co., Cupertino, California, *personal communication*.

45. Groves, W. O., Herzog, A. H., and Craford, M. G., "The Effect of Nitrogen Doping on GaAs_{1-x}P_x Electroluminescent Diodes," *Appl. Phys. Letters*, vol. 19 (Sep. 1971) pp. 184-186.

46. Hakkli, B. W., "Electroluminescent Properties of InGaP Grown by IPE on GaAs," *Electrochem. Soc. Meeting*, Los Angeles, Calif. (Spring 1970) paper 74.

47. Onton, A., and Lorenz, M. R., "Electroluminescence in Indium Gallium Phosphide," *Proc. Third Intl. Symp. on Gallium Arsenide and Related Compounds*, Inst. of Physics (1970) pp. 222-230.

48. Nuese, C. J., Sigai, A. G., and Gannon, J. J., "Orange Laser Emission and Bright Electroluminescence from In_{1-x}Ga_xP Vapor-grown p-n Junctions," *to be published*.

49. Rupprecht, H., Woodall, J. M., and Pettit, G. D., "Efficient Visible Electroluminescence at 300°K from Ga_{1-x}Al_xAs p-n Junctions Grown by Liquid-Phase Epitaxy," *Appl. Phys. Letters*, vol. 11 (Aug. 1967) pp. 81-83.

50. Blum, J. M., and Shih, K. K., "The LPF of Al_xGa_{1-x}As for Monolithic Planar Structures," *Proc. IEEE*, vol. 59 (Oct. 1971) pp. 1498-1502.

51. Dierschke, E. G., Stone, I. E., and Haisty, R. W., "Efficient Electroluminescence from Zinc-Diffused Ga_{1-x}Al_xAs Diodes at 25°C," *Appl. Phys. Letters*, vol. 19 (Aug. 15, 1971) pp. 98-100.

52. Pankove, J. I., Miller, F. A., and Berkeyheiser, J. E., "GaN Electroluminescent Diodes," *Intl. Electron Devices Meeting*, Washington, D.C. (Oct. 1971) paper 10.1; see also Pankove, J. I., Miller, E. A., Richman, D., and Berkeyheiser, J. E., "Electroluminescence in GaN," *J. Luminescence*, vol. 4 (July 1971) pp. 63-66.

53. Geusic, J. E., Ostermayer, F. W., Marcos, H. M., Van Uitert, L. G., and Van der Ziel, J. P., "Efficiency of Red, Green, and Blue Infrared-to-Visible Conversion Sources," *J. Appl. Phys.*, vol. 42, (April 1971) pp. 1958-1960.

54. Lorenz, M. R., and Onton, A., "Electronic Structure of III-V Alloys from Luminescence Studies," *Proc. 10th Intl. Conf. on the Physics of Semiconductors*, Cambridge, Mass., 1970.

55. Thompson, A. G., Cardona, M., Shaklee, K. L., and Wooley, J. C., "Electroreflectance in the GaAs-GaP Alloys," *Physical Review*, vol. 146, (June 10, 1966) pp. 601-610.

56. Herzog, A. H., Groves, W. O., and Craford, M. G., "Electroluminescence of Diffused GaAs_{1-x}P_x Diodes with Low Donor Concentrations," *J. Appl. Phys.*, vol. 40, (March 15, 1969) pp. 1830-1838.

57. Kressel, H., Lockwood, H. F., and Nelson, H., "Low Threshold Al_xGa_{1-x}As Visible and IR Light Emitting Diode Lasers," *J. Quantum Electronics*, vol. QE-6 (June 1970) pp. 278-284.

58. Potter, R. M., Blank, J. M., and Addamiano, A., "Silicon Carbide Light-Emitting Diodes," *J. Appl. Phys.*, vol. 40 (April 1969) pp. 2253-2257.

59. Kressel, H., and Ladany, I., "Electroluminescence in Al_xGa_{1-x}P Diodes Prepared by Liquid-Phase Epitaxy," *J. Appl. Phys.*, vol. 39 (Oct 1968) pp. 5339-5340.

Operation and application of NUMITRON digital display devices

F. J. Feyder

Digital display devices having a brightness of 7000 foot-lamberts considerably broaden the application possibilities. The NUMITRON devices have this capability and, with their incandescent-type seven-segment construction, provide sharp, high-contrast, clutter-free displays in virtually any color with controllable high brightness. They operate at a nominal voltage of 4.5 V at 24 mA/segment and are compatible with integrated-circuit decoder/drivers.

NUMITRON DEVICES are presently available to display the numerals 0 through 9 with or without a decimal point; the numeral 1 preceded by either a plus or minus sign; and a plus or minus sign only. The DR2000-series devices have a character height of 0.6 inch and can be mounted on 0.8-inch centers; the smaller DR2100-series devices have a character height of 0.4 inch with mounting on 0.5-inch centers. The electrical characteristics of both series are the same. Fig. 1 shows the various types of RCA's NUMITRON display devices.

Electrical operation

NUMITRON digital display devices are designed for optimum operation at 4.5 V/segment, which results in a nominal segment current of 24 mA and an average power dissipation of 108 mW (see

Fig. 2). Any value of segment voltage between 3.5 and 5 V, however, gives satisfactory operation with due consideration for brightness and operating life (see Fig. 3). Fig. 4 shows the relative

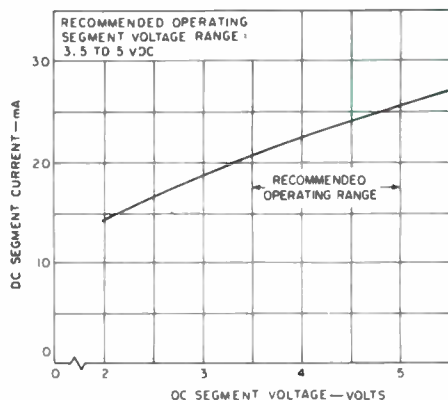
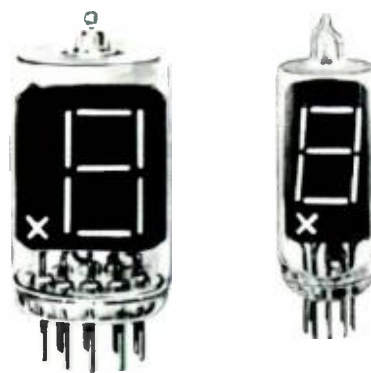


Fig. 2—Direct current through coil segment as a function of the segment voltage.

Frank J. Feyder, Ldr.
 Special Products Engineering
 Receiving Tube Engineering
 Entertainment Tube Division
 Electronic Components
 Somerville, New Jersey

received BSEE in 1955 from Newark College of Engineering. In 1947 he joined RCA Receiving Tube Engineering, Harrison, N. J., and served in various assignments while attending evening classes at Newark College of Engineering. In 1953 he transferred into the Test Engineering department where he was responsible for the Qualification Approval program on military tube types and prepared specifications on industrial and premium tube types. In 1958, Mr. Feyder became an Engineering Leader in Test Engineering where he was responsible for both electrical and environmental testing on Industrial, Military, and Premium tube types. From 1962 to 1967 he was an Engineering Leader in Industrial Tube Applications, Advanced Product Development, and Nuvistor Development. Since June 1967 Mr. Feyder has been in the Special Products Engineering and Services department with responsibility for the Measurement Standards Laboratory and application work on new products.



DR2000

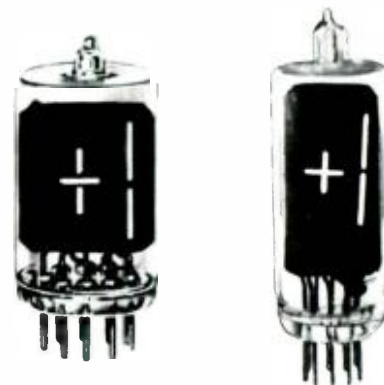
DR2100

0 through 9

DR2010

DR2110

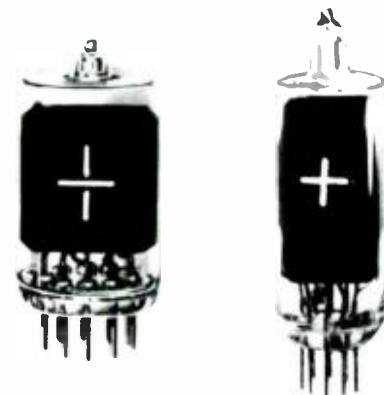
0 through 9
with decimal point



DR2020

DR2120

Plus-minus sign
and numeral 1



DR2030

DR2130

Plus-minus sign



Fig. 1—Several examples of RCA's NUMITRON digital display devices.

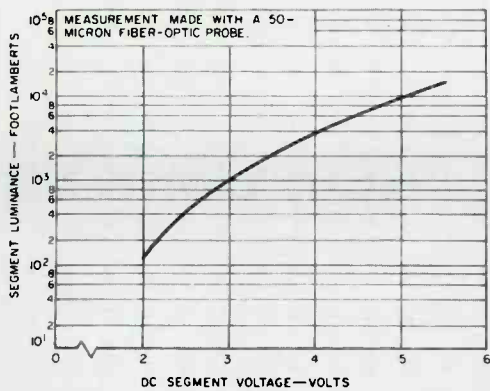


Fig. 3—Luminance of a coil segment as a function of the segment voltage.

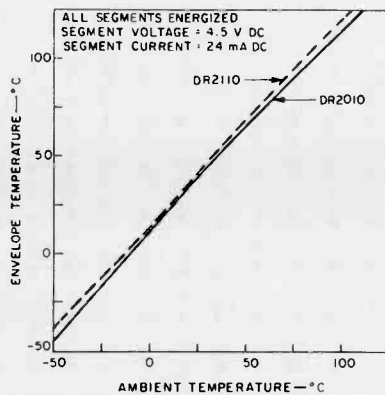


Fig. 5—Envelope temperature as a function of ambient temperature.

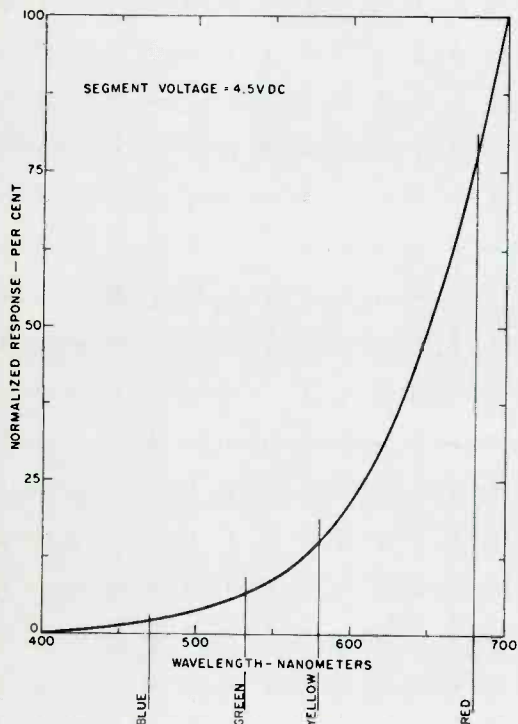


Fig. 4—Spectral intensity distribution within visual spectrum.

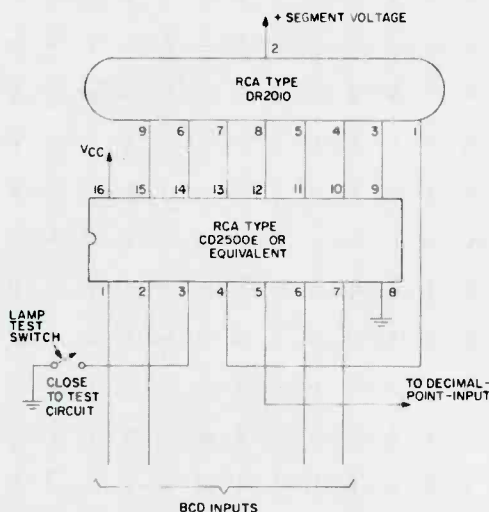
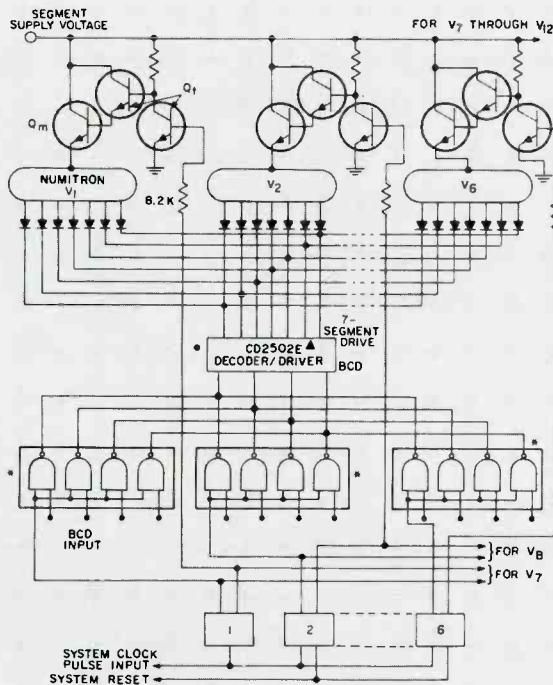


Fig. 6—Basic interconnection of a NUMITRON device with an integrated-circuit decoder/driver.



CD2302 or equivalent

▲ Selection of the CD2502E rates for operation at 12 volts.

● The CD2502E can drive up to six Numitrons. Eight Numitrons may be multiplexed provided that a suitable decoder/driver (rated for operation at 15 volts and 60 milliamperes) is used. Required decoder/driver ratings are determined from Fig. 9.

Fig. 7—Basic components required for multiplex operation of NUMITRON devices.

Display	BCD INPUT (8-4-2-1 CODE) TO DECODER DRIVER			
	D (TERM. 6)	C (TERM. 2)	B (TERM. 1)	A (TERM. 7)
0	0	0	0	0
1	0	0	0	1
2	0	0	1	0
3	0	0	1	1
4	0	1	0	0
5	0	1	0	1
6	0	1	1	0
7	0	1	1	1
8	1	0	0	0
9	1	0	0	1

Notes:

1. D, C, B, and A represent the BCD code 8-4-2-1, respectively, which are the four input to the decoder/driver required to illuminate the corresponding digit on the Numitron.

2. 0=low-level input, 1=high-level input.

Table 1—Decoder inputs required to form numerical characters on the DR2000 NUMITRON.

light-output intensity within the visible spectrum at nominal segment voltage. Because the coil segments have small mass and relatively low operating temperature, NUMITRON devices remain cool during operation. Fig. 5 shows that the bulb temperature is maintained at approximately 14 C above the ambient temperature.

Direct IC decoder/driver operation

The NUMITRON devices that provide the readout of numerals 0 through 9 are compatible with the RCA CD2500E series of integrated circuit decoder/drivers. In addition, other decoder/drivers such as the Fairchild 9317, Texas Instruments SN7447, and Motorola MC7447P can be used to operate the NUMITRON device. The integrated circuit decoder/driver accepts four-line input in binary code decimal (BCD) form (8-4-2-1 code) and decodes it into an output representing a decimal number from 0 through 9.

The RCA CD2500E has a decimal-point driver circuit, and Fig. 6 shows the basic interconnection to the NUMITRON device along with the lamp-test circuit. When pin 3 is grounded by closing the LAMP TEST SWITCH, all segments light up, including the decimal point. The decoder inputs required to form the numerical characters are shown in Table 1.

Multiplex operation

In the conventional direct-drive method of operation, a given number of NUMITRON devices requires an equal number of decoder/drivers for the simultaneous display of the numerical output data. However, one decoder/driver can be made to drive a number of NUMITRON devices sequentially by use of a time-multiplex system. If the multiplexing repetition rate is greater than 50 Hz, there is no noticeable flicker of the numerals being displayed.

One possible method of multiplex operation is shown in Fig. 7. One RCA CD2502E decoder/driver is used to drive up to a maximum of six DR2000 NUMITRON devices with a duty factor of 16.7%. When DR2010 NUMITRON devices are used, a separate drive circuit for the decimal points must be incorporated. The multiplex circuit incorporates a ring counter which, in sequence, controls the BCD data in the NAND gates and then the segment-voltage pulses, which pass through drive transistor Q_m to the common terminal of each NUMITRON device. In this way, the ring counter determines which device in the series will provide the proper numerical display at a given time. The illumination of the proper coil segment to form the desired numeral on each NUMITRON is still controlled by the decoder/driver in response to the BCD inputs. Isolation diodes are used in series with each coil segment of the NUMITRON to prevent simultaneous lighting of coil segments in adjacent devices.

As shown in Fig. 8, multiplex operation of the NUMITRON device is possible at pulse voltages significantly higher than the maximum recommended value of 5.0 V specified for DC operation, provided that the appropriate duty factor is observed. During this operation, however, care should be taken to ascertain that the breakdown voltage rating and the maximum output current rating of the decoder/driver will not be exceeded. Also, transistor Q_m should be carefully selected to ensure that it can handle the maximum current required. Fig. 9 shows the peak voltage (E_p) and current (I_p) of the NUMITRON device for various duty factors.

Brightness control

During operation with the decoder/driver, a 0.3 to 0.5-V drop occurs across the driver transistor in the inte-

grated circuit. Therefore, a DC supply of 5 V is required to obtain the desired segment voltage of 4.5 to 4.7 V. For fixed-brightness operation, the NUMITRON display device may be operated directly from the 5-V (V_{cc}) supply of the integrated circuit decoder/driver, providing the current capability is available.

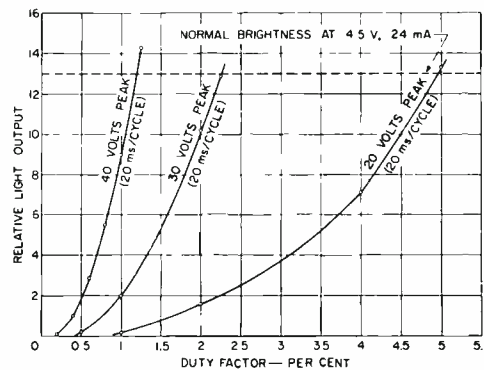
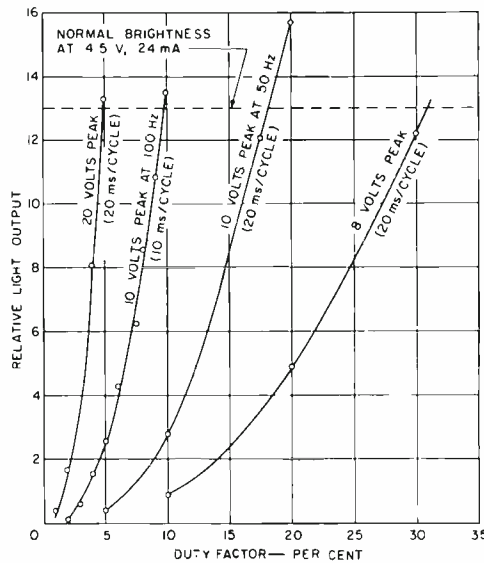


Fig. 8—Relative light output as a function of duty factor and pulse magnitude for multiplex operation.

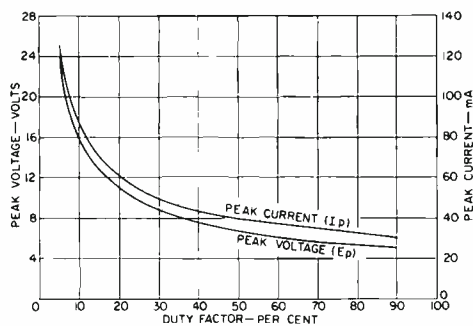


Fig. 9—Peak pulse voltage and current required to produce a NUMITRON device display of the same brightness as a DC segment voltage of 4.7 volts as a function of duty factor.

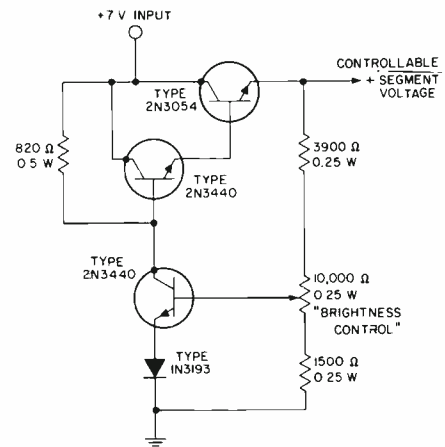


Fig. 10—Series regulator circuit for brightness control of NUMITRON devices.

If controllable brightness is desired, a separate power supply with a regulator circuit is recommended. Fig. 10 shows a schematic of a simple series voltage-regulator circuit that may be used to control the brightness. The circuit operates from a DC input of 7 V and provides a variable voltage output of approximately 2.5 to 5 V. With this variable voltage applied to the common coil-segment connection (pin 2) of the NUMITRON device, the brightness of the display can be varied by adjustment of the brightness-control potentiometer in the regulator circuit.

Ripple blanking

Zeros at both ends of a multi-digit display can be automatically blanked out to provide easier reading. For example, the number 0014.0250 is better displayed as 14.025. This suppression of the unwanted zeros is accomplished by grounding the RB_i terminal of the most significant digit of the whole number and the least significant digit of the fraction. Fig. 11 shows a ripple blanking circuit. In this circuit, the RB_o of the most significant digit of the whole number is connected to the RB_i of the next lower digit, and the RB_o of this latter digit is, in turn, connected to the RB_i of the following digit. On the fraction side, the RB_o of the least significant digit is connected to the RB_i of the next higher digit, and so on. In this manner, the ripple signal flow originates from the most significant digit of this whole number and the least significant digit for the fractional part.

Dimmer control

The ripple-blanking output terminal can also be used simultaneously as an intensity (dimming) control when the seg-

Table II—Mechanical specifications for NUMITRON devices.

Test	Conditions	DC segment voltage (V)	MIL-STD	Method
SHOCK				
a)	100g, 1 ms. half-sinewave	4.5	1311	1041
b)	50g, 11 ms. half-sinewave	Non-operating	MIL-F-1F 1311	4.3.3 1042A
VIBRATION				
a)	Variable frequency: 10 to 44 Hz, 0.1-inch DA, and 44 to 200 Hz, 10g	4.5		
b)	Variable frequency: 200 to 800 Hz, 1g	4.5		
c)	Variable frequency: 800 to 2000 Hz, 10g	4.5		
d)	Variable frequency: 10 to 50 to 10 Hz, 0.08-inch DA, 10g maximum	4.5	1311	1031A
e)	Fatigue: 25 Hz, 2.5g, 96 Hr	4.5	1311	1031A

ment supply voltage is fixed. The dimming is achieved by the variation of the pulse width of the signal at the intensity-control input as shown in Fig. 11.

Shock and vibration

The NUMITRON display devices utilize a rugged, well-supported, single-plane unit construction that, together with the relatively small mass of the coil segments, results in extremely rugged devices. The coil segments have a mechanical resonance in the frequency range of approximately 200 to 800 Hz. However, this effect can be overcome by the proper use of vibration isolators in the mounting of the equipment utilizing the NUMITRON.

Table II outlines the mechanical capability of the NUMITRON device, which will also meet the aeronautical specifications for operational and crash safety shock tests for instrument panel locations.

Applications

By far, the most common digital measuring instruments are the digital

counter/timer and the digital voltmeter. A brief discussion of each follows, which shows basically no change in the instruments except the decoder/driver and the NUMITRON devices. This information is widely applicable to other types of digital instruments.

Digital counter/timers

Digital electronic counter/timers are the most accurate and convenient instruments for measurements of frequency and time intervals. In counter operation, shown in Fig. 13, the main gate is opened for a precise period of time controlled by the time base oscillator and decode dividers. During the gating interval, the number of input cycles are totaled in the decade counter assembly and then displayed on the NUMITRON devices. The display timing control selects the sample rate, resets the counters, and operates the buffer/store which stores one count while the next count is being made by the decade dividers. The output (BCD 8-4-2-1 code) of the buffer/store controls the decoder/driver which, in turn, lights the

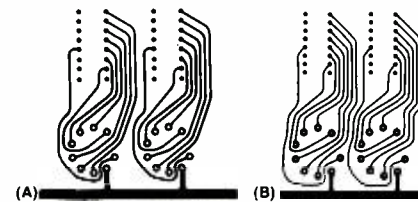


Fig. 12—Printed-circuit board layouts for two NUMITRON devices and associated CD2501E integrated-circuit decoder/driver: a) direct-mounting arrangement; b) with NUMITRONs mounted in a commercial socket. (Actual size, 0.8 inch centers).

proper segments of the NUMITRON.

Mounting

The DR2000 series NUMITRON devices fit into standard 9-pin miniature electron tube sockets. However, for printed-circuit-board applications, where horizontal mounting space is limited, a commercial socket (Methode Manufacturing No. PN-8610) is available which permits 0.8-inch center-to-center mounting. In addition, the base pins are solderable and may be mounted directly on the board.

Fig. 12 shows suggested printed-circuit board layouts for 0.8-inch centers on a single-sided board for direct mounting and for the commercial socket. The line width of the conductors is 0.025 inch while the width of the common bus for pin 2 is determined by the number of NUMITRON devices used. A 0.100-inch wide bus is adequate for five NUMITRON devices.

The DR2100 series NUMITRON display devices are manufactured in two electrically identical versions: the DR2100

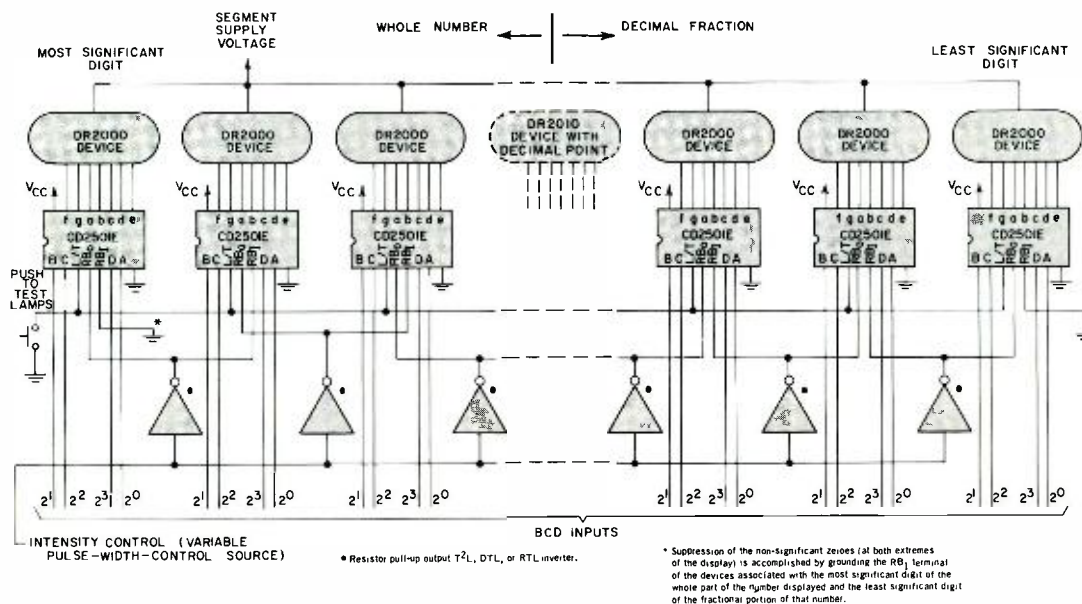


Fig. 11—Typical ripple-blanking and intensity-control application diagram using RCA CD2501E and NUMITRON devices DR2000 or DR2100.

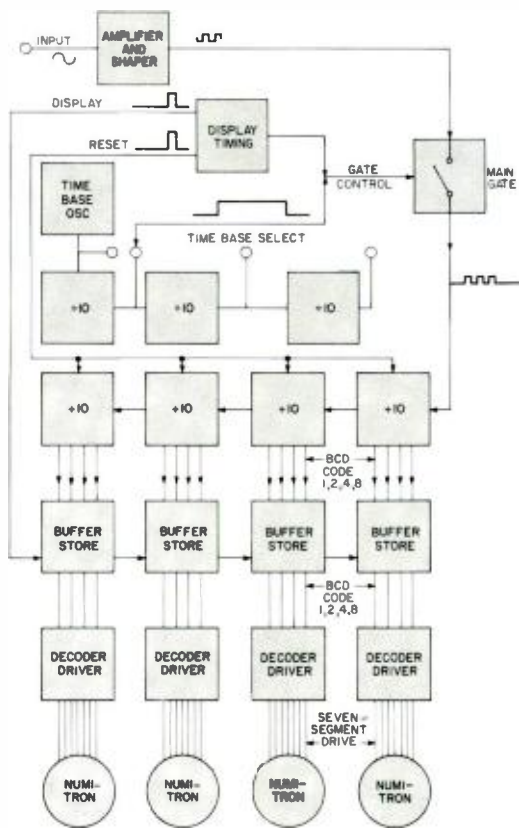


Fig. 14—Ramp type of digital voltmeter using NUMITRON devices to provide the visual readout.

series has straight solderable leads and the DR2100V1 series has formed solderable leads to facilitate direct printed-circuit-board mounting. The DR2100 uses a standard TO5-style 10-pin socket for mounting on 0.5-inch centers; while the DR2100V1 is mounted directly on the PC board, also on 0.5-inch centers. The PC board layout would be similar to Fig. 12, but with smaller center-to-center dimensions.

Reliability

Numerous life tests are presently operating with production devices to establish failure-rate information. The life tests are operating in several different modes to cover known applications. There are life tests operating on DC and AC at accelerated conditions, on-off cycling, square-wave pulse conditions, and multiplex operation. In addition, life tests are run on each production lot to assure continuing reliability of the product. The results to date are good and indicate the ability to exceed 100,000 hours operation at rated conditions.

Digital voltmeters

Several different methods can be used

to digitize the analog input signals; all of the methods, however, require digital readouts and counting similar to that of the single-ramp method shown in Fig. 14. In this method, the DC signal is compared to an accurate ramp. The width of the output signal from the comparator is proportional to the DC voltage being measured. This signal operates a gate that allows a number of oscillator cycles through the gate in direct proportion to the input voltage. With 1 V at the input, exactly 1000 cycles pass through the gate and are totaled on the counters. Similarly, an input of 0.500 V results in exactly 500 cycles or counts. The display timing circuit operates the buffer/store which causes the new reading to be displayed. The extra digit "1" (the overload digit), and the polarity indication are displayed on the DR2020 type NUMITRON which is controlled as shown in Fig. 14.

Decade counter section

Decade counter sections consist of a divide-by-10 counter, a buffer/store, a decoder/driver, and a NUMITRON. The BCD output of the decade counter changes continuously during the counting. These signals are applied to the buffer/store, which consists of four storage

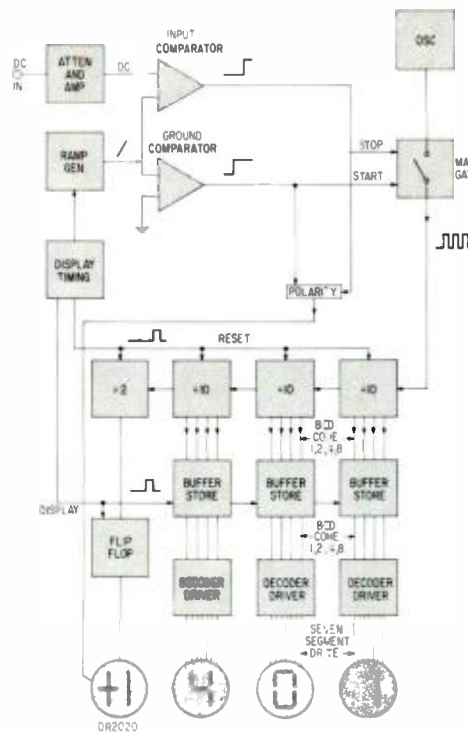


Fig. 13—Digital counter timer using NUMITRON devices to provide the visual readout.

flip-flops that store only the resultant total and ignore the intermediate changes. A change appears in the BCD output of the buffer/store only when the new final count differs from the preceding one. This BCD output is connected to the decoder/driver and sometimes to external terminals for interconnection with other digital equipment such as recorders. In the decoder/driver, the BCD input is converted into 7-line output that lights the appropriate segments of the NUMITRON.

Acknowledgements

The author wishes to thank Mr. Raymond Robertson and Mr. A. M. Liebman of Receiving Tube Engineering and Mr. J. Lee of Digital Circuit Engineering, Solid State Division for their invaluable help in supplying the data for curves and circuit development.

References

1. RCA Electronic Components, *Digital Display Devices*, Bulletin dated April, 1970.
2. RCA Electronic Components, *Digital Display Devices*, Application Note AN-4277.
3. RCA Solid State Division, *BCD to 7-Segment Decoder/Drivers*, Bulletin dated November, 1969.
4. Luxenberg, H. R., and Kuehn, R. L., (editors), *Display Systems Engineering* (McGraw-Hill Book Company)
5. RCA Solid State Division, *Digital Integrated Circuits*, Application Note IC AN-6294.

Design and construction of NUMITRON digital display devices

R. D. Reichert

The NUMITRON is a low-cost low-voltage digital display device with good brightness, contrast, and reliability. The market features and applications of this device have been described in other articles in this issue; this paper describes the design features and methods of fabrication. Implications for future devices of this type are also discussed.

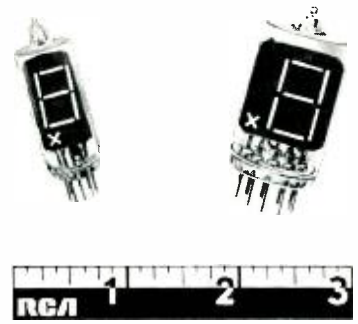


Fig. 1—NUMITRON digital display devices.

Robert D. Reichert, Mgr., Receiving Tube Design and Applications Engineering, Entertainment Tube Division, Electronic Components, Somerville, New Jersey, received the BSEE from the Polytechnic Institute of Brooklyn in 1951 and the MS in Industrial Engineering from Stevens Institute of Technology in 1956. Mr. Reichert joined RCA in 1951 and after completing the Specialized Training Program was assigned to the Receiving Tube Design Department of the Electron Tube Division. In this capacity he was responsible for the design and development of a variety of receiving tubes ranging from small-signal IF amplifiers to high voltage rectifiers and shunt regulators. In addition to having published a paper on Receiving Tube Design, Mr. Reichert holds several patents including those for the basic designs of the 3A3 and 6BK4 tubes. In 1955 he transferred to the Eastern District Field Office where he served as a Field Engineer and later as a Sales Engineer to one of RCA's largest customers. In 1959 he became Administrator of Market Planning for small power tubes after which he returned to Receiving Tube Design as an Engineering Leader. In 1967 he became Manager of the Receiving Tube Design Department and recently assumed the responsibility of Manager, Receiving Tube Design and Applications Engineering.



WE ARE CONSTANTLY FINDING new and additional needs for the retrieval of digital information. If one were to list the number of times that we interface with numerical information in the course of a day, the length of the list would be astounding. Realizing the rapidly increasing need for numeric information and the desire to display this data, Electronic Components, in 1968, undertook a program to design and develop a digital display device. A study was first made of the advantages and disadvantages of display devices then available, with the idea that a new device should include as many desirable features as possible. In addition, the desired characteristics for a new display device were formulated. With this information as a starting point, the concept of the NUMITRON seven-segment incandescent digital display device evolved.

Display device requirements

A list of basic requirements for any character-display device is presented below along with the features of the NUMITRON digital display device:

Operating voltage—The operating voltage should be compatible with semiconductor drive circuitry. The rated drive voltage of the NUMITRON display device is 4.5 volts for each segment.

Operating power—Having established an operating voltage and desiring as low an operating power as practical, the challenge becomes one of designing a device with as low an operating current as possible while maintaining other desirable features such as brightness and long life. The NUMITRON uses filamentary incandescent segments that consist of a single helical coil of very fine tungsten wire wound at very high TPI (turns per inch). The individual coils draw 24 mA at 4.5 V. The input power is therefore 108 mW/segment or approximately $\frac{3}{4}$ W/digit.

Reprint RE-17-6-4

Final manuscript received January 31, 1972.

Brightness—High brightness is necessary for satisfactory viewing under high ambient-light conditions. The NUMITRON segment luminance of 7000 footlamberts is extremely bright and permits viewing in direct sunlight. In addition, the brightness is fully controllable by means of drive voltage adjustment.

Contrast—The advantage of high brightness can be lost if the contrast between the character being displayed and its background is insufficient. The background of the NUMITRON display device is a black ceramic, which provides a high contrast with the lighted character. Another contrast to be considered is the difference in brightness between lighted and unlighted segments. This ratio is extremely good in the NUMITRON, inasmuch as unlighted segments are practically invisible.

Viewing angle—The design factor that limits the viewing angle of most display devices is the depth of the character within its enclosure. The planar construction of the NUMITRON permits a wide viewing angle compared to devices with "stacked" digits.

Freedom from clutter—The planar construction of the NUMITRON provides freedom from the clutter associated with designs which stack individual characters on top of one another.

Reliability—The high brightness levels of the NUMITRON display device segments are obtained at a coil temperature of 1400°C, which is considerably below the typical

design value of 2500°C for lamp bulb filaments. Therefore, evaporation of the tungsten wire is negligible. In fact, calculations relating tungsten evaporation to filament temperature indicate that the tungsten evaporation burnout mechanism, which causes failure in lamp bulbs, is essentially nonexistent in the NUMITRON. Accelerated life tests on RCA's NUMITRON display devices indicate a life expectancy in excess of 100,000 hours.

Color selection—Multicolor displays that use inexpensive color filters are desirable. The range of color filter selection is dependent on the width of the light spectrum emitted by the display device. The light output of the NUMITRON has a wide incandescent spectrum that permits an unlimited choice of color filters.

Size—Character size depends on the particular application. RCA's NUMITRON digital display devices presently offer a choice of two character sizes. The DR2000 series of display devices have a 0.6-inch numeral height and mount on 0.8-inch centers, while the DR2100 series offer a 0.4-inch numeral height and mount on 0.5-inch centers. In actual operation, an optical illusion causes lighted characters to appear larger than they actually measure.

Cost—RCA's NUMITRON display devices are manufactured on high-speed receiving-tube equipment, so costs are low. In addition, the sockets required are standard low-cost items.

Components of the NUMITRON

Fig. 1 shows a photograph of both series of NUMITRON display devices. Each size is offered in four basic configurations: seven-segment without decimal point, seven-segment with decimal point, plus or minus, and plus or minus 1. The actual character dimensions are shown in Fig. 2. Each device contains a group of incandescent single-helical coil segments in an evacuated glass envelope. During operation, specific coil combinations are lighted to form the desired character. Any satisfactory switching system can be used to address the proper coils; however, the usual technique is to use integrated-circuit decoder-drivers such as the RCA CD2500F or CD2501E.

Fig. 3 shows an exploded view of a NUMITRON. The various parts are described below:

Stem—The stem used on the DR2000 series NUMITRON is essentially the same as the stem used on T6-½ miniature receiving tubes, so DR2000 devices can use standard miniature receiving tube sockets. The stem leads are silver clad so that the device can be soldered directly into printed circuit boards if so desired. The DR2100 series employs a 9-pin sub-miniature stem designed to mate with commercial sockets

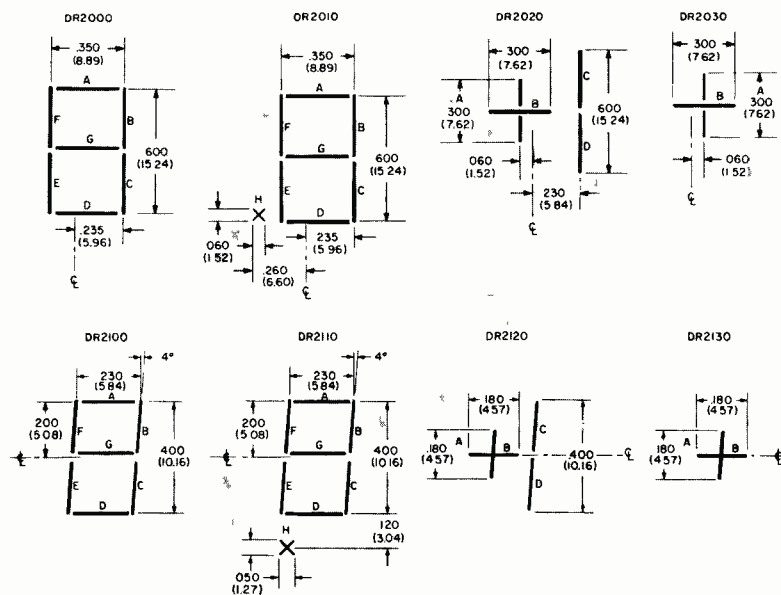


Fig. 2—Character dimensions of NUMITRON display devices given in inches and millimeters.

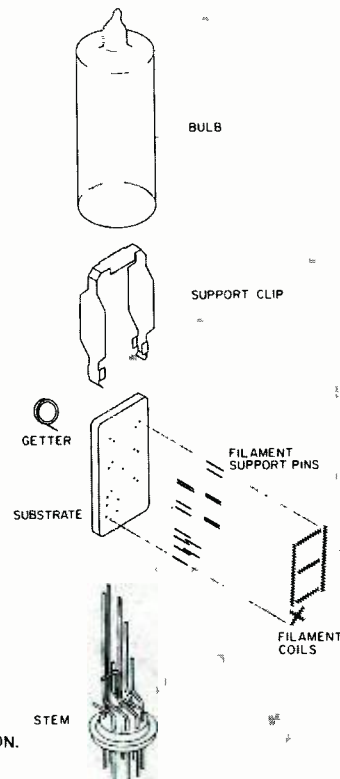


Fig. 3—Exploded view of a NUMITRON.

that are currently available for TO-5 IC packages. The DR2100VI series has formed leads for direct printed-circuit board mounting. The center-to-center mounting distance is 0.5 inch, including space for an inter-unit light shield.

Substrate—The substrate that supports the seven incandescent segments is molded from alumina ceramic material. The alumina is blackened by the addition of metal oxides to provide a high-contrast background for the lighted segments. After being molded, the ceramic is fired to a permanent set. The finished substrate, which is 0.075-inch thick, contains the necessary holes and indentations required for inserting and fastening the filament-support pins.

Filament-support pins—The individual filament-support pins are made from 0.014-inch Kovar wire cut to the required lengths. For the decimal eight configuration, there are sixteen individual pins.

Support clip—The substrate support clip, stamped and formed from 0.005-inch steel strip, supports the mount firmly within the bulb. The surface is blackened to eliminate reflections within the device.

Filament coils—The individual segments are 0.002-inch-diameter helical coils of 0.0004-inch tungsten wire that is specially doped with other materials to provide the required metallurgical properties. The coil segments in the finished device have approximately 800 turns per inch. The coils are initially wound at a higher TPI and are stretched into position during assembly.

Getter—The getter is the barium compound type regularly used in receiving tubes. Its purpose is to maintain a high degree of vacuum in the finished device.

Bulb—The bulb is made from 008 lime glass and is of the tubing variety so as to have good optical properties. A tubulation extends from the top end for evacuation purposes.

Construction

In NUMITRON display device fabrication, a substrate-pin-stem assembly and a filament-frame assembly are made individually. For the substrate-pin-stem assembly, the filament-support pins are loaded into the ceramic substrate in a suitable jig. A liquid glass frit is applied to the back of the substrate, and the assembly is then fired at 1000°C to set the frit and secure the pins in place. The substrate-pin assembly is then welded to the formed stem.

The filament-frame assembly is used in mounting the very fine filament coils. Fig. 4 shows a typical filament-frame assembly. The 0.0004-inch tungsten filament wire is wound in the form of a single helical coil on an 0.0012-inch

molybdenum mandrel. Segments of the continuous coil and mandrel assembly are then welded to stainless steel frames. The entire filament-frame assembly is then immersed in an acid solution to dissolve out the molybdenum mandrel, leaving the tungsten coil welded to the steel frame as shown in Fig. 4.

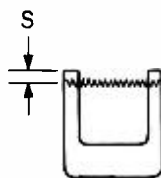


Fig. 4—Filament frame assembly.

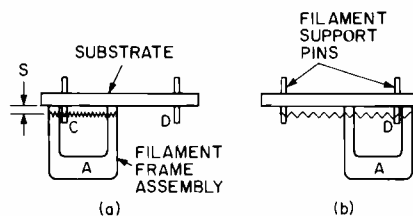


Fig. 5—Filament coil welding

The filament coil is welded to the substrate-pin-stem assembly by the two-step process illustrated in Fig. 5. The filament-frame assembly is held at point A and pressed against the substrate. Dimension S in Figs. 4 and 5a, which was fixed when the coil and mandrel were welded to the frame, is thus automatically set into the finished device. The coil is welded to the support pin at point C and broken off of the left frame leg. The frame assembly is then moved to the right as in Fig. 5b thereby stretching the coil a fixed amount. A second coil-to-support-pin weld is made at point D, after which the support frame is separated and discarded. The same operation is repeated five times to form the seven individual segments; the vertical segments require an additional center weld. The frame thus provides a handle for holding the filament coil during the welding operation, and serves as a gauge to position and stretch the coil.

NUMITRON display devices that include a decimal point require two additional coils mounted in the form of a small x. The two filaments that form the decimal point are connected in series on the back of the substrate. The series combination of coils for the decimal point,

like each of the seven segments of the figure eight, operate at 4.5 V.

Finishing and testing

After a getter has been welded to the back of the mount and the filament support pins have been positioned for good filament alignment, the support clip is placed over the substrate and the mount is inserted into the bulb. The device is then sealed and exhausted in a manner similar to that used for miniature receiving tubes. The completed device is operated for several hours, after which it is tested for both electrical and visual criteria. The major characteristics for the RCA DR2000 and DR2100 series of NUMITRON digital display devices are listed in Table I.

Future developmental programs

Additional devices presently under consideration include a "flat-pack" version of the standard seven-segment configuration, a twelve-segment "wagon wheel" pattern for displaying position, magnitude or direction information, and reduced power versions of the present NUMITRON display devices. Fourteen- or sixteen-segment devices capable of displaying alphabetic as well as numeric characters could be designed and manufactured provided there was sufficient market demand. As the fields of data collection, data processing and data display continue to expand, so too will the need for character display devices.

Table I—Published characteristics of the DR2000 and DR2100 series of NUMITRONS.

	DR2000 series	DR2100 series
Mechanical		
Mounting position	any	any
Maximum overall length (in.)	1.875	1.660
Maximum seated length (in.)	1.625	1.450
Maximum diameter (in.)	0.785	0.485
Base (9-pin)	miniature	0.230 pin circle
Electrical (dc segment voltage is 4.5 V unless otherwise specified)		
Recommended dc-segment voltage range (V)	3.5 to 5.0	3.5 to 5.0
Segment current (mA)	24	24
Mean life expectancy at 95% confidence level (h)	100,000	100,000
Visual (dc segment voltage is 4.5 V)		
Viewing angle (included angle)	140°	120°
Typical segment luminance (fL)	7000	7000
Response times (ms): typical ascent (to visibility) descent (to 50% of luminance)	15	15
Max. segment deflection from straight line (in.)	<20	<20
	0.005	0.004

Liquid-crystal dynamic scattering for display devices

H. C. Schindler

For the past several years, RCA has been developing practical fabrication techniques for liquid crystal devices to be used in numeric-readout displays. This development work has led to several devices that are both feasible and desirable. In this paper, the design and construction of several types of liquid-crystal numeric-readout devices will be discussed in some depth.



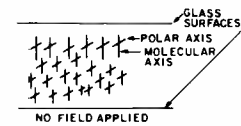
Henry C. Schindler
MOS IC & Liquid Crystal Products
Solid State Division
Somerville, N.J.

received the BChE from Cooper Union in 1955, and the MS in Physics from the Stevens Institute of Technology in 1959. Mr. Schindler was employed for four years at Picatinny Arsenal where he formulated and tested rocket and jet devices. Subsequently, he joined General Instrument Corporation as a senior engineer in developing semiconductor devices. In June 1962, Mr. Schindler was engaged by the RCA Superconductor Materials and Devices Laboratory of the Special Electronic Components Division at Princeton, N.J. He participated in the development of the niobium tin vapor deposition process and studies of the effect of the physical, chemical, and electrical properties of Nb_3Sn films. As a result of this work, he received the RCA Laboratory Outstanding Achievement Award. In April 1964, Mr. Schindler transferred to the RCA Superconductive Products Operation. He was initially involved with the development and electromagnetic evaluation of superconductive ribbons for magnet applications. In 1968, he assumed full responsibility for the design and assembly of all commercial-magnet systems and, subsequently, in 1969, he assumed additional responsibility for ribbon development and pilot-line production. In 1970, Mr. Schindler joined the Liquid Crystal Engineering Activity where he is involved with the design, evaluation, and applications of liquid-crystal devices.

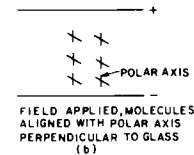
LIQUID-CRYSTAL materials were discovered by H. Reinitzer in 1889. These materials flow like a liquid, yet the molecules are somewhat ordered and, consequently, behave to some degree like a solid. Until recently, liquid crystals were curiosity items; however, in 1968, the electro-optical phenomenon called *dynamic scattering* was discovered at the RCA Laboratories.

Dynamic scattering is observed when a thin film (6 to 25 μm) of nematic liquid crystal material is placed between transparent conducting electrodes and a voltage differential exceeding about 7 volts is applied. Dynamic scattering is caused by the interaction between free space charge and elastic and dielectric forces. The space charge can be produced either by the anisotropy in the conductivity or by the production of ions due to injection of carriers from the electrode.

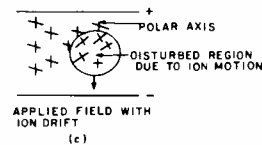
The molecules of the liquid are rod-like, with the polar axis displaced from the geometric axis. The liquid is also *birefringent*: its index of refraction depends on the light direction. When the liquid-crystal material is placed in thin films between conductively coated glass plates, the molecular axis of the molecules can be aligned in one of three orientations: 1) randomly, 2) parallel to the glass, or 3) perpendicular to the glass. In all RCA displays, the molecular axis is aligned perpendicular to the glass with the polar axis displaced as shown in Fig. 1a. However, when an electric field of sufficient intensity is applied, the polar axes of the molecules align themselves parallel to the field, Fig. 1b. If some ions are present in the liquid crystal, they will be



(a)



(b)



(c)

Fig. 1—Dynamic scattering in nematic liquid crystals.

forced to move to the negative electrode, Fig. 1c. The motion of the ions causes localized disturbances in the electric field and disrupts the ordered molecular array. This disruption results in regions of varying indices of refraction. Any light passing through the liquid crystal, with its varying degrees of refraction, will be diffusely scattered by the activated regions; those regions appear like frosted glass. Material in the unactivated state is clear. Since the device does not generate light, but solely scatters light, the activated portions will appear brighter as ambient light is increased. By designing displays with some regions clear and other regions capable of scattering the available light, numeric and animated images can be generated.

A major advantage of liquid-crystal displays is that they scatter available light; therefore, washout in high-light-intensity areas (so prevalent with light-generating devices) is not a problem. In addition, and of extreme importance, these displays do not generate light, thus, requiring negligible power. In fact, liquid crystals require the least power of all available displays. The major potential applications for nematic liquid-crystal displays are in areas of numeric display, such as in portable instrumentation, calculators, and panel meters.

Liquid-crystal devices can be constructed for use in either a transmissive or

Reprint RE-17-6-2
Final manuscript received February 24, 1972.



Fig. 2—Assembled single- and four-digit 7-segment displays.

a reflective mode. In the transmissive mode, the front and back electrodes are transparent and the display is illuminated from the back. When back lighting is not available, the back electrode is made reflective and available light is used. If power is at a premium, such as in portable instrumentation, the reflective mode is usually used. Assembled single- and four-digit (7-segment digits) displays currently marketed by RCA are shown in Fig. 2.

Liquid-crystal materials

Many naturally occurring organic compounds are known to behave as liquid crystals. Each of these substances has distinctive properties, and each has its own operating temperature range; in most cases, the ranges are too narrow and too high above room temperature to be of practical value. In addition to the discovery of dynamic scattering in thin films, one of the major developments over the past few years has been the development of several stable liquid-crystal mixtures that will operate at normally-encountered temperatures. One of these formulations is a multicomponent system operating from 5°C to 55°C. This temperature range makes the system useful in indoor applications, such as in panel meters and calculators. Other liquid-crystal formulations with different operating-temperature ranges have been developed over the past few years for custom applications.

Each liquid-crystal mixture has a sharply defined maximum operating temperature above which dynamic scattering completely ceases. This temperature is variously called the *N-L point* (the material goes from a nematic liquid to an ordinary liquid) or the "isotropic temperature" (the material goes from "scattering" to "non-scattering" at this temperature is reversible and is in no way harmful to the device. Similarly, there is a lower temperature at which a liquid-solid transition takes place. This point is referred to as the *C-N point* (crystalline to nematic). This change in state is also reversible and non-harmful.

During the cooling of a liquid-crystal display, the liquid-crystal material, sandwiched between glass plates spaced at only 5×10^{-4} inch, frequently super-cools because of the strong surface forces. In this supercooled state, the dynamic scattering phenomenon in some mixtures persists to temperatures considerably below the *C-N point*. Many claims for "non-freezing" or very-low-freezing-point materials are the result of a quick quench allowing no time for nucleation or crystallization. This results in the formation of a glassy state which may have a long holding period during which, due to the high viscosity of the liquid crystal, no change is observable. This supercooling property can be used provided crystallization does not occur after long periods of storage. The liquid-crystal formulation previously described has an operating range of 5°C to 55°C, and will not freeze in devices at the low end of this temperature range even after storage at the low temperature for several months.

Measuring electro-optical characteristics

Before discussing the electro-optical characteristics of liquid-crystal devices, it will help to understand how these characteristics are defined and measured. The electro-optical measurements of delay-time, risetime, and decay-time are made, typically, in either a transmissive or reflective mode, depending on liquid-crystal cell type, and at a specified voltage, frequency, and temperature. For example, since RCA liquid crystals are used in conjunction with RCA cos/mos circuits, a

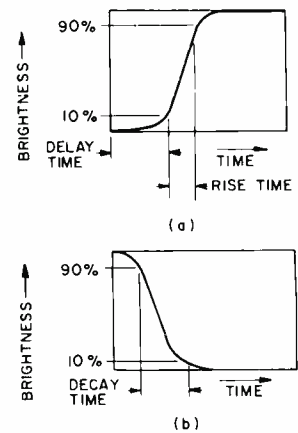


Fig. 3—Typical oscilloscope traces for (a) rise time and (b) decay time taken with the apparatus of Fig. 4.

15-volt symmetrical squarewave supply at 60-Hz has been selected. The electrical parameters are defined as follows:

Delay-time: The time from the initiation of the *on* pulse to the 10% level of the transition, Fig. 3a.

Rise time: The time interval required to change the element from the inactive to the active state defined as 10% to 90% of the transition, Fig. 3a.

Decay-time: The time interval required to change the element from an active to an inactive state defined as 90% to 10% of the transition, Fig. 3b.

Contrast ratio: Ratio of the light intensity in the *on* to the *off* state.

A diagram of the test apparatus is shown in Fig. 4. In the transmissive mode, a light source is mounted approximately 6 inches behind the cell and at an angle of 45 degrees from normal to the surface, as shown in Fig. 4. A brightness meter is mounted in front

PHOTO-RESEARCH BRIGHTNESS METER 1505-UB OR EQUIVALENT

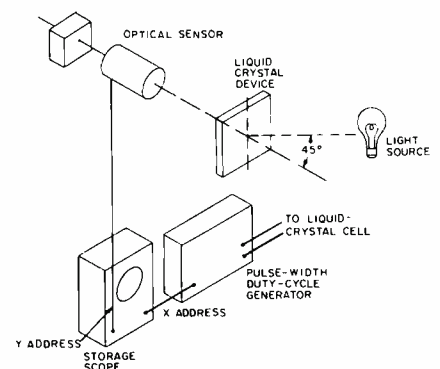


Fig. 4—Apparatus used to measure liquid-crystal electro-optical characteristics.

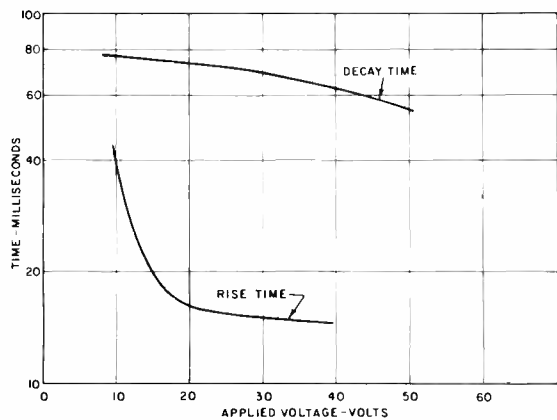
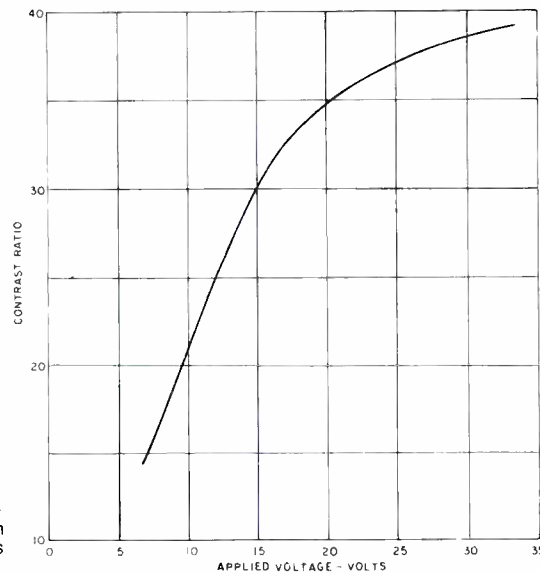


Fig. 5—Rise and decay time as a function of applied voltage (symmetrical squarewave at 60 Hz) for transmissive and reflective cells with 0.0005-inch electrode spacing.

Fig. 6—Contrast ratio as a function of applied voltage for transmissive and reflective cells with 0.0005-inch electrode spacing. Applied voltage is a symmetrical squarewave at 60 Hz.



and normal to the cell. In the inactive state, no dynamic scattering occurs and most of the incident light is transmitted without reaching the sensor. Upon activation of the element, however, the dynamic-scattering phenomenon is produced, and most of the incident light in the active-element region is diffusely forward scattered to the sensor.

In the reflective mode, a light source is mounted in front at an angle of 45 degrees away from the perpendicular to the cell. The light intensity is measured with a brightness meter in front and normal to the cell. When the cell is inactive, the incident light from the light source is specularly reflected and little light reaches the meter. When the cell is activated, the incident light is diffusely scattered, and the light meter measures an increased light intensity.

The electro-optic measurements are made with a pulse-width generator, storage oscilloscope, and photometer. The liquid-crystal cell is triggered with 12-second pulses, each pulse consisting of 5 seconds during which the cell is *on*, and 7 seconds during which the cell is *off*. The luminance of the liquid-crystal cell is measured with a Photo Research Spot Brightness Meter, Model 1505-UB, or equivalent.

Electrical-device characteristics

The electrical performance of a liquid crystal display is strongly influenced by the spacing between electrodes, liquid-crystal resistivity, operating voltage,

operating frequency, and operating temperature.

Spacing of conducting electrodes

The spacing between conducting electrodes influences all of the optical and electrical parameters in a liquid-crystal display. The nominal spacing between the electrodes of a liquid crystal is 5×10^{-4} inches. The decay time of the device, that is, the time required for the activated material to return to the unactivated state, is approximately proportional to the second power of cell spacing. The spacing is thus a compromise between the closest practically achievable spacing without shorting the electrodes and sufficiently rapid optical-response times. If response time is not critical in a particular application, the spacing between the electrodes might be increased to facilitate production.

Liquid-crystal resistivity

In the very pure state, liquid-crystal-material resistivities in the order of 1×10^{11} to 5×10^{11} ohm-cm can be achieved. However, since the scattering phenomenon involves the movement of ions within the liquid-crystal material, a sufficient number of these ions must be present. This requirement places an upper limit of approximately 10^{10} ohm-cm on the liquid resistivity. The liquid crystal resistivity increases as the temperature is lowered, and is a maximum at the lowest operating temperature. It is therefore necessary that the 10^{10} ohm-cm resistivity not be

exceeded at this lowest operating temperature. Current RCA cells are approximately 5×10^8 ohm-cm at room temperature (25°C). If higher resistivity liquids are required because of limited available battery power, the lower end of the operating temperature range will be slightly higher. These considerations are of prime importance in applications, such as watches, in which the available power supply is limited and in which materials of the highest available resistivity consistent with a wide operating temperature range must be used.

Operating voltage

As a general rule, all transmissive and reflective liquid-crystal displays can operate in the dynamic-scattering mode with voltages as low as 7-volts RMS; however, better contrast and faster rise and decay times can be achieved at somewhat higher voltages. Because these are appearance factors, which are somewhat subjective, trade-offs can be made to best suit the particular application. The rise and decay times as a function of voltage for a cell with electrodes typically spaced at 0.0005-inch are shown in Fig. 5. The degree of contrast as a function of voltage is shown in Fig. 6. The contrast ratio is the ratio of the light intensity when the liquid crystal is activated to light intensity when it is unactivated. While the display can be operated at low voltages, a 15- to 18-volt level has been selected as optimum because of the good readability achieved at this voltage; this voltage level can be varied.

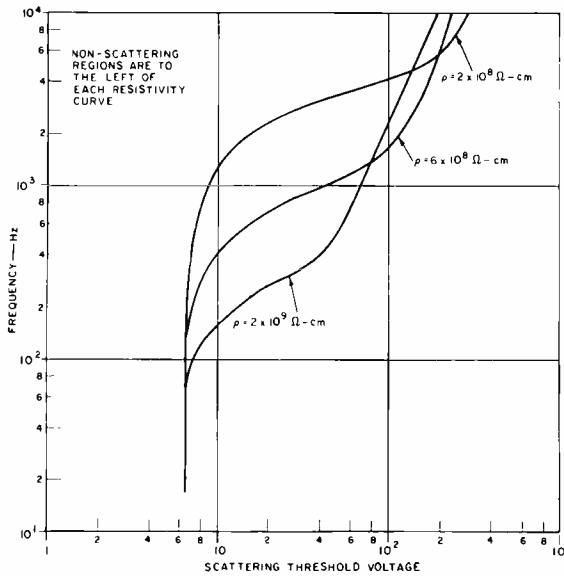


Fig. 7—An operating phase diagram for several liquid-crystal resistivities showing scattering threshold voltage as a function of frequency.

Operating frequency

Two important frequency parameters are the frequency above which the display will not operate, commonly referred to as the cut-off frequency, and the capacitive power associated with the operation of the display at the desired frequency.

Cut-off frequency

When applying any symmetrical wave to a liquid-crystal display while simultaneously increasing the operating frequency, a frequency will be reached above which the display does not operate. This is commonly referred to as the *cut-off frequency* and is related to the distance that the ions in the liquid-crystal material can travel during a given polarity swing. As the frequency increases, the time the ions are acted upon decreases and, consequently, the distance they travel also decreases. When this distance becomes so small that the molecular regions that cause scattering cannot be effectively rotated, scattering ceases.

For any given liquid-crystal resistivity, the cut-off frequency depends on the operating voltage. In Fig. 7, an operating phase diagram is shown for several liquid-crystal resistivities. The non-operating regions are to the left of each material resistivity. For example, for a resistivity of 2×10^8 ohm-cm, the region

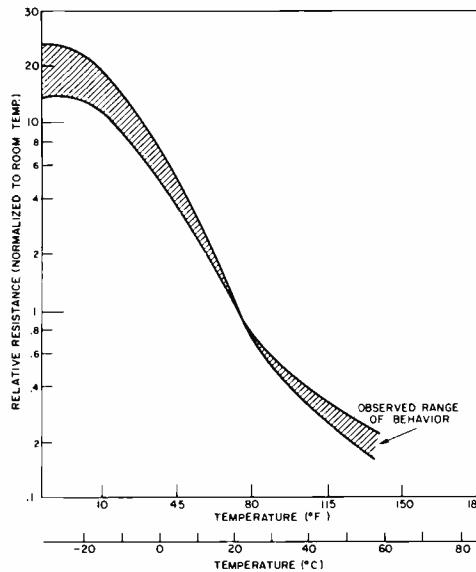


Fig. 8—Relative resistance as a function of temperature.

to the left and above the resistivity curve represents conditions under which scattering will not occur. As the resistivity of the material increases, a greater portion of the voltage-frequency domain becomes non-scattering.

Capacitive energy

If the available power for a liquid-crystal display is limited, the display should be operated at as low a frequency as possible to minimize the capacitive power losses associated with the switching of the display devices. However, operation with a symmetrical square wave at frequencies of less than 25Hz may cause flicker depending on the age and vision of the observer. The appearance of the display, then, provides a guideline to a possible minimum operating frequency. In terms of obtaining long life and minimum capacitive power, it has been established that operation in the 30- to 60-Hz frequency range is desirable.

Operating temperature

As the temperature of the liquid-crystal decreases, the liquid becomes more viscous. A higher viscosity, in turn, causes the resistivity of the liquid to increase; this condition is shown in Fig. 8. With increased liquid viscosity, the time required to generate and relax scattering regions also increases; this is

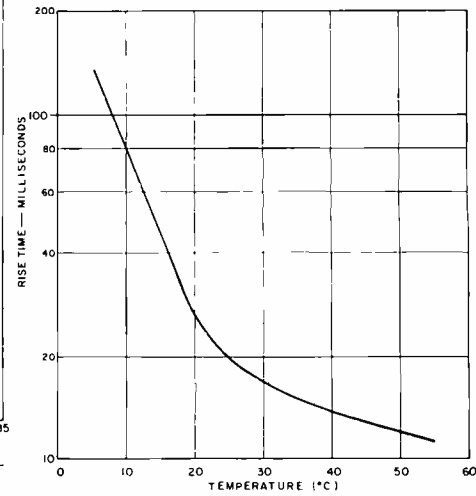


Fig. 9—Rise time as a function of temperature for transmissive and reflective cells with 0.0005-inch electrode spacing. Applied voltage is 15 V (symmetrical squarewave) at 60 Hz.

demonstrated in Figs. 9, 10 and 11, in which the rise time, decay time, and contrast ratio are plotted as functions of temperature. It is evident from these graphs that both the rise and decay times are prolonged with decreasing temperatures, whereas the degree of contrast is relatively insensitive to temperature over the operating range.

Design criteria

The design of a liquid crystal display involves topological problems, electrical-design considerations, and power consumption.

Topological layout

In the pattern layout of a liquid-crystal display, it is essential that only the desired pattern be activated, and that all other areas remain inactive. A typical design for a 4-digit 7-segment numeric display is shown in Fig. 12. The conductive surfaces for the front and back plates of the device are shown in Figs. 12a and 12b, respectively, and the assembled front to back electrodes are shown in Fig. 12c.

Note that the conductive surfaces face each other only in those areas that are to be activated. Although the inner portions of the digits have conductive surfaces facing each other, no scattering occurs because no leads are provided for activation. The lead patterns are designed such that they will not coin-

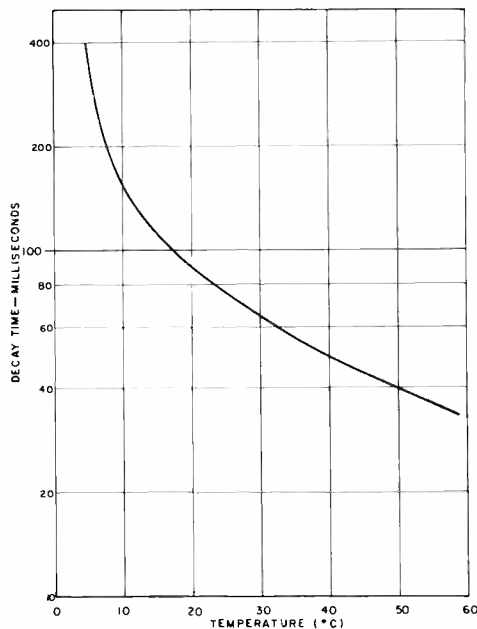


Fig. 10—Decay time as a function of temperature for transmissive and reflective cells with 0.0005-inch electrode spacing. Applied voltage is 15 V (symmetrical squarewave) at 60 Hz.

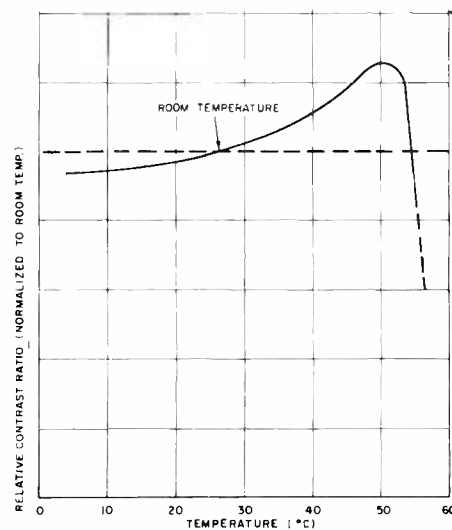
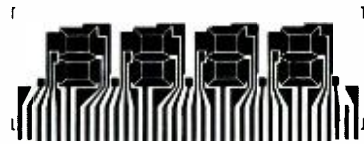


Fig. 11—Contrast ratio as a function of temperature for transmissive and reflective cells with 0.0005-inch electrode spacing. Applied voltage is 15 V (symmetrical squarewave) at 60 Hz.



a) Front plate. Dark areas are conductive coating.



b) Back plate. Dark areas are conductive coating.



c) Assembled display. Dark areas are activated segments.

Fig. 12—Light areas of liquid-crystal display are conductive areas.

side with (or overlap) a pattern on the opposing surface except for areas forming the activatable segments of the display. This arrangement assures that the lead patterns will not be activated at any time. The conductive surface is a thin, transparent coating of tin-oxide or indium-oxide on a glass substrate. This construction technique and patterning system permits the design of displays of considerable sophistication and complexity.

Electrical leads

It is desirable to maintain the voltage drop along the lead lengths of a display at less than 1% of the available operating voltage to permit the device to operate at 99% of available voltage; operation at this voltage level will assure maximum response time. Since most displays operate in the 15- to 20-V region, lead voltage drop should not exceed 0.15 to 0.20 V.

The voltage drop along the leads is easily calculated after the lead and activatable area resistances are known. To obtain these resistance values, the number of squares in the lead layout is multiplied by the total resistance per square for the conductive coating, typically 500 ohms per square. With a liquid-crystal-cell spacing of approximately 5×10^{-4} inch, the average resistance for a 1-inch-square activatable area is 250,000 ohms. The voltage drop

of the leads, therefore, is the drive voltage multiplied by the ratio of the lead resistance to the sum of the lead resistance plus the fixed resistance of the activatable area. Should the voltage drop of the leads exceed 0.15 to 0.20 volts, the lead width can be readjusted to achieve the desired design level.

Power consumption

The combination of liquid-crystal display and cos/mos driving circuitry produces a display system that consumes less power than any other known electronic display system. As an example, the RCA TA8040 display consisting of four 0.6-inch-high by 0.4-inch-wide 7-segment digits plus 5 decimal points consumes only about 100 μ A at 15 volts or 1.5 mW with all segments operating. Since the normal duty cycle of the segments in a numeric display is 65 to 70%, the power consumption is further reduced to approximately 1 mW. If the display is considered to be driven by the energy of a single D cell, such as the type T-50, and if 70% efficiency is experienced in converting the available 1.5 volts to a 15-volt operating voltage, then the energy of the D cell is sufficient to operate the liquid-crystal display 24 hours/day for 300 days. The power can be reduced further and display life increased by a factor of five by slightly increasing the resistivity of the liquid-crystal material. However, as previously discussed, this advantage is

somewhat offset by a slight reduction in the operating temperature range.

Conclusion and commercial prospects

Since the initial RCA announcements on dynamic scattering in 1968, several years have been devoted to developing practical fabrication techniques. The point has now been reached at which many commercial products appear feasible and desirable. This paper confines its discussion to liquid-crystal numeric-readout displays. These displays can be either single- or multi-digit types, or they can be custom designed. Liquid-crystal displays have been designed to meet desired operating parameters in terms of rise and decay time, operating voltage, and temperature. These devices and present technologies are ideally suited for digital-readout equipment, clocks, and calculators. Circuitry involving cos/mos technology is presently evolving to complement the liquid crystals. As materials and technology advance, other applications, such as watches and outdoor displays will be realized.

Bibliography

1. Heilmeyer, G. H., "Liquid-Crystal Display Devices," *Scientific American*, Vol. 222, No. 4, (April 1970) pp 100-106.
2. Castellano, J. A., "Now That the Heat Is Off, Liquid Crystals Can Show Their Colors Everywhere," *Electronics*, Vol. 43, No. 14, (July 6, 1970).

Facsimile printer using a liquid crystal array

J. Tults | D. L. Matthies

Liquid crystal cells can be used to build various display and light-modulating devices. The construction of such devices is simple and their power consumption very low since rather than producing light, the liquid crystal cells modify the characteristic of incident light. This paper describes the construction of an optical facsimile printer where a linear array of liquid crystal cells is employed as a light modulator.

Juri Tults, Consumer Electronics Research Laboratory, RCA Laboratories, Princeton, New Jersey received the BSEE and MSEE from Purdue University in 1964 and 1965 respectively. Since 1965 he has been employed by RCA Laboratories where he has worked on research projects related to color television, character recognition, electroluminescent and liquid-crystal displays, and digital communication systems. Mr. Tults is a member of IEEE and Tau Beta Pi.

Dennis L. Matthies, Consumer Electronics Research Laboratory, RCA Laboratories, Princeton, New Jersey received the BS in Physics from Rensselaer Polytechnic Institute in 1968 and the MSE from Princeton University in 1970 and the MA from Princeton University in 1971. He is presently pursuing the PhD at Princeton, specializing in device physics. Mr. Matthies joined the staff of RCA Laboratories in July 1968 and has engaged in research dealing with liquid crystal displays, holography, glow discharge material synthesis, and thermoplastic recording. He has participated in the Research Training Program and the Graduate Study Program. He was the recipient of an RCA Laboratories Outstanding Achievement Award in 1970 for contributions to a team effort in devising and improving the processing of storage media for high density recording. Mr. Matthies holds one patent and has two others pending. He is a member of the IEEE, Eta Kappa Nu, and Sigma Pi Sigma.

Authors Matthies and Tults (left to right).



IN THE PAST FEW YEARS, several papers have been published by G. H. Heilmeyer and his co-workers at RCA Laboratories describing the phenomenon of dynamic scattering in liquid crystals.^{1,2} This phenomenon has been used in displays consisting of a suitable arrangement of cells containing liquid crystal material. In the facsimile printer, the array of liquid crystal cells operates as a very low-loss light modulator driven by only a negligible amount of power supplied at a moderate voltage level. The method of exciting the cells was chosen to reduce, as much as possible, the response time of the liquid crystal cells to maximize the speed of the printer.

Basic system

The basic printer is illustrated in Fig. 1. The light sensitive recording surface can be, for example, Electrofax paper which travels at a constant speed past the exposing station. A projection lens focuses an enlarged image of the linear array of liquid crystal cells upon the recording surface. The light transmission characteristics of the individual cells of the array are controlled by excitation voltage waveforms obtained from signal processing circuits.

Array construction

The construction of a typical liquid crystal cell array for the facsimile printer is shown in Fig. 2. The structure consists of two quartz plates separated by 1/2 mil-thick spacers with the space between the plates filled by liquid crystal material. The inside surfaces of the quartz plates have transparent, conductive coatings that are etched to form the desired electrode patterns. Cells are formed where the electrodes on the top and bottom plates overlap—these areas are shown shaded in Fig. 2. In this structure, the single strip-electrode on the top plate is common to all cells. The length of the shortest side of a single cell must be at least about five times larger than its thickness to reduce the relative magnitude of fringing effects between adjacent cells.

The equivalent circuit of a liquid crystal cell is a resistor and a capacitor connected in parallel. In a 10-mil-square cell, the capacitance is about 0.1 pF, and the resistance is typically 10⁹ ohms.

Reprint RE-17-6-1
Final manuscript received June 17, 1970

Electro-optic characteristics

Normally, a liquid crystal cell is transparent to radiation in the wavelength range from about $0.3 \mu\text{m}$ to $2 \mu\text{m}$. When a voltage is applied to the electrodes of the cell, the liquid crystal material switches into what is called the dynamic scattering mode. In this mode, light traveling through the cell is scattered in the forward direction.

Fig. 3 shows the electro-optic transfer characteristic of a typical liquid crystal cell in the array when the light is incident upon the cell at an angle of 30° to the normal, while the detector is pointed directly at the cell. As the voltage approaches 10 volts, the dynamic scattering effect becomes noticeable and increases with the applied voltage. Saturation is reached at about 30 or 40 volts. The excitation voltage can be DC, or AC at a frequency less than about 500 Hz. The life of the liquid crystal cells can be significantly increased if AC excitation is used.

The optical characteristics of a liquid crystal cell, illustrated in Fig. 4, are also of great importance in the design of the printer. These characteristics show that for most efficient utilization of the incident light the beam should be normal to the cell ($\theta=0^\circ$). However, under those circumstances the cell is a rather poor light valve since the ratio of the relative brightness values of the cell when clear and then scattering, commonly known as the *contrast*, is only about 3 (Fig. 4c). It is possible to enhance this low value of contrast optically by methods described later in this article. Of course, as can be seen from Fig. 4c, a contrast of about 10 can be obtained by aiming the light beam on the cell at an angle of 30° to the normal. The peak brightness of the cell in this case is decreased by a factor of about 30 (from $\theta=0^\circ$) resulting in very inefficient use of the available light.

Dynamic operating characteristics

In addition to the static electro-optic performance, the dynamic operating characteristics of liquid crystal cells are also of great importance in applications like the facsimile printer. Fig. 5 shows actual waveforms illustrating the dynamic response of a liquid crystal cell excited by discontinuous AC signals. In Fig. 5a a low-frequency excitation waveform is applied across the cell for

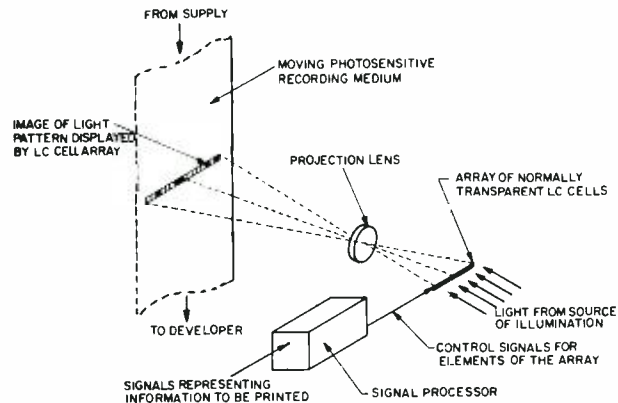


Fig. 1—Basic elements of facsimile printer employing a linear array of liquid-crystal cells.

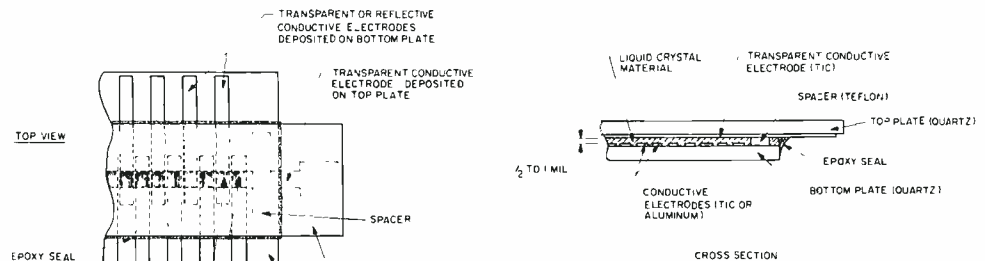


Fig. 2—Construction of a linear array of liquid-crystal cells. [Drawings are not accurately scaled.]

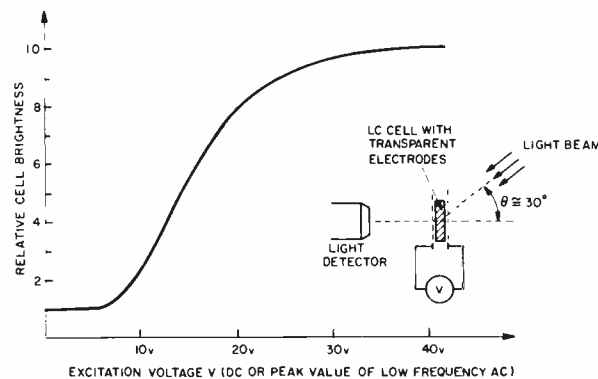


Fig. 3—Static electro-optic transfer function of a typical liquid-crystal cell.

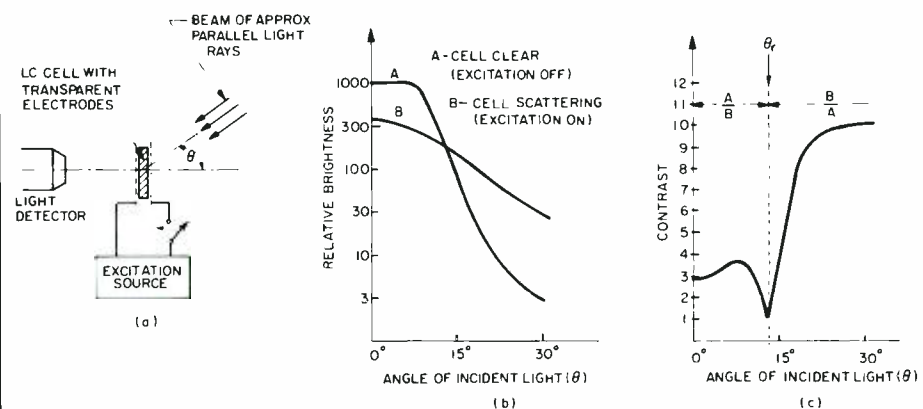


Fig. 4—Brightness and contrast of liquid-crystal cell as functions of angle of incident light.

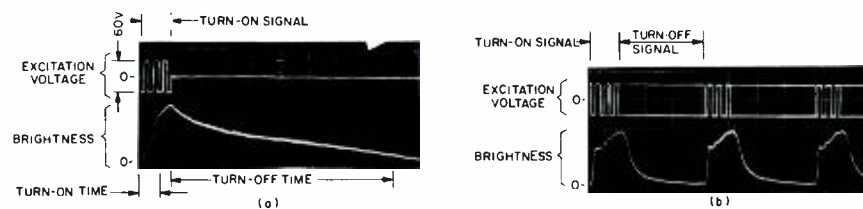


Fig. 5—Dynamic electro-optic response of liquid-crystal cell excited with AC waveforms.

a period of about 10 ms. The resulting changes in the brightness of the cell are shown by the lower waveform. The decay time of the brightness, of about 100-ms duration in this case, is obviously much longer than the risetime.

The decay time can be dramatically reduced by applying a high frequency AC signal across the cell during periods when the brightness of the cell should be low. This is illustrated in Fig. 5b which shows a 20-kHz turn-off signal applied to the cell whenever the low frequency excitation signal is not present. The decay period is thus reduced to about 5 ms, and the risetime of the brightness response is also decreased by a noticeable amount. With this technique, the speed of response can be increased to the point where the cell can be switched from one brightness state into another at intervals as short as about 10 ms.

Optical system

The optical system of the facsimile printer (Fig. 6) is basically a slightly modified slide projector. On the extreme left is a point source of light, e.g. a mercury-arc lamp. A condenser lens focuses the image of the light source on the center of the aperture plane of the projection lens. The array of liquid crystal cells is placed into the path of the light beam where ordinarily a slide would be inserted in a slide projector. Rather than an array of square cells, one consisting of rectangular cells is employed to intercept a greater frac-

tion of the output beam of the condenser lens. For a fixed length of the array, this fraction is proportional to the height/width ratio of the individual cells in the array. Without the cylinder lens shown in Fig. 6, the projection lens would form an undistorted image of the array on the recording surface. However, with the lens inserted, this image is compressed along the vertical axis and, as a result, the desired image consisting of an array of square cells is obtained. The optical system is arranged to produce an image where the side dimension of a cell is about 5 to 10 mils. This is an adequately small size for resolution elements in many applications, e.g. for printing typewriter-size alphanumerics.

One very important aspect of the projection system is its ability to enhance the contrast of the projected image. On basis of the characteristics in Fig. 4, the contrast in the plane of the array of liquid crystal cells, when looking in a direction normal to the array, is only about 3. To obtain a recording of good contrast on Electrofax paper, like the Dennison HS, the ratio of the maximum and minimum intensities of the incident light must be at least about 5. A ratio of 10 can actually be obtained at the image of the projection system. This becomes possible by using a projection lens of small aperture. At the same time, the aperture should be at least as large as the image of the light source formed at the aperture so as not to reduce the brightness of the image. Under those

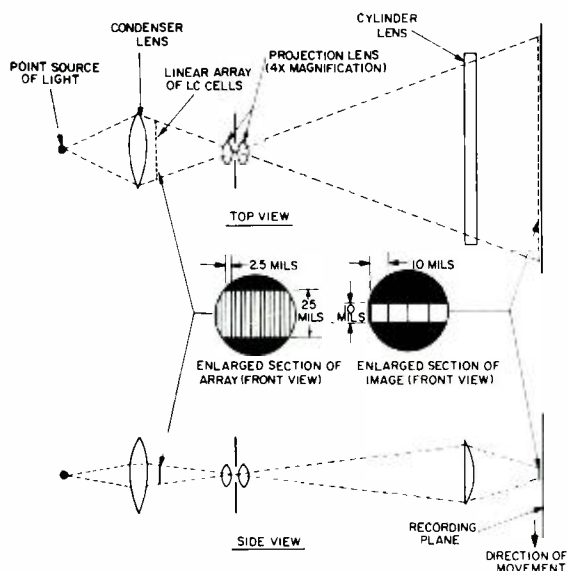


Fig. 6—High efficiency projection printer.

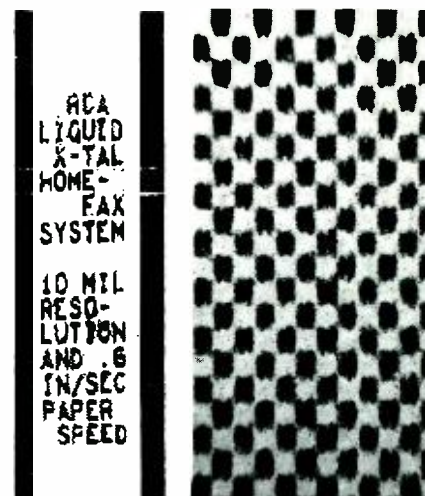


Fig. 7 Fig. 8
Records printed with projection-type crystal printer.

conditions, all the light intercepted by a clear cell in the array passes through the aperture and arrives at the recording plane, whereas only a fraction of the total light from a scattering cell can pass through the projection lens. The size of this fraction is directly related to the area of the aperture.

It may be of interest here that the liquid crystal material exhibits dynamic scattering for wavelengths in the range of 0.3 μm to 2 μm ; thus, recording media with various spectral sensitivity characteristics can be used. It is only necessary to select a light source with a peak spectral emission characteristic at a wavelength approximately equal to that of the response characteristic of the recording medium.

Signal processor

The experimental facsimile printer which has actually been constructed employs a 0.6-inch-long array of 60 rectangular liquid-crystal cells. The electrical excitation signals for the cells are obtained from a signal processor.

In this signal processing system, the video input signal is quantized into binary samples to represent either white or black picture elements. Such a system is entirely adequate for printing alphanumeric and graphical data. The printing speed is 60 lines/second and is set by the field rate of the TV signal. This is close to the maximum printing rate of about 100 lines/second which is directly related to the previously mentioned shortest practical switching interval of 10 ms for liquid crystal cells.

A more complicated signal processing system is needed when the incoming information is, for example, in the form of ASCII codes representing serially arriving alphanumeric character data. Assuming that the output of such a printer consists of 8-inch-long rows of typewriter-size characters where one resolution element is a 10-mil square, then the characters can be printed at a rate as fast as 576/second.

Experimental results

The records shown in Fig. 7 were printed with the facsimile recording system which has been described. The recording medium was Dennison HS Electrofax paper moving at a speed of 0.6 in/s. One resolution element on those records is of a size approximately equal to a 10-mil square. The contrast of the recordings is sufficiently good for excellent legibility. The somewhat uneven appearance of the characters is caused by the fact that the video source was supplying an analog-type signal to the printer which was then converted into a digital signal by the signal processor. The photographs of the magnified recordings in Fig. 8 demonstrate more convincingly the resolution and contrast capabilities of the printer. These records were made with a signal obtained from a synthetic pattern generator. The true width of the elements on these magnified records is approximately 10 mils.

Principles of a contact-type printer

Another interesting possibility for constructing a facsimile printer using a linear array of liquid crystal cells has been investigated. The principle of operation of this printer can be explained with the aid of Fig. 9, which shows two cross-sectional views of the recorder. The array of liquid crystal cells is similar in structure to the unit shown in Fig. 2. The recording surface is not placed into immediate contact with the structure of the array as one might expect, but is separated from it by a transparent structure containing a set of parallel and light absorbing planes. The center-to-center spacing W of these planes is identical to that of the liquid crystal cells.

The purpose of the structure in Fig. 2 is to produce contrast enhancement in a manner which is really basically the same as in the projection printer. By

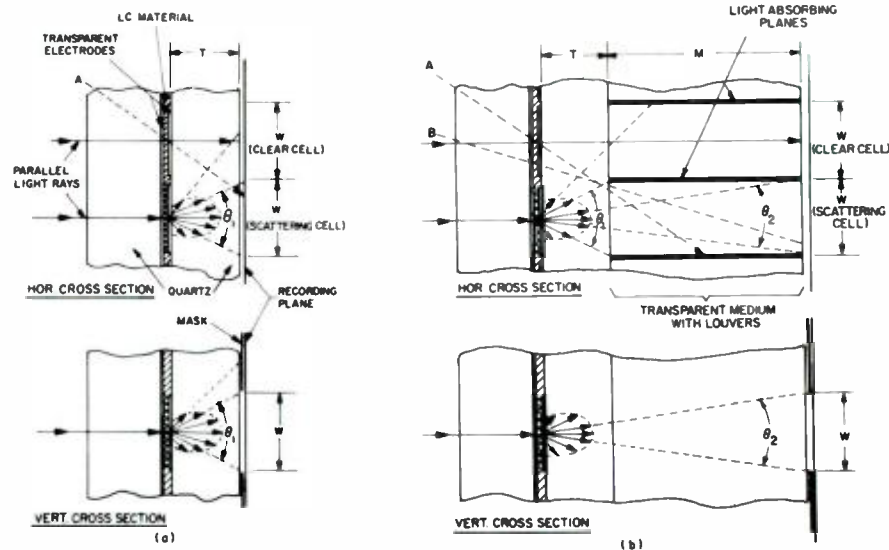


Fig. 9—Contact printing with liquid-crystal-cell array.

increasing the separation M between a scattering liquid crystal cell and an area of the same size on the recording surface directly opposite to the cell, the light falling on this area from the cell decreases. On the other hand, assuming the rays of light remain parallel while traveling through sections of the array where the cells are clear, areas on the recording surface opposite to these cells receive a constant amount of light regardless of the distance M between the recording medium and the array. As a result, the levels of light intensity at the recording plane corresponding to the clear and scattering cells have a ratio which increases with the separation M , and a recording of high contrast is produced.

The light-absorbing planes and the mask adjacent to the recording surface prevent any light rays from a scattering cell reaching areas on the recording plane other than an elemental area of size $W \times W$ directly opposite the cell in question. These planes also have the important function of reducing optical crosstalk which results when the rays from the light source are not perfectly parallel.

The contact printing system is attractive because it is more compact than the projection printer. However, in the contact printer, the array of liquid crystal cells prints a record which has a width equal to the length of the array. For most practical applications it is, therefore, necessary to provide a light source which can supply a broad beam

of parallel light. Unfortunately, a cheap and efficient way of constructing such a source has not been found. Practical ways for realizing the structure of the louvered medium also need to be investigated.

Conclusion

The feasibility of modulating light with an array of liquid crystal cells in an optical facsimile printer has been demonstrated. Liquid crystal cells require only modest operating voltages and consume little power. It is, therefore, possible to construct the signal processor with integrated circuits. The speed of such a printer is limited to about 100 lines/second. In the form described in this article, the printer is not capable of recording information in intermediate shades of gray.

Acknowledgement

The idea of the liquid-crystal printer originated with B. J. Lechner and R. F. Sanford at the RCA Laboratories. The optical contrast enhancement schemes were suggested by J. Y. Avins and D. Matthies. Valuable technical assistance was provided by W. E. Carpenter, R. N. Friel, E. L. Kaschak, and L. A. Zaroni.

References

1. Heilmeyer, G. H., Zaroni, L. A., and Barton, L. A., "Dynamic Scattering: A New Electro-Optic Effect in Certain Classes of Nematic Liquid Crystals," *Proc. IEEE*, Vol. 56, No. 7 (July 1968) pp. 1162-1171.
2. Heilmeyer, G. H., Zaroni, L. A., and Barton, L. A., "Further Studies of the Dynamic Scattering Mode in Nematic Liquid Crystals," *IEEE Transactions on Electron Devices*, Vol. ED-17, No. 1 (January 1970) pp. 22-26.

Storage tubes for computer displays

F. J. Marlowe

In the late 1940's storage tubes showed some promise as computer memories. The Selectron¹—invented at RCA Laboratories, the Williams tube² and the Haeff tube³ are historic electrostatic memories from that era. In those early days, the job was being done clumsily by vacuum-tube flip flops, so by comparison a single tube that could store a few hundred bits was attractive. However, the magnetic core memory, invented in about 1950, was so successful that storage tubes disappeared entirely from the computer scene. In the intervening years, storage tubes found use in radar and television, mainly as scan converters. Development continued and improvements were made, but they were never competitive with cores as main-frame memories. Recently, though, the growing use of video displays with graphics capability as computer output devices has opened some special applications for which modern storage tubes are better suited than magnetic cores or other conventional types of memory.

COMPUTER VIDEO OUTPUT DEVICES that display graphics are particularly good applications for storage tubes because, unlike ordinary CRT's, storage tubes can retain an image without the need for continuous refreshing. In the computer, graphics typically are stored compactly as a list of parameters (e.g., slope or curvature, length, and starting point) for each line. To display those lines, the list is scanned sequentially and fed to the video output device

where it is converted to a picture. Use of a storage tube, which requires no refreshing, in the output device permits efficient utilization of the computer because the list of parameters need only be scanned once each time a picture is constructed. The gain in bits displayed over bits stored in main memory can be enormous. For example, using for this purpose a garden variety storage tube with resolution equal to that of standard TV, a short list of parameters

Frank J. Marlowe, Communications Research Laboratory, RCA Laboratories, Princeton, N.J., did his undergraduate work at Pratt Institute during which time he was a co-op student with the Brooklyn Navy Yard. In 1963, he received the BSEE and joined RCA Laboratories on the research training program. In 1965, he received the MSEE from Princeton University. He is presently working towards the PhD at Rutgers University. At RCA Laboratories Mr. Marlowe has worked on semiconductor lasers, laser digital devices, liquid crystal matrix displays, and most recently storage display systems. He is the holder of one U.S. patent.



in main memory can be converted to a display having 250,000 bits. In this application, the storage tube is not equivalent to a 250,000-bit conventional digital memory because an individual stored bit cannot be addressed and read out by the computer; only the collective array of bits making an image constitutes an output. In general, a storage tube in a video output device is used only as a limited type of memory which stores information that is not to be read out and interpreted by the computer, but is only to be displayed to a human observer.

An increasingly important application of video-graphic output devices is in time sharing terminals that are linked to a computer by telephone lines. Because of the limited phone-line bandwidth, graphics must be transmitted in condensed parameterized form, and then converted at the terminal to an image. Furthermore, the terminal must be able to store that image long enough so that it can be constructed piece by piece as data arrive relatively slowly over the phone line and so that it remains long enough to be comprehended by the terminal operator. Storage tubes not only permit piece-by-piece image construction, but also can retain images for long periods of time. Most important, the nature of time sharing terminals requires that terminal cost be a fraction of the computer cost; using a storage tube for the terminal memory a graphic image can be stored and displayed far less expensively than using a conventional type of computer memory.

In the remainder of this paper three different types of storage tubes that are used as computer output devices are described. The *cathodochromic storage tube* is a direct-view tube that displays on its faceplate a visible image which remains indefinitely, or until it is intentionally erased. The *bistable direct view storage tube* also displays a stored image on its faceplate, but the storage of that image depends upon continued application of electrical power. The *silicon storage tube* stores a volatile charge pattern that cannot be seen directly, but must be scanned electronically, and displayed on a TV monitor. Other types of storage tubes exist and can be used for computer

Reprint RE-17-6-11
Final manuscript received October 25, 1971

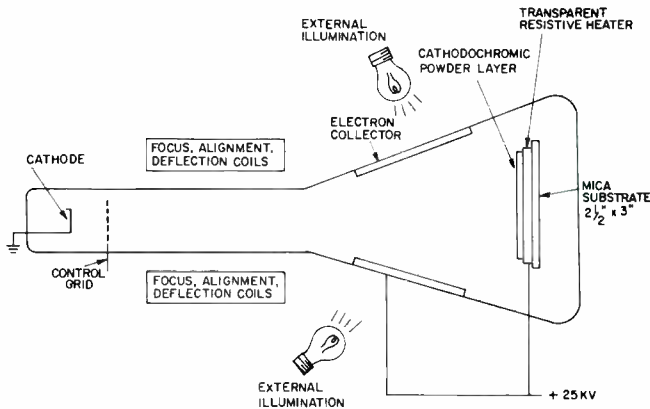


Fig. 1—Cathodochromic storage tube.

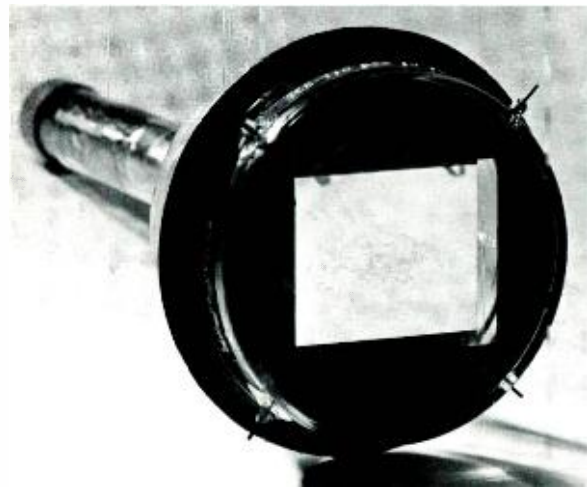


Fig. 2—An RCA cathodochromic tube with stored image.

graphics, but these three are currently the most prominent, and are likely to become more so in the future.

Cathodochromic storage tube

During World War II dark-trace tubes were used for radar displays requiring long persistence. In those tubes a *KCl* coating on the faceplate turned dark when bombarded by a high energy electron beam. Persistence could be varied from seconds to hours depending on incident light and temperature. Unlike phosphors, the *KCl* coating gave off no light, but could only be viewed under reflected or transmitted illumination.

The modern cathodochromic storage tube is an outgrowth of the old dark-trace radar displays. Fig. 1 is a schematic of an experimental tube⁴ developed at RCA Laboratories. The cathodochromic material is thermal-erase sodalite: *Br*, which turns dark under bombardment by the electron beam. The contrast ratio depends on exposure time, with a maximum in excess of 10:1. At room temperature, image persistence is permanent; however by activating the resistive heater, a stored picture can be erased in two seconds. Although the storage target shown in Fig. 1 is illuminated from the rear, the stored image can also be viewed under reflected ambient light alone.

The cathodochromic storage tube has a number of features that make it attractive as a computer video output device:

- 1) Resolution is very high. Spots of 1 mil diameter can be written and resolved.

- 2) Tube structure is nearly as simple as a plain black and white kinescope.
- 3) Since the image can be viewed under reflected light, it is not washed out by a bright ambient background.
- 4) Storage time is indefinite without requiring application of power.
- 5) Gray scale images can be displayed.

On the other hand, some disadvantages are:

- 1) Two seconds required for erasure is objectionably long for some applications such as an interactive time sharing terminal.
- 2) The storage/viewing area, limited at present to not much more than 2½ inches x 3 inches, is too small for many purposes. To solve this problem artificial means of increasing the size, such as projection, must be employed.

As an example of its storage/display capability an RCA cathodochromic tube with a stored computer-drawn image is shown removed from its socket in Fig. 2.

The cathodochromic storage tube has only had limited application as a computer output device. In addition to some experimental systems such as one built at RCA Laboratories, one company has introduced a computer terminal employing cathodochromic tubes. Also, another company marketed a terminal based upon a photochromic tube, which is similar to the cathodochromic one, but uses a light-emitting phosphor excited by the electron beam to darken the storage/display medium. In general, cost of cathodochromic terminals has been high, which, coupled with the disadvantages of long erase time and need for projection magnification, has with-

held the terminals from widespread general-purpose applications. However, cathodochromic storage tubes still hold promise for special purposes where the needs for high resolution and/or permanent storage predominate.

Bistable direct-view storage tube

Currently the most widely used computer output storage tube is the bistable direct-view type manufactured by Tektronix. This tube is incorporated in a number of products including an interactive graphics and alphanumeric terminal shown in Fig. 3. Early bistable direct-view storage tubes employed an insulator-coated mesh to store the charge pattern, which in turn controlled the landing of electrons on a phosphor-



Fig. 3—Bistable direct-view storage tube in a computer display terminal. (Courtesy of Tektronix, Inc., Beaverton, Oregon.)

coated faceplate. In the modern simplified bistable direct-view tube, a charge pattern is stored directly on a phosphor-dielectric target using the bistable secondary emission properties of the insulating phosphor. That charge pattern controls the landing of electrons on the phosphor-dielectric, producing a corresponding visual output.

A schematic of the tube's internal structure is shown in Fig. 4.³⁻⁶ The target is made of two layers on the glass faceplate: the transparent conductor serves as an electron collector for secondary electrons; the phosphor-dielectric layer both stores the charge pattern and emits light. Two flood guns continuously bombard the target with electrons which both maintain the charge pattern and excite the phosphor. The writing gun shifts selected points on the target from the erased or dark state to the bright state.

The secondary emission ratio of the phosphor-dielectric layer is plotted in Fig. 5. Under uniform illumination from the flood guns, each particle of phosphor-dielectric is stable at either zero volts relative to the flood guns—in which case no electrons land on the phosphor—or at V_C —in which case 150-V electrons land and excite the phosphor. The transparent conducting layer is able to both collect secondary electrons and serve as a reference for

the higher stable target voltage, V_C , because the phosphor-dielectric particles are dispersed. The write gun shifts target points from the lower-voltage stable point (erased) to the higher-voltage one by bombarding the phosphor-dielectric with very high energy electrons which generate secondary electrons, causing a net positive potential shift. Erasure is done by momentarily decreasing the target-to-flood-gun potential below the first crossover and then gradually returning it to 150 V.

The bistable direct-view tube has features that are adequate, but not exceptional, for a computer video output device, and has no serious deficiencies. The size of the display, 21cm x 16.2cm, is right for one or two viewers. Resolution of 400 x 300 line pairs⁷ is more than that of commercial television but is less than that of the cathodochromic storage tube. A storage time of 15 minutes with power applied gives ample time for an image to be drawn and comprehended by the viewer. Erase time of about 1/5 second is considerably better than that of the cathodochromic tube. However, unlike the cathodochromic tube, the bistable storage target has no capability for gray-scale display. Due to its simplified structure (simple relative to earlier bistable tubes, but not as simple as the cathodochromic tube, which has

no flood guns), the price of video output devices using the tube is within reach of many computer users. One minor deficiency of the tube is that because the phosphor particles on the screen must be dispersed, brightness of the display is sacrificed. However, users quickly accommodate themselves to low brightness, and the other features of the tube have made it the current most widely used storage tube for computer output devices with graphics capability.

Silicon storage tube

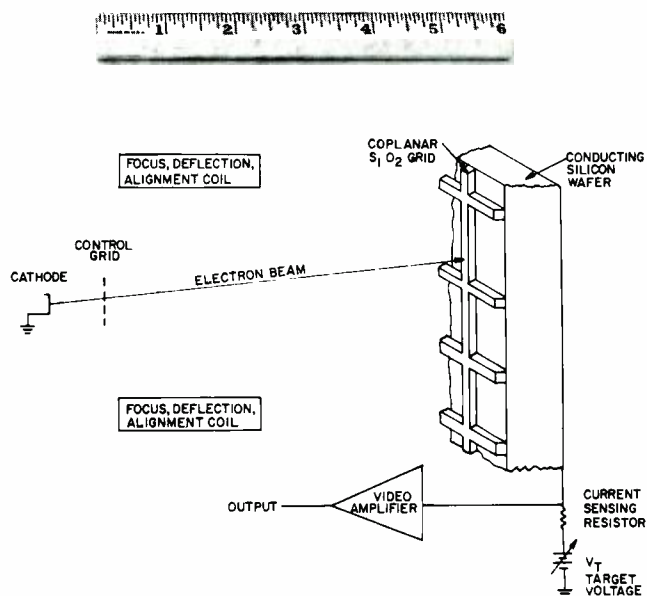
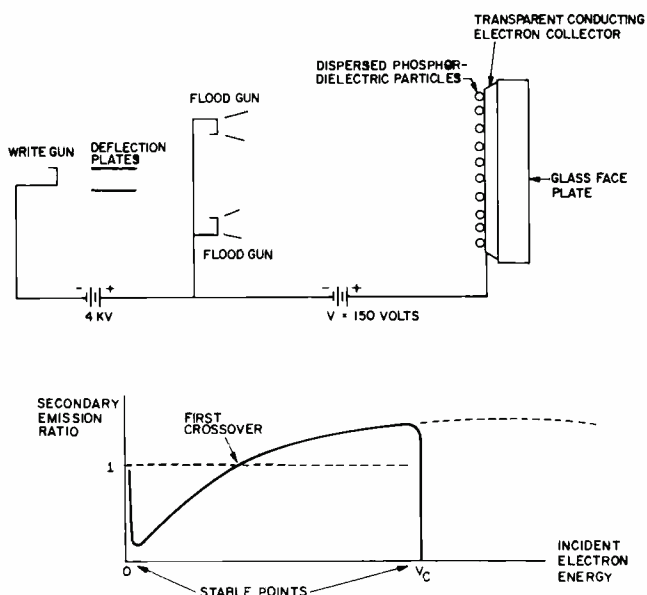
The silicon-target storage tube, a relative newcomer introduced only a year or two ago, looks and operates very much like a vidicon television camera tube. As such, it has many advantages compared to other types of storage tube. It is small in size, of rugged construction, and—most of all—low in cost. Even though both resolution and storage time are poorer than those of the first two types of storage tube discussed, the silicon tube in its short life has been the object of considerable activity. RCA and at least four other companies have manufactured the item. Fig. 6 shows an RCA one-inch diameter silicon storage tube. [The RCA silicon storage tube is similar in operation to the RCA Alphechon tube, which used an insulator-coated wire mesh for

Fig. 4—Structure of bistable direct-view storage tube (top left).

Fig. 5—Secondary emission ratio of an insulator near a reference potential, V_C (lower left).

Fig. 6—RCA one-inch-diameter silicon storage tube (top right).

Fig. 7—Structure of silicon storage tube (lower right).



storage.] One-and-one-half inch diameter tubes with correspondingly better resolution are also available. Much of the interest lies in the area of TV picture processing, but the tube has features that also make it attractive as a computer output device.

The basic operating principle of the tube⁸ is that a charge pattern is stored on a SiO_2 dielectric grid that is part of and approximately coplanar with the surface of a conducting silicon wafer. Figure 7 is a schematic of a silicon target and tube. Readout is like that in a vidicon, namely by the electron beam, which scans the target with a TV raster.

The charge pattern stored on the coplanar SiO_2 grid controls the amount of beam current landing on the conducting silicon wafer, thereby producing an electrical output signal, which can be amplified for display on a TV monitor. Writing, which consists of charging the SiO_2 positively, is done with the target raised to a potential above first crossover (refer to Fig. 5) so that the secondary emission gain of the SiO_2 under electron bombardment is greater than unity. Gray scale is obtained by modulating the electron beam current during writing. Erasure is done with the target biased below first crossover so that those areas to be erased are charged negatively by the electron beam down to cathode potential. Fig. 8 shows a read-erase-write cycle of the target. Notice that in the read mode the storage grid is negative relative to the cathode. Because of this, electrons do not land on the SiO_2 during readout, so the stored charge pattern can be scanned repetitively without discharging. In practice, however, the target is discharged after a few minutes of readout by positive ions, which come from residual gas atoms ionized by the electron beam. The readout time is a parameter that the tube designer can control. For example, by increasing the target capacitance (thinner SiO_2) readout time is increased, but so also is the time required to erase.

The silicon storage tube has a number of features that make it exceptionally versatile as a computer video-graphics output device:

- 1) Because the output is electronic, the stored picture can be displayed on a TV monitor having excellent contrast and brightness. Furthermore, multiple monitors can display the picture simultaneously.
- 2) The output signal can be processed

electronically for a variety of display applications such as superposition with live TV, broadcast over an RF channel, or slow-scan input to a facsimile printer, to name a few.

- 3) Stored graphics can be selectively erased.
- 4) In a tube designed for fast erasure, the entire stored image can be erased in 1/30 sec.
- 5) Gray-scale images can be stored and displayed.
- 6) Small regions on the target can be magnified by "zooming" the electrically variable raster scan.

In spite of its flexibility, the silicon storage tube is not yet widely used as a computer output device—primarily because of its limited resolution. There is a broad range of resolution performance claimed by the various manufacturers, and some of this range is due more to differences in measuring methods than in device quality. However, generally speaking, resolution of the 1-inch diameter tubes is comparable to that of standard television, and that of the 1½-inch diameter tubes a little better. Work is presently under way both at RCA Laboratories and by other manufacturers of the silicon tube to make computer terminals based upon it. The future is certain to see them in applications where flexibility and low cost are important, but resolution requirements do not demand the capability of the bistable direct-view tube.

Conclusion

Which tube makes the best computer video graphic output device? The price performance combination of the bistable direct-view storage tube has made it the solid front-running storage tube for today's general-purpose computer users. The cathodochromic stor-

age tube is both stronger than and weaker than the bistable one. In particular, resolution and storage time are better, but display size and erase time are not as good. As the use of computer video graphics increases, more special applications will emerge which will require the strong points of the cathodochromic tube and for which its weaknesses will not be serious limitations. Use of the silicon storage tube in computer displays can be expected to pick up in proportion to the adoption of computers by the general population. For such purposes, high resolution will not be mandatory; the versatility of the tube will be important; and its low cost will be a compelling advantage. One thing is certain: the growth of computer video graphics has returned storage tubes to the hierarchy of viable computer memories.

References

1. Rajchman, Jan. "Selective Electrostatic Storage Tube." *RC4 Review*, Vol. 12, (1951) p. 53.
2. Williams, F. C. and Kilburn, T. "A Storage System for Use with Binary-Digital Computing Machines." *Proc. Inst. Elec. Eng. (London)* Vol. 96, Part 2, (1949) pp. 183-202.
3. Haeff, Andrew V. "A Memory Tube." *Electronics* Vol. 20, No. 9 (Sept. 1947) p. 80.
4. Heyman, P. M., Gorog, I., and Faughnan, B. "High Contrast Thermal-Erase Cathodochromic Sodalite Storage-Display Tubes." *IEEE Transactions on Electron Devices*, Vol. ED-18, No. 9 (Sept. 1971).
5. *Instruction Manual for Type 601 Storage Monitor* (Tektronix Co.; Beaverton, Oregon; 1968).
6. Winningstad, C. Norman. "A Simplified Direct-View Bistable Storage Tube in Computer Output Applications." *Technical Session, Proceedings of the SID, Eighth National Symposium* (May 1967); 1971.
7. *Catalog for Tektronix Co.* (Beaverton, Oregon; 1971) p. 335.
8. Silver, R. S. and Luedicke, F. "Electronic Image Storage Utilizing a Silicon Dioxide Target." *IEEE Transactions on Electron Devices*, Vol. ED-18, No. 4 (April 1971).

Bibliography

1. Knoll, M. and Kazan, B. "Storage Tubes and Their Basic Principles." (John Wiley and Sons, Inc.; 1952).
2. Kazan, B. and Knoll, M. "Electronic Image Storage" (Academic Press; 1968).

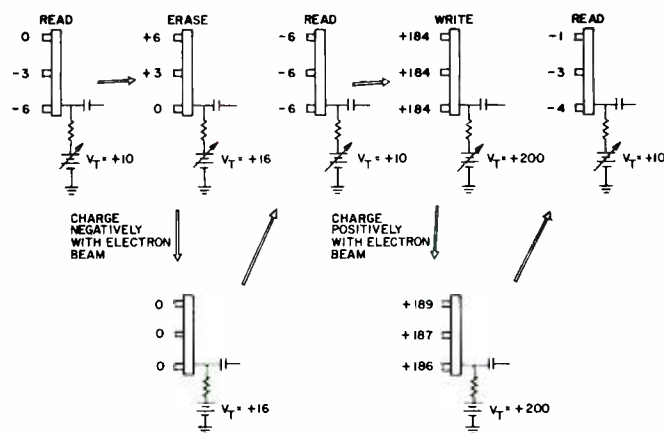


Fig. 8—Target of silicon storage tube in read, erase, write cycle (all voltages are relative to the cathode).

Display system using the Alphechon storage tube

F. Marlowe | F. Wendt | C. Wine

An exciting new display system based on an Alphechon storage tube has been built at RCA Laboratories. The Alphechon is a single-gun electrical-input electrical-output storage tube that was developed in 1968 by Ed Smith and co-workers of the Industrial Tube Division in Lancaster. The tube has a number of important features such as: standard television resolution, gray-scale capability, single-frame time writing and erasure of a complete stored picture, selective erase, and the structural simplicity of an ordinary one-inch diameter vidicon tube. This paper will begin with an indication of certain general types of display systems that require a storage tube. That will be followed by an explanation of how the Alphechon storage tube works, and that in turn by a description of the display system that was built using an Alphechon tube.

WHY USE A STORAGE TUBE? A television monitor requires as input 30 complete picture frames/second even if the displayed picture is not moving. In some applications, however, it is not possible to transmit 30 frames/second from a video source directly to a TV monitor. For example, the monitor may be part of a remote time-sharing terminal linked to a computer by a low bandwidth telephone line. You would like to have the computer display a still picture on the monitor, but the phone line does not have sufficient bandwidth to allow transmission of 30 frames/second. If a storage tube is included at the terminal, though, the computer can transmit over the phone line to the storage tube in a slow-scan mode. The storage tube stores the picture and then reads it out repetitively to the monitor at 30 picture frames/second. In this way, the monitor receives the proper input in spite of the bandwidth limitation on the telephone line. An additional benefit derived from the use of a storage tube is that once the computer transmits the picture to the storage tube, it can ignore that terminal insofar as the displayed picture is concerned until that picture is to be changed.

Reprint RE-17-6-12

Final manuscript received October 22, 1970.

A second type of display system that uses a storage tube is one in which a video source feeds a number of monitors over a common video line, but not all the monitors necessarily display the same picture. For example, the video source could be a computer in a stockbroker's main office in New York City and the monitors could be located in branch offices in towns between New York and Philadelphia. The cost advantage of using a common video line to link such widely separated terminals is apparent. In this example, the video source would continuously transmit frames of stock market information, each frame preceded by some coding so that a user located in one of the branch offices can select the frame that he wants. When the selected picture frame arrives, it is written into a storage tube, and thereafter until another frame is selected, that storage tube ignores the video line and reads the stored picture out to its monitor at a rate of 30 frames/second.

Although there are many other applications for storage tubes than those indicated above, we are primarily interested in those two, and in fact the display system that was built operates in both of the ways indicated. In particular it can accept random-scan inputs from a computer at slow scan rates over a telephone line, and it can accept single frame inputs of live TV from a video line.

Having justified the need for a storage tube in certain types of display systems, let us next consider the Alphechon tube.

How the Alphechon storage tube works

The Alphechon tube (Fig. 1) is structurally similar to an ordinary one-inch diameter vidicon. At the left end is the electron gun, while at the right end is the dielectric storage target. Deflection is electromagnetic and focus is a combination of electromagnetic and electrostatic. The aquadag coating that can be seen covering most of the inside of the glass is the electrostatic focus electrode.



Fig. 1 — Alphechon tube.

Charles M. Wine

Communications Research Laboratory
RCA Laboratories
Princeton, N.J.

received the BEE (cum laude) from the City College of New York in 1959 and joined the technical staff at RCA Laboratories. He has done some graduate work at Princeton University. At RCA Laboratories he has been involved in work in the following fields: psycho-acoustic subjective testing, the application of tunnel diodes to home instruments, ultra-high-speed tunnel diode logic and memory circuits and systems, high speed cryogenic logic elements and memory systems, read-only memories, character generators, and low cost displays for time sharing systems. Most recently he has been working on both hardware and software aspects of computer peripheral equipment and systems. Mr. Wine is the holder or co-holder of twelve issued patents with another dozen pending. He is a senior member of IEEE, a member of AAAS and ACM. He is also a member of Eta Kappa Nu and Tau Beta Pi.

Frank S. Wendt

Information Sciences
RCA Laboratories
Princeton, N.J.

obtained the BS in physics from the University of Richmond in 1949, after completion of active duty with the U.S. Navy as a radar technician. In 1950, he became a member of the technical staff of the RCA Laboratories, where he spent three years in the acoustical research laboratory. Mr. Wendt then joined a U.S. Government Agency for several years of classified work. In 1956 he became a member of the research staff of General Motors Corporation, developing electronic instrumentation for automated highways and automobile safety devices. After a short stay with a small electrohydraulic servomechanism company, Mr. Wendt returned to RCA Laboratories in 1959 where he has designed and built instrumentation and hardware for many diversified projects. Mr. Wendt has held membership in the Acoustical Society of America and the Audio Engineering Society and is presently a member of the IEEE. He has been granted two patents and has received an RCA Achievement Award.

Authors (left to right) Wine, Marlowe, and Wendt. Mr. Marlowe's biography is included with his other paper in this issue.



A schematic diagram of the internal elements of an Alphechon is shown in Fig. 2. The storage target is a wire mesh, or grid, covered with a thin coating of dielectric. The dielectric does not block the holes in the mesh so electrons from the cathode can pass through the grid. When the Alphechon is in the read-out mode, the surface of the dielectric is negative relative to the cathode with some regions being more negative than others in accordance with the stored image. The electron beam scans the target with a TV raster, and those regions of the target that are more negative allow less electrons to pass through the grid and conversely those regions that are less negative allow more electrons to pass. A potential of -6 V on the dielectric surface relative to the cathode prevents any electrons from passing through the storage target, so -6 V is the target cutoff potential. Electrons that pass through the storage target are picked up by the metal backplate and constitute the video output current, while those that are turned back are collected by a separate grid called the collector grid.

An important point is that in the read mode, since the entire dielectric surface is negative relative to the cathode, no electrons from the cathode actually land on the storage target. Thus, the read-out mechanism is nondestructive. However, the vacuum inside the tube is not perfect so there are gas molecules present. Some of the gas molecules are ionized by collisions with electrons and some of the positive ions thus formed land on the negative storage target. By this means, a stored picture is gradually washed out during read out. Stored gray-scale pictures have been read out continuously for as much as one half hour without objectionable deterioration and stored digital black-and-white pictures can be read out continuously for over one hour without objectionable deterioration.

To see how a stored picture is erased and written, first notice in Fig. 2 that the storage grid is connected to a voltage source, V_T , by a resistor and then refer to Fig. 3. In Fig. 3, the storage dielectric and V_T are shown for the three modes of operation: read, erase, and write. In the read mode, Fig. 3a, the dielectric surface is negative relative to the cathode, as explained above, and V_T equals 30 V. To erase, V_T is increased by 6 V to 36 V and capacitive

coupling causes the dielectric surface also to increase by 6 V. This situation is shown in the lower part of Fig. 3b. Notice now that all parts of the dielectric surface are positive (or zero in the limiting case) relative to the cathode so electrons from the cathode will land on the target, charging those areas where they land negatively down to cathode potential. If the entire stored picture is to be erased, the beam scans the target with a TV raster; alternatively, if only selected portions of the target are to be erased, the beam scans with a random or selective scan. The upper part of Fig. 3b shows the storage dielectric in the erase mode after the dielectric surface has been charged down to cathode potential. At this point if the Alphechon were returned to the read mode by returning V_T to 30 V, the erased regions would be at -6 V—the target cutoff potential.

Writing is done by secondary emission. If electrons are made to strike the dielectric surface with sufficient energy, more electrons will be kicked back out than originally arrived at the dielectric. In this way, the target can be charged positively by a beam of negative electrons. Electrons are given high impact energy by raising V_T to $+200$ V. Again capacitive coupling causes the potential of the dielectric surface to increase, in this case to about 170 V—a value well above the secondary-emission unity-gain crossover voltage (refer to the lower part of Fig. 3c). If a complete TV frame is to be written into the Alphechon, the beam scans the target with a TV raster and the video input appears as beam-current modulation, thereby controlling the amount of positive charge deposited at each point of the target. Alternatively, if input is to be by random scan—and this is what is meant by random scan—the beam position is made to jump from point to point. While the beam position is moving, the beam current is blanked off. Then when the beam position is steady at a point, the beam current is unblanked long enough to write a dot at that point. In this way, lines of random length and direction can be drawn as sequences of dots. The upper portion of Fig. 3c shows a possible configuration of the storage dielectric after writing is completed.

To summarize the operation of the Alphechon tube: in the read mode no electrons land on the storage dielectric;

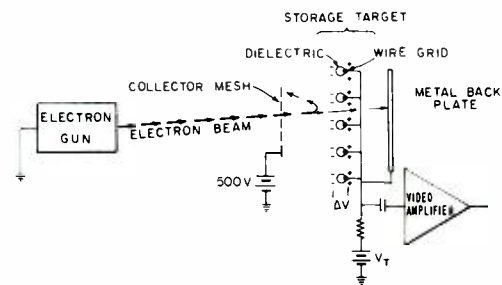


Fig. 2—Alphechon tube in the read mode.

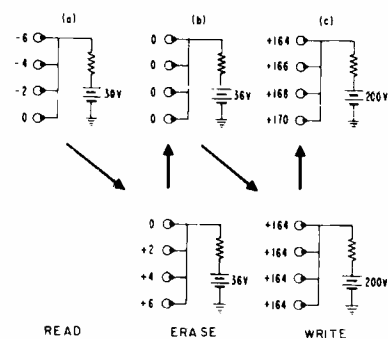


Fig. 3—Alphechon target during read-erase-write sequence.

in the erase mode the dielectric is charged negatively down to cathode potential; and in the write mode it is charged positively by secondary emission.

Display system using the Alphechon

The display system that was built is shown in block-diagram form in Fig. 4. An operator at a keyboard communicates with the computer via an acoustic coupler and telephone line. The computer sends back instructions in ASCII code to the vector generator, which interprets these instructions as control signals for the Alphechon and deflection levels for random scan. For purposes of this discussion, the vector generator can be considered to be a black box that delivers the proper control signals to the Alphechon control circuitry.

Part of the Alphechon control circuitry is the scan selection scheme shown in Fig. 5. Either TV scan or random scan can be selected by closing the appropriate switch to ground. These switch closures to ground are done electronically under control of the vector generator. If TV scan is desired, the center pair of analog gates is turned on and horizontal and vertical voltage ramps are fed to the horizontal and vertical deflection amplifiers. Alterna-

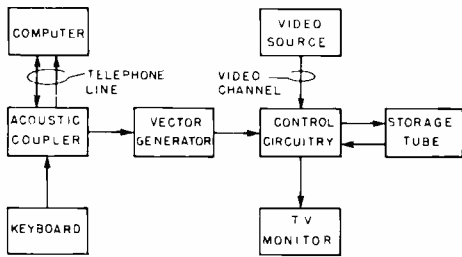


Fig. 4—Block diagram of flexible display system.

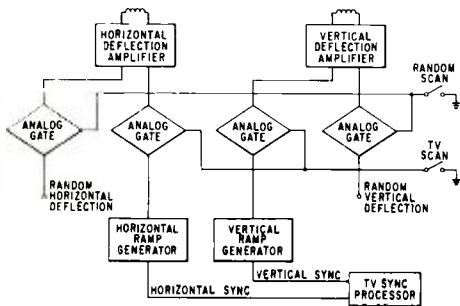


Fig. 5—Scan selection scheme.

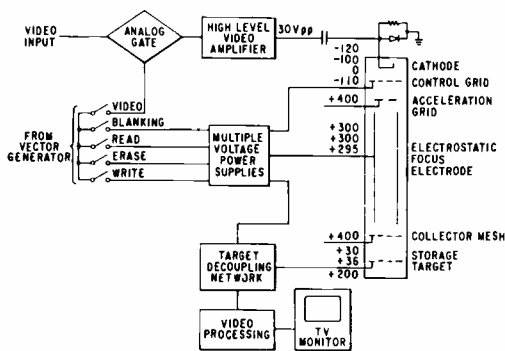


Fig. 6—Alphechon electrode biasing circuitry.

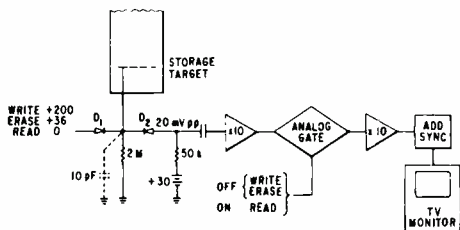


Fig. 7—Target decoupling and video processing.

tively if random scan is required, the outer pair of analog gates is turned on and deflection levels from the vector generator are fed to the deflection amplifiers. The deflection amplifiers cannot be of the resonant type normally used in televisions but must be DC amplifiers due to the requirements of random scan.

Also included in the Alphechon control circuitry is the electrode biasing circuitry shown in Fig. 6. When a frame of video is to be written into the Alphechon, the video input is gated into a high-level video amplifier. The output of this amplifier is fed to the cathode of the Alphechon by means of a diode DC restorer. Also from the vector generator are controls for blanking, read, erase, and write. These controls go to multiple-voltage power supplies which set the electrode voltages for each of the modes. The only electrode that is negative is the control grid which ranges in voltage from -120 V for beam-current blanking to 0 volts for maximum beam current. Maximum beam current, incidentally, is required to erase an entire stored picture in a single TV frame time. In the description of how an Alphechon works, the voltages applied to the storage target were explained. Both the acceleration electrode and the collector mesh are maintained at $+400$ v DC. The only remaining electrode is the electrostatic-focus electrode which is normally held at $+300$ V, but is decreased to $+295$ V when the Alphechon is in the write mode. The reason for the change during writing is that in the write mode the storage target is raised from $+30$ or $+36$ V (read or erase modes) to $+200$ V—a voltage increase that is high enough to perturb the electron trajectory and defocus the beam. Consequently, to keep the beam in focus during writing, the electrostatic focus voltage is decreased by 5 V when the Alphechon switches to the write mode.

Notice that none of the voltages applied to the Alphechon is exceptionally high, and all of the voltages that must be switched are low enough to be handled by ordinary transistor switching circuits.

The target decoupling network and video processing circuitry are shown in Fig. 7. In the read mode, the video amplifier senses millivolt signals, but

when the Alphechon switches to the erase or write modes, a large voltage step amounting in the latter case to nearly 200 V is applied to the target. To protect the sensitive video amplifier from these large voltage steps, it must be decoupled from the target whenever the Alphechon is switched out of the read mode. This decoupling is done by diodes D_1 and D_2 shown in Fig. 7. The voltages for each of the modes applied to D_1 are shown at the left. In the read mode, D_1 is turned off and D_2 is turned on by the 30-V source and 50-k Ω resistor. Then in the erase and write modes, D_1 is turned on, turning D_2 off. Clearly, only in the read mode is the video amplifier coupled to the target by D_2 biased on.

The decoupling network, however, introduces an additional problem. When D_2 turns off, the current in the 50-k Ω resistor also turns off producing an IR drop at the input to the video amplifier amounting to about 1-V. Although a 1-V step is not enough to damage the video amplifier, it is enough to drive some of the later stages of gain into saturation or cutoff. The problem is that the recovery time is too long—tens of milliseconds—if the Alphechon is to be used in a time-sharing computer terminal. Information to be written into the Alphechon arrives at the terminal over a telephone line at slow scan rates, so it may take several seconds to write a complete picture. However, during much of that time, the Alphechon is not actually writing but merely waiting for inputs to arrive. It would be best if the Alphechon could remain in the read mode while it was waiting for inputs to arrive and switch to the write mode momentarily only when actually writing. The result would be that the viewer has the impression that new information is being written into the Alphechon simultaneously while the stored picture is being read out. A typical duty cycle for such operation is 1 ms of write followed by 10 ms of wait, followed in turn by 1 ms of write, etc. Clearly if the video amplifier takes more than 10 ms to recover from the write mode, no signal information will pass thru the video amplifier. This problem was solved by inserting an analog gate in the middle of the video chain as shown in Fig. 7. In the read mode, the gate is on, allowing video to pass; in the erase and write modes, the gate is turned off, preventing the later stages from saturating.

There is one remaining problem: the bandwidth limitation imposed by the 10 pF of stray target capacitance. To develop a voltage with good signal-to-noise ratio, the 50-k Ω current sensing resistor is required. However, 50 k Ω in parallel with 10 pF gives a cutoff frequency of only about 300 kHz. Consequently, the video amplifier must be strongly peaked at the high frequencies to give the overall video processing system a bandwidth of 4 MHz.

The screen of a TV monitor displaying a resolution test pattern that is stored in the Alphechon tube is shown in Fig. 8. The resolution is 300 TV lines vertically by 400 TV lines horizontally. Fig. 9 is a stored gray scale picture that was entered into the Alphechon in a single TV-frame time using live TV as a video source.

An example of computer-generated text is shown in Fig. 10. These letters were written into the Alphechon using the random-scan mode whereby each line is composed of a sequence of closely spaced dots. The characters originated in a software character generator in the computer and were transmitted to the Alphechon time-sharing display terminal by telephone lines.

Some simple computer generated graphics are shown in Fig. 11; Fig. 12 shows the same stored picture with one line selectively erased. Selective erase also used a random scan, but in this case sequences of closely spaced dots are erased instead of written.

It is an easy matter to combine a stored gray-scale picture with computer generated text or graphics by superimposing both types of input on the storage target. First the gray scale input is entered into the Alphechon using TV scan; then the computer input is written over the stored gray-scale picture using random scan. The computer input can consist of either white or black lines depending on whether the Alphechon is biased in the write or erase mode respectively at the time the inputs are entered.

Another feature of the Alphechon display system is that a stored still picture can be combined electrically with a moving TV picture. For example, a printed subscript stored in the Alphechon can be added to a live TV transmission.

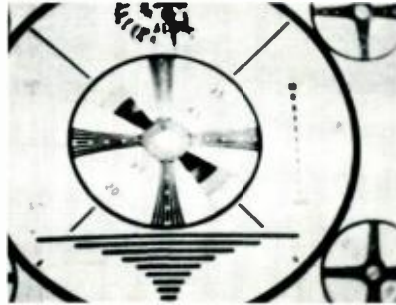


Fig. 8—Stored resolution test pattern.



Fig. 9—Stored gray-scale picture.

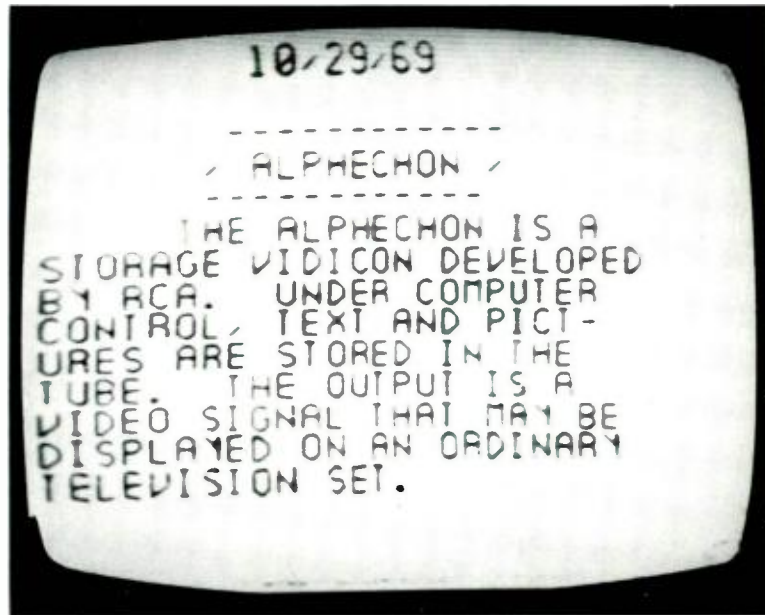


Fig. 10—Stored computer-generated text.

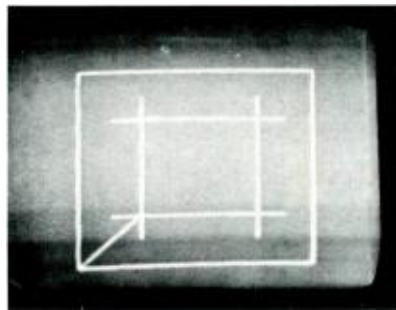


Fig. 11—Computer generated graphics.

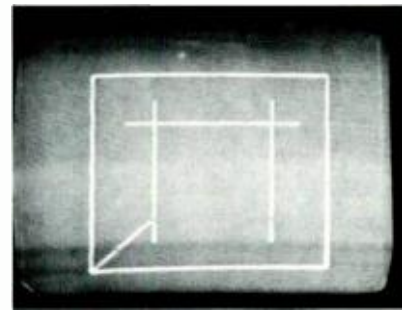


Fig. 12—Same as Figure 11 with a line selectively erased.

Summary

A display system based on the Alphechon storage tube has been built that can operate as: 1) a time-sharing terminal linked to a computer via telephone line, 2) a video single-frame freeze, or 3) a combination of both. The display has TV resolution, gray-scale

capability, ability to write or erase a complete stored picture in a single TV frame time, and selective erase. The system demonstrates that the Alphechon, due to its structural simplicity and modest addressing requirements, could be the store in a flexible low-cost display terminal.

Data storage and retrieval device for aircraft

P. L. Nelson | R. H. Norwalt

A multimode storage and presentation system capable of handling both video and audio information has been developed to provide necessary flight information to a pilot. The audio portion of the system is a voice-response system suitable for pilot warning, automated oral landing/take-off instructions, and weather and air traffic broadcast. The video consists of fixed format data such as maps, charts, drawings, and alphanumeric text which can be presented in real time. The storage and presentation system was configured based on the combination of a TV raster display, a digital code-to-analog converter, and a random-access optical ROM. A holographic rom implementation was chosen for image stability and resolution requirements. Lenseless Fourler transform recording is used; readout is with parallel light. Dust and scratch immunity are provided by hologram redundancy. A HeNe laser provides the readout beam; access and display time is less than 0.1 second to any one of 100 holograms in an x-y matrix on a storage card.

AS OPERATOR/MACHINE INTERACTION becomes more vigorous, increasing processor time will be required to effect data transfer to the operator. Much of this information will be in the form of fixed data such as charts, tables, drawings, audio instructions, and archival documents. At present, this type of data is stored in digital form in large disc files which must be connected through buffers to the operator's console.

To reduce the storage cost and control time required to provide an operator with a page of information, low-cost multimode storage and presentation systems are required. Such systems must be capable of producing data on the operator's console with minimal address and routing information. In addition, these systems should be able

Reprint RE-17-6-7
Final manuscript received February 24, 1972.

to display real-time alphanumeric and graphic data in conjunction with the fixed format audio and video data.

A specific example of this type of equipment need is found in a pilot information system. To meet the increased system requirements resulting from higher vehicle speeds and greater vehicle complexity, data on critical vehicle performance parameters must be provided when these parameters are either being exceeded, or are in danger of being exceeded if existing conditions continue. A vocal instruction or a group of instructions directing the pilot's attention to the monitor at such time would be desirable. The system monitor should also be capable of presenting real-time alphanumeric information provided by an on-board processor or from a ground-based data bank. And presentation of selected video data in the form of landing patterns and profile

charts is also highly desirable.

System approach

The system is based on the combination of a TV raster display, a digital-code-to-video converter, and a random-access optical read-only data store. This configuration requires only the monitor itself to be located within the operator's immediate area; all ancillary components may be located in more favorable areas.

This approach was chosen because of the multimode nature of the fixed data and the need to present real-time changing alphanumeric and graphic information. The optical random-access read-only memory (ROM) can provide both video and fixed alphanumeric information with a minimum of external control data. It is also possible, utilizing a slow-scan mode on the video sensor, to play back audio messages stored in the same



Perry L. Nelson (left)
Design and Development Engineering
Advanced Technology Laboratories
Van Nuys, California

received the BS in physics and mathematics from St. Olaf College, Minnesota, and did graduate work in physics at Montana State University. While at RCA, Mr. Nelson has been actively engaged in research and first-stage design of new projects. He has been engaged in programs such as a near-surface burst capacitive fuze for bombs, an optical fuze employing GaAs laser diodes and optical portions of a signaling system for submarines. Following this, Mr. Nelson studied possible uses of piezoelectric ceramics in the Ordnance area. He developed and tested a unique piezoceramic sensor and has done work on a solid-state piezoelectric transformer and a piezoelectric S&A device. In 1970, he became active in the area of voice-response techniques. This project includes a holographic storage and he has specifically been responsible for the holographic facility and research leading to a random access non-movable store of audio and video information.

R. H. Norwalt, Ldr. (right)
Advanced Technology Laboratories
Van Nuys, California

joined RCA after receiving his undergraduate degree from the University of Southern California in 1961. Before 1961, Mr. Norwalt was actively involved in the design and development of magnetic drum memory systems and associated solid-state control circuitry for Litton Industries and Magnavox Research Laboratories. From 1962 through 1964, he was responsible for the design and development of several memory systems. During 1965 and 1966 he was responsible for specialized military displays and the EASD display research and development programs. From 1966 through 1969, as Leader of the Military and Advanced Displays group, he was responsible for a number of special Military video display systems as well as for the development of a low-cost Military alphanumeric/graphic video display system. He is presently responsible for the development of advanced techniques for optical memories and large-scale solid-state integrated circuitry. Mr. Norwalt holds a patent on a semiconductor-controlled pulse shaper and has a number of disclosures pending. He is a member of the Society for Information Display and American Management Association.

memory. The digital-code-to-video alphanumeric converter is used in conjunction with the fixed memory in an information update mode. Standard message formats can be stored in the ROM with blank spaces for changeable data insert. In this manner, only the address of the format and the changeable data codes are required. This significantly reduces the amount of data which is required of the processor to present a complex display.

System description

The multimode data storage and presentation (MDSP) system (Fig. 1) was designed to operate under the control of a central on-board processor. This processor, which generates requirements for both fixed and real-time data, will direct the appropriate data to the data control module. The display may therefore operate in a number of modes; operation in a warning mode and in an information mode is briefly described.

Warning mode

In the vital-data or warning mode, a signal from the processor, representing data requiring immediate attention or a specific out-of-tolerance condition, will be fed into the data control module. This module will determine by word structure that a warning sequence will be initiated. This sequence may consist of an audio alert followed by a visual message presented on the cockpit display. In the event that a message of higher priority is sensed, the previous message is interrupted and the new one presented in its place.

Information mode

In the information mode, which may be the result of an operator inquiry or a data transmission, a control word is fed to the data control module which determines the subsequent sequence from the word structure. The data control module first selects the desired fixed format, either text or pictorial data, from the ROM. It then requests the variable or update information from the processor. This information is then supplied to the digital-code-to-video alphanumeric converter from either the processor or the data link. The output of the converter is fed through the video mixer and is presented on the display.

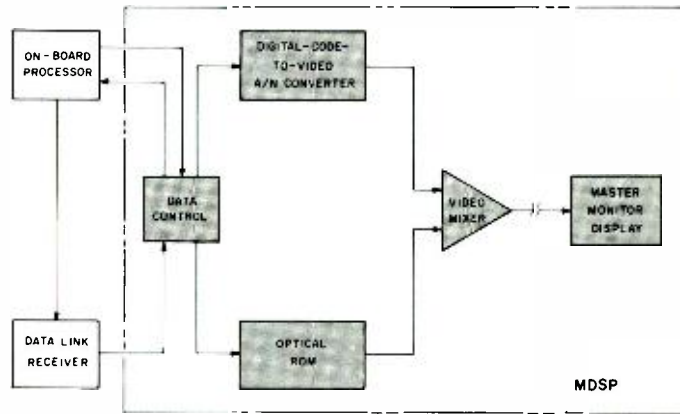


Fig. 1—Multimode data storage and presentation (MDSP) system, block diagram.

Optical storage and retrieval sub-system

Requirements

The function of the optical storage and retrieval subsystem (the optical ROM) is to provide the basic fixed memory for the system. It provides the high density random access storage required to reduce storage cost and size and control time. In providing this memory function, it must be capable of satisfying several requirements, the most basic of which is multimode storage. The information to be stored in the memory will be of two types: stationary video and audio. Stationary video data consists of charts, tables, landing patterns, and drawings. Audio data consists of vocal directives and instructions. This information is stored in a format which is randomly accessible by the data control module.

The information shown on the monitor of the MDSP system must remain stable even though the remote storage unit is subjected to vibration and shock.

Image redundancy is required to limit the loss of information due to scratches and dust. The optical memory design should utilize a minimal number of parts and provide for an easily expanded storage capability.

Design approach

To satisfy the requirements for high density multimode storage with random-access capability, a coherent optical approach was selected. This approach, which utilizes a deflector-addressed two-dimensional matrix of holograms, features rapid access without mechanical movement, insensitivity to dirt and scratches, and image stability at the sensor.

There are many types of holograms. Each of these may be classified as one of two generalized types, near-field and far-field. Image redundancy may be achieved with either type, but image stability is achieved only in the far-field type of recording. This type of hologram, which includes both Fraunhofer and Fourier-transform holograms, is

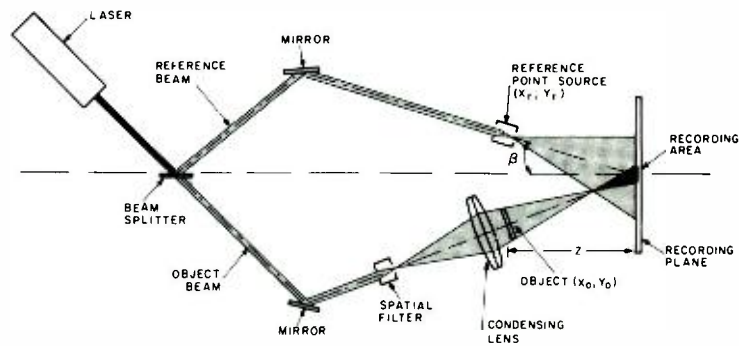


Fig. 2—Fourier transform recording geometry.

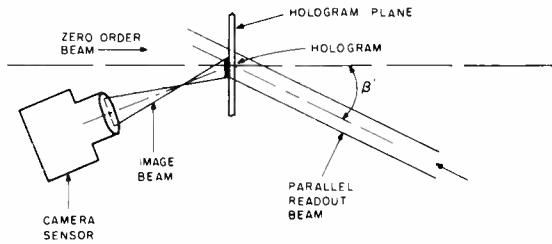


Fig. 3—Readout of lensless Fourier transform holograms utilizing parallel light.

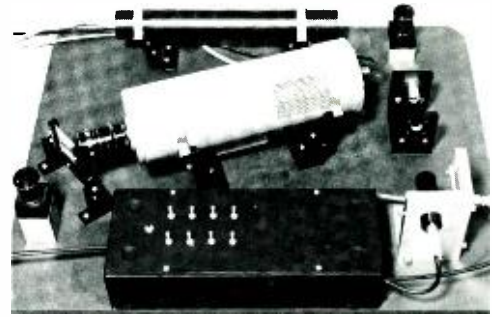


Fig. 4—Breadboard holographic payout unit.

recorded in such a manner that the object appears to be at infinity relative to the storage medium. Small movement of the medium during payout is thus irrelevant. To minimize the complexity of the playback system, Fourier-transform holograms were chosen for the storage and retrieval subsystem.

A typical physical setup for recording holograms of the lensless Fourier transform type is shown in Fig. 2. The beam from the laser is divided at the beam splitter into reference and object components. The object beam is spatially filtered and expanded. At some point, this light is collected by a lens and focused through the object toward the recording plane. The reference beam in this case is a spherical wave diverging from a point source coplanar with the object. The spherical wavefronts of the object and reference waves form a linear grating pattern when they inter-

sect at the film plane. The recording medium thus sees an approximately constant-spatial-frequency grating formed for each object point. This is an approximation of a true far-field hologram that has been achieved without the aid of a transforming lens. Resolution of Fourier transform hologram is theoretically very high, since the recording is not resolution limited by any lenses between the object and film. However, when a grating is used to provide redundancy with a transparent object, the resolution is determined by the period of this grating.

Readout of a Fourier transform hologram is possible in one of two ways: 1) with parallel light and an appropriate lens, or 2) with the conjugate of the original reference beam and no lens. The parallel light readout was chosen because it could be implemented with a simpler lens system.

Fig. 3 shows a readout schematic for Fourier transform holograms using parallel light. The hologram is illuminated with parallel light from the side opposite to that originally exposed by the object and reference beams. The angle β' which the payout beam makes with the hologram center line must be equal to the construction angle β (Fig. 2) which the reference beam made with the hologram center line. The reconstructed object wavefront is projected in space toward the position of the original object, but focused at infinity. Placing a positive lens at some place in this wavefront causes an image of the original object to be formed in the focal plane of the lens.

Parallel light payout is an approximation of the divergent reference beam used in construction. Because of this approximation, during construction the total angle that the recorded hologram subtends with the point reference source must be small (generally less than 10°).

Readout breadboard

A breadboard model of a payout unit, capable of addressing a matrix of holograms and detecting the reconstructed image, was designed and built. It incorporates a small HeNe laser, expansion optics, two piezoelectric deflectors for x-y address, a matrix of holograms, and a TV camera. The completed model is shown in Fig. 4.

The HeNe laser is capable of 1.5 mW of single-mode output power. The beam is expanded and recollimated to a diameter of approximately 2.4 mm. The two piezoelectric deflectors then direct the beam to the hologram matrix. The image wavefront from the selected hologram is reflected from a stationary mirror into the collecting lens of the camera. A remote monitor then displays the reconstructed image.

The expansion optics are a 20X microscope objective and a simple collecting lens. The deflectors are based upon the principle of deflection of a piezoceramic beam when voltage is applied across the material. A mirror is attached to the end of piezoceramic material and is deflected through an angle in response to the applied voltage as shown in Fig. 5. Each deflector produces a scan, the length of which is directly proportional to the amplitude of the 60-Hz sinusoidal voltage applied.

A ± 50 Vp-p signal achieves a total deflection angle of 4.5° . This is enough deflection to address a 1-inch-square matrix of 100 holograms. The deflection circuitry is capable of address times of 250 μ s.

Position selection must be accomplished because of the AC scan. This can be done by placing a simple light modulator operating in an on-off mode at some position in the beam and synchronizing with the deflectors and the camera.

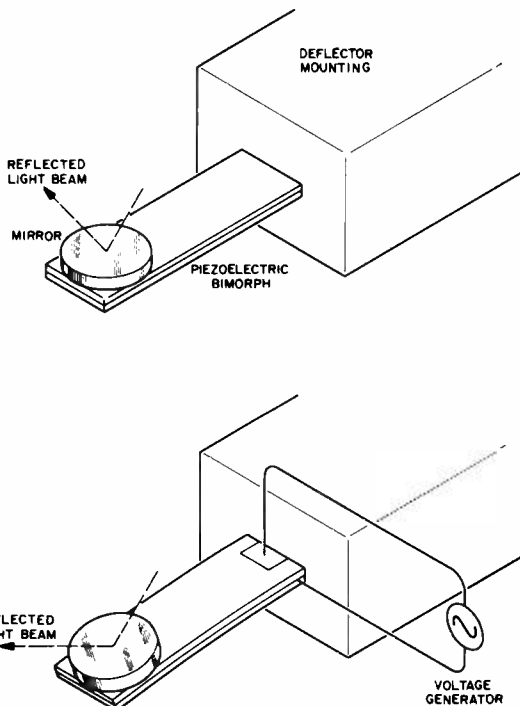


Fig. 5—Piezoelectric deflector.

The total access and display time is considerably greater than 250 μ s. This is due mainly to the mechanical movement of the piezoelectric deflectors. The initial address voltage must overcome the mechanical inertia of the deflector beam. The movement of the deflector must then be allowed to stabilize after an initial overshoot of the desired location. The total time required for a stable image on the display screen is now approximately 0.1 second.

At present, the pickup sensor is an RCA PK-501 camera. The standard vidicon may be replaced with a slow-scan vidicon to accommodate slowly scanned audio information.

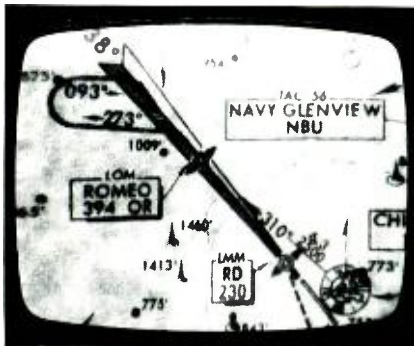


Fig. 6—Hologram of approach chart reconstructed on TV cockpit monitor.

Information recording and readout

The information to be stored in the holographic memory is both audio and video. The recording of the video information is accomplished in two steps. A positive transparency of the desired information is reduced to the required object size and a hologram is then made of this object. Fig. 6 shows an approach chart, after reconstruction, on a cockpit monitor.

There are several requirements placed on the audio information before it is stored in holographic form. It must first be recorded on film in an area and format which is compatible with the desired hologram information areas. A transparency in the correct object size is then made of this information format, and a hologram is again formed from this object/transparency.

The hologram matrix consists of square information areas (see Fig. 7). The audio information must therefore be

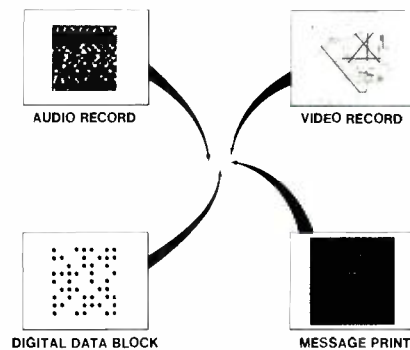


Fig. 7—Hologram matrix.

stored in a raster scan format of parallel lines. The audio is presently limited to voice messages one to three seconds long per information area.

Several methods can be used to form the master audio record; the most common of these are density, frequency, and amplitude modulation. The audio is recorded by modulating, with the desired audio information, a light beam which is raster scanning a recording film. Due to the limitations of the equipment available to affect the recording, amplitude modulation and frequency modulation were hampered by low signal-to-noise and distortion. Density-modulated recording provided a greater signal-to-noise ratio and less distortion. A typical audio record is shown in Fig. 8.

Readout of an audio hologram is accomplished by first addressing that hologram in a matrix. The stored audio format is restored on the face of the vidicon. The vidicon is modified so that the readout beam serially traces the lines of information. This information is then restored through a loudspeaker.

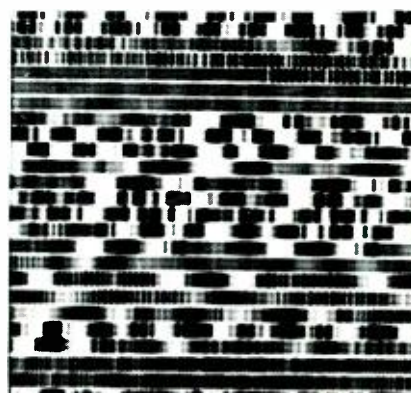


Fig. 8—Audio record.

The actual recording of density-modulated audio was accomplished with a camera and a modified Tektronix 535 oscilloscope. The oscilloscope was modified so that its beam intensity can be modulated by the desired audio information. The x and y yoke drivers were also modified to enable the beam to write 30 parallel lines on the oscilloscope face. Each line was 33 ms long, thus giving a 1-second density-modulated message. A picture was taken of this format as it was being written on the oscilloscope face, and was later reduced to the desired positive transparency.

Preliminary readout evaluation of the recorded audio was performed by placing the picture negative on the face of the Tektronix 535 oscilloscope and tracing the lines of audio information with an unmodulated beam. The playthrough beam, modulated by the information on the negative, was detected by a photodiode, amplified, and analyzed. Results of this evaluation indicate that highly intelligible audio can be obtained with a bandwidth of 2.5 kHz (50 Hz to 3.0 kHz).

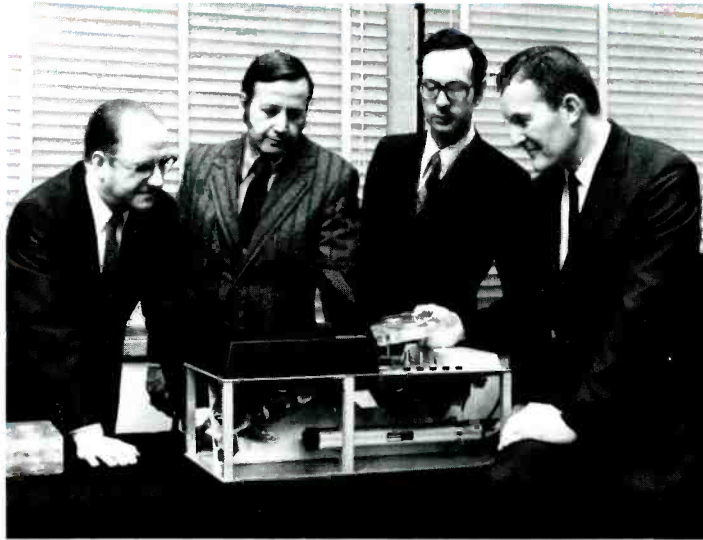
Distortion can be kept negligible only if the registration between the tracing beam and the recorded information line is kept accurate. One method of providing registration is to record a single frequency signal on both the top and bottom of each information line. These frequencies act as negative feedback to the drive circuitry of the tracing beam, forcing the beam to accurately follow the information line.

Readout of an actual audio hologram requires the readout vidicon to trace the lines of audio displayed on its face. This is accomplished by modifying the deflection circuitry of the vidicon so that the beam is capable of tracing the same format in which the audio is written.

Conclusion

The multimode data storage and information system is capable of presenting in-flight audio or video information to a pilot. Only the monitor and loudspeaker are located in the cockpit with all other components located elsewhere in the aircraft. This feature allows room for system expansion; the ROM-storage approach provides both the capacity and the flexibility.

Team Award in Science



Robert E. Flory, Robert J. Ryan, Michael J. Lurie, William J. Hannan



Dainis Karlsons (posthumous award)

For outstanding technical leadership of a large team in the successful development of a holographic prerecorded video system.

Messrs. **Hannan, Flory, Karlsons, Ryan,** and Dr. **Lurie** of RCA Laboratories, Princeton, N.J., led a large team that pioneered the development of holotape, a system for playing low-cost color movies through a home TV set. This research involved developing a material for recording surface-relief holograms, and developing processes for recording color-encoded object transparencies, for recording highly redundant holograms, for fabricating metal-master tapes, for embossing holograms on low-cost vinyl tapes, and finally designing and constructing a player to demonstrate overall system performance.

Among the technical firsts accomplished by this team are: first to replicate holograms by an embossing process, first to record highly redundant speckle-free holograms, first to demonstrate flicker-free movies from continuously moving Fraunhofer holograms, first to demonstrate a two-beam vidicon (Bivicon) camera, and first to demonstrate embossed-groove stereo sound track.

Because of its stop-action and variable-speed capabilities, the holotape system has good potential in audio-visual systems for instruction and training. As a result of holotape research, the Aerospace Systems Division in Burlington, Mass., has obtained several holographically oriented contracts, e.g., "Moving Map Display." Also, the Bivicon camera developed for this system may find use as a low-cost color camera for live pickup when used with a magnetic video tape recorder or for use in "professional" color cameras or film chains for slides or film.

Messrs. **Burke, Dietz,** and **Neilson** of Solid State Division, Somerville, N.J., and Messrs. **Grundmann** and **Lemke** of Consumer Electronics Indianapolis, Ind., have conceived, designed, and implemented a new solid-state horizontal deflection system. This effort has enabled RCA to move aggressively into all-solid-state TV instruments, establishing a leadership position in the field. The development of a successful solid-state horizontal deflection system had been a major stumbling block, requiring new directions in devices and circuitry for uncompromised instrument performance, competitive cost, and improved reliability. These goals were met. Following RCA's lead, these deflection innovations are being adopted by other instrument manufacturers around the world. The availability of a deflection system with unlimited energy capability has been a contributing factor to kinescope and yoke developments presently underway.

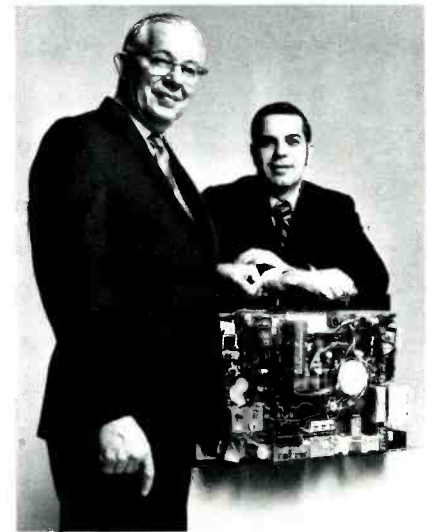
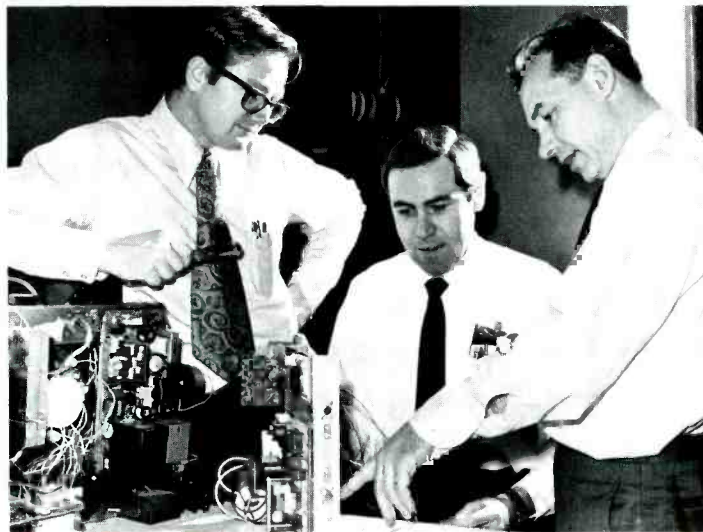
While the original role for thyristors (as opposed to competitive transistor systems) was originally relegated, because of apparent cost and circuit complexity, to large-screen wide-angle color, the inherent reliability, reproducibility, and total systems cost have made SCR deflection a contender for smaller screen color and even black and white. All RCA solid-state color sets have used SCR deflection and, while still early, the field history shows the promise of significant improvement over tube systems.

In addition to use within RCA, substantial business is developing through other equipment manufacturers who may purchase components from the Solid State Division. In addition there is potential for patent royalty revenue where RCA has a strong position.

For the highly successful development of the thyristor horizontal deflection system and required components for television receivers.

Donald E. Burke, John M. Neilson, Wolfgang F. Dietz

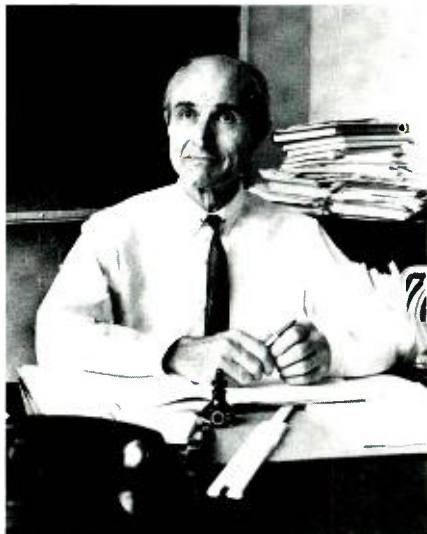
Gustave L. Grundmann (retired) and Eugene Lemke



Team Award in Engineering



Individual Award in Science



Edward G. Ramberg

Dr. **Ramberg** of the RCA Laboratories, Princeton, N. J., has—throughout an entire career spanning 30 years—applied his knowledge of theoretical physics to important practical developments in electron microscopy and electron optics.

His extensive work on holography, intensely pursued in the last three years, is a characteristic example of Dr. Ramberg's work. He has contributed greatly to the understanding of a variety of possibilities and limitations of holography—e.g., grain-size and its connection with resolution; "speckle noise", its origin and mitigation; optical aberrations versus resolution; 3D-color-storage in thick hologram-recording media, and the general theoretical characteristics of holographic systems designed to supply optical magnification.

Also, in the development of thermoelectric semiconductor materials and their application to heat-transfer systems, Dr. Ramberg is RCA's foremost theoretical expert. As such, he translated solid-state physics into practical guides, helping experimenters in this field choose their exploratory course and defining the physical limitations which set absolute bounds to optimism in the search for the ultimate in efficient thermocouple materials.

His most prolific field of endeavor has been in the development of cathode ray tubes in all of their forms: electron microscopes, kinescopes, TV cameras, electron multipliers. This activity spans his entire career, and it continues today with recent contributions to the theory of manufacture of still better dichroic filters. He has also contributed much to the design of better luminescent screens.

But his greatest contributions, by far, have been a continuous stream of theory and practical applications and inventions in the area of electron optics.

In honor of an entire career of uncommonly valuable theoretical and practical contributions in fields of importance to RCA.

The 1972 David Sarnoff Outstanding Achievement Awards

RCA's highest technical honors, the annual David Sarnoff Outstanding Achievement Awards, have been announced for 1972. Each award consists of a gold medal and a bronze replica, a framed citation, and a cash prize.

The Awards for individual accomplishment in science and in engineering were established in 1956 to commemorate the fiftieth anniversary in radio, television and electronics of David Sarnoff. The awards for team performance were initiated in 1961. All engineering activities of RCA divisions and subsidiary companies are eligible for the Engineering Awards; the Chief Engineers in each location present nominations annually. Members of both the RCA engineering and research staffs are eligible for the Science Awards. Final selections are made by a committee of RCA executives, of which the Executive Vice President, Research and Engineering, serves as Chairman.

In recognition of his outstanding technical leadership in building RCA's pre-eminence in the field of radar and defense systems.

Dr. **Weinstock** of the Missile and Surface Radar Division, Moorestown, N. J., has made technical contributions to the development of the radar and the weapon system for the AEGIS program. Initially serving as technical director of the RCA/Martin preliminary study, his technical judgment prompted the contracting agencies to request that he become consultant to the Navy on this program. His excellence as the RCA system representative in this effort was a major factor in RCA's ultimate acquisition of the \$250 million AEGIS contract, which could develop into the largest defense contract RCA has ever received. In 1968, he assumed the technical direction of the RCA/Raytheon/Bendix team during the formal contract definition phase. After the contract was awarded in 1968, Dr. Weinstock directed the DoD-initiated AEGIS System Simplification study. He was called upon to perform in this role as the only individual within RCA who had both the technical knowledge and the management perspective, coupled with the capability of interfacing with his counterparts in the Navy. He is currently the key technical focal point within RCA and to the Navy for the basic AEGIS system design.

From 1965 to 1968, Dr. Weinstock served as senior technical consultant on a number of the advanced systems studies. This effort covered the preliminary design and analysis of midcourse and terminal measurement systems, and active and passive intelligence sensors.

Dr. Weinstock has developed a considerable national reputation in the radar community not only for his overall capability in the radar field, but also in the specific area of radar Target Modeling. "Weinstock Models" have become accepted as extensions of the Swerling Cases and are included in lectures as such. He has also materially contributed to the field of radar, as a major contributing author to the classic textbook *Modern Radar*.

Walter W. Weinstock



Individual Award in Engineering

Constant-rate digital vector generation

L. W. Poppen | J. J. Lyon

This paper discusses a technique for generating lines (vectors) upon a CRT display. The basic technique uses a digital generation of x- and y- signals (count pulses) so that one axis is always counting at the maximum system capability; this produces vectors which are of uniform intensity regardless of length. Since this basic system requires two additions in one clock interval, it has a hardware speed limitation. To overcome this, a new algorithm was developed which requires only one addition but operates with equal capability.

J. J. Lyon, Electromagnetic and Aviation System Division, Van Nuys, Calif., received the BS in Engineering cum laude, from UCLA in 1968 and completed the MS in Engineering in 1971 also at UCLA. Mr. Lyon joined RCA in 1968 and has been involved in logic design programs on the TACFIRE system on a clock track writer and simulator, and on the AVSAD drum system. He was assigned complete logic design responsibility for the AN TPO-27 display system. Mr. Lyon also designed and tested the phase comparator for a multiple drum system on an RCA independent research and development program. He has just completed the logic design of a high-speed, digital vector generator on another research program and is presently involved in the logic design on an automatic bowling scoring system. He is a member of Tau Beta Pi and the IEEE.

L. W. Poppen, Ldr. Military Display Design, Electromagnetic and Aviation Systems Division, Van Nuys, Calif., received the BSEE with highest distinction from Purdue University in 1956 and the MSEE from the University of Southern California in 1958. Mr. Poppen has had extensive experience in military display design. At RCA he was program director on the AN TPO-27 display subsystem which consisted of two alphanumeric displays, one of which was capable of displaying radar PPI data. He also participated in the preliminary study effort on the three-dimensional AN TPS-59 radar displays consisting of PPIs and RHIs using storage CRTs. Mr. Poppen has just completed development programs on a digital vector generator and on a 4000-character alphanumeric display. Prior to joining RCA, Mr. Poppen was leader on the three-dimensional AN TPS 32 radar display subsystem at ITT Gillilan and on the MTDS command and control system at Litton DSD. He is a member of Tau Beta Pi, Eta Kappa Nu, the IEEE, and the SID.

Authors Poppen (left) and Lyon.



COMPUTER-GENERATED DISPLAYS frequently require the placement of lines (vectors) upon a CRT. To retain the total system accuracy and stability, digital techniques are generally applied to do this. The following paragraphs describe an approach for generating vectors which provides vectors of uniform intensity regardless of their length and without compensating for intensity.

Vector generation

The deflection system of a CRT display receives an analog voltage representing the present *x*-position of the electron beam and another voltage representing the *y*-position (see Fig. 1). In a digital display, these voltages are derived by digital-to-analog converters fed from a digital storage register. If a value is loaded into this register, the electron beam will move to that location. If these registers are also counters and if pulses are fed to the *x*- and *y*-counters, a vector will be drawn. For this vector to be straight, the pulse rates on the two (*x* and *y*) lines must be uniform. For the angle to be correct, the pulse rates must be at the proper ratio. In a 10-bit (1024-position) system, 1023 pulses must be sent to a counter to draw a full diameter vector. The number of pulses on one axis should not deviate from the required number by more than one pulse or it may be noticeable. The requirements of vector generation, therefore, are two uniform pulse rates at the proper ratio.

“Constant” rate vectors

Vectors are generally drawn using either of two basic approaches: 1) all vectors take equal time, or 2) all vectors are drawn at the same rate.

The first approach is generally simpler to implement, but produces vectors of different intensity (unless there is video compensation) and does not make maximum use of the speed capability of the system. The second approach has the major disadvantage of being more complex. For these reasons, it seemed desirable to save implementation time and hence put more data on the display if a relatively simple system could be found to meet the requirement.

Reprint RE-17-6-8
Final manuscript received August 23, 1971.

In a truly constant-rate system, it is necessary to modify both x - and y -count rates depending on $R(\sqrt{x^2 + y^2})$. To eliminate this additional complexity, the longer axis of a vector was made to operate at the clock rate, and the smaller axis would operate at a rate reduced from this. This means that a vector on the axis moves at the clock rate, while one at 45° moves 40% faster ($\sqrt{2}$) than the clock rate, thus producing a vector of slightly less intensity. This phenomenon is not observable, however, because of the logarithmic nature of the response of the eye. In contrast to the truly constant-rate system, which draws on-axis vectors at a rate slower (by $\sqrt{2}/2$) than the clock rate and which does not make maximum utilization of the system capability, the approximation of the "nearly" constant rate system results in all the advantages of true constant-rate vector generation, but with reduced complexity.

Basic technique

The requirement is to accept x and y -coordinates of the beginning and end points of a vector and convert these coordinates into two pulse trains: the clock pulse for the longer axis and a proportionately lower frequency pulse train of approximately evenly spaced pulses for the shorter axis of the vector. The following paragraphs explain the basic techniques and the actual implementation of the constant-rate system.

Preprocessing

The data for vector generation consists of the starting point (x_1, y_1); and the end point (x_2, y_2) of the vector. The first operation that must be performed is to determine the x and y values of vector length: $\Delta x = x_2 - x_1$; $\Delta y = y_2 - y_1$. Since the signs of the coordinate are handled by the "count direction" line in the display, then Δx and Δy are treated as absolute magnitudes. The resultant values of Δx and Δy , therefore, are always positive. The sweep counters are jammed to the value of x_1, y_1 , and the first subtraction of $x - y$ is done to determine which is larger. The clock is then routed to the sweep counter of the larger number as soon as the actual vector generation is started.

Theory of Operation

The process is one of simulating division by repetitive subtraction. The

smaller number, b , is subtracted from the larger, a . Then b is subtracted from the remainder, R . This is continued until $R - b$ becomes negative. At this time the following division is simulated:

$$a/b = Q_1 - (d_1/b)$$

where Q_1 is the quotient and equals the number of subtractions necessary to produce a negative remainder, and d_1 is the remainder. At this time, Q_1 pulses have been put out on the a line, and one pulse on the b line. After the negative result, a is added back in to the previous remainder and the process continues. The second division, for example, is:

$$(a - d_1)/b = Q_2 - (d_2/b)$$

The process continues until $Q_1 + Q_2 + \dots + Q_n = a$. Therefore, a pulses have been put out on the a line and, as shown in the proof in the Appendix, b pulses have been put out on the b line. The following example shows that the pulses on the b line are quite evenly spaced. For this example, let $a=7$; and $b=5$.

Example

	R	a -line	b -line	
Start				
$(R-b)$ 1st subtraction	2	1		First
$(R-b)$ 2nd subtraction	-3	1	1	division
$(R+a)$ adding a	4			Second
$(R-b)$ 3rd subtraction	-1	1	1	division
$(R+a)$ adding a	6			Third
$(R-b)$ 4th subtraction	1	1		division
$(R-b)$ 5th subtraction	-4	1	1	
$(R+a)$ adding a	3			Fourth
$(R-b)$ 6th subtraction	-2	1	1	division
$(R+a)$ adding a	5			Fifth
$(R-b)$ 7th subtraction	0	1	1	division
		7	5	

Note that a negative (or zero) result means that the subtraction produced an overflow and a pulse is put out on the

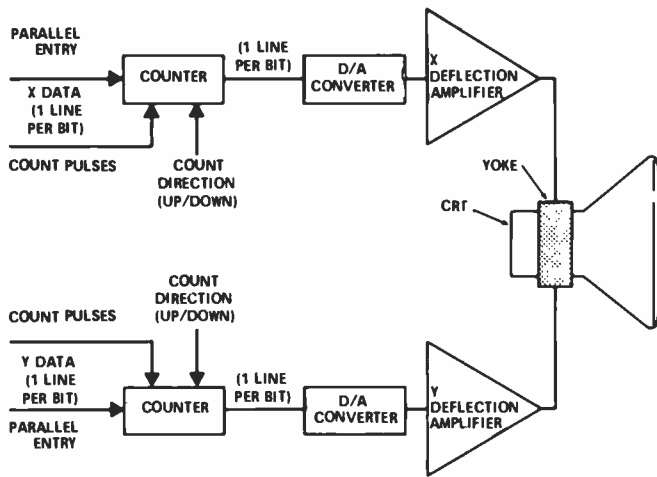


Fig. 1—Typical CRT magnetic deflection system.

b line. If this were put into a division format the results would be as follows:

Division with negative remainder "Normal" division

1. $\frac{7}{5} = 2 - \frac{3}{5}$	$\frac{7}{5} = 1 + \frac{2}{5}$
2. $\frac{7-3}{5} = 1 - \frac{1}{5}$	$\frac{7+2}{5} = 1 + \frac{4}{5}$
3. $\frac{7-1}{5} = 2 - \frac{4}{5}$	$\frac{7+4}{5} = 2 + \frac{1}{5}$
4. $\frac{7-4}{5} = 1 - \frac{2}{5}$	$\frac{7+1}{5} = 1 + \frac{3}{5}$
5. $\frac{7-2}{5} = 1 - \frac{0}{5}$	$\frac{7+3}{5} = 2 + \frac{0}{5}$

Division with a negative remainder is somewhat different than normal division. The result of any specific step may be different and may result in slightly different pulse spacing, but the result is the same. Functionally, it is easier to detect a negative remainder.

From the above example, the following should be noted:

- 1) The number of divisions is b .
- 2) The sum of the quotients is a .
- 3) The last remainder is always zero (see Appendix for proof).
- 4) The specific quotient for one division is the number of steps to put out one pulse on the "b" line.

Application

Fig. 1 is a block diagram of the actual implementation of the basic system. The selection gating determines whether Δx or R will be routed to the left channel and whether Δy or R will be routed to the right channel. The polarity gating determines whether a process is an add or subtract. The control logic sets the selection and polarity gates, depending on the sign of R and whether Δx or Δy was larger.

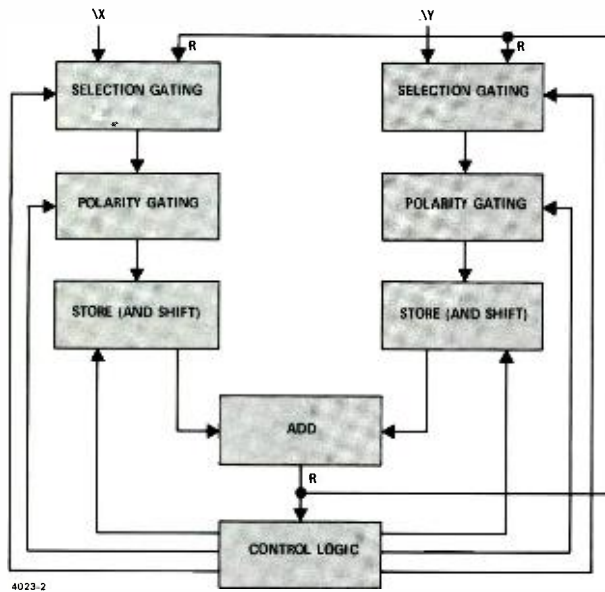


Fig. 2—Block diagram of vector generation.

Operation	Left channel		Right channel		Conditions	
	Var.	Sign	Var.	Sign	Larger No.	Previous Sign of R
1. $\Delta x - \Delta y$	Δx	+	Δy	-	Δx	1st oper.
2. $R - \Delta y$	R	+	Δy	-	Δx	+
3. $\Delta x + R$	Δx	+	R	+	Δx	-
4. $\Delta y - \Delta x$	Δx	-	Δy	+	Δy	1st oper.
5. $R - \Delta x$	Δx	-	R	+	Δy	+
6. $R + \Delta y$	R	+	Δy	+	Δy	-

After the initial determination of whether Δx or Δy is larger, steps 1 through 3 or 4 through 6 are enabled. If Δx is larger, $\Delta x - \Delta y$ (step 1) is enabled. After time has been allowed for the signals to arrive at the storage registers, they are clocked into the registers. The adders then perform the addition. After allowing time for the addition process, the control logic determines the sign of R . If the sign of R is positive, the gates are enabled to perform $R - \Delta y$ (step 2) at the next clock time and a pulse is put out on the x line. If the sign of R is negative, $\Delta x + R$ (step 3) must be accomplished before the next clock time. Pulses are put out on the Δx and Δy lines. The process of subtractions (and additions where necessary) is continued until the number of subtractions equals Δx .

It was noted in the above discussion that, after a subtraction produces a negative result, an addition must be performed with both operations being performed in one clock interval. This imposes a significant speed limitation. In the specific application, integrated

circuit adders were used. These were not fast enough to be able to perform two additions in one clock interval at the desired clock rate. In any case, it would be inefficient to perform two operations when one would suffice, since the system would have to operate at one-half the speed capability of the adders. It was deemed desirable to find a new algorithm which would require only one addition per clock period. This new algorithm is discussed in the following paragraphs.

Alternate approach

To utilize the maximum speed capability of the basic system, a new implementation of the system had to be derived. Specifically, the problem is that a subtraction ($R - b$) produces a negative result and must be followed by an ($R + a$). The total combination, therefore, to be performed in one clock period is $R - b + a$. This can be accomplished by $R - (b - a)$. If $(b - a)$ is sent into either channel of Fig. 2, however, the selection gates will require three choices. Eighteen bits (nine per x and nine per y) of a choice of three inputs requires a large amount of gating. Thus, an alternative was implemented. This alternate approach is discussed in the following paragraph.

Operation of alternate approach

Since it is inefficient to implement the $R - b + a$ operation in one step, a two-

step approach was taken. If two steps are taken, the second step of necessity will coincide with an existing step. The two steps must be examined as a pair. There are two possible operations in each clock interval. If the remainder of the previous operation was plus, it is $R - b$; if it was minus, it is $R + a$. The left column below shows the first step as $R - b + a$ and the second step as either $R - b$ or $R - b + a$. The middle column shows the sum of the two steps; and the right column, an alternate pair of steps which yields the same result.

Comparison of regular and alternate approaches

	Regular pair	sum	Alternate pair
Pair No. 1:	$R - b + a$ $R - b$	$R - 2b + a$	$R + a$ $R - 2b$
Pair No. 2:	$R - b + a$ $R - b + a$	$R - 2b + 2a$	$R + 2a$ $R - 2b$

The following example is given to demonstrate the difference between the two algorithms. In this example $a = 8$ and $b = 6$.

Example

Basic Approach

	R	a pulse	b pulse
$R = a$	8		
$R - b$	2	1	
$R - b + a$	{ -4 +4	1	1
$R - b + a$	{ -2 +6	1	1
$R - b + a$	{ -0 +8	1	1
$R - b$	2	1	
$R - b + a$	{ -4 +4	1	1
$R - b + a$	{ -2 +6	1	1
$R - b$	-0	1	1
		8	6

Alternate Approach

	R	a pulse	b pulse
$R = a$	8		
$R - b$	2	0	
$R - b$	-4	1	1
$R + a$	4	1	
$R - 2b$	-8	1	1
$R + a$	0	1	1
$R - 2b$	-12	1	1
$R + 2a$	4	1	
$R - 2b$	-8	1	1
$R + a$	-0	1	1
		8	6

In the basic approach, when an $R - b$ results in a negative answer, a is added in the same step. In the alternate approach, when an $R - b$ results in a negative answer, a is added in the next step.

This amounts to a delay. The alternate approach, therefore, starts counting a steps at the second subtraction. This results in the proper number of pulses being put out on the two lines. Because of the delay, it does not necessarily result in a final remainder of zero nor does it result in identical pulse spacing. The alternate approach yields correct results when started one pulse late (as shown) in all cases except when $a=b$.

Then a one pulse shortage occurs in that value selected to be b . In this next example, $a=5$ and $b=5$.

Example

	<i>Basic approach</i>		
	<u>R</u>	<u>a pulse</u>	<u>b pulse</u>
$R=a$	5		
$R-b+a$	{ -0 +5	1	1
$R-b+a$	{ -0 +5	1	1
$R-b+a$	{ -0 +5	1	1
$R-b+a$	{ -0 +5	1	1
$R-b$	-0	1	1
		—	—
		5	5

Alternate approach

	<u>R</u>	<u>a pulse</u>	<u>b pulse</u>
$R=a$	5		
$R-b$	-0		
$R+a$	5	1	
$R-2b$	-5	1	1
$R+a$	-0	1	1
$R-2b$	-10	1	1
$R+2a$	-0	1	1
		—	—
		5	4

Because of the separation of steps in the alternate approach, the $R+a$ results in a positive remainder and no b pulse. From that point on, pulses are put out on both a and b . If $a=b$, therefore, b will be one pulse short at the end regardless of the value of a and b . In the actual application of this technique, the final coordinates of the vector were entered into the counter at the end of the vector so that any error (including this one) would be corrected.

Summary of alternate approach and implementation

The alternate approach has four operations. The operations and rules of their use are listed below:

<i>Operation</i>	<i>When performed</i>
$R+2a$	When previous $R+a$ resulted in a negative result; performed after $R-2b$.
$R-2b$	After every $R+a$ or $R+2a$.
$R+a$	When previous subtraction ($R-b$ or $R-2b$) was negative, unless conditions for $R+2a$ exist.
$R-b$	When previous subtraction produced positive results.

The block diagram (Fig. 1) shows both the implementation of the basic approach and the alternate approach. The only additional requirement of the alternate approach is that multiplication of a or b by 2 is required. This is done in the storage registers by performing a shift up, which requires just a small additional amount of time.

The letters a and b have been used to represent the larger and smaller numbers, respectively. Either x or y can be a or b , and the initial comparison determines this. If they are equal, the result is arbitrary. A separate counter (not shown) has the value of a entered in it at the start of the cycle. When this is counted down to zero, a pulses have been put out and the operation is terminated.

Appendix—division by multiple subtractions

Proof that the number of subtractions equals the dividend.

The constant-rate generating technique requires the simulation of division by multiple subtractions. The smaller of two numbers is repetitively subtracted from the larger. When the result is negative, a pulse is put out on the line representing the smaller number. The number of subtractions performed equals the larger number. The first division of a (the larger number) by b (the smaller number) is:

$$a/b = Q_1 - (d_1/b)$$

This division represents Q_1 subtractions in the actual process. When the overflow occurs (remainder is minus), one count is accrued for the smaller number. This process is repeated by adding the remainder to a and dividing by b . The process is terminated when the number of subtractions ($Q_1 + Q_2 + \dots + Q_n$) is equal to a . It is therefore, necessary to prove that the number of operations, n , is equal to b .

For the second division, subtract the difference from the previous division from the dividend, then divide

$$(a-d_1)/b = Q_2 - (d_2/b)$$

Once again, subtract the difference, resulting from the previous division, from the dividend, then divide. Continue until n divisions have been performed.

$$\begin{aligned} (a-d_2)/b &= Q_3 - (d_3/b) \\ &\vdots \\ (a-d_{n-1})/b &= Q_n - (d_n/b) \end{aligned}$$

Each equation is now multiplied by b , and the remainders are repetitively substituted into the equations to yield the remainder after the n th quotient.

$$\begin{aligned} a &= bQ_1 - d_1 \\ a &= bQ_2 - d_2 + d_1 \\ &\vdots \\ a &= bQ_n - d_n + d_{n-1} \end{aligned}$$

or

$$\begin{aligned} d_1 &= bQ_1 - a \\ d_2 &= bQ_2 - a + d_1 \\ &= b(Q_1 + Q_2) - 2a \\ d_3 &= bQ_3 - a + d_2 \\ &= b(Q_1 + Q_2 + Q_3) - 3a \\ &\vdots \\ d_n &= bQ_n - a + d_{n-1} \\ &= b(Q_1 + Q_2 + \dots + Q_n) - na \end{aligned}$$

That is

$$d_n + na = b(Q_1 + Q_2 + \dots + Q_n) \quad (1)$$

or

$$\frac{d_n}{b} + \frac{na}{b} = (Q_1 + Q_2 + \dots + Q_n)$$

But since

$$a = (Q_1 + Q_2 + \dots + Q_n)$$

(as stated, the operation is terminated when the sum of the quotients = a) then

$$\begin{aligned} \frac{d_n}{b} + \frac{na}{b} &= a \\ \frac{d_n}{b} &= \frac{ab - na}{b} \\ d_n &= a(b-n) \end{aligned} \quad (2)$$

Since d_n and a are positive, $(b-n)$ must be positive or zero. Therefore

$$b \geq n$$

but d_n is the remainder of a division by b ; therefore

$$d_n < b$$

and

$$a \geq b$$

hence

$$a > d_n$$

Substituting this inequality into Eq. 2:

$$\begin{aligned} a &> a(b-n) \\ 1 &> b-n \end{aligned}$$

Since $b \geq n$ and b and n are integers, the only value of $b-n$ which solves the equation is

$$b-n=0 \quad (3)$$

Therefore

$$b=n$$

Substituting this result back into Eq. 2

$$d_n=0$$

It has been proved, therefore, that the number of overflows and, hence, the number of pulses on the b line equals b , the smaller number. It is further noted that the last remainder is zero and that a pulse must be put out on this overflow (i.e., zero must be considered negative).

Digital and optical techniques for image enhancement

Dr. W. W. Lee | Dr. P. C. Murray

Television pictures, as they are received from a satellite, contain noise and distortion, causing some information to be lost. Processing cannot add information which is not there, but it can make the information present in the picture more readily available to observers. A project was conducted at AED to establish the groundwork for an optimum method for improving satellite pictures.

OPTICAL IMAGE ENHANCEMENT is based on the Fourier transform properties of lenses. It has been known since the turn of the century that the diffraction pattern in the focal plane of a lens could be described in terms of the Fourier transform of the object function. Only with the advent of the laser, with its properties of coherent light emission, did this fact become of practical value. The major advantage of Fourier-plane processing is that one single operation affects the entire picture. The processing is holistic, not point-by-point. This allows Fourier processing to be done extremely rapidly with simple equipment. The major disadvantage is that this form of processing is analog and hence subject to all the inaccuracies and non-linearities inherent in analog processes. In addition, very high quality optics are needed to reduce noise susceptibility of coherent optical systems.

Digital processing is inherently almost noise free. The only extraneous noise introduced is usually in the reproduction system and, by proper design, this can be held to a minimum. The processing is however point-by-point, and this has two effects. First, it requires either

a large machine (computer) or a long time to process a picture of even moderate information content. Second, for reasonable machine sizes and program lengths, it confines operations on a picture point to areas reasonably near that point. If the information is so distorted that it is uniformly spread over a large area, the digital approach becomes excessively demanding. Fortunately for most real life cases, the bulk of the information is found immediately adjacent to its original position.

Approach

Optical processing

To perform optical data processing, a coherent plane wavefront of high purity is desirable. The wavefront should be spectrally pure and have good spatial and temporal coherence, although as path differences are short, the spatial coherence is more important than the temporal. It is not essential that the wavefront as it emerges from the collimator be absolutely plane. Small amounts of sphericity can be tolerated, although they are inconvenient.

Diagrams of the optical data processing facility are shown in Fig. 1, and a photo-

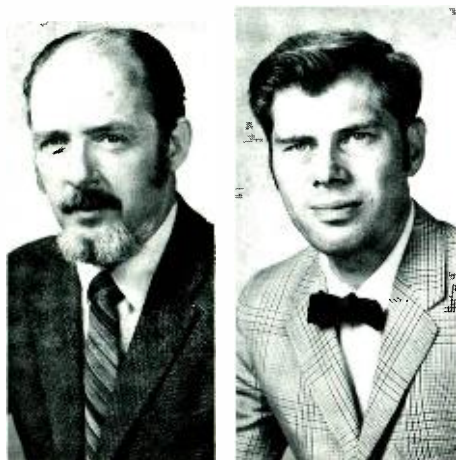
graph of the processing unit is shown in Fig. 2. In Fig. 1a, the collimated beam passes through the input transparency (at "G") and through a transform lens. In the focal plane of the lens, the Fourier transform is found, and here the various filtering operations are performed. Next is an inverse transform lens, which produces the picture after the operations are performed. All the optics used in coherent processing must be of considerably higher quality than is needed ordinarily. Failure to use these high quality optics will result in excessively noisy systems and seriously degrade the final output.

To record the picture, two modes are used. The recreated picture may either be recorded directly on film or, for immediate availability, a closed-circuit television system is used to give a real-time reproduction and to allow changes to be seen instantly.

The optical data processing facility is mounted on a Gaertner rectangular bench with built-in air suspension to provide vibration isolation. The light source is a 2-mW helium-neon laser designed for high stability and single-mode operation.

The beam is deflected to a convenient height (about 9 inches) above the bench by two folding mirrors. It then passes through a rotatable polarizer, which is used to adjust its intensity. A third mirror directs the beam into a spatial filter.

This filter consists of a microscope objective and a 50- μm pinhole. Focusing and x and y alignment adjustments are provided on the pinhole. The laser beam is focused on the pinhole, from where it diverges. This eliminates noise



Dr. W. W. Lee* (left), Astro-Electronics Division, Princeton, N.J., received the BA in Physics from the University of Virginia in 1951 and the PhD in Physics from the University of Paris in 1959. His work at AED involved lasers and holography, with special reference to optical data processing. Before joining AED, Dr. Lee was employed by the Bendix Corporation, where he was engaged in research and product development in the electro-optic field. Some of the areas in which he was active included laser range finders and target designators, celestial sensors, computer memories, and optical encoders. He has ten patents and has published four papers in the optics and electrooptics field.

*Since this article was written, Dr. Lee has left RCA.

Dr. Paul C. Murray* (right), Astro-Electronics Division, Princeton, N.J., received the BEE from Cornell University in 1946, the MS in Physics from the University of Delaware in 1948, and the PhD in Physics from Purdue University in 1954. He joined RCA in 1959 after five years as a senior project engineer at the Sperry Gyroscope Company. His recent accomplishments include the supervision of the installation of an RCA ColorScanner and a Data General Super Nova computer image-processing facility, and computer restoration of degraded images using a number of software programs. Dr. Murray received the AED Engineering Excellence Award in March 1969 for his work on multispectral registration.

*Since this article was written, Dr. Murray has left RCA.

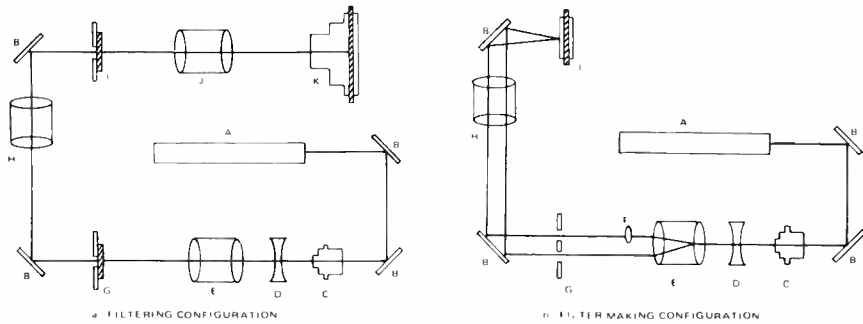


Fig. 1—Optical data processing equipment configurations. LEGEND: A) laser, B) deflecting mirror; C) spatial filter, D) beam expander, E) collimating lens, F) reference beam lens, G) input plane, H) transform lens, I) Fourier plane, J) inverse transform lens, K) output plane.

and spatial incoherence caused by dust particles or imperfections associated with the mirrors or polarizer.

From the filter, the light passes through a collimator consisting of a simple concave lens and a projection lens, the latter having an aperture of 10.16 cm (4 in.) and a focal length of 35.56 cm (14 in.). The concave lens spreads the beam so that the central maximum of the diffraction pattern from the 50- μm pinhole fills the projection lens which then collimates the light to a high degree.

If a filter or hologram is being made, the input is altered to the Rayleigh interferometer configuration (Fig. 1b) as detailed below. For normal filtering operations, however, the input transparency is placed in a holder at this point, surrounded by suitable baffling to eliminate stray light.

Because space is limited on the rectangular bench, a folding mirror deflects the light 90° to the transform lens. Because of vignetting, this mirror also acts as a system stop in the horizontal direction, limiting the usable field to a quasi-ellipse 10.16 cm (4 in.) long by 6.35 cm (2.5 in.) broad.

After folding, the light passes through the transform lens at the end of the optical bench. Another folding mirror deflects it through 90° to pass along the bench side.

Because of the sharply convergent nature of the light leaving the transform lens, this second mirror does not affect the system aperture.

A mount with screw drives is located in the Fourier plane to provide three degrees of translational freedom. A fixture is available to provide a degree of rotational freedom about the optic axis. Centering adjustments allow the center of the pattern to be aligned with the fixture's center of rotation.

Next in the optical path is the inverse transform lens, which forms the modified image of the input transparency in the output plane. The unit is so designed that either a plate holder may be placed in this plane to record the image directly, or the output may be picked up by a high-resolution television monitor (in this case, a Cohu Electronics 6000-series camera, set for 1125 lines/frame).

Certain modifications are made to this configuration to make filters. As a filter is usually made by taking the Fourier transform (with the phase preserved) of a given input, the plate holder is moved from the output plane to the Fourier plane. A reference beam is used to record the phase in the filter. This is done by placing a short focal-length lens in front of the input plane such that its focus falls in the input plane. This acts as a point source to the transform lens, and hence the transform lens produces a collimated beam which interacts with the transform to preserve the phase.

Digital processing

The basic approach taken in the digital portion of the effort was considerably different. Here, conceptually if not actually, the picture is presented as an array of binary numbers available usually in sequence. (In practice, an actual picture is taken and subsequently digitized, for convenience.) The picture is then operated on, point by point, and reconstructed by scanning.

To achieve this, an RCA Graphic Model 70/8802 color scanner was interfaced to a Data General Super Nova Computer by means of analog-to-digital and digital-to-analog conversion units. The computer's basic clock rate is 0.8 μs , which allows considerable processing at color-scanner data rates.

The color scanner contains a scanning head that views light transmitted through a transparency in three color bands simultaneously. In graphics applications, these bands are matrixed in an analog color computer to provide proper outputs for producing color printing plates. For image processing application, the input is generally black-and-white imagery. For this case, a point in the color scanner computer is chosen where the image signal is representative of film density. This signal (the log of film transmission) is digitized by the computer and serves as input image data. The digital-to-analog converted data from the computer is reentered into the color scanner circuitry at essentially the same point. When the computer is instructed to echo input data, a film is produced which, in all appearances, is identical to an analog reproduction.

For optimum utilization of the digital computer with the color scanner, a synchronization system was required. Initially this took the form of a once-around sync start pulse generated on the color-scanner drum by a light-source phototransistor circuit. Picture-element (pixel) timing was done by the computer as follows: New data was alternately digitized from the scanner and processed data outputted for a predetermined number of pixels/line. The computer program processed the stored digital imagery after the last pixel was inputted and then waited for the next line sync to occur. This format works fairly well for up to 1024 pixels/line.

As the number of pixels/line increases, drum rotational instability is visible in output imagery. Thus, a pixel clock was added to the scanner drum periphery, to define the location of each pixel.

The system provides a combination of scanning and film reproduction, together with digital and analog image computation capability. The system is

Fig. 2—Optical data processing unit



adaptable, through numerous programs, to solving many image problems and demonstrating processing of differing signal sources. Further, the input and output formats can be readily changed.

The fast-multiply option, available with the Super Nova Computer (3.8 μ s), was obtained because the basic operation of picture processing by digital means is matrix multiplication. At least one matrix multiplication must be carried out for each picture point. The quality of the processing increases (although not in a simple fashion) as the matrix grows larger. Since the number of multiplications necessary to find the product of the two n th-order square matrices is n^3 , even a small decrease in multiplication time results in substantial savings in total processing time.

The theory of digital computer picture processing is too complex to describe in great detail here. It is covered thoroughly in Rosenfeld.¹ Basically, the information at any point is considered to be affected by the information at surrounding points. The given point is considered to be the center of an n th order square matrix whose other elements are the n^2-1 surrounding points. This matrix is then multiplied by a weighting matrix specifying the distribution of the information at the surrounding points. Usually, only the value of the central matrix need be calculated. For more accurate work, it is sometimes necessary to calculate the entire product.

Typical of the types of operations that are easily accomplished by this sort of technique are noise removal, edge sharpening, shading correction, etc. This type of technique is most easily implemented when the processing is position independent; that is when the

weighting matrix is not a function of point position. Theoretically, there is no reason why the matrix should not be position dependent, but as a practical matter, the requirements on machine capability and processing time make it hard to realize. Fortunately, most of the commonly desired operations are position independent.

Optical processing

The first step in the investigation, after the setting up and debugging of the facility, was the making of two-dimensional holograms for use as filters. This was done using the setup described above with a lens to provide a reference beam. As the relative intensity of the reference and signal beam is important, a second polarizer may be inserted in either beam to vary its relative intensity. The beams should be balanced so that fringes are partially visible in the brightest section of the transform plane.

After a filter is made, reproductions are made using the filter as a hologram. A successful reproduction does not guarantee successful performance as a filter, but failure to reproduce guarantees failure as a filter.

The making and reproduction of holograms was not only the first step in testing the newly setup facility but also provided numerical measures of the response of the system. The frequency response was measured by reconstructing a hologram of a three-bar, Air Force test pattern. The reconstruction cut off at 40 cycles/mm. Visual inspection of the image through a microscope indicates that the limiting factor is the optics; not the film used (Polaroid P/N).

The system noise arises from three sources: 1) the inherent "speckle" noise of the laser; 2) the noise due to

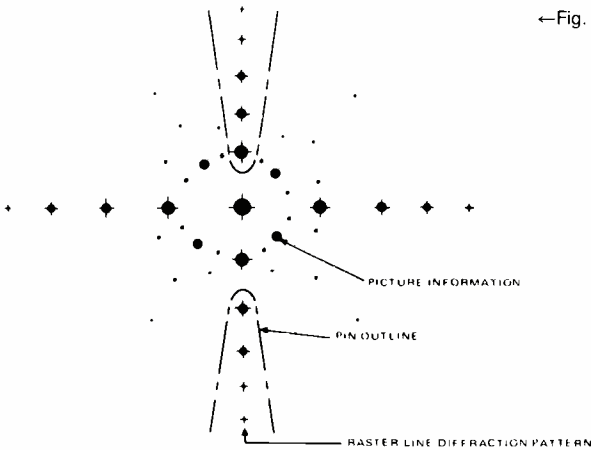
dust, scratches, streaks, etc. in the optical path; and 3) the granularity of the film used. For Kodak 649F plates, the grain is so fine that its contribution to the total noise figure can be neglected.

Removal of coherent noise

The first attempt at removing coherent noise was made by using the matched-filter approach to remove raster lines. This is a three-step process. A transparency of a blank raster was obtained. A two-beam hologram of this was made. This hologram was then put in the Fourier plane and a picture with raster lines was projected through it. Where the original raster lines had struck the plate, there were, of course, opaque patches. Hence when the light of the raster lines in the picture struck these same points it would be stopped, but the light from the picture would go through. Reconstructions from filters made in this manner were acceptable images of the original. Attempts were therefore made to remove raster lines from a variety of pictures, including continuous tone, and resolution test patterns. The raster lines were indeed removed, but owing to the lack of a liquid gate, substantial amounts of noise were introduced.

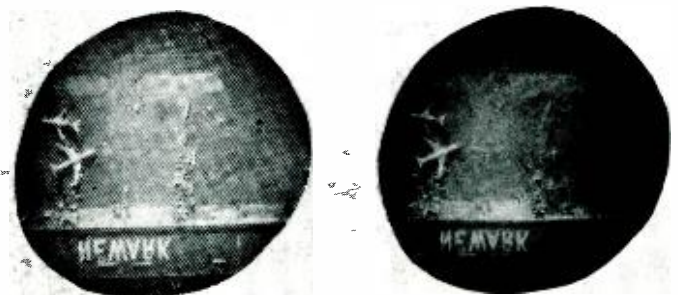
As the noise is introduced by inhomogeneities in that portion of the Fourier plane through which light passes, it was decided to attempt to remove raster lines by placing two mechanical stops to block the spatial frequencies due to the raster lines. A depiction of the Fourier plane without the raster lines is shown in Fig. 3.

Lines were successfully removed from several pictures with this method. Typical results are shown in Fig. 4. Note that there is no apparent degradation of picture quality. A measure of the



←Fig. 3—Image of Fourier plane with raster lines removed by mechanical stops.

Fig. 4—Effect of raster line removal



information loss encountered was made on a resolution test pattern, and it was concluded that there is no loss of information along the raster lines and that the resolution limit at right angles to the raster lines is reduced to 75% of its original value. As there is no phase medium in the Fourier plane, essentially no noise is introduced.

Matched filtering

Matched filtering is a technique used to permit recognition of an image from a noisy background. This is a theoretically well-grounded procedure in both electronics and optics.²

To discuss the technique in a little more detail, all the strictures of the two-beam filter discussed above apply here also. The reference beam must be almost parallel to the signal beam. Their intensities must be properly balanced. Exposure times must be appropriate. Also, and the most restrictive requirement on this technique, for optimum results the pattern should be binary. Patterns showing gray scale do not filter well, if at all. They can be used to make filters if there are hard edges of sufficient contrast, but objects with soft edges do not show readily identifiable diffraction patterns. Fortunately this would not appear to be an insurmountable obstacle in real world applications.

The remaining constraint on matched filtering in practice is that the filter must be well centered on the optical axis. The filter must be in the same location both when it is made and when it is used. This may be done by use of fiducial locating marks, but it proved simpler and just as accurate in practice to center the filter by using a microscope and a well known diffraction pattern.

No difficulty was encountered in making the Fourier transform of the pattern or a negative from this by contact printing. As the filters are essentially binary masks, no special care in development was needed. It was found that the dynamic range of light present in the pattern was such as to exceed grossly the dynamic range of the film. The central maximum was always an indecipherable blob if any trace of the higher orders was visible. By trial and error, it was found that the optimum exposure was that which showed the most detail in the first-order section of the diffraction pattern. This, of course, varied from one object to another, so no quantitative values are given.



Fig. 5—Effect of matched filtering.

An underexposure reveals nothing. As exposure is increased, the first thing to appear is the correlation peak in the desired pattern. Then as exposure is further increased, the entire desired pattern appears. Finally with longer exposures, patterns similar to the desired pattern appear and finally all patterns on the film, of whatever nature, appear. Typical exposure values and the results are as shown in Table I using Polaroid P/N film.

In Fig. 5, two photos are shown. The first shows an array of patterns used for a test. The target pattern is the thick cross in the top line.

The second picture shows an exposure through a filter tuned to this cross. The target cross is clearly visible, and the intensity of the other images depends on their similarity to the target pattern as explained below:

Exposure (s)	Image
4	Nothing on film.
6	Correlation peak visible.
8	Entire pattern (a cross) visible; correlation peaks present in smaller crosses.
10	All crosses visible.
15	Crosses and X's visible; circles faintly visible.
20	All patterns visible.

From these data, it can be seen that there is adequate rejection and sufficient exposure latitude to allow this technique to be useful in real life. Unfortunately, the exposure time for each pattern is different and depends not only on the type of pattern but also on the average transmission of the transparency being used.

As regards x and y alignment with the optical axis, the intensity of the correlation peak appears to vary approximately linearly, disappearing completely when the center of the filter is half the width of the central maximum from the optical axis.

The filter is somewhat less sensitive rotationally. It appears to lose its filtering action when the first-order maximum of the filter is completely displaced from the first order of the diffraction pattern. The degradation is not linear. It drops off quite slowly at first and then declines steeply.

It also appears that the characteristic of rejection depends more on the high frequencies than the low. Since the thick-arm cross differs more from the target crosses in high-frequency content than do the short- and long-arm crosses, we infer from the following data that the discrimination is better at high frequencies:

Type of target	% Attenuation
Target cross	—
Long-arm cross	5
Short-arm cross	5
Thick-arm cross	~50
Circle	>95
X	>95

This is born out by two facts. First, the high frequencies are more spread out on the photographic plate and allow for better alignment. Second, the low frequencies are found near the central maximum where detail is lost due to the low dynamic range of the film.

Image enhancement

Since basically image enhancement involves selectively attenuating certain spatial frequencies, it would appear to be readily achievable by Fourier-plane processing. To turn a photograph into a line drawing, as it were, would involve selectively reducing the amplitude of those frequencies near the optical axis and allowing those further away to pass through unchanged. The resulting picture would then be amplified during the development process. Due to the coherent noise problem already mentioned, no quantitative results were to be expected, although it was hoped that useful information could be obtained on gross effects of filtering and filter construction. These would be useful in aperture correction and motion-blurring work. In this sort of work, filters which have a transmission that is an arbitrary function of position are necessary.

Motion blurring

An attempt was made to correct motion blurring, or the effect seen when the camera is moved as the shutter is actuated. Like all other aberrations, this

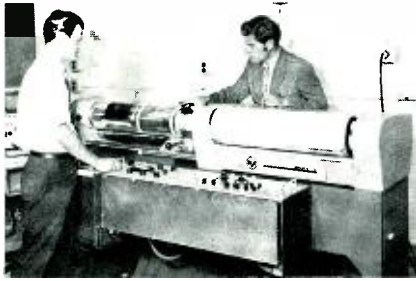


Fig. 6—Color scanner.

can be seen as a change of phase and amplitude. If this change in the Fourier plane is represented by some pair of functions $A(r, \theta)$; $\phi(r, \theta)$ and a filter whose transmission as a function of r and θ is $1/A$ and phase retardation is $1/\phi$, and sufficient noise-free amplification is available, then the effect of the filter will cancel out the aberration of motion blurring.

To make a filter whose characteristics are suitable for removing motion blurring or aberrations, it is essential that there be a capability for making filters which have a positionally arbitrary transmission function. This has hitherto not been possible except for certain simple functions or functions showing certain symmetry conditions. R. Horton of AED suggested a new and novel approach to this problem which has resulted in much superior filters of a perfectly general nature. These are also much cheaper and easier to produce. A patent disclosure has been submitted for this idea.

To provide motion-blurred pictures under controlled conditions, a special fixture has been made. This is a piece of support equipment which moves the input transmission during exposure.

Digital processing

For the digital effort, the color scanner has been set up and interfaced with the digital computer, and restored/processed pictures are available. The color scanner is shown in Fig. 6.

The main thrust of the digital effort has been restoring blurred pictures. A typical aerial photograph was taken and a one-for-one duplicate made on the scanner. The only difference was that the aperture in the pickup head was increased so that it received light from several adjacent picture elements simultaneously. This is equivalent to a somewhat defocused picture. The result is shown in Fig. 7.

Knowing the size of the pickup aperture, a 3×3 matrix was calculated to restore the original. Specifically, the 3×3 matrix restoration program stores three data lines in memory. The "center" line is processed a pixel at a time. In effect, the pixel value is compared to (convolved with) the values of the eight surrounding pixels. Where the surround differs from the pixel value, these differences are multiplexed by a constant(s) [high frequency data]. This process has its greatest effect at the sample frequency rate where adjacent picture elements may differ most in value. To a first approximation, the process is the inverse of the falling off of response of a sensor system or film image at higher frequencies. The results of this restoration are shown in Fig. 8.

The steps required to demonstrate the image-restoration process are 1) with a large scanning aperture, defocus the image and transfer the image to film and 2) digitally restore the defocused image and record on film. To perform a meaningful experiment, the fall-off in the modulation transfer function for step 1) was measured. With this as a base, the matrix restoration constants were set so that data at the sampling rate would be restored by a factor approximating the degradation factor.

The results of the restoration process showed that the restored image closely resembled the direct digital transfer of the image with a very distinct improvement over the defocused image. When less than the required restoration constants were tried, some improvement was noted. When more than the

required restoration constants were used, the resulting image contained brightness reversals at boundaries, as expected. The matrix convolution essentially adds a local derivative of the slope to the value. When the strength of the derivative is approximately correct, it sharpens edges. When the strength exceeds the correct value, the derivative of the image becomes dominant in determining the image density value; that is, objects are outlined with black or white halos.

Conclusions

It appears from the results of the optical section of the project that the following benefits can be readily obtained by optical processing: 1) objects can be readily recognized from among noisy backgrounds by matched filtering techniques (the noise contribution of the filter is slight; it can be easily produced and the alignment requirements, while stringent, are not prohibitive); and 2) coherent noise such as raster line may be readily removed without undue information loss or artifact production.

Digital processing has shown that there is great capability in the area of edge enhancement and deblurring. Some feel has been obtained for machine and time requirements and for the level of digitization and scanning necessary to produce usable pictures.

References

1. Rosenfeld, A., *Picture Processing by Computer* (Academic Press: 1969).
2. Stoke, G., *Introduction to Coherent Optics and Holography* (Academic Press: 1966).

Fig. 7—Blurred photo.



Fig. 8—Blurred photo after restoration



Mechanical and optical limitations on the performance of photomasks

H. O. Hook

Present optical performance in mask making is within a factor of three of the theoretical limits. The use of at least partially coherent light for optical printing has been used for wafer exposure. The supposed inferior resolution of coherent illumination is shown to be inapplicable to the way images are used in mask making. When properly used, coherent illumination produces slightly better edge definition in masks than incoherent illumination. Mechanical-positional precision is not a limitation in most mask making. Electron-beam exposure seems likely to play a role in pattern generation for mask making and may be used for wafer exposure if the economics of equipment now in development prove favorable.

IN ALL PHOTO FABRICATION PROCESSES, a photomask is used to define the geometry of the device being fabricated. The information in device geometry is usually transferred from the photomask by contact printing on a photoresist coating on the device-to-be. The precision of the final device can be no better than the precision of the photomask used to make it. A mask may be inadequate by having either mislocated or improperly defined patterns. The limitations of photomask precision can be considered in two parts: 1) fundamental or theoretical limits on possible precision, and 2) practical or state-of-the-art limitations.

Several years ago, it was estimated

(with good justification) that minimum sizes for semiconductor device elements would be unlikely to require mask geometries smaller than $10\ \mu\text{m}$. Today many devices use elements $1/10$ that size (one acoustic wave device has been reported using $0.15\text{-}\mu\text{m}$ lines with $0.3\text{-}\mu\text{m}$ spaces), and one would be foolhardy to predict a limit to how small device elements may ultimately become. Current device production uses elements as small as $1\ \mu\text{m}$, but $3\ \mu\text{m}$ is more common as the smallest device line width.

Fundamental mechanical limitations on precision are negligible since mechanical surfaces are definable to an atomic layer or so (a few angstroms) and this

limit is far below the limits imposed by theoretical light optics and practical device fabrication. The theoretical limits on precision imposed by optics are determined by the wavelength of light, and are in the range of a few tenths of a micrometer (μm). Shorter wavelength radiation such as x-rays, electrons, or ions all have better theoretical (and actual) resolution but also have attendant practical shortcomings.

The practical limits of precision are not as easy to delineate as being either mechanical or optical, since theory is neater than practice. Even so, the practical mechanical limits on precision are about $1/5$ of the size of the optical limits. Today's mechanical systems are repeatable to $0.2\ \mu\text{m}$ (10×10^{-6} in.) and optical limits are about $1\ \mu\text{m}$ (40×10^{-6} in.). The absolute mechanical accuracy is about $1\ \mu\text{m}$ (40×10^{-6} in.).

Let us consider the nature and sources of some of the real-world limitations due to mechanical factors, light optics, and the economics of higher resolution masking using means other than light.¹

Mechanical limitations

The mechanical problem is mainly that of locating a movable member precisely. Some years ago, Sir Robert Hooke (no known relation) proposed that stress is proportional to strain. Thus, all structural members are springs. All structures have mass and are springy; masses mounted on springs oscillate when vibrated; therefore, vibration control is needed. Almost all structural members change dimension with temperature. Therefore, temperature effects must be considered.

Reprint RE-17-6-17

Final manuscript received May 14, 1971

Some of the material in this paper is adapted from the author's contribution to Ref. 1

Harvey O. Hook, Mgr.

Photochemical and Chemical Processing
RCA Laboratories
Princeton, N.J.

received the BA with chemistry major from Elon College in 1947 and the BEE from North Carolina State College in 1949. In 1950 he received the MSEE from the same College. Since 1950 Mr. Hook has been with the RCA Laboratories where he is Manager of the Photochemical and Chemical Processing Group. He holds several patents relating to display-storage tubes and solid-state display devices. As a member of the Technical Staff, he worked on opto-electronic computer components, vacuum technology, color picture tubes, and the optics of displays. Mr. Hook is a Senior Member of IEEE and a member of the Instrument Society of America, the American Vacuum Society, and the Society of Photographic Scientists and Engineers.



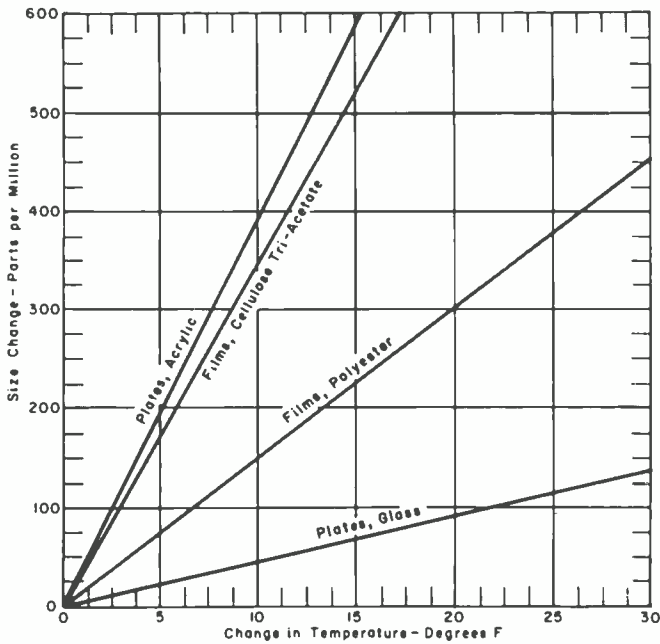


Fig. 2—Dimensional changes with temperature for artwork media.

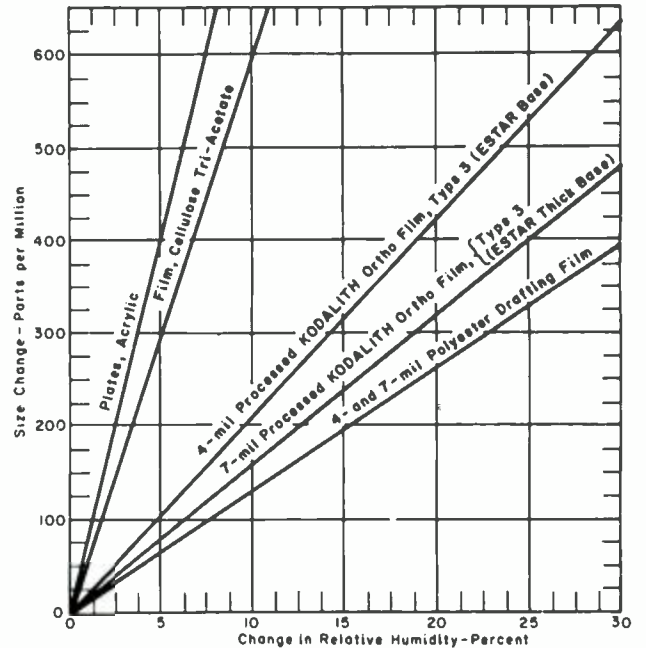


Fig. 3—Dimensional changes with humidity for artwork media.

Keeping these principles in mind, let us now examine a successful design of a step-and-repeat machine which positions a glass photographic plate precisely with respect to an image produced by its projection system. The design philosophy is to 1) build the highest possible basic accuracy into the machine, 2) measure the location as precisely and reliably as economically feasible, and 3) whenever possible arrange to compensate and cancel the residual errors. Fig. 1 shows a Jade step-and-repeat machine. The glass plate to be exposed is mounted back-to-back with a master ruling which will be used to determine that the x-y table has moved to the proper place. Errors due to thermal effects in the ways and drives, drifts in oil film thickness on screws, screw wind-up, thrust bearing shift, etc. are thus minimized. Micro-



Fig. 1—Jade step-and-repeat machine.

scope and photocell sensors on the top arm tell the machine logic the proper location to expose the plate to the image from the optical tower below. The microscope arm is a rugged casting rigidly coupled to the optical exposure tower which is also in a rigid casting. Shock mounts are provided both at the base of the stand and between the stand and the massive granite slab. The microscope lamp is mounted on a thin metal bracket and the light piped in through fiber optics to avoid excessive heat. It is a well-engineered design. However, testing showed a slow drift in position between start and end of a long job, if it was the first one done after the machine was turned on. The cause turned out to be the radiation from the microscope lamp housing to the massive cast-iron arm supporting the microscope. The cure was to mount a shiny aluminum radiation shield between the lamp housing and the arm.

This case history illustrates the care with which all mechanical perturbations must be eliminated to assure precision in mask making. All makers of such machines specify a narrow temperature span in which precision is acceptable. Usually this span is about 1°C ($\approx 2^\circ\text{F}$). Even within these limits, temperature transients should be avoided.

Similar precision location control is required on the machines which produce the master artwork and the reduction cameras. Table 1 indicates the

expected precision of several artwork production means. A couple of case histories illustrate the importance of apparently minor design features. Early Gerber Model 32 plotter tables had the stepper-motor power supplies mounted beneath the heavy steel table so the high-current motor leads could be short. The resultant heat expanded the table enough with respect to the drive screws (which are exposed to the room ambient above the table) to cause the zero location on the table to shift as much as 0.015 in. from a cold start. Moving the power supplies to an adjacent room effected a complete cure. In a more recent (and much more precise) machine built by Concord Control for Max Levy in Philadelphia, the Teflon [[®]Du Pont] nuts which run on the ball screws to provide safety stops at the ends of the carriage created enough frictional heating of the screws to produce a small but easily detectable error in long ruling runs. For certain runs, these mechanical limit stops must be disconnected.

In addition to temperature control, humidity control is necessary to prevent size change in the peel film or photographic film used for master artwork. Fig. 2 is a graph of changes in dimensions vs. temperature. Fig. 3 is the same for humidity. If glass is used as the master artwork substrate, its flatness becomes the critical factor. The bow in a glass plate can produce magnifica-

tion errors in camera reduction. Table II illustrates the sources of error in a typical mask problem. None of the schemes assures that the desired precision will be maintained, but since the errors shown are cumulative for the worst case conditions, one can expect some error cancellation and a reasonable yield of good masks from the best of the processes.

In addition to displacement-of-image errors, mechanical imperfection can produce out-of-focus images resulting in loss of size control and rounding of corners. (The high contrast of the processes used usually assures adequate edge definition).

Standard-flatness glass plates are frequently used to contact print working masks. Their lack of flatness can cause imperfect contact which results in imperfect images. Also, and less obvious, an overall curvature may be produced at the contact surface which results in the copy being either larger or smaller than the original depending on whether the copy is on the outside or inside of the curve.

Some contact printing machines use pressure platens and air pressure to control this distortion. Fig. 4a is a sectional view of a contact printing arrangement. The master plate is held at its edges on a gasket in the lower frame. The unexposed plate is placed over it, the back of the frame is closed with a rubber flap which provides a vacuum seal, and the frame is evacuated causing atmospheric pressure to push the plates together. Another design, Fig. 4b, places the master against an optical flat and uses hydraulic pressure behind a rubber diaphragm to force the unexposed plate against the master. A third, Fig. 4c, design is similar to the first except that the unexposed plate is held against a flat lapped pressure-pad by vacuum. Pneumatic pressure is then applied to the gasketed side of the master and to a piston on the pressure pad to drive the master and unexposed plate into contact.

Even with such extreme measures to assure contact, emulsion-to-emulsion contact prints containing less than $3 \mu\text{m}$ (0.1 mil) lines are not really reproducible. Contact fluid is a tremendous help by reducing diffraction effects, by nearly eliminating reflections from emulsion surfaces and by eliminating the refraction effect (see Fig. 5). Con-

Table I—Expected precision of artwork for photomasks.

Drawing means	Accuracy (μ)	Precision (ppm)	Finest line (μ)	Basis
Manual	± 250	± 250	250	Precision based on artwork 1-meter square (40 x 40 in.)
Machine-aided (manual coordinatograph)	± 25	± 25	500	
Machine-drawn (automatic scribe plotter) 10 x 10 cm to 1 x 1 or cut meter	± 25	± 25	50	
Machine-drawn (reticle generator), programmed step and flash with programmed rectangle 1 to 100-mm square	± 12	± 12	5	Precision based on 5-cm square (2 x 2 in.)
	± 1	± 5		
Machine-drawn (mask generator), drawn actual size for semiconductor marks 25 to 100-mm square	± 1	± 5	0.3	Projection based on state of the art. Not yet in existence. Precision based on 5-cm square (2 x 2 in.)

Table II—Sources of errors in typical photomask operations.

Specification	Errors (ppm)		
	Film (0.007 in.)	Ultraflat glass	Microflat glass
Artwork, 25X, (± 0.0005 in. in 25 in.)	± 20	± 20	± 20
Temperature error at 75°F ± 1 °F	± 15	± 4	± 4
Humidity error at 35 to 45% RH	± 80		
Processing size change	$+50$ to -80 †		
Total artwork error	$+165$ to -195	± 24	± 24
Reduction camera, 75 in. to lens:			
Copyboard, ± 0.001 in.	± 13 ±		
Large glass flatness		± 160 †	± 20
2 x 2-in. glass flatness	± 14	± 34	± 14
Total copying error	± 14	± 184	± 34
Total overall error	$+179$ to -219	± 208	± 58

†Trouble; far out of tolerance.

±Repeating error which may be neglected if only requirement is registry within a set of masks.

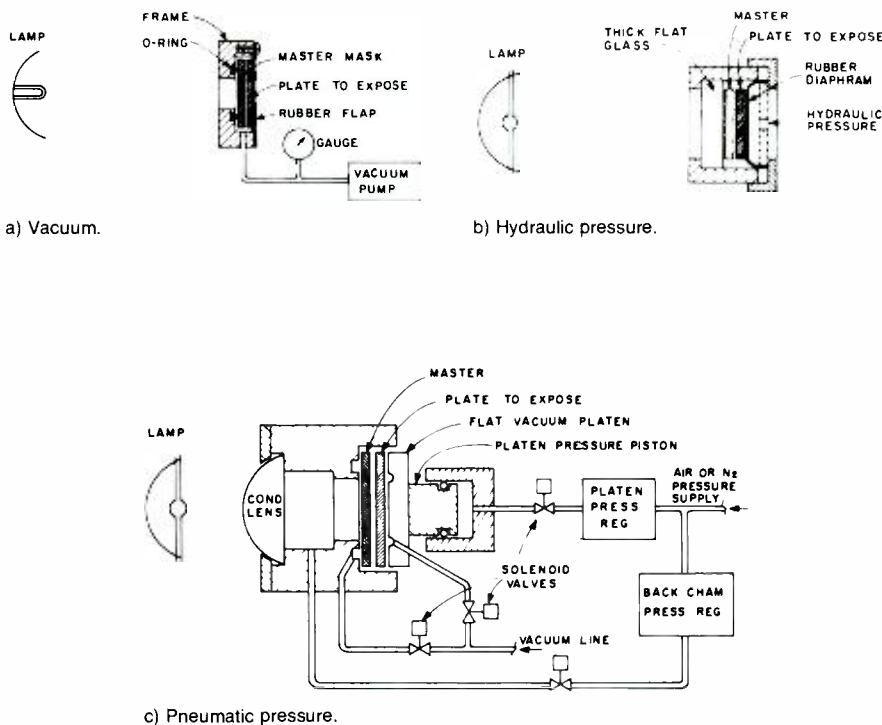


Fig. 4—Contact printing frame designs.

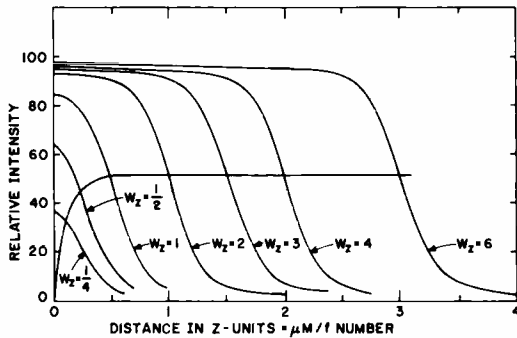


Fig. 5—Improvement in contact printing by using contact fluid.

tact fluids are messy and are therefore usually avoided. An ideal fluid would have an index of refraction of 1.50 to 1.55, be volatile enough to evaporate without a separate cleaning step, and low enough volatility to avoid forming vapor bubbles during exposure. It would wet the surfaces of master and print emulsion easily without swelling or otherwise chemically or physically affecting its properties. Methanol, isopropanol, and glycerol are sometimes used although their indexes of refraction are lower than desired. Some fluorocarbons and silicones look more promising but are not yet widely used. But we have drifted into the realm of optical problems.

Optical limitations

Several formulas for resolution have been proposed. For our purpose, it is only necessary to note that the form is $d = a\lambda/(NA)$, where d is the minimum resolved spot size, a is a constant which depends on the criterion of "resolved," λ is the wavelength of the irradiation, and NA (numerical aperture) represents the sine of the convergence angle at focus. The important thing to note is that resolution improves as the wavelength is decreased and the numerical aperture is increased.

The most common optical limitations on mask precision affect the edge locations of geometric features more than their centers. This lack of precision thus appears more as a lack of component dimensional control than as misregistry. Lens distortion, the main exception (is this optical or mechanical?), produces displacement of images from their theoretically correct placement, but since it is always the same in a given lens and setting, this distortion does not cause misregistry of masks made the same way for several layers. Low distortion is desirable,

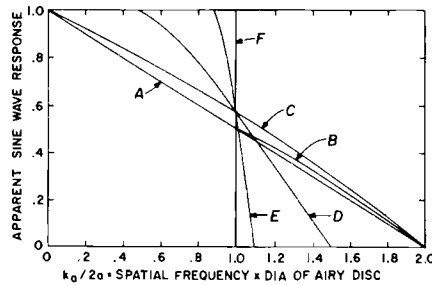


Fig. 6—Spatial frequency response with spatial coherence as a parameter (95% modulation at input).

however, since masks from different processes may sometimes be required and exact placement of images within the lens field is less critical. (Masks made by different processes are rarely mixed in sets for silicon device fabrication, but in other processes, notably evaporation masks for solid state TV camera devices, mixed process masks have been matched to $5 \mu\text{m}$ over a 100-mm mask). In modern computer-designed lenses for mask making, the distortion is low enough so that it contributes a negligible deterioration to mask quality.

The most significant optical limits on present mask performance are due to diffraction and, less important, residual lens aberrations. An optical image is always degraded with respect to the object being imaged. The situation is quite like that of pulse deterioration due to bandwidth limitation and delay distortion in an electrical transmission line. Amplifying and clipping at the receiving end can help to clean up some of the distortion, but if pulse edge location (timing) and width are crucial, the choice of clipping level makes a significant difference in the results.^{2,3} The bandwidth limitation in an optical systems depends on the focal length and aperture or *f*number of the lens, the wavelength of light, the index of refraction of the medium in which the image is formed, and the degree of spatial coherence of the illumination. [Unfortunately the term *coherence* is used to refer to two distinct properties of light. *Spatial coherence*, the coherence referred to here, is achieved when a point source of illumination is used with the image of the point source focused in the aperture of the imaging lens. The light may be polychromatic. *Temporal coherence* refers to the coherence length or monochromaticity of a light source. The "speckle" typical

of scattered laser light illustrates that temporal coherence is not destroyed by diffusing the light source. Coherence lengths of a few μm occur with gas-arc sources and coherence lengths of several meters may be obtained with lasers. Lasers generally have both types of coherence. Both types of coherence, when present, require that wave amplitudes be summed in evaluating illumination; whereas for incoherent illumination, the intensities (powers) are summed.]

Mask makers usually have only the last factor under their control. The economics of lens manufacture are such that nearly diffraction limited lenses with effective *f*numbers less than 1 and fields large enough to be useful in mask making are not likely to be available soon. The high-index glasses necessary to correct spherical aberration limit the shortest optical wavelength transmitted to about $0.4 \mu\text{m}$. The indexes of refraction of all photosensitive materials suitable for mask making are between 1.5 and 1.6. Thus the spatial coherence of the illumination is about all that one can manipulate. Fig. 6 is a plot of the spatial frequency response as the spatial coherence is varied. The area under the curve remains almost constant. At full incoherence, the cut-off frequency is double that of the fully coherent illumination. Analysis of the situation indicates that the fraction of full response (contrast) required determines how coherent the illumination should be. If 10% response is adequate, incoherent illumination will allow frequencies nearly twice as high as coherent illumination. Most mask-making processes require 40 to 70% modulation which indicates equality or superiority for coherent illumination. The main disadvantage of coherent illumination is that imperfections anywhere in the system cast shadows that produce flaws in the masks.

We can now consider the effects of coherence and exposure as they relate to the smallest line geometries which can be adequately reproduced. Several authors have considered imaging and coherence which provide background for this discussion.^{5,6,7,8} Fig. 7 is a group of curves of density vs. log exposure for Kodak high-resolution plates developed in D-8. For development times of 3 to 5 minutes, an image contrast range of a factor of 2 (log exposure change of 0.3) results in a den-

sity range of about 2 in the developed plate. Since the contrast range of 100 (density change of 2) is adequate for a mask to be used with photoresist, a log exposure range of 0.3 is reasonable as the minimum image contrast necessary to expose a mask.

Let us now propose some definitions to provide a working base for talking about exposure, contrast, and resolution. Proper exposure and processing will produce all geometries in their correct size. Fig. 8a graphs the log intensity in the image plane for several widths of slits as objects, and coherent illumination. Fig. 8b is the same for incoherent illumination. The assumed zero-response value for these curves is 1000 cycles/mm. This value corresponds to an $f/1$ diffraction-limited lens and 5000 Å light, and approximates the response of best current step-and-repeat lenses. Log intensity is used so the 2:1 (0.3 log exp) exposure range is represented by a constant-width band which can be moved up and down to represent different exposures. Clearly there is no "proper" exposure that will reproduce all slits at the correct size. The smaller slits have a lower maximum intensity and the 0.25- μm slits will not reproduce at all if the middle of the 0.3-log exposure range is set at the nominal slit width for wider slits. This leads to the first definition:

Optimum exposure places the center of the exposure band such that larger slits are reproduced in their correct size.

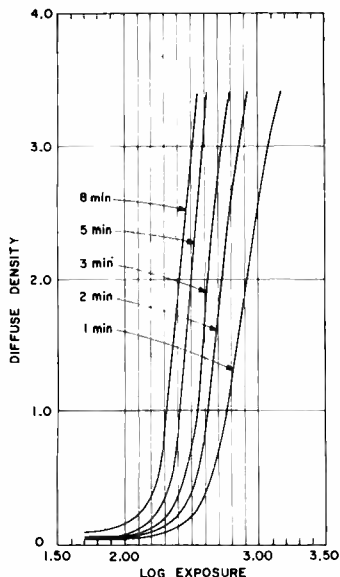


Fig. 7—Density vs. log exposure for Kodak high resolution plates.

The resulting density at the edge is approximately 0.6 or 25% transmitting. For the 1000 line/mm assumed for the curves, the edge transition is approximately 0.25 μm . The nominal width occurs at $\frac{1}{2}$ of the unmasked intensity for incoherent illumination, and at $\frac{1}{4}$ of the unmasked intensity for coherent illumination. The second definition follows logically:

Minimum useful line width is the smallest line produced in its correct dimensions at the same exposure which produces all larger lines in their correct dimensions.

For both incoherent and coherent light, 2 μm is the minimum line width. For coherent light, the 1- μm line is too wide; but there is a line width between 0.5 and 1 μm which would be reproduced in its correct width. For incoherent light, the 1 μm line will not reach full density. The "ringing" caused by the sharp cut-off of coherent illumination may result in line-width modulation of nearby lines. Also, the loss of higher spatial frequencies in coherent illumination is evident in that the narrowest slits are imaged at higher intensity by incoherent light than coherent. Fig. 9 is an enlarged portion of Figs. 8a and 8b overlaid to show the difference in the images produced by coherent and incoherent illumination. Increased exposure can be represented by moving the exposure band downward on the graphs. If one requires that a neutral density of 2 be reached in the center of the reproduced bar, object lines narrower than some minimum width will all be reproduced at the same width. The extra exposure required will increase the size of all larger lines. For example, all curves representing images of slits less than 1 μm for coherent and 0.5 μm for incoherent illumination can be superimposed by a vertical (intensity) scale shift.

So far, we have been considering the situation of illuminated slits on a dark background. Small dark areas on a light background are much more difficult to handle. To see why, compare Fig. 10 with Fig. 8b. Fig. 10 is computed for dark lines on an infinite light background. The narrower lines vanish much more rapidly than with illuminated slits and no amount of exposure compensation can restore them because the image contrast is too low. Note, however, that the minimum useful line width as previously defined

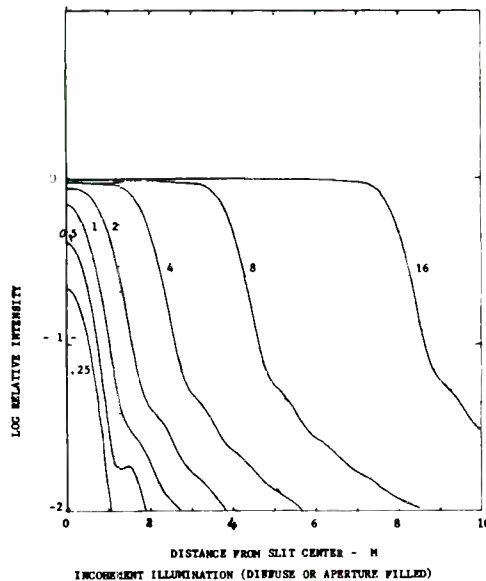
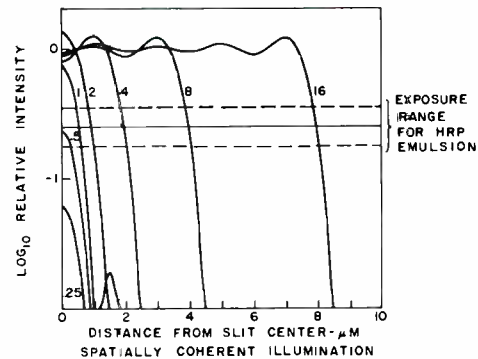


Fig. 8—Log intensity in images of slits—Coherent and incoherent illumination.

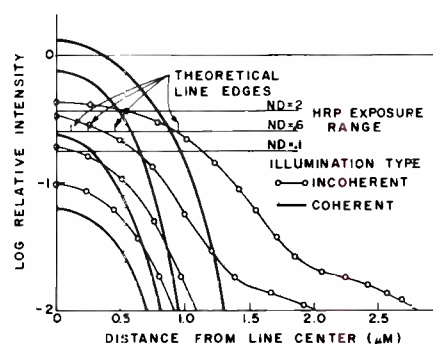


Fig. 9—Comparison of coherent and incoherent slit images near limiting resolution (normalized to optimum exposure intensities).

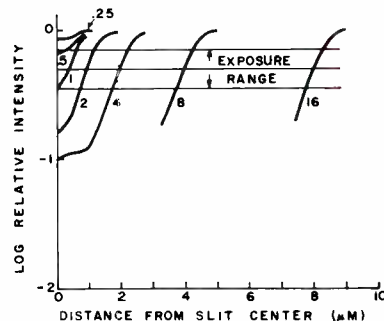


Fig. 10—Log intensity in images of dark stripes in light field.

is still reproduced at approximately the correct size. This observation leads to an alternate definition of the *minimum useful line width* as the smallest line reproduced with equal width in a clear line and a dark line from equal width objects.

Step-and-repeat cameras designed to expose photoresist using blue light with lenses approaching *f*/1 can get slightly higher cut/off resolution due to shorter wavelength of light. The lower effective gamma (contrast) of photoresist, however, requires a higher-contrast image and loses some of the advantage. Dyed high-resolution plates⁹ keep their high contrast while reducing the scattering of blue light and produce the highest demonstratable resolution. The Tropel *f*/1.6 lens in the Jade step-and-repeat machine at RCA Laboratories has shown an experimental cut-off resolution of at least 1100 lines/mm. It's theoretical cut-off resolution is about 1200 lines/mm. The response at 1000 lines/mm is 10 to 20%, which is too low for satisfactory photoresist exposure. At 500 lines/mm, the response is 44% to 50%, which is the minimum for satisfactory photoresist exposure. Since the theoretical limiting resolution is about 3000 lines/mm in air using 435-nm light and a numerical aperture of 1.0 (*f*/0.5), these lenses are within a factor of 3 of the best one could possibly do. The highest resolution lens available today for an image in air seems to be the E. Leitz metallurgical microscope objective with 80X magnification and a NA of 0.95. As a reducing lens, it can produce images about 0.5 μm over a field about 0.4 mm in diameter—far too small to expose the chips being made today. It can be used only for very special work where the expense of drawing line-by-line is justified.

The cost of serial point-by-point generation of a mask can be appreciated if one allows 10⁻⁷ s/element for exposure time (a fairly optimistic number) and considers that a 50-mm-dia (2-inch) wafer contains about 2 × 10⁹ 1-μm spots. The resulting minimum exposure time is about 200 seconds, if the control system can supply the data fast enough. The cost of such a system is about 10 times the cost of a mask aligner and printer, and the time to expose is 10 times as long. The resulting 100 times cost/exposure is uneconomical for production exposure on wafers but could be quite acceptable for making original masks.

Table III—Comparison of parallel-electron-beam exposure systems for masking.

Method	Image Photocathode	Image Aperture	Parallel beams (fly's eye)
Workert(s)	O'Keeffe ¹²	Koops, Mollenstedt ¹¹	Newberry
Company	Westinghouse	U. Tubingen, Ger.	G.E.
Image size	50mm circle	1 × 1 mm	25mm sq.
Obj. size	50mm circle	3 × 3 cm	?
Resolution	7.5 μm		1.5 μm
Alignment	± 2 μm		?
Exposure	15 to 20 s		
Cycle time	20 to 30 min		
Expected exposure	5 s		
Expected cycle	1 min		
Expected alignment	± 0.1 μm		
Comments:	Limited photocathode life	2 masks needed + mechanical translation	difficult to match lenses in array for magnification and distortion. 0.080-in. chip

Table IV—Comparison of scanning-electron-beam systems for masking.

Workert(s)	Samaroo ¹³	Broers ¹¹	Taru ¹¹	Lindsay
Company	Western Elec.	Hatzakis	Denda	
Beam current	1 to 10nA	IBM	JEOI	
Accel. volts	15kV	1μA	10nA	
Sens. mat'l.	HRP	?	?	
Field size	5 × 5 cm	PMMA	KPR	
Total bits	~ 10 ⁹	1 × 1 mm	2 × 2 mm	5 × 5 cm
Exp. time	1000 s	10 ⁶	1.7 × 10 ⁷	
Min line	4 μm	0.1 to 5 s	40 s	0.5 μm
Beam control	computer	1 μm	1 μm	
Bits/sec	10 ⁶	flying spot	computer	
5 × 5 cm exp.	1000 s (max)	2 × 10 ⁹ to 10 ⁷	4 × 10 ⁶	
	10 to 300 s (usual)	250 to 12500 s	25000 s (max)	
			250 to 8000 s (usual)	

Notes: HRP is a high-resolution plate.
PMMA is polymethyl methacrylate.
KPR is Kodak photoresist.

Wavelengths < 100 nm

The two main potential benefits of very short wavelength radiation are increased resolution and increased depth of field. The basic resolution equation [$d = a\lambda/(NA)$] discussed above shows the inverse relation between wavelength and numerical aperture or convergence angle in the focused image. 10kV electrons have a wavelength of about 0.122 angstroms. The wavelength-limited resolution is therefore much better than needed since atomic spacings are of the order of a few angstroms. The angle of convergence can therefore be made quite small resulting in a large depth of field. For 10kV electrons and a 1-μm spot, the depth of focus is a few millimeters.

X-rays

X-ray wavelengths are much shorter than light, but they are not used in masking except for a few peripheral things like chemical spread function evaluation in photographic material. The two main reasons for disuse are 1) masks must be thick to be sufficiently dense to x-radiation which places a severe limitation on resolution, and 2) no effective high-resolution focusing means exists for x-rays. Molecules have similar limitations in that mask resolu-

tion is limited since masks must be apertured (*e.g.*, etched or electroformed metal) and focusing is not feasible. However, vacuum evaporation through apertures has been used to make some very sophisticated devices.¹⁰ Conventional means are used to make the masks, so the potential resolution improvement has not been exploited.

Ions

Ions can be focused into very fine beams and used for point-by-point scanning. However, the deflection and focusing power is several hundred to several thousand times that required to focus and deflect electrons. Also, no small-sized, high-current-density ion sources capable of yielding beams with power density comparable to electron beams are available. Therefore, although ion implantation is an important semiconductor fabrication technology, it is not used for generation or replication of masks by scanning or imaging. (The use of structures on the wafers to mask ion implantation in self-aligning patterns is an important use of "aperture" type masks).

Electron-beams

Electron-beam exposure is the most promising means of using short-

wavelength energy for mask making, in spite of a number of difficulties. Electron beams of 10^{-16} ampere, 250-nm in diameter, have been reported.¹¹ Why not just scan such a beam across the wafer or mask substrate and expose a high resolution mask? The answer is aberrations. Lenses for light can have a high order of correction over wide fields because many glass surfaces can be used with differing kinds of glass to produce near-perfect images over a wide field. Electron optics are not so fortunate. Only electric and magnetic fields can be used as lenses. For high resolution, the beam cannot be allowed to strike the field-forming electrodes. The electron optician is faced with a situation similar to a light optician forced to work with lenses made of balloons filled with high index gas and constrained at the margins. The result is that the angular fields over which really high resolution can be obtained is small compared to light optics. Broers¹¹ reports a 1-mm field about 4000 elements across. By comparison, the lenses for 1:1 projection printing reproduce about 20,000 elements across a 60-mm field. Serial-scan electron-beam mask generation seems destined to use mechanical motion or step-and-repeat to produce a full wafer-sized exposure.

Several parallel-electron-beam exposure schemes have been proposed; see Table III. A "fly's eye" electron lens array was built by workers at G.E. in Schenectady, where several patterns could be scanned in parallel. There were some press releases a few years ago, but no information has been released since. A projection system similar to a transmission electron microscope in reverse has been built at the University of Tubingen in Germany by H. Koops and G. Mollenstedt. It is reported to project a pattern with 50-nm resolution about 1 mm square. None of these systems have included any means of registration of successive exposures for multi-layer device fabrication, although electronic sensing of registry marks and using the information to register automatically the current exposure should be possible.

The electron exposure equipment closest to being ready to expose wafers in a production environment was developed at the Westinghouse Research Center in Pittsburgh.¹² It images a masked photocathode at 1:1

onto a wafer loaded in a vacuum chamber. The electron-sensitive resist on the wafer must not be photosensitive since the ultraviolet light that is used to illuminate the transparent photocathode also falls on the wafer. The forthcoming commercial machine is expected to use automatic registration, sensing registry marks on the wafer and tilting the focusing magnetic field to achieve registry. Workers at Western Electric Engineering Research Center have developed a scanning-electron-beam system which meets the requirements of 10X reticle production quite well.¹³ Working on high resolution photographic plates, 4- μ m lines over a 50×50 -mm area are expected. The reported results were for a 4×4 -mm field. An eventual addressable array of $100,000 \times 100,000$ points was predicted, but much higher stability than yet achieved is needed. In this application, the ease of scanning of the electron beam is exploited rather than the high resolution or depth of field. The mask is used in further optical processing steps which require flat glass and will limit resolution as well. JEOL has reported a system similar to a scanning electron microscope for mask work.¹⁴ Resolution of 1 μ m and exposure times of 1.5 to 2 hours are achieved. Registration by scanning previously applied patterns allows application to device fabrication; recent work on scanning-electron-beam systems is summarized in Table IV.

Conclusions

This has been a rather sketchy report of where we stand today in photomask technology. As device makers find needs for smaller structures, the mask makers will be called upon to produce suitable masks. As long as visible or near-ultraviolet light is used to make the final image on the device, the smallest geometries will not be smaller than a few tenths of a micrometer. Electron imaging seems to be the most promising means of improving on light imaging with at least one electron-beam wafer-printing device nearing commercial reality. Several scanning-electron-beam equipments are being used for experimental mask making (often for convenience of scanning rather than the higher resolution capability). Fig. 11 is a summary of the capabilities of diffraction limited optical systems in mask making.

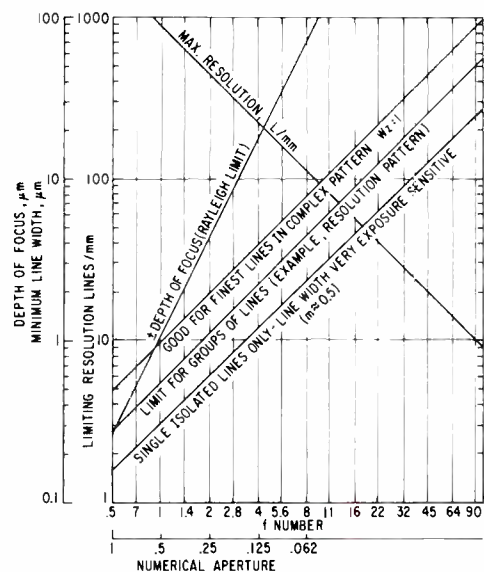


Fig. 11—Guide to mask making capabilities of diffraction-limited optical systems.

Acknowledgment

Dr. E. G. Ramberg provided the mathematical forms from which the intensity curves were computed and was an able consultant on questions involving the connection between the mathematics and the real world.

References

- Ryan, R. J., Davidson, F. B., Hook, H. O., Chapter 14 "Photofabrication," Harper, C., ed.; *Handbook of Materials for Electronics* (McGraw Hill: New York, 1970).
- Schade, O. H. *J. OF SMPLE*, Vol. 13 (1964) pp. 18-119.
- Johnson, H., "Restoration of High Frequencies in Photomask Line Patterns by Photographic Non-Linearity," *SCP and Solid State Technology*, Vol. 10, No. 7 (July 1967) p. 50-53.
- Swing, R. E. and Clay, J. R., "Ambiguity of Transfer Function With Partially Coherent Illumination," *J. Opt. Soc. Am.*, Vol. 57, No. 10 (1967) p. 1180-1189.
- Altman, J. H., "Photography of Fine Slits Near the Diffraction Limit," *Photographic Science and Engineering*, Vol. 10, No. 3 (May-June 1966) p. 140-143.
- Considine, P. S., "Effects of Coherence on Imaging Systems," *J. Opt. Soc. Am.*, Vol. 56 (1966) p. 1001-1009.
- Kotler, F. and Perrin, F. H., "Imagery of One-Dimensional Patterns," *J. Opt. Soc. Am.*, Vol. 56 (1966) p. 377-388.
- Kinzy, R. E., "Images of Coherently Illuminated Edged Objects Formed by Scanning Optical Systems," *J. Opt. Soc. Am.*, Vol. 56 (1966) p. 9-11.
- Keirwin, R. E., "Dyed Photographic Emulsions for Improved Recording of Projected Images," *Applied Optics*, Vol. 8, No. 9 (1969) p. 1891-1895.
- Kodak Pamphlet, "Kodak High Resolution Plate, Type 2," p. 226.
- Kodak Incidental Intelligence*, Vol. 8, No. 2 (1970).
- Weimer, P. K., U.S. Patent No. 3,488,508; also paper presented at IEEE Int. Conv. (March 1971).
- Broers, A. N. and Hatzakis, M., "Micro Circuits Made Through Microscopes," *Industrial Research* (March 1970) p. 56-58.
- O'Keefe, T. W., "Fabrication of Integrated Circuits Using The Electron Image Projection System (EIPS)," *IEEE Trans. on Electron Devices*, Vol. ED-17, No. 6 (June 1970) p. 465-469.
- Samaroo, W. R., Ramot, J., and Parry, P. D., "An Electron-Beam Pattern Generator," *IEEE International Convention Digest*, Session 2C (March 23, 1970).
- Miyauchi, S., Tanaka, K., and Russ, J. C., "IC Pattern Exposure By Scanning Electron Beam Apparatus," *Solid State Technology* (June 1970) p. 56-64.

Advanced laser beam image reproducer for very-high-resolution image recording

S. M. Ravner

The image recording capabilities of the RCA Laser Beam Image Reproducer have been significantly upgraded. The current third-generation design faithfully reconstructs imagery on film with a resolution in excess of 18,000 picture elements per scan at a scan rate of 1000 lines per second and with a flat dc-10MHz video response.

Stephen M. Ravner, Mgr.
High Resolution Displays
Astro-Electronics Division
Princeton, New Jersey

received the BSEE and the MSEE from the Polytechnic Institute of Brooklyn in 1959 and 1963, respectively. He has been active in the design and development of advanced television and display devices at RCA during the past nine years and was responsible for the development, at AED, of a high resolution Laser Beam Image Reproducer (LBIR). Previously, he was associated with ITT Federal Laboratories, where he was concerned with design and development of training simulators and display devices utilizing television techniques. Mr. Ravner joined AED in 1961 and shortly became a lead engineer for the electrical-system design, integration and testing of the Nimbus Ground Stations; he was also responsible for the study and design of a high-resolution line-scan kinescope display for a dielectric-tape camera system. After his promotion to Leader Engineering in 1965, Mr. Ravner was responsible for the design and development of all AGE for a classified program as well as early design phases of the improved Apollo Television Scan Converters for NASA. In 1968, he was promoted to Manager of High Resolution Displays and has devoted the major portion of his efforts toward directing the LBIR advanced development program at AED. Mr. Ravner is a member of the IEEE and the Society for Information Display.

THE MAJOR OBJECTIVE of a development program at AED is to demonstrate the potential capability of the RCA Laser Beam Image Reproducer (LBIR) in faithfully recording images on film with high modulation transfer function (MTF) response at spatial frequencies corresponding to 18,000 to 24,000 picture elements (pixels) per scan, at a scan rate of 1000 lines per second, and with an analog video bandwidth up to 25 MHz (-3dB). This capability is needed to meet the requirements of future space programs, such as later-generation Earth Resources Technology Satellite (ERTS) missions. Imaging sensors already exist which provide 10,000 pixels per scan resolution, such as the RCA $4\frac{1}{2}$ -inch Return Beam Vidicon (RBV) camera, and higher resolution sensors are currently being developed.

The basic approach to the upgrading

program was to utilize the maximum amount of already existing LBIR design and hardware. Fig. 1 shows the configuration of the advanced LBIR.

In addition to the major objective of improving the resolution of the LBIR by reducing the optically formed scanning spot size, emphasis was also placed on extending the performance of other LBIR subsystems so that they would be compatible with the higher resolution aspects of the image. Performance improvements included the ability to maintain uniform focus over the full $9\frac{1}{2}$ -inch film width and the elimination of non-uniform line-to-line spacing caused by the film transport or the scanner. These factors were already satisfied for the 6,000-pixel LBIR design, but were unsatisfactory for the desired 18,000- to 24,000-pixel design. The satisfaction of these requirements is much more difficult at the higher resolution.

Background of LBIR development

The LBIR was developed originally in 1967 at AED to provide a means of recording the high-resolution imagery produced by the then newly developed RCA 2-inch RBV camera.

The objective of this original effort was to construct a machine which would reproduce the imagery in a 9×9 -inch photographic transparency format with no significant degradation of image

Fig. 1—Advanced Laser Beam Image Reproducer (LBIR).

Reprint RE-17-6-15

Final manuscript received December 20, 1971



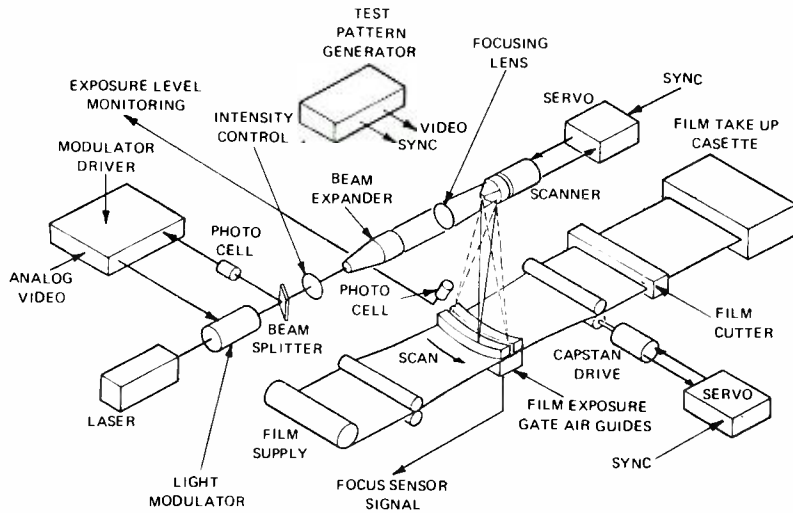


Fig. 2—Pictorial diagram of advanced LBIR.

quality. The resultant prototype LBIR design provided 75% response (including film) at a resolution of 6,000 pixels per scan, had a gray scale dynamic range in excess of 100:1, and had excellent geometric fidelity. Since the 2-inch RBV camera had a limiting resolution of 4,500 pixels per scan and a 50:1 dynamic range, the LBIR appeared as a "transparent window" in the total imaging system.

A second-generation LBIR¹ was developed in late 1968 to provide several basic improvements essential for field operational equipment; it provided additional image fidelity improvements as well. Several functions were

automated, alignment stability was greatly improved, and a continuous film transport was added to provide operational mode versatility and rapid sequential frame capability. However, the basic image reproduction parameters, such as resolution and gray scale, were not significantly changed. This design satisfied the needs of the three-camera 2-inch RBV system being designed for the ERTS program.

However, early in 1970, the need for a higher resolution image reproducer became evident. Sensors capable of providing up to four times the LBIR resolution (24,000 pixels per scan) were being investigated for advanced ERTS

Table I—LBIR performance characteristics (2nd and 3rd generation comparison).

Characteristics	Previous LBIR	Present LBIR
Resolution:		
Pixels per scan	6000	18,000
Corresponding cycles/mm	13.2	39.5
MTF (with film)	80% (Kodak RAR1496)	56% (Kodak 3414)
MTF (electro-optics only)	94%	75%
Gray scale:		
Dynamic range	100:1	250:1
Maximum film density	2.3 (Kodak RAR2496)	2.0 (Kodak 3414)
Video bandwidth	dc-5MHz (-3dB)	dc-10MHz (-0.5dB) dc-25MHz (-3dB)
Signal to noise ratio (electronics)	50dB	50dB
Horizontal blanking	10%	10%
Nominal line scan rate	1250 lines per second	1000 lines per second
Nominal scanner speed	18,750 r/min	15,000 r/min
Scanner sync jitter	100ns p-p, <10Hz bandwidth	50ns p-p, <10Hz bandwidth
Scanner	1-inch diameter, air bearings	1-inch diameter, air bearings
Number of facets	4	4
Line-to-line spacing	38 μm	12.7 μm
Line-to-line jitter	±1.0 μm	±0.3 μm
Transport speed range	25 to 100 mm/sec	1 to 100 mm/sec
Recording gate	Fixed curved platen	Air-guide curved platen
Film supply capacity	9½-inches wide by 125 feet (RAR2496)	9½-inches wide by 250 feet (3414)
Laser power	15 mW @ 632.8nm	15 mW @ 632.8nm

missions. As a result, AED undertook a program to upgrade the LBIR to a third-generation version which would be compatible with these very-high-resolution sensors.

LBIR description

A pictorial diagram of the current LBIR is shown in Fig. 2. The basic imaging process consists of scanning a finely focused, intensity-modulated laser beam across the width of a continuous web of film. The 9½-inch wide film is shaped to a precise curvature by an air-bearing exposure gate, and the beam is deflected across the film by a rotating four-sided pyramidal scanning mirror. The optics and scanning geometry are such that the phase-locked constant-speed scanner produces a linear scan rate, with perfect focus and uniform exposure, across the entire width of the film. Vertical scanning is accomplished by moving the film perpendicularly to the exposure scan line.

The performance characteristics of the improved (third generation) LBIR are compared to the previous design in Table I. The modifications and improvements which were implemented to achieve the higher resolution performance are described in the following paragraphs.

Light modulation system

The new LBIR light modulation system consists of the modulator driver (video) electronics, the light modulator, and the optical feedback beam splitter mirror and photo cell. The intensity control, which is a high-quality polarizer used to establish the gross exposure level in the LBIR, was retained from the previous LBIR design. The electronics are

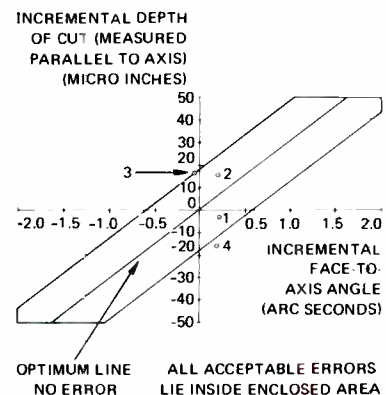


Fig. 3—Scanner geometric error diagram.

all-solid-state. The light modulator is a low-voltage electro-optic transverse field type.

The new set of light modulation components features automatic null-bias control for "hands-off" full-time contrast optimization; an overall electronics-optics feedback loop for highly accurate and repeatable continuous gray-scale recording; and light modulator transfer characteristic linearization. Along with these features, the wide bandwidth and dynamic range of this system, as indicated in Table I, permit rapid-rate recording of sharp high-resolution images. For example, an image consisting of $20,000 \times 20,000$ pixels, or a total of 400 million picture elements, is reproduced by the LBIR in only twenty seconds.

Optics and scanner

The major optical components in the LBIR are the beam expander, focusing lens, and scanner. These components determine the diffraction limited scanning spot size. The beam expander enlarges the modulated laser beam to completely fill the aperture of the focusing lens.

The scanner axis is coincident with the optical axis; each facet, therefore, intercepts 25% of the converging focused beam emerging from the lens, and deflects it radially (the facets are at 45° to the axis).

The rotation of the scanner causes the facet passing through the lower quad-



Fig. 4—Air-guide exposure gate.

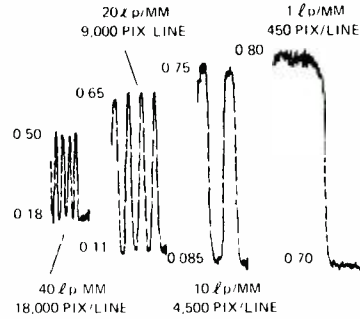


Fig. 5—Microdensitometer traces for various horizontal burst frequencies.

rant of the beam cross section to scan the film. All other beams are blocked so as not to expose the film. The optics are focused for diffraction limited performance, with the scanner facet being the limiting aperture.

Although the 1-inch scanner diameter is the major limitation in extending the resolution, analysis indicated that it could still provide significantly higher resolution than had previously been achieved. Therefore, the scanner size was not increased, thereby avoiding a major scanner subsystem re-design effort. The scanner itself, however, was replaced with a new one which was built to extremely tight geometric tolerances, commensurate with the $12.7\text{-}\mu\text{m}$ line-spacing requirement. The actual measured geometric errors in the new scanner are plotted in the scanner geometric error diagram of Fig. 3. The parallelogram in Fig. 3 encompasses the permissible combination of depth-of-cut and face-to-axis angle errors which are needed to produce the scan line spacing accuracy of $\pm 0.3\ \mu\text{m}$. The achievement of these accuracies represents a major breakthrough in precision scanner fabrication and optical finishing. One facet (point 4, Fig. 3) was slightly out of tolerance, but not sufficiently so to leave any doubts about the success of the technique.

The scanner shaft is actually the armature of the drive motor. It is supported entirely by air bearings (both journal and thrust) to provide vibration-free rotation (no ball bearing noise). The scanner servo utilizes optical tachometer feedback derived from the scanner mirror facets which are used for scanning. The scan synchronization jitter is virtually unmeasurable on a line-to-line basis, and restricted to 50 ns peak-to-peak over a cycle period of more than a hundred scan lines.

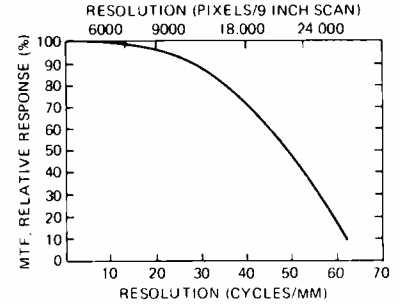


Fig. 6—MTF plot.

Film transport and air-guide exposure gate

The film transport was modified in two major areas: The servo electronics were modified to reduce line-to-line spacing jitter and to extend the lower end of the speed range, and the air-guide exposure gate was substituted for the fixed platen in the original transport.

Table I shows the extended speed range and jitter characteristics of the transport. The $\pm 0.3\text{-}\mu\text{m}$ jitter in line-to-line spacing corresponds to a worst-case value of less than 5% line-to-line spacing error for the $12.7\text{-}\mu\text{m}$ line spacing. This value insures that "banding" (random horizontal streaks in the image due to scan line bunching) is below the visibly detectable level.

The air-guide exposure gate, shown in Fig. 4, provides a uniform cushion of air above and below the film as it shapes it to the precise curvature. The film is supported within the gate by the air bearing and does not touch any part of it. The depth of focus control thus achieved is at least five times better than the allowable depth of focus needed to maintain the MTF performance indicated in Table I. This is one of the most important modifications made in the LBIR for improving the high-resolution performance.

The lower half of the air-guide contains several photo diodes located in positions across its full width. A high-resolution bar target transparency is inserted in the air-guide during optical alignment, and an unmodulated beam is swept across it. Focus adjustment is made while monitoring the diode outputs. This technique results in optimum focus alignment since it is made during actual operating conditions (the scanner at nominal speed, and the air-guide shaping and supporting the film).

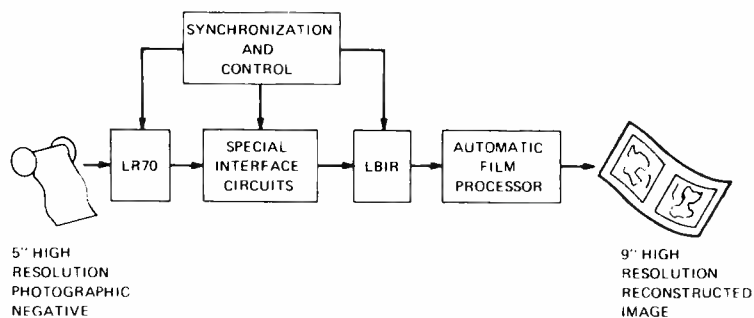


Fig. 7—LR70/LBIR combination.

The film type used in the new LBIR, Kodak 3414, is a high-definition aerial film. The exposure sensitivity of 3414 is approximately ten times less than the Kodak RAR2496 originally used for the lower resolution recording. The laser power in the LBIR (15 mW @ 632.8nm) was more than adequate for the 2496 film but not sufficient to fully expose the 3414 film. This condition was corrected by eliminating the vertical aperture mask. The mask was used to create merged scan lines in the lower resolution LBIR, and was not needed for initial testing of the higher resolution LBIR. This improved the optical efficiency enough to expose the 3414 film to densities in excess of 2.0.

Test pattern generator (TPG)

The TPG was re-designed primarily to provide horizontal burst frequencies as high as 10MHz (18,000 pixels per scan) to facilitate high resolution MTF measurements. The TPG also provides a variety of gray scales, vertical frequency burst patterns, geometric linearity patterns, and a composite of all of these in a single frame.

Performance

TPG measurements

The third-generation LBIR was tested extensively using the TPG as a calibrated input source. Microdensitometer traces for various horizontal burst frequencies

Table II—Horizontal resolution, 3rd generation LBIR.

Pixels per scan line	TPG burst freq. (MHz)	Cycles/mm on film	MTF of 3414 film (%)	MTF of LBIR and film (%)	MTF of LBIR without film (%)
450	0.25	1	100	100	100
4,500	2.5	10	95	94.5	99
9,000	5.0	20	87	84.5	96.5
18,000	10.0	40	75	56.0	74.0

are shown in Fig. 5. The calculated values of MTF based on these measurements are given in Table II, and the MTF is plotted in Fig. 6.

Table II indicates that the film MTF is a significant factor in the overall system performance. For that reason, the LBIR MTF with the film effects removed is tabulated, thereby giving an indication of the potential LBIR resolution capability with finer grain (or grainless) hard-copy media.

The horizontal resolution achieved in the upgraded LBIR (with the film effects removed) compares favorably with theoretical optical calculations. These calculations take into account the aperture shape (scanner facet), the complex illumination profile across the aperture, the wavefront distortions in the optics, and the path-length differences. Higher resolution performance may be directly extrapolated from these figures to determine the required scanner diameter. For example, the horizontal MTF of the LBIR optics can exceed 90% with a 1.4-inch diameter scanner.

Since the vertical aperture mask is not used in the upgraded LBIR, it is not possible to modify the vertical dimension of the scanning spot. As a result, the individual scan lines are clearly visible under high (30X) magnification. For this reason, MTF measurements were not made in the vertical direction; it was obvious that the vertical resolution was "too good," and spot elongation is needed to optimize the system. In a later phase of this program, a higher power laser will be installed in the LBIR, and the vertical aperture will be reinstalled, thereby allowing adjustment for optimum scan line merging while maintaining maximum vertical resolution.

Gray-scale tests demonstrate the large dynamic range capabilities of the LBIR,

as well as the highly accurate density repeatability. The latter is a direct result of the automatic null-bias circuitry.

Geometric measurements indicate an accuracy of better than one part in 2×10^5 on a fine scale (any 10×10 pixel area) and better than one part in 2×10^4 on a large scale (100×100 pixel area or larger). The large scale geometric accuracy could be improved to match that of the fine scale by cancelling out the 50-ns scanner jitter effects with an electronically variable video delay line, a technique which is commonly used in transverse-scan wide-band magnetic tape recorders.

Imagery tests

Nothing is as convincing in evaluating an imaging device as a picture of a real scene generated by that device. In previous years, the LBIR performance could always be demonstrated by providing a real scene video input generated by the 2-inch RBV camera. However, in order to demonstrate the new improved high-resolution LBIR, a sensor of comparable capability had to be found.

Fortunately, RCA has also been developing a wideband laser signal recorder/reproducer system, designated the LR70, which utilizes 5-inch wide photographic film as the recording medium. The LR70 has the necessary optical resolution, scan rate, signal bandwidth, and dynamic range to scan a scene transparency and produce an analog video signal suitable for feeding the new LBIR.

Some minor modifications were made to the LR70 in order to optimize its image scanning performance. A very high-resolution 5-inch aerial camera negative transparency was used as the scene input. The LR70/LBIR combination was interfaced as shown in the block diagram of Fig. 7, and images were scanned and reproduced simultaneously. An example of the resultant output is shown in Fig. 8, and a 25 times enlargement of a small area of this scene is shown in Fig. 9.

The general appearance of the LBIR output is that of a conventional photographic transparency, and not of a scanned image. Only under high magnification is it apparent that the scene is indeed scanned and reconstructed in a raster format. This demonstration

confirms the suitability of the improved LBIR for future ultra-high resolution imaging system applications.

Summary and conclusions

The major changes to the previous LBIR during the improvement program were the substitution of a 25-MHz light modulation system in the place of the original 5-MHz system; the replacement of the scanner mirror with a new one of much higher quality; the addition of a precision air-guide film exposure gate with integral focus sensors; the modification of the film transport servo system to provide much finer line-to-line spacing control; the use of a higher resolution film; and the re-design of the LBIR TPG to provide higher bandwidth test signals. In addition, the film transport and scanner mirror servo electronics were modified to operate at the scan rates commensurate with the higher resolution scan parameters, and the optical components were checked and critically aligned.

The resultant performance exceeds expectations, in that the recorded

images are photographic-like, and the MTF of the entire system was measured to be nearly the theoretical value for the components used.

The LBIR improvement program is continuing at AED. However, the major objective of demonstrating its extended high-resolution performance capability potential has been achieved. The major problems associated with higher resolution operation, such as film transport and scanner induced banding and precise focus control across the entire format, have been solved.

Higher values of LBIR MTF will not be useful however, unless a better image recording medium is used. Additional modifications are currently in progress which will facilitate recording on lower sensitivity materials which offer a considerable improvement in resolution. The LBIR MTF can easily be increased by increasing the limiting aperture, namely, the scanner and associated optical components. This in itself does not present a difficult technological challenge, rather it only involves engineering re-design.

The LBIR is currently a highly developed and tested image recording device, which has satisfied its purpose in the past. Based on the progress of the current improvement program, there is no doubt that it will also satisfy the needs of future higher resolution imaging systems as well.

Acknowledgment

The LBIR advanced development work was done at the Astro-Electronics Division primarily under the direction of Carmine Masucci, with the extensive support of Dick Groves. The author thanks Bob Thompson and Larry Dobbins of the Communications Systems Division for the use of the LR70 and their timely support during the image recording phase of the program.

Reference

1. Ravner, S. M., "Laser Beam Image Reproducer," SPSE-Sponsored ELIMS-70 Symposium, April 1970 (and published in proceedings of that symposium). Subsequently published as RCA Reprint RE-17-2-16.
2. Dobbins, L. W., "High-speed facsimile system employing the LR70 laser scanner," *this issue*.

Fig. 8—Photograph reproduced by LBIR.



Fig. 9—Portion of photo of Fig. 8, magnified 25 times by LBIR.



High-speed facsimile system employing the LR70 laser scanner

L. W. Dobbins

A high-speed facsimile transmission system utilizing the LR70 laser scanner has been demonstrated. In the LR70 unit, a laser beam is focused to a small spot and mechanically scanned across the width of a 5-inch film transparency. The light energy, modulated by variations in film density, is collected and focused on a photo-multiplier tube. The result is a serial stream of data representing the scanned imagery in a raster format. This data is the input to a similar device which reproduces the original imagery with very little degradation.

MECHANICAL SCANNERS are not new. They were, in fact, the first scanners. But now, a new generation of technology enables the mechanical scanners to greatly exceed the performance of electronic scanners in two areas:

- 1) Number of picture elements; or pixels, per scan
- 2) Geometric fidelity

A typical system output image has demonstrated that straight lines in the original image can be reproduced as

straight lines. Servo control of scan velocity (ScanLoc) permits spot position error to be kept to one part in twenty-thousand. Electronically Variable Delay Lines (EVDL) permit an improvement in control of spot location by an order of magnitude.

Development of transverse scanning devices at RCA

The majority of the laser scanning devices developed at RCA have been of the transverse scan type. In these devices, the focused laser beam line-scans perpendicular to the direction of film motion. These transverse scan

devices developed along two parallel paths, image scanner/recorders and signal recorder/playback units.

In 1967 the prototype Laser Beam Image Reproducer (LBIR) was built (see Fig. 1, upper left). The LBIR recorded a single 9-inch frame on film. This device had 75% Modulation Transfer Function (MTF) at 6000 elements per scan. This unit was upgraded in 1969 to permit continuous recording. Eighteen thousand picture elements can now be recorded per scan at 75% MTF. The LBIR is described in this issue and in several published papers.^{1,2}

Signal recording

Signal recorders were developed when the availability of high-powered lasers made it possible to record much higher frequencies on silver halide film than had been possible with magnetic tape. The original wideband laser signal recorder (lower left, Fig. 1) was developed in 1966 and has undergone continual improvement. Its present capability is 80-MHz video bandwidth with a time base stability of better than 1 ns.

LR70 series

This growing technology led to the LR70, which has demonstrated capability in recording and scanning both imagery and signals. The facsimile system discussed here consists of the LR70 scanner coupled to the LBIR. Some capabilities

Reprint RE-17-6-22
Final manuscript received January 7, 1972.

Lawrence W. Dobbins, Recording Equipment Operations, Communications Systems Division, Camden, N.J., received the BSEE from Auburn University and has completed course work for the Master's Degree at Drexel Institute of Technology. Mr. Dobbins joined RCA in 1955 and has done design work on transverse scan magnetic recorders, optical correlators, and spectrum analysis devices. He also took an active role in the design of optical and electronic systems in the LR70. Mr. Dobbins is presently a Senior Member of the Engineering Staff. He is a member of the IEEE, the Society for Information Display, and the Society of Photo-optical Instrumentation Engineers.



Table I—Image scanner characteristics (LR70PIX).

Parameter	Performance
Resolution (α 50% MTF)	20,000 pixels [*] per scan
Geometric fidelity	1 part in 20,000
Gray scale	14, $\sqrt{2}$ steps
Video bandwidth	dc to 75 MHz
Format	5-inch-wide film up to 1500 ft long
Scan rate	Up to 5000 scans/s
Film speed	0.25 in/s and higher, continuously variable
Time required to scan a 5-inch square frame	48 (at maximum data rate)

*Picture elements

Table II—Signal recorder/playback characteristics (LR70CVR).

Parameter	Performance
Bandwidth:	
Direct record	250 KHz to 75 MHz (-6 dB)
Digital	100 MBit/s
Video, with FM system	dc to 30 MHz
Record time	35 min
Film width	5 in
Scanner speed	833 in/s (50,000 f/min)
Scan speed	20,000 in/s
Film speed	10 in/s

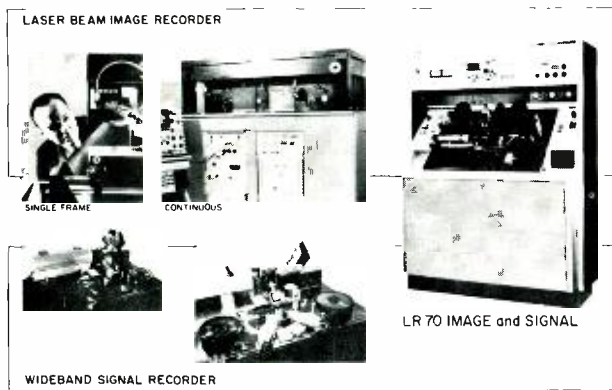


Fig. 1—Development of RCA laser scanning and recording devices.

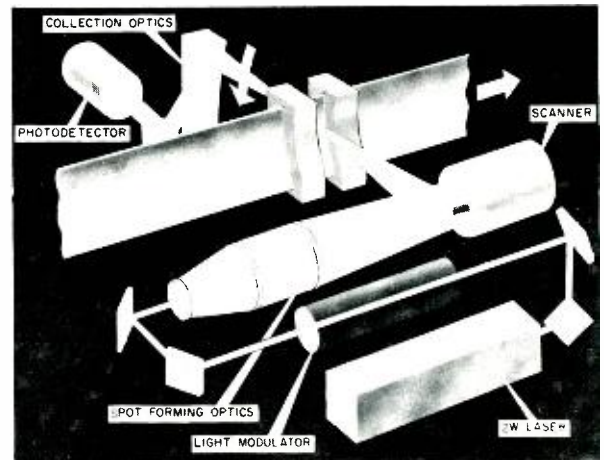


Fig. 2—Optics system of the LR70. →

of the LR70 are considerably greater than those required in the particular facsimile link with the LBR. The maximum performance characteristics of the LR70 as an image scanner are listed in Table I. As a signal recorder/reproducer, designated LR70VR, its performance parameters are different, but related. These characteristics are listed in Table II. At present, the LR70 which extends some of these capabilities is being assembled.

LR70 optics

Fig. 2 is a diagram of the optics of the LR70. The light source is a 2-watt argon laser. This laser is grossly overpowered for image scanner applications, but was selected to permit direct recording of 75-MHz signals on low-sensitivity film.

The laser beam is directed through a 140-MHz light modulator. When the LR70 is operated as a scanner, the light modulator is not required and is either removed or biased to provide a constant light output.

After emerging from the light modulator the beam is directed to the spot-forming optics which consists of a beam expander and a spot-forming lens. The spot-forming lens forms one spot on its optical axis. A rotating mirror scanner is placed on the optical axis to deflect this focused spot to the film platen. As the mirror rotates, the scanned spot generates a circular locus concentric to the scan axis. This approach permits uniform resolution to be achieved over the entire scan, and diffraction-limited performance can be achieved with off-the-shelf lenses. The film is supported within the focal depth with a precision air bearing film guide.

Film motion causes succeeding spots to scan adjacent lines on the film in a raster pattern. As the light passes through the film, it is modulated by the density variations, collected with a curved mirror, and directed to a photomultiplier tube.

Laser noise measurements

It was found that laser noise is a function of laser reflector tuning. The laser configuration used has a wavelength selector prism which makes it possible to operate with about equal power at 4880\AA or 5145\AA . No tuning adjustment of the laser cavity about the 4880\AA line reduced noise without also reducing light power. The broadband signal-to-noise ratio was measured and found to be 34 dB at 4880\AA .

The laser was next tuned to the green line at 5145\AA . Various adjustments of the wavelength selector prism were able to tune hard noise components through the low megahertz range as

shown by the spectral plots in Figs. 3(a) and 3(b). The broadband signal-to-noise ratio was approximately 31 dB for this group of adjustments.

Further tuning, as shown in Fig. 3(c), removed the hard noise components, leaving only the plasma noise which decreases with increasing frequency. The broadband signal-to-noise ratio was 46 dB. These measurements were made without film. Fig. 3(d) indicates the measurement system noise with the light blocked. The large signal at the left is the zero frequency characteristic of the spectrum analyzer.

Kenville^{3,4} describes how longitudinal laser mode noise can be reduced with an etalon, which is a secondary resonant cavity within the laser resonator. The measurements described above were made without an etalon.

Calculation of photodetector noise

For an image scanner without film, the peak-to-peak current in the terminating

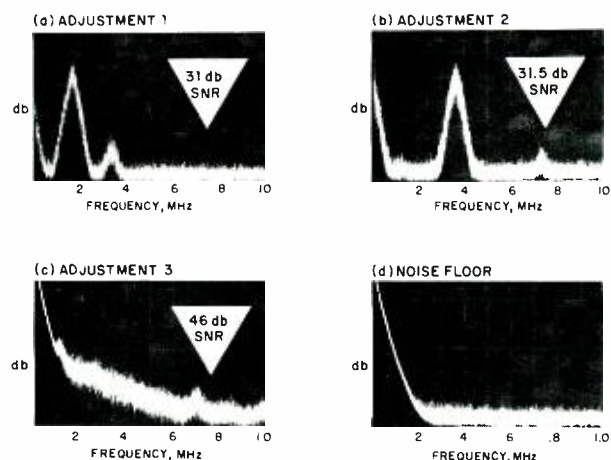


Fig. 3—Laser noise at 5145A

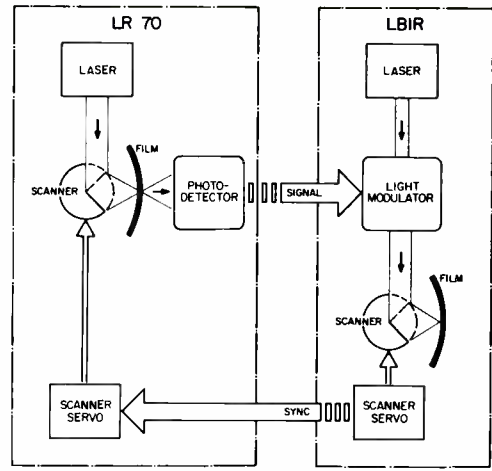
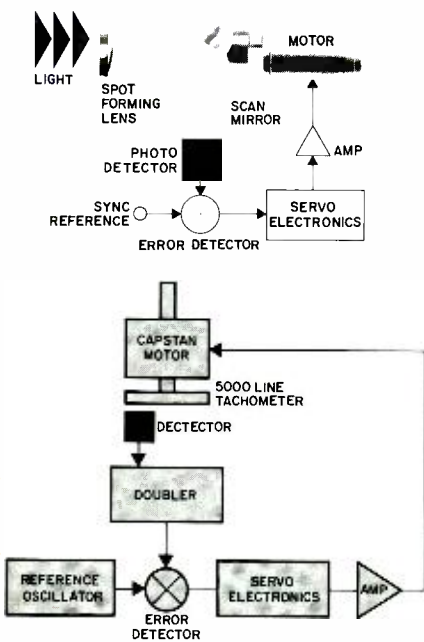


Fig. 4 (upper left)—ScanLock servo control.

Fig. 5 (left)—Film drive system.

Fig. 6 (above)—High-speed facsimile system.

load resistor is given by:

$$i_{sig} = \mu I_K \quad (1)$$

where μ is the tube current gain; and I_K is the average photocathode current. The noise current^{4,5} in the terminating load is written

$$i_n = \mu [3eI_K \Delta f]^{1/2} \quad (2)$$

where e is the charge of an electron; and Δf is the bandwidth.

The contrast ratio which can be achieved is determined by the signal-to-noise (S/R) ratio. S/N is calculated by combining equations (1) and (2).

$$S/N = \frac{p-p \text{ signal}}{rms \text{ noise}} = \left[\frac{I_K}{3e\Delta f} \right]^{1/2} \quad (3)$$

For a 10-MHz bandwidth and 5- μ a photodetector current (data from the test described herein) the photodetector provides a S/N ratio of 60 dB. This signal is then amplified by the electron multiplier within the photomultiplier tube so that S/N ratio is not reduced significantly by the terminating resistor and amplifier.

Number of gray levels which can be transmitted

The contrast ratio determines the number of gray levels which can be transmitted and is given by the S/N , defined as the ratio of peak-to-peak signal to rms noise. The important noise sources are: the laser, the film, and the photo-

detector. Film noise is discussed in papers by Kenville.^{3,4} The light power level in the LR70 is high enough to make photodetector noise small. Laser noise, therefore, is the most significant remaining noise source and constitutes another limit on the overall S/N .

The relation between S/N and gray levels is written

$$S/N = (\sqrt{2})^N \quad (4)$$

where N is the number of $\sqrt{2}$ gray levels.

Since the broadband S/N is limited by the laser to 46 dB, the maximum number of gray levels which can be scanned is greater than 15.5. Film base plus fog would reduce this to an actual 14.5 gray levels.

Geometric fidelity in the scan direction

Geometric fidelity in the scan direction is controlled by moving the spot at a constant velocity across the film. A diagram of the ScanLoc servo is shown in Fig. 4. Motor speed is sensed by detecting a spot of light from each facet of the scan mirror. Comparison with a reference signal provides an error signal used to control the motor. In this particular test, 1000 scans/s from a 6-facet scanner resulted in a rotational rate of 166.6 r/s. The error between the ScanLoc pulse and sync reference was ± 25 ns peak-to-peak. This error can be reduced by an order of magnitude with an EVDL.

Geometric fidelity in the vertical direction

A servo-controlled printed circuit motor (see Fig. 5) drives the film at the very low speed of 0.25 in/s. The resulting error in the location of the scan lines on the film was $\pm 0.3 \mu\text{m}$ or $\pm 5\%$ of a scan line.

High-speed facsimile system

Fig. 6 shows the LR70 scanner connected to the LBIR, forming a high-speed facsimile system. This is the system which transmitted the aerial photographs shown in Fig. 7. Continuous lengths of 5-inch-wide film transparencies from an aerial camera were placed in the LR70 and scanned. Transmission variations in the film modulated the light received by the photodetector producing an electrical signal. This signal was fed to the LBIR where it controlled the intensity of a scanned spot. The LBIR recorded on continuous lengths of 9.5-inch-wide film, providing a magnification of approximately 2:1 in the transmitted images.

A scanner servo is used in each machine to control the velocity and phase of the scanner. In this case the LR70 was slaved to the LBIR, although either equipment may serve as the reference. The operating parameters for this system were: 20,000 pixels/scan, 20 seconds per frame, and a 10-MHz data rate.

Fig. 7 shows a typical aerial scene scanned by the LR70 and recorded by the LBIR. The entire width of a 9.5-inch-film from the LBIR is shown.

Electronic vs mechanical scanning

Table III compares resolution and geometric fidelity for electronic and mechanical scanning. First, comparing resolution, the electronic scanners such as cathode ray tube, return beam vidicon, or electron beam recorder have an upper practical limit on the

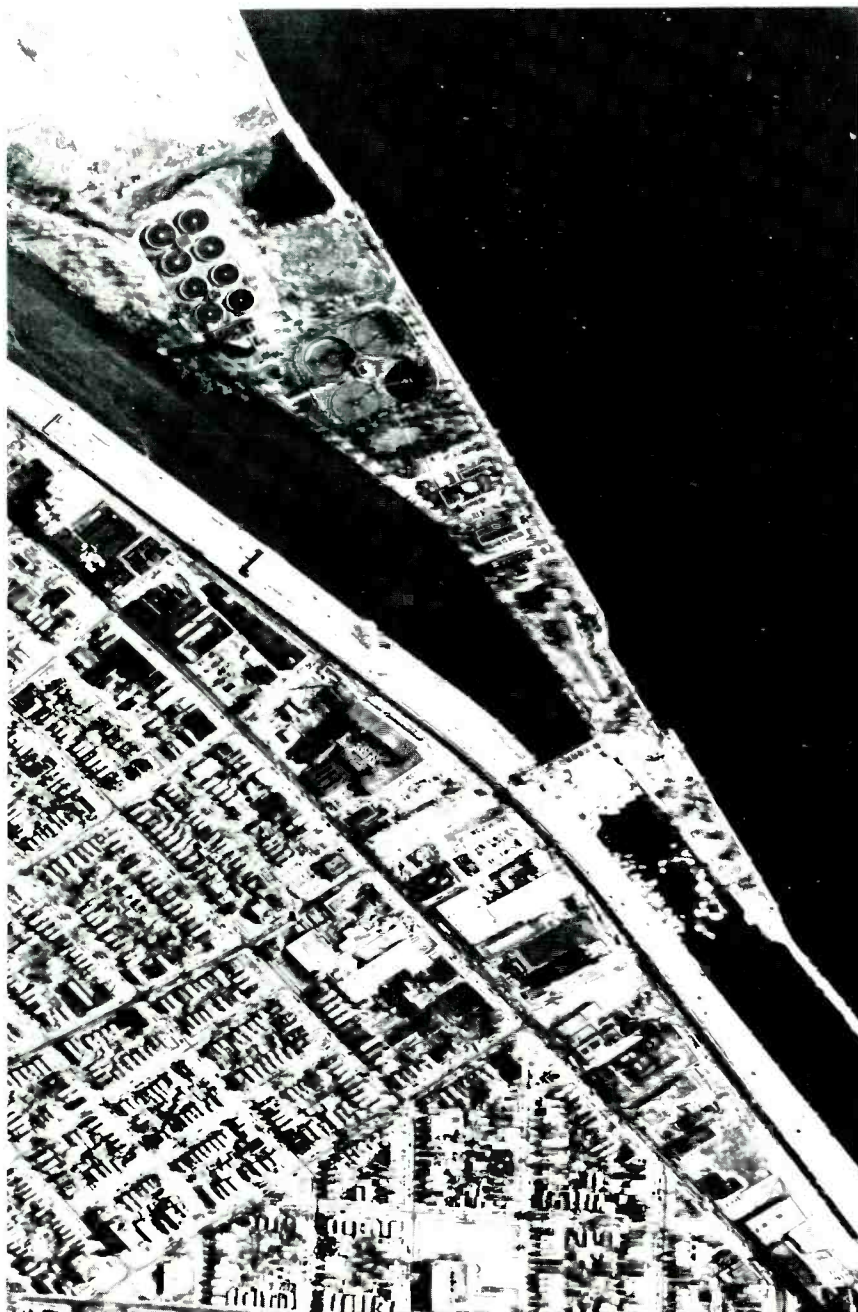
Table III—Comparison of high-resolution scanning—electronic and mechanical scanners.

Parameter	Electronic (CRT, RBV, or EBR)	Mechanical	
		Laser recording	LR70/LBIR
Pixels/scan at 50% MTF	10,000	30,000	20,000
Geometric errors (peak-to-peak)	0.05%	0.0005%	0.005%
Error in number of spots	2.5 (with 5K spot device)	0.15	1.0

number of picture elements per scan of about 10,000.⁶ At this point, the deflection system requires a S/N ratio of 100 dB. The mechanical scanners provide 20,000 pixels per scan at 50% MTF with a conservative growth capability beyond 30,000 pixels per scan.

Second, comparing geometric fidelity, a good 5000-spot electronic scanner device can provide 0.05% accuracy, an error of 2.5 spots in five thousand. Mechanical scanners without electronic correction can provide 0.005% error which corresponds to one spot in 20,000.

Fig. 7—Transmitted image of an aerial scene.



With the EVDL, the performance of mechanical scanners can be improved by an order of magnitude to 15% of one spot error out of 30,000 spots.

Applications

The LR70 series can be applied to a wide range of both signal and imagery applications. Its resolution, data rate, and data format can be easily tailored to each system requirement.

As a signal recorder it can record analog data with a bandwidth of up to 75 MHz

or 100 MBit per second digital data. Time base error can be less than 1 ns, rms. At maximum data rate, a record time of 35 minutes is provided.

In a facsimile system, the LR70 operates as a high-performance scanner, as demonstrated. Other image applications include:

- 1) Color recording—Color or other multi-channel information is encoded on black-and-white film. The information is reproduced on a separate display device which allows image enhancement. This technique, developed at RCA, is described in more detail by Corsover.⁷
- 2) Graphic arts—An entire newspaper page can be recorded with high fidelity on a single frame.
- 3) Computer input/output—Variable data rate and resolution give the LR70 the versatility to interface with computer systems.

Conclusion

The LR70 and the LBIR are line scanning devices which read and write high-resolution imagery with very little degradation. The geometric fidelity and resolution are unequalled by other scanning devices, including electronic scanners. As a signal recorder/reproducer (LR70 VR), the 75-MHz data rate and nanosecond time base stability are state-of-the-art. For a wide range of signal and image applications, the designed-in versatility of the LR70 series provides a solution to many high-performance record/reproduce system problems.

References

1. Ravner, S., "Laser Beam Image Reproducer (LBIR)," Proceedings of Electronic Imaging Systems Symposium Sponsored by SPSE (Palo Alto, Calif., April 1970), pp. 181-198.
2. Woywood, D. J., "Laser Recording: Key to High Resolution Image/Signal Reproduction," *Laser Focus* (February 1968).
3. Kenville, R., "Noise in Laser Recording," Proceedings of Electro-Optical System Design Conference, (New York 1971) pp. 68-75.
4. Kenville, R., "Noise in Laser Recording," *IEEE Spectrum* (March 1971) pp. 50-57.
5. *RCA Phototubes and Photocells*, Technical Manual PT-60, RCA (1963) pp. 55-58.
6. Brewer, G., "The Application of Electron/Ion Beam Technology to Microelectronics," *IEEE Spectrum* (January 1971) pp. 23-37.
7. Corsover, S., "Multi-Spectral Recording Encoded in Black and White Film," Proceedings of Electro-Optical System Design Conference (New York, 1971) pp. 85-92.

Acknowledgments

The author wishes to acknowledge the design work of Messrs. D. Lannin and J. Warring and the many helpful suggestions of C. Horton, C. Mascucci, S. Ravner, C. R. Thompson, and G. T. Rogers.

Hardware-software tradeoffs for a CRT phototypesetting system

S. A. Raciti

To create a finely meshed hardware-software control system such as the CRT Phototypesetting System, a decision-making process is vital in determining the hardware-software tradeoffs. This decision-making process is applicable to virtually any computer-aided process control problem. The basic decision-making flow chart may be expanded to ask further questions dependent upon the particular process control system being investigated.

THE CRT PHOTOTYPESSETTING SYSTEM is part of a much larger Photo-composition System as depicted in Fig. 1. The input to the CRT Phototypesetting System is a composed magnetic tape (from a large-scale computer system), which describes in complete detail the pages to be typeset by the CRT Phototypesetting System. This detail includes hyphenated and justified text data and font file data. The font file data describes to the Phototypesetting System how to write text characters on the CRT.

Referring again to Fig. 1, the CRT Phototypesetting System comprises an

input magnetic tape unit, a control processor (process control computer), a CRT/camera control electronic unit, and a CRT/camera unit.

The process involved in creating text images on film is illustrated in Fig. 2. Within this system, the control processor performs the following functions:

- 1) Reads the composed magnetic tape and converts the data received into commands understandable to the CRT/camera control electronic unit;
- 2) Stores within its memory the working font files as required by instructions contained in the data received from the composed tape;
- 3) Sends soft-logic control commands to the CRT/camera control electronic unit that describe in all detail (e.g., positional detail) what is to be written on the CRT;
- 4) Initiates image generation on the CRT by pointing to the proper font file data within

Salvatore A. Raciti, Ldr.
Project Management
AEGIS Program
Moorestown, New Jersey

received the BEE from Manhattan College in 1951 and the MEE from New York University in 1960. Prior to joining RCA in 1958, Mr. Raciti spent seven years in the general areas of radar and data processing. In 1960, he became a group leader at Missile and Surface Radar Division at Moorestown where he was responsible for design and development of radar data processing equipment. In 1965, he joined the Graphic Systems Division and was responsible for the logic design of Videocomp systems and allied components. Since leaving Graphic Systems, Mr. Raciti has been with the AEGIS program.

Reprint RE-17-6-21
Final manuscript received March 1, 1971

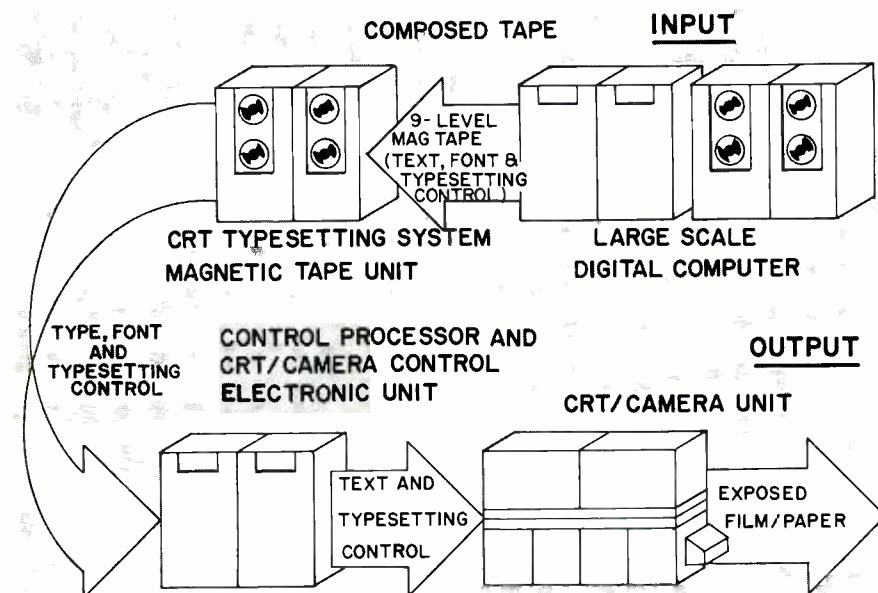


Fig. 1—CRT phototypesetting system.



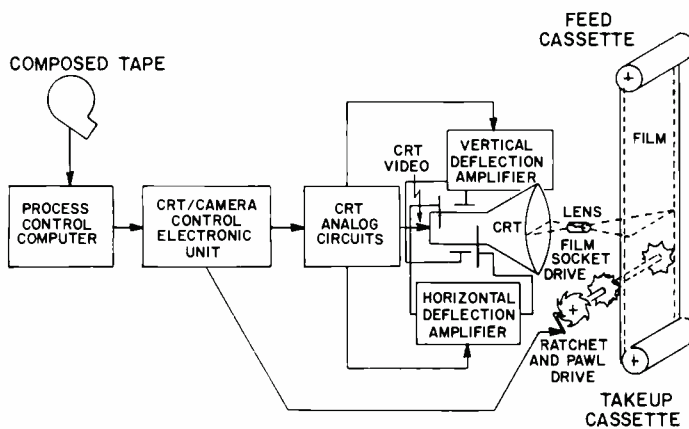


Fig. 2—Process control system for creating text images on film.

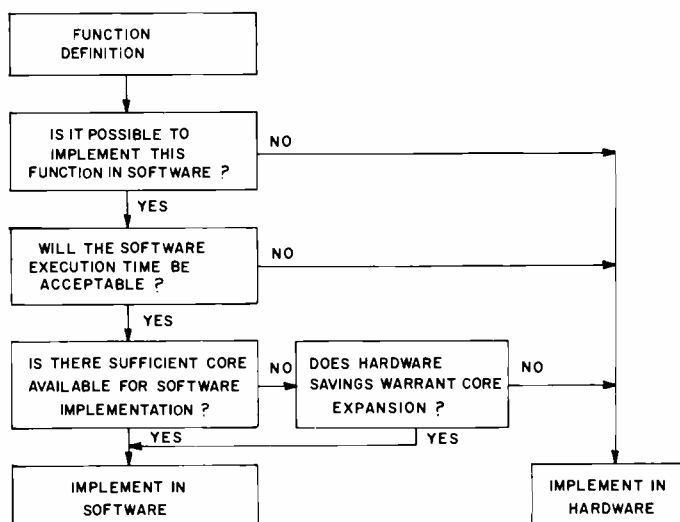


Fig. 3—Decision-making flowchart.

its own memory so the CRT/camera can fetch this data as required; and
5) Initiates the movement of film through the camera unit and specifies the amount of film to be moved.

The CRT/camera control electronic unit converts the commands and font file data received from the control processor into video, positional, and scan *on-off* signals that drive the CRT analog circuits and the camera ratchet and pawl drive.

The Phototypesetting System is, therefore, organized as a process control system with the control processor as its heart. As a result, the total system is a finely meshed soft-hard logic system.

Process of decision making

During the course of the design of a process control system such as the CRT Phototypesetting System, many software-hardware tradeoffs are made. Each function to be performed is examined and a decision is made to either implement the function in the control processor software or in hardware. The function is examined against the decision-making flow chart of Fig. 3.

First the function is defined in terms of what is required to meet the equipment product specification. If it is at all possible to implement the function

in software, an estimate is made of the software execution time. This estimate may show that software execution of the function nearly meets the equipment requirements. A decision to modify the equipment specification allows further examination of the function for software implementation. When it is determined that software execution of the function is an acceptable approach, an estimate of the amount of processor core is required. If there is sufficient core available, the function is implemented in software. If not, the hardware cost savings is compared against the cost of core expansion. If it is more economical to expand the core, this leads also to a software implementation. If not, a hardware implementation is decided upon. Going through the decision tree for a number of functions that are economically implemented in software may also lead to the necessity of core expansion.

CRT phototypesetting functions and tradeoffs

There are many areas of CRT and camera control wherein hardware-software tradeoffs are made during the course of design. The major functions investigated are:

- Character writing
- Horizontal spacing of characters
- Vertical spacing of lines of text
- Oblique control (italics)
- Geometry, dynamic focus, and dynamic astigmatism

Character writing

Character writing is broken down into many sub-functions:

Scan control—Characters are written by a series of adjacent vertical strokes on the CRT. Here, the CRT traces must be controlled such that the stroke linearity (i.e., after a stroke is started a controlled interval of time must pass) is assured and the CRT beam *on-off* (video) is correct for proper character generation. Trace control is also important in assuring that stroke spacing is correct.

These functions are implemented in hardware since they are all high-speed functions which are not software controllable without a serious degradation of system speed.

Font file data—Font file data must be decoded (unpacked) such that it may be easily converted to video *on-off* information. Font file data are stored in variable length words that define video *on-off* length. The information defining the word length must be stripped out and a binary number defining black or white segment (video) length derived.

Software unpacking of the font file is a possibility, but the time and core required to unpack the font file into variable length words significantly reduces system performance. Again this leads to a hardware implementation of the function.

Height control—Height of a character may be varied by either varying the CRT scan velocity or the rate of counting out the segment lengths derived from the font file. Scan velocity and counting frequency must be selected.

Since character size is infrequently changed, a software implementation does not change system performance. The amount of core used is a very small percentage of the total amount of core required for the processor control program. Therefore, a software decoding should be used to select scan velocity and counting frequency.

Width control—Width of a character is varied by changing the spacing between CRT scans as a function of the desired width. The contents of a horizontal register defines the horizontal placement of a CRT scan. The number of increments between scans controls the character width.

This again is a high-speed function not implementable in software. Hardware is used to calculate the CRT scan position during the previous scan interval. The software specifies the character width by defining the number of horizontal increments between strokes; the hardware defines each stroke scan position.

CRT dot size and brightness—As the spacing between CRT scans is increased, the CRT dot size must be increased so that the scans properly overlap. Brightness must also be increased such that the total energy per unit area received by the CRT remains a constant. Brightness is also increased whenever the CRT scan velocity is changed, again to keep the energy per unit area constant.

This particular problem posed a dilemma. Software implementation is reasonable, core and time required are not inordinate to decode the various functions required; but implementing in this manner led to an increase in hardware required because it significantly increased the number of interface signals between the CRT/camera control electronic unit and the CRT analog circuits. These interface signals require costly line driver/receiver circuits. As a result this function is implemented by hardware.

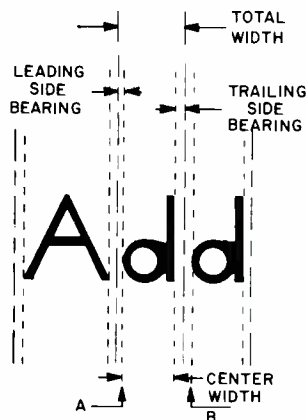


Fig. 4—Horizontal control of a character.

Horizontal spacing of characters

Here again, this function may be broken down into sub-functions:

Character Spacing—Fig. 4 shows the total width of a character broken down into three horizontal widths: leading and trailing side bearings and center width. CRT scans take place only within the center width portion of the character. Spacing of characters is then the sum of the center width (CW) and trailing side bearing (TSB) of the character just written and the leading side bearing (LSB) of the character to be written. This, then, must be summed with the initial horizontal position (point A, Fig. 4) of the character just written to yield a new horizontal position (point B, Fig. 4) for the next character.

Since software can easily perform these sums during the character writing interval with a negligible amount of core, this function is software implemented.

Word spacing—Word spacing is carried out in a manner similar to character spacing. In addition to summing CW, TSB, and LSB, the interword spacing quantity is also summed by the software yielding a new horizontal position for the start of a new word.

Line start position—The starting position of a line is a function of photomaterial width (the photomaterial centered with respect to the CRT center) and any line indent information supplied on magnetic tape. Here again the software simply calculates the horizontal starting position of a line. In addition, the software through a simple program loop waits out the necessary time for the CRT beam to retrace to the new line start position prior to specifying the first character to be written.

Vertical spacing of lines of text

The vertical spacing of lines in a CRT Phototypesetter is controlled by both a mechanical movement of the photomaterial through the camera and a vertical displacement on the face of the CRT. The mechanical movements are coarse while the electronic movements are fine. It is determined that software may accomplish this control with a negligible

amount of core, with speeds negligible with respect to the vertical movement time.

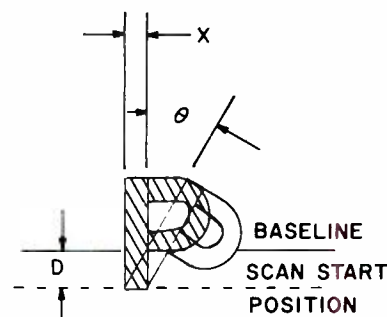


Fig. 5—Oblique control of a character.

Oblique control (italics)

When a text character is rotated on the face of a CRT it is rotated from the lower left corner as depicted in Fig. 5. It must then be displaced horizontally by the quantity X . It is determined that this calculation slows down system speed by an order of magnitude when typesetting italic characters; therefore, this function is implemented in hardware.

Geometry, dynamic focus, and dynamic astigmatism corrections

The flat CRT faceplate, deflection yoke fringe field effects, and nonsymmetry introduce many distortions into the system. Those of major concern are pin-cushioning of the CRT image (geometry distortion), spot growth, and astigmatic distortion.

Geometry corrections and focus corrections are theoretically calculable but software routines would be inordinately long, thereby materially reducing system performance. Dynamic astigmatism corrections are not predictable and tables in excess of 15,000 words are needed for corrections. As a result, none of these functions are implemented in software.

Acknowledgment

The author is grateful to T. Appleyard for preparing the illustrations in this paper.

References

1. Maymon, G. W., "Diagnostic Programs for Video Comp Phototypesetters," *Information Display* (Nov. Dec. 1969) pp. 31-36.
2. Stevens, M. E. and Little, J. L., "Automatic Typographic-Quality Typesetting Techniques, A State of the Art Review," National Bureau of Standards Monograph 99 (April 1967).
3. Walter, G. O., "Typesetting," *Scientific American* (May 1969) pp. 60-69.
4. Raciti, S. A., "Digital Control of a CRT Phototypesetting System," *Computer Design* (Nov. 1970) pp. 107-112.
5. Klensch, R. J. and Simshauser, E., "The CRT in Phototypesetting Systems," *IEEE Spectrum* (Sept. 1969) pp. 75-80.

The RCA 4506 ultra-high-resolution cathode-ray tube

O. Choi | C. T. Widder

The cathode-ray tube (CRT) is a device designed to produce a spot of light on specified two-dimensional coordinates for a given duration of time. The spot of light is generated by the fluorescence of a phosphor screen on a CRT faceplate excited by a beam of high-velocity electrons. To utilize fully the generated pattern of light on the phosphor screen, the structure of the CRT must be such that the dimension tolerances are compatible with those of the electron beam. This paper describes the design parameters of the electron gun, phosphor screen, and glass envelope used in the RCA 4506, 7-inch ultra-high-resolution CRT. The flatness of the faceplate and structural rigidity of the various parts of the tube are also discussed.

FROM AN ELECTRON-OPTICAL POINT OF VIEW, a CRT can be divided into four components: 1) the source of electrons comprising the cathode and the point of crossover, 2) the limiting aperture and focusing lens system, 3) the deflection field, and 4) the focused spot and the screen. Fig. 1 is a schematic diagram of a cathode-ray tube and these four components.

The system requirements limit some of the CRT parameters such as screen diameter, overall length of the tube, and maximum operating voltage. In the case

Reprint RE-17-6-14
Final Manuscript received January 31, 1972

of RCA type 4506 ultra-high-resolution CRT (shown in outline in Fig. 2), the screen diameter is 15.8 cm, the overall length 55.7 cm, and the maximum operating voltage 20 kV. Within these limitations, the objective of the CRT design is to achieve a maximum spot density at the fluorescent screen. However, there remain two very fundamental constraints inherent in the nature of the electron beam. These constraints are the Langmuir limit of cathode load and the effect of s —space charge.

D. B. Langmuir¹ showed that the maximum peak image brightness, ρ_0 , can



O. Choi

Christopher T. Widder*
Advanced Technology
Electronic Components
Lancaster, Pa.

received BSE from University of South Florida in August, 1967. Since coming to RCA in 1967, Mr. Widder worked on supporting development of advanced cameras such as the 3-inch image-isocon camera. He also developed a new frit sealing technique for special and advanced image tubes. He is a member of the American Society for Metals and Society for Experimental Stress Analysis

*Since this article was written, Mr. Widder has left RCA.

O. Choi
Project Development
Electronic Components
Lancaster, Pa.

received the BS in Physics from Franklin and Marshall College. After three years of graduate study at University of Pennsylvania and University of Colorado, he joined Tube Division at Lancaster, Pa. in 1959. His current activities are mainly in design of ultra-high-resolution cathode ray tubes. His past activities with RCA have been in design work in high-resolution TV camera tubes, including image orthicons, image isocons, and infrared vidicons.

be expressed in terms of ρ_c , the cathode load, and the beam half angle, θ , as shown in Eq. 1:

$$\rho_0 = \rho_c [(eV/KT) + 1] \sin^2 \theta \quad (1)$$

where e is the electron charge in coulombs, V the accelerating voltage, K the Boltzman constant, and T the absolute temperature of the cathode. Langmuir's equation shows that if V and ρ_c are fixed, the only way to increase the spot density is to increase the aperture diameter, hence a larger half angle, θ . Increasing the aperture diameter, however, produces two additional, serious problems: spherical and chromatic aberrations of the spot. The former is manifested in excessive spread of the beam and the latter in distortion of the spot image away from the center of the screen. These aberrations are also functions of the magnetic fields generated by the focusing lens and the deflection yokes. One certainty clearly indicated by Eq. 1 is that there exists a maximum value of spot density for a given cathode load, regardless of all other design factors. This value is the first of two fundamental physical limitations, the other being the one imposed by space-charge effect. The main task of a CRT designer, therefore, is to arrive at a practical compromise between an acceptable level of aberrations while seeking a largest possible value for the beam convergence half angle. Not to make the half angle as large as permissible is to dissipate a useful beam current, thus sacrificing some of the possible spot density. Conversely, if the magnetic components can be improved upon so as to permit a larger beam diameter without a corresponding increase in aberrations, a better CRT would result.

Langmuir's equation is a very generalized expression and, in actuality, there are many variations modifying each of the terms. For example, the term, ρ_c , is a value assignable only for cathodes in which there is a uniform flow of electrons at uniform velocity. There are no such cathodes in existence. But to obtain the predicted maximum value of spot density, ρ_0 , as shown in the Eq. 1, an attempt should be made to create a uniform ρ_c in the cathode. A conventional oxide cathode surface is characterized by non-uniformity in topography. Its surface is loose and spongy. Consequently, the variation in spacing between the cathode surface and the

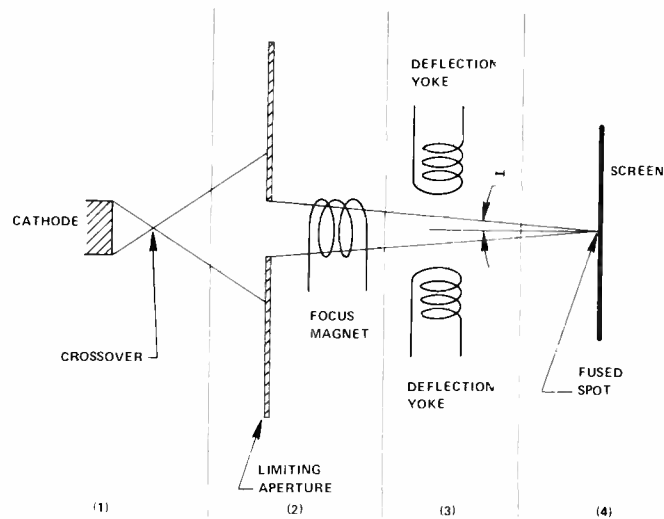


Fig. 1—Schematic diagram of CRT.

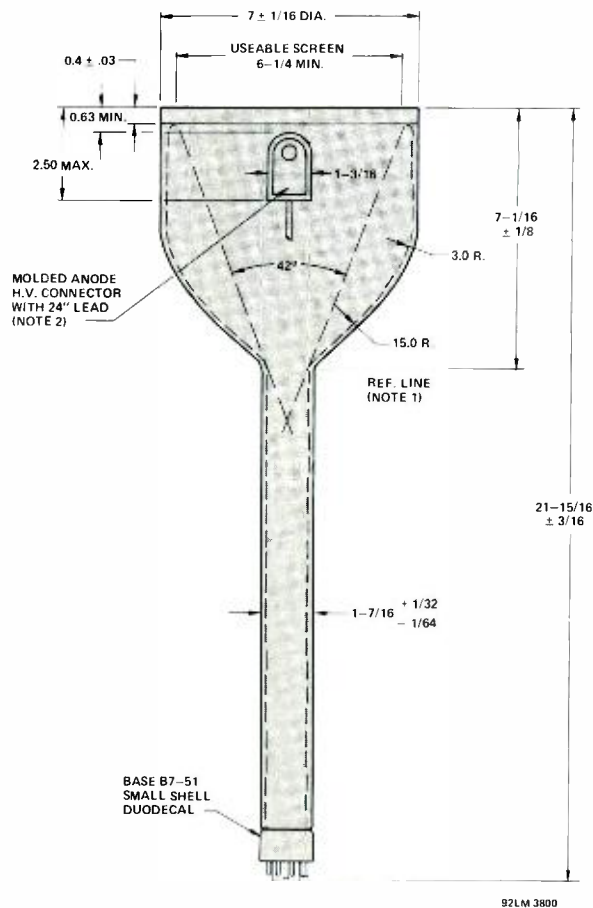


Fig. 2—4506 dimensional outline.

grid structure is on the order of 100 to 200 μm . In the case of RCA 4506, the spread is reduced to the order of 20 to 30 μm . Topography of the cathode is not the only parameter contributing to non-uniformity of ρ_c . But because ρ_c is a function of the uniform portion of ρ_c , an increase in cathode load results in increased spot density. In the case of the RCA 4506, the gain due to the increased uniformity is apparent in the focused beam diameter at the screen, which is measured to be 18 to 19 μm at 50% of the beam profile.

J. W. Schwartz² has shown a function of p (a ratio of beam radius at the screen to the initial radius of the gun) which has a relationship with a Gaussian space-charge condition such that in a normalized form

$$f(p) = \frac{j^{1/2}}{V^{3/4}} \frac{z}{r_i} \quad (2)$$

where r_s represents the radius of the undeflected spot. The significance of Eq. 3 in design consideration is considerable. Its main significance is the limitation on maximum r_s by ρ_c for fixed practical values of V and T . As an example, an electron gun operating at a cathode temperature of 1054°K with a 10-kV operating voltage and an r_s of 18 μA would impose a cathode-loading limit of several amperes/cm². Because Eq. 1 is based on a 100% uniform ρ_c , the RCA 4506 with a cathode emission of 3 A/cm² is operating near the maximum attainable spot density. In other words, a search for a higher current density alone would

where z is the distance from center of deflection to screen and r_i the radius of the beam at deflection. Combining Eq. 2 with Langmuir's thermal limitation (Eq. 1) it can be shown² that

$$\sqrt{\pi e / K T} \cdot \sqrt{\rho_c / \sqrt{V}} \cdot r_s = f(p) \quad (3)$$

where r_s represents the radius of the undeflected spot. The significance of Eq. 3 in design consideration is considerable. Its main significance is the limitation on maximum r_s by ρ_c for fixed practical values of V and T . As an example, an electron gun operating a cathode temperature of 1054°K with a 10-kV operating voltage and an r_s of 18 μA would impose a cathode-loading limit of several amperes/cm². Because Eq. 1 is based on a 100% uniform ρ_c , the RCA 4506 with a cathode emission of 3 A/cm² is operating near the maxi-

mum attainable spot density. In other words, a search for a higher current density would not contribute to a better resolving beam. On the contrary, the space-charge effect would cause blooming of the beam. The only other practical approach to improving the beam characteristic is to take advantage of the Langmuir thermal term of Eq. 3. Interestingly, the contribution of the thermal term is equally as important as the space-charge term, as seen in Eq. 3.

From the system point of view, a fine beam of electrons is of little use if the amount of current is not stable over a period of time. In graphic arts applications, an unstable beam current would manifest itself in non-uniform thickness of type fonts and in an uneven grey shade in half-tone pictures—defects considered unacceptable by printers. The RCA 4506 gun design has taken this problem into consideration. The completely redesigned gun structure in this new tube has successfully overcome the persistent beam-stability problem of conventional guns. It is not uncommon to observe a drift of 10% in GI drive voltage for a given cathode current within 100 hours of turning on the tube. The new gun in RCA 4506 has shown a stability within 1 to 2% for a period of 150 hours.

Screen

The fine electron beam, as produced by the gun, must be faithfully translated into corresponding light output, to realize all its potential benefits. There are four major characteristics which must be satisfied to comply with the electron beam and the systems requirements. First, the screen should not degrade the ultra-high-resolution quality of the electron beam. In general, the thinner the screen, the finer is its resolving range. Reduced thickness, however, is accompanied also by a lower light output and an increase in pinholes. The design criterion, therefore, is to arrive at an optimum compromise. The RCA 4506 is in this respect an excellent compromise, for there are no pin-holes in the dimensional range of the beam diameter, i.e., 18 μm , and resolution is not sacrificed. Secondly, the light output must be of high efficiency and uniformity throughout the usable screen area. For this purpose the 4506 utilizes a specially developed phosphor which has shown an increase in peak effi-

ciency of 50% over that of the conventional P11. As shown in Fig. 3, the spectral distribution of the new phosphor slightly favors the ultra-violet region where the photographic emulsion is more sensitive. The overall gain in coupling efficiency between the electron beam and photographic emulsion is, therefore, greatly increased. The uniformity of light output over the entire screen of the RCA 4506 is within 5% of the peak. Thirdly, the decay time of light emission from the screen after cessation of excitation should be as short as possible. Decay time is largely a fundamental characteristic of the chosen phosphor. A faster decaying screen allows a higher frequency display, hence a greater output for the system. As shown in Fig. 4, RCA 4506 decay time to 10% of peak output is consistently below 5 μs . The fourth major design consideration for the screen is blemish population and distribution. In some applications the output is displayed, one line of characters at a time, on the same area of the screen. Thus, a blemish in the form of lower light output would exhibit a characteristic streak of vertical lines in the finished photographic plate. Such a streak exaggerates the minuscule defects of the screen. To reduce blemishes, the entire screen preparation process is conducted in a super-clean laminar-flow room. The results confirm the importance of using such a dust-free environment for screen preparation.

Envelopes

The faceplate and funnel are two important component parts and require substantial consideration in the development of a high-resolution cathode-ray tube. The funnel shape must be easily produced by standard glass-working techniques and must be such that no adverse stress concentrations are developed on its surface. The type of glass used should be capable of withstanding the high-temperature bakeouts involved in tube processing and also must closely match in thermal expansion other glasses that will be sealed to it.

The shape of the faceplate is a simple round disc. This disc, however, must survive atmospheric loading and have negligible deviation from flatness. The faceplate glass must also closely match the funnel in its thermal expansion characteristics. This glass must also be

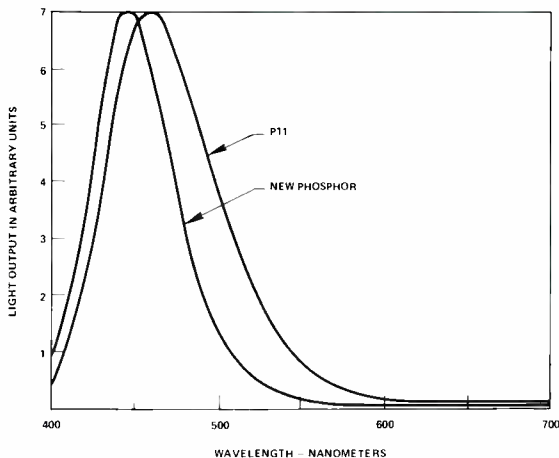


Fig. 3—Spectral response curve.

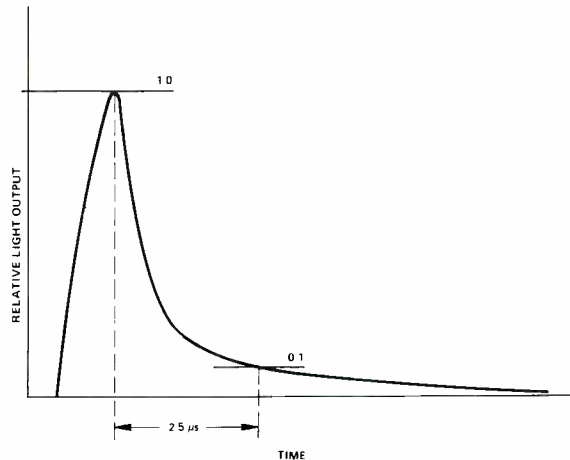


Fig. 4—Decay curve.

non-browning, i.e., its transmission characteristics are not degraded by electron bombardment as a result of tube operation. The surface of the glass must be resistant to the chemical reagents, humidity, etc., encountered in the normal handling and is able to retain a highly polished finish.

In current glass technology, there are two basic types of glass that one may choose from, *hard* glass or *soft* glass. The terms *soft* and *hard* qualitatively refer to the softening temperature, *hard* being the higher temperature of the two. The common readily available glasses (hard and soft) considered and their properties are:³

	0080 (soft)	0120 (soft)	7052 (hard)	
Strain	470	395	435	°C
Anneal	510	435	480	°C
Soften	695	630	710	°C
Thermal exp. (to 300°C)	92.0	89.0	46.0	°C

There are many other types of glasses available to the design engineer, but the economics of using a different type glass would be too costly to justify. The glass chosen for this CRT is "0120" lead (*Pb*) glass, commonly known as G12. It represents an optimum combination of good workability for funnel shapes and an extended low-temperature annealing range highly suitable for frit sealing and flame sealing of the gun mount. Another very significant reason for choosing G12 is that "non-browning" G12 faceplates are readily available for use. The shape of the funnel is dictated more by glass-working techniques than by stress considerations. More often than not these techniques usually result in structurally sound shapes with the thickness

of the glass being used to increase the safety factor if the need should arise.

Because the faceplate shape is defined, the only parameters of interest are its thickness and its intrinsic properties. The proper thickness is determined through the use of equations derived from simple plate and shell theory. The applicable equation is⁴

$$\sigma_t = \sigma_r = -(3W/8\pi m t^2)(3m+1) \quad (4)$$

where $W = w\pi a^2$ and w is the magnitude of the uniform loading, a the radius, and $m = 1/\nu$, ν being Poisson's ratio.

This equation results from considering the disc to be uniformly loaded and simply supported at the edges. This equation gives the magnitude of the stress at the center of the faceplate. The maximum allowed stress at the center of the faceplate is on the order of 1000 lbf/in².

Optical consideration also must be considered because the curvature of the faceplate, due to atmospheric loading, can destroy the resolution of the image to be projected. Customer specifications dictate that the deflection at the center be no more than 0.003 inch. Of these two considerations—optical and mechanical strength—the more severe of the two will determine the proper thickness. For this particular tube type, the optical performance determined the proper thickness.

The intrinsic properties of the glass are the next consideration. The choice for this tube type is not singular since there are several varieties available from dif-

ferent manufacturers. The primary requirement for this faceplate, besides being a good optical glass, is that it must not *brown*. Browning is caused by displacement of electrons from their normal positions to form color centers which absorb light in a characteristic range of wavelengths, mainly those in the ultra-violet region. For many glasses, this range overlaps the visible spectrum so that the glass color darkens on exposure; the color is usually a yellow or brown. The addition of certain elements dilutes this effect drastically, most notably oxides of the transition elements and also cerium oxide. Cerium has the added advantage of not coloring the glass. Common non-browning glass and their pertinent properties are:⁵

	Corning 9025	Corning 9019	Pitts- burgh Plate 5533	Pitts- burgh Plate 3459	
Strain	417	455	471	467	°C
Anneal	458	487	501	493	°C
Soft	651	675	694	675	°C
Thermal Exp. (25 to 300°C)	90	99	94.5	94.5	°C

For this cathode ray tube, two glass types were chosen; type 3459 and Corning Code 9025. These glasses were developed for use as a clear-optical-quality, non-browning panel glass for cathode-ray tube faceplates. The expansion behavior of these glasses provides an excellent match for frit sealing to 0120 glass and other metals and ceramics.

After the appropriate materials for both the faceplate and the funnel are chosen, consideration must be given to how these two pieces can be joined together

to form a vacuum-tight structure. There are two techniques available: flame sealing and frit sealing. Flame sealing of the faceplate involves temperatures in excess of 800°C in the area of the seal. These temperatures are high enough to distort the glass faceplate. This distortion, however minute, is enough to disqualify it as a possible sealing technique.

The other possibility involves "solder" glass for frit sealing. This glass family has the unique capability of changing its inherent structure during the application of heat in the sealing process. This change in structure allows the solder glass to be reheated to a higher temperature than it was sealed at without detrimental effects. One such material is used on this tube type, namely Corning's Pyroceram® brand solder, glass Code 7575. The properties of this material are shown below:⁶

<i>Coefficient of thermal expansion</i>	84–92 × 10 ⁻⁷ cm/cm/ie
<i>Softening temperature</i>	370°C
<i>Sealing temperature</i>	440° to 450°C
<i>Sealing time</i>	60 minutes

There are distinct advantages in using this type process, the most important being that faceplate distortion is held to an absolute minimum. At the same time, however, the process allows the faceplate to be processed separately from the funnel, thus simplifying the process requirements in attempting to meet the objective goals of this tube type.

After a faceplate is frit sealed to the funnel to form a vacuum-tight envelope,

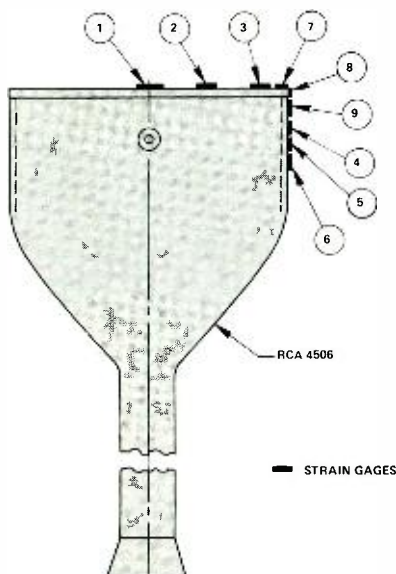


Fig. 5—Strain gage locations.

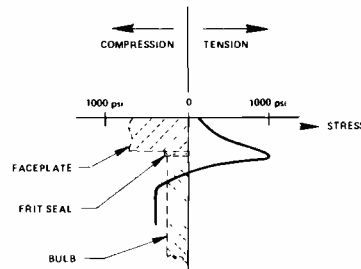
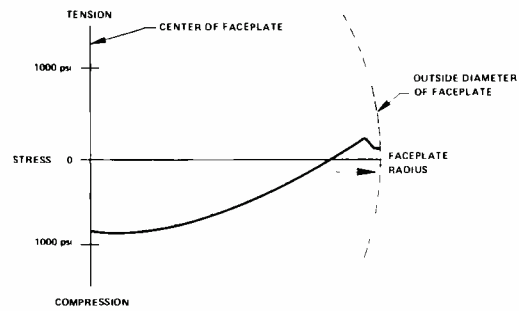


Fig. 6—Stress distribution of faceplate and bulb wall.

the bending stresses developed at the outside surface near the frit seal are measured. A conventional technique for this measurement is the use of strain gages. For this measurement, nine stress gages are cemented to the bulb at various locations as shown on Fig. 5. After each gage is stabilized, the bulb is evacuated and resulting strains measured. Because the gages are in the same direction as the principal stresses, direct conversion into stress quantities is reached by multiplying the strain readings by 10. Considering that

$$\sigma = \epsilon E$$

where E is Young's modulus (lb/in²), ϵ is the strain reading obtained on machine ($\mu\text{in}/\mu\text{in}$), and σ the stress (lb/in²) (5)

and noting that Young's Modulus for 0120 glass is 10.2×10^6 , sufficient accuracy is obtained for the level of stress distribution. Fig. 6 demonstrates the distribution magnitude of the stresses found in the bulb after evacuation. The highest level of stress measured is close to 1000 lb/in², which is an acceptable level of stress for normal handling.

Conclusions

The RCA 4506, is a suitable vehicle for a computer-composed graphics output for hard copy. Its application, however,

is not limited to graphics composition for printers. The tube should be an excellent vehicle as the flying-spot scanning source for an optical character reader of high resolution and in other applications in which an ultra-high-resolution video signal has to be monitored and recorded.

Acknowledgments

The authors are deeply indebted to the contribution of a colleague, D. R. Tshudy, for developing and fabricating the near-perfect screen for this tube type. Without his untiring effort, this tube and indeed this paper would not have been possible. Also the technical guidance and advice of M. D. Harsh and J. A. Zollman are gratefully acknowledged. The fabrication and data taking as well as construction of support equipment were due to Messrs. J. J. Donches, A. L. Hollinger, W. H. Tucker, R. A. Mickle, and R. J. Conn; the authors are deeply indebted for their efforts.

References

- Langmuir, D. B., "Theoretical Limitations of Cathode Ray Tubes," *Proc IRE* 25, pp 977-991 (1937).
- Schwartz, J. W., "Space-charge limitations on the Focus of Electron Beams," *RCA Review* 18, pp 3-111 (1957).
- Hutchins, J. R., Harrington, R. V., *Enycl. Chem. Techn.*, 2nd Edition, Volume 10, (Wiley, 1966) pp. 533-604.
- Roark, R. J., *Formulas for Stress and Strain* (McGraw-Hill, 1954)
- Private communications
- Corning Data Sheet (Aug. 1965)

Precision CRT tester

E. D. Simshauser

A precision CRT tester was developed by the Graphic Systems Division in 1970 to test cathode ray tubes, deflection yokes, focus coils, various circuits and other items commonly used in photocomposers. Special emphasis has been placed on getting components to be tested into and out of the machine quickly and easily.

THE PRECISION CRT TESTER has a wide variety of test capabilities. Among them, it can test CRT's ranging in diameter from 5 to 10 in. and requiring ulior voltages ranging from 10 to 30 kV and second anode voltages ranging up to 2 kV. The tests include spot size and profile, phosphor blemishes, light output, and light-output rise and fall times.

Deflection yokes can be tested for deflection sensitivity, yoke settling time, deflection linearity, astigmatism and hysteresis.

Focus coils can be tested for spot size at best focus, inherent astigmatism and settling time of the focus yoke.

In addition, the pincushion-correction, dynamic-focus and dynamic-astigmatism circuits are arranged in plug-in fashion so that they can be modified as desired. The dynamic-astigmatism circuit also includes a static astigmatism adjustment.

Other facilities include three ramp generators, amplifiers (six ampere) for vertical and horizontal deflection and various other function generators such as digital-to-analog converters for various rasters. The deflection amplifier has a bandwidth from DC to 300 kHz at the 3 dB-down point. In addition, its settling time with a 60 μ H yoke is about 50 μ s to get within 1 tenth of 1% of the final rest position of the spot. The blanking amplifier used for driving the CRT can be modulated to a rate of about 10 MHz and has a switching time (*on* or *off*) of approximately 50 ns.

Two sets of cards are also provided to change the control function of the machine. With one set of cards in place, the machine is controlled by its own internal switches and programming controls. With the other set of cards in place, the machine can be controlled by a type-1600 controller which is normally used to drive the RCA VideoComp. When used with the controller, the CRT tester provides suf-

ficient features to enable testing the ability of a particular tube or deflection components to write satisfactory text and other graphic output material. When used in this mode, the output is photographed on high-quality film and then may be viewed or used for offset printing.

Part of the tester is visible in the author's photograph. The unit is about 9-ft long, 6-ft high, and 2 ft wide. The CRT is mounted on the moveable carriage on top of the machine. This

Elvin D. Simshauser*
Graphic Systems Division
Computer Systems
Princeton, N.J.

graduated from Kent State University with the BS in Physics in 1951 and joined RCA at that time. After completing the engineering training program, he was assigned to the Special Devices Section where he did development work on sound-powered telephones, aircraft and submarine intercom systems, and miscellaneous transducers. After two years in the Army as a computer technician, he returned to RCA (Surface Communications Division) in 1956, working on headset and microphone development for the Air Force. From 1958 to 1963 he worked on several classified communications programs. In 1963 he transferred to the RCA Tucson plant and worked on a variety of small communications devices, including a low-power signaling device, a low-power long-distance radio, and a bundle-drop marker radio. In 1966 he transferred to the Graphic Systems Division of RCA and since that time has worked in the Advanced Development Group on kinescope photocomposing systems.

*Since this article was written, Mr. Simshauser has left RCA.



Reprint RE-17-6-13
Final manuscript received January 25, 1971.

permits the tube to be moved forward near the control panel for viewing with a microscope while operating the controls. Conversely, for using film, the CRT can be moved to the rear of the machine so that the film plane may be mounted near the controls to permit focusing and other adjustments to be made. All important operating controls are mounted on the front panel, among these are; focusing controls, pattern generation control, DC offset in both *x* and *y* axes, gain for both *x* and *y* axes, grid bias for the control grid (*G₁*) and a continuous-run 1-shot switch—the latter being used when photographs are taken so that the pattern is exposed to the film only once.

Secondary operating controls are accessible from the left side of the machine and include power supply switches and voltage adjustments, and several large plugs that switch the deflection yoke to various current sources. In addition, all plug-in circuits are on the left side. Access to wiring and large items such as the main deflection amplifier are from the right side of the machine.

A functional block diagram of the CRT tester is shown in Fig. 1; only the important operational blocks and monitoring facilities are shown. In addition to the functions shown on the diagram, the A functional block diagram of the CRT tester is shown in Fig. 1; only the important high-speed high-current switch used in testing settling times of deflection yokes; a +current/off/ -current switch for yoke hysteresis tests, circuits for automatic turnoff of high voltage in the event of grid-bias failure; and automatic spot defocusing when in the DC spot (no deflection except DC offset) mode. Other items used with the CRT tester are several 100-power microscopes, a slit analyzer, miscellaneous lenses, cameras and oscilloscopes.

Three different mounting plates for 5, 7 and 10-in. tubes have been initially provided with the machine. The tube is mounted by simply setting face down on the mounting plate and securing it with a clamping ring and three nuts. This entire assembly may then be mounted in the CRT tester with no further adjustments. Translation and gimbaling adjustments in both horizontal and vertical directions are provided for the deflection coil and focus yoke. In addition, mounts are provided for centering and beam alignment coils.

The shield is easily moveable since it is mounted on the same rails as the CRT mount itself. Slots are provided in the shield so that yoke adjustments may be made with the shield in place.

A key feature of the tester is the ease with which items to be tested can be inserted and removed. An example of this is the ability to remove a CRT by unloosening six screws and unplugging the high voltage lead and the socket. Similarly, only three screws are used to hold the focus and deflection yokes in place (plus screws necessary to connect them electrically). The shield for the cathode ray tube is mounted on a set of tracks so that it can be rolled on and off of the tube quickly without danger to the CRT or the operator. Most circuits (except power supplies and the main deflection amplifiers) are mounted on plug in cards or can be plugged in to permit easy changing or servicing.

A complete rundown on all the tests possible with the CRT tester would not be appropriate to this article. Only a few of the more representative tests will be described to give the reader some idea of the machine's capability.

Spot size and profile

Probably the most commonly made CRT test involves the spot size and profile and the decay time of the light output. Spot size can be measured by putting a raster on the screen and shrinking the size of the raster down until the lines just merge to form a uniform-appearing field as viewed in a microscope. The raster width divided by the number of lines then gives the spot size. This method is quick and convenient but does not have the accuracy of other methods and thus is used mostly as a quick check. The most accurate way of measuring spot size is to use a slit analyzer. The unit used on the CRT tester has a single slit. A raster is generated which consists of two lines scanned alternately at about 6 mils apart (see Fig. 2). These two lines are scanned slowly sideways. The lines are focused by means of a lens onto a very narrow slit (in comparison with the spot width) with a photomultiplier tube behind it.

As the two lines move slowly past the slit (they are parallel with the slit), the output from the photomultiplier is proportional to the light entering the slit. The

magnitude of the output represents the intensity of the spot and the duration of the output represents the width of the spot. Since the lines are known to be 6 mils apart, the time between the two output peaks is thus calibrated as 6 mils and measurements of the spot width can be taken directly from the output on the oscilloscope or a photograph of the output.

Because spot size and shape is affected somewhat by the amount of beam current (which is proportional to cathode current), it is common practice to take measurements at the cathode current used for normal tube operation. Since for phototypesetting applications this current is very high in comparison to that necessary to damage the tube, it is necessary that the spot scan at a high velocity. If the spot were scanned across the slit at that velocity, the scan time across the slit would be about 0.4 μ s. Thus because light output rise and fall times are many μ s, the sweep time across the slit would be shorter than the rise and fall time of the light output and so a grossly distorted impression of the spot size would be created. This problem is circumvented by scanning

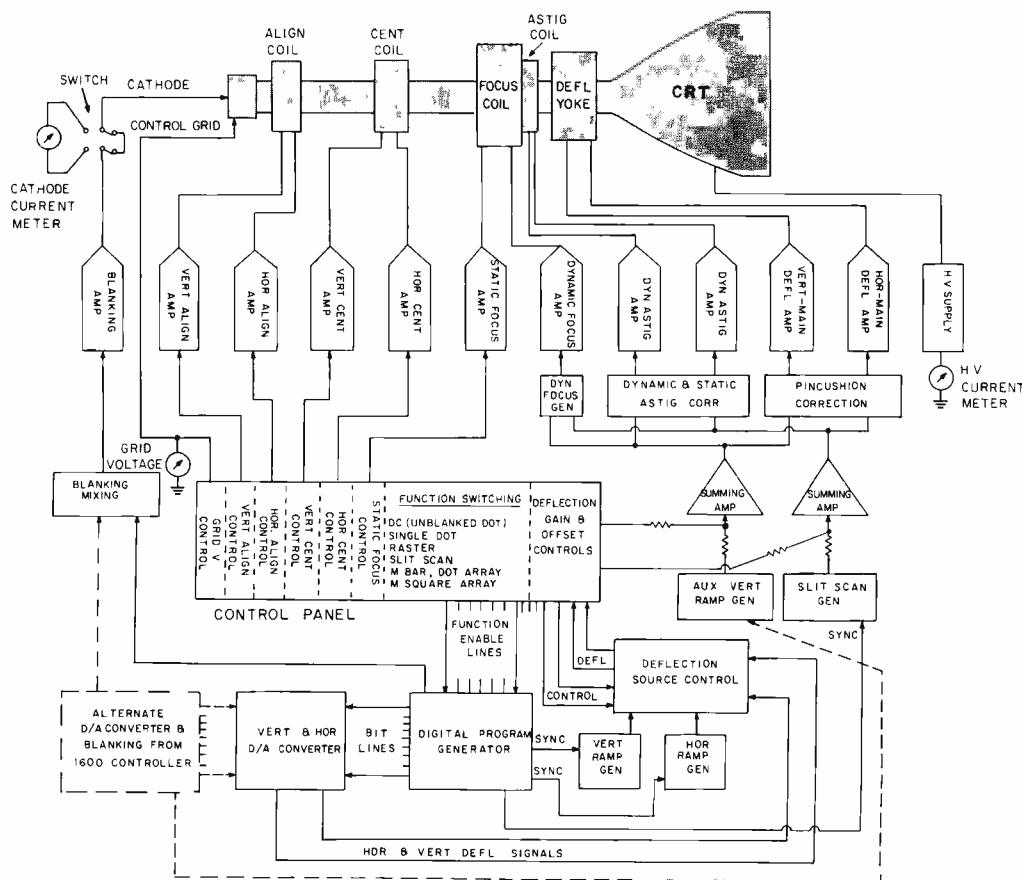


Fig. 1—Functional block diagram of the CRT tester.

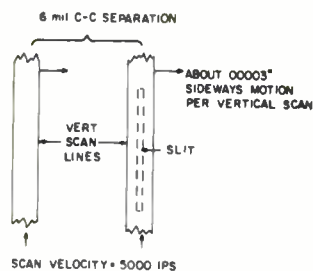


Fig. 2—Raster for spot-size and profile test.

the spot parallel to the slit and moving it a little bit further over the slit for each scan. In this way, the total scan time across the slit for each vertical stroke is about 1 ms and the total scan time across the slit is about 30 to 60 ms and so the problem with light and rise and fall time is avoided. Typical parameters used for 7-in. photocomposer CRT's are 1 μ A of cathode current with a scan velocity of 5000 in./s on the face of the tube.

Decay time

Decay times of the light output are also measured by using the slit analyzer. For this application, the slit is opened very wide so that the entire spot can shine through onto the photomultiplier tube. The photomultiplier used is type 5819 whose spectral response is similar to that of the films most commonly used in photocomposers. The 5819 is used with a 1000-ohm final dynode resistor and all other resistors are relatively low values; thus its response time is measured in nanoseconds. For most common CRT's, this is quite adequate for measuring rise and fall times of the light output. The procedure is simply to use a stationary spot; turn it *on* for a few microseconds; and then back *off*. The rise and fall time of the light output is observed on an oscilloscope or the oscilloscope trace photographed.

Yoke linearity

One of the more interesting tests that can be performed on the CRT tester is that of yoke linearity. Deflection linearity is commonly specified in terms of deflection angle rather than deflection distance since deflection yokes are usually reasonably linear with respect to deflection angle versus deflecting current. The measurement consists of focusing the spot of the CRT through a 1:1 lens (which type of lens can have very low distortion) onto a very accurately calibrated screen with grid lines on it. The spot is first left in the undeflected position and the screen lined up

so that the spot rests on the zero axis of the screen. Next the spot is deflected until it comes to the next calibrated mark on the screen, and the deflection current is measured with a digital voltmeter. The current is measured across a precision sampling resistor. By this means, deflection current vs. deflection distance can be accurately calibrated. Then by means of comparing the ratio of the current necessary to deflect two known distances (2 inches and 1 inch, for example) the deflection angle can be calculated knowing the trigonometric relationships between the tangents of two angles. This procedure also allows one to locate the effective deflection center of the yoke with a high degree of precision. Yoke linearity measurements to about 0.1% are possible, and the center of deflection can be located to an accuracy of about ± 10 mils.

Test results

To date, the CRT tester has been used for testing four tube types, three types of deflection yokes, and two types of focus coils plus miscellaneous dynamic astigmatism generation circuits. Several very significant factors have been revealed. Among them that light output rise and fall times of currently available *P-11* tubes are markedly faster than indicated by either data sheets for the standard *P-11* phosphor or by direct conversations with vendors. Vendors have indicated that the phosphors currently used on tubes called *P-11* are really not the standard *P-11* phosphor but "improved" versions thereof. Also in photocomposers, the tube is usually run at a much higher beam-current density than that used for most rise and fall time measurements. Thus the combination of a slightly different phosphor and the higher beam current density is the apparent cause for the considerably faster performance.

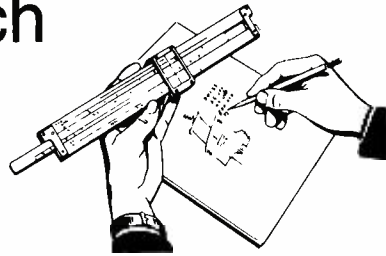
The CRT tester has also shown that the requirements on the deflection amplifiers are very severe indeed (first discovered in photocomposer usage). For example, if the peak-to-peak noise is to be no more than 10% of a spot width in a system able to resolve about 6,000 lines across the face of a tube then the peak-to-peak signal to peak-to-peak noise ratio must be 96 dB. These requirements are extremely severe particularly since the bandwidth is from DC to 300 kHz. Measurements on the CRT

tester have indicated that even the best currently available deflection amplifiers do not meet this requirement, about 80 dB being normal. The result is about a 30% increase in apparent spot size. The second problem that has shown up involves settling times of the amplifier itself. This is, of course, principally determined by such things as switching speed of the deflection transistors and other such parameters. However, another item, thermal settling time is normally neglected in measurements because it is usually less than 1%. Thermal effects do show up in the deflection amplifier and can take as long as 30 ms to settle out. The problem is serious in photocomposer applications because 1% errors are painfully visible under some circumstances and so it is necessary to slow the writing speed.

Another phenomena associated with controlling spot size is that of focus yoke settling times. Focus yokes are normally machined from solid iron rather than laminated structures because of the high precision required in machining the gap. As a result of the solid structure, considerable eddy current loss is experienced in the yoke, and measurements have shown that from 1 to 3 ms is required for the spot to settle to minimum size after a change in focus current occurs. This is significant because photocomposers employ dynamic focus to maintain optimum focus over the entire face of the tube. Hence, when the beam is deflected quickly, the focus current must also be changed quickly. This problem can be reduced considerably by the use of high resistivity nickle-iron alloys but results in a very expensive yoke.

Another problem that has been demonstrated on the CRT tester is that of irregularity in the required dynamic astigmatism corrections. Classic astigmatism theory indicates that the required astigmatism correction should be symmetrical about the zero deflection axis for both *x* and *y* deflections. However, mostly as a result of winding irregularities and irregularities in the shape of the pole pieces, it has been found that there is, in most deflection yokes, a sizeable departure from the symmetrical astigmatism pattern. As a result, to obtain best spot size on the face of a tube it is necessary to go to what are essentially random pattern generators for generation of the dynamic astigmatism function.

Engineering and Research Notes



Brief Technical Papers
of Current Interest

Penetration-type cathode-ray tubes for multicolor displays

Donnavon D. Shaffer
Entertainment Tube Division
Electronic Components
Lancaster, Pa.



The novel tube, illustrated in Fig. 1, may be used in a multicolor display for a computer output, for an airport-traffic control system, or for other information systems.

An electron gun (18) in the neck is adapted to project a beam of electrons (20) toward a viewing screen (22) on the window in conjunction with voltages applied to the conductive coating (24) on the funnel, the grill (26) across the funnel, and the reflective metal layer (34) of the screen. Deflection of the beam is achieved by known means, such as a deflection yoke (28).

Cascade-type screen

The cascade-type screen shown in detail in Fig. 2) has a first phosphor layer (30) adjacent to the window (14), a second phosphor layer (32) thereon, and then a light-reflective metal layer (34) on the second phosphor layer. The second phosphor layer (32) consists essentially of built-up particles, one of which is shown in Fig. 3. Each particle consists of a second core (36) of a blue-emitting short-decay cathodoluminescent phosphor—such as silver-activated zinc sulfide; second nonluminescent layer (38)—such as silica—thereon; and an outer skin (40) of a red-emitting medium-decay cathodoluminescent phosphor—such as yttrium europium oxysulfide. The first phosphor layer (30, Fig. 2) consists also of built-up particles, one of which is shown in Fig. 4. Each particle includes a first core (42) of a

green-emitting long-decay photoluminescent phosphor—such as copper-activated zinc cadmium sulfide—and a first nonluminescent layer (44)—such as silica. The first nonluminescent layer (44) has a thickness equivalent to the combined thicknesses of the second luminescent layer (38) and the outer skin (40) of the other built-up particle. The built-up particles may be made by the methods disclosed by Pritchard,¹ Kell,² or Messineo, et al.,³ and may consist of phosphors with different emission characteristics. The first and second layers may be deposited by methods known in the art; for example, by settling.

In operating the tube, the beam (20, Fig. 1) scans the screen (22). At lower voltages (e.g., 10 kV), the outer skin (40, Fig. 3) luminesces, displaying to the viewer a medium-decay red pattern on the screen. At higher voltages (e.g., 16 kV), the second cores (36) emit a short-decay blue luminescence, which excites the first cores to luminesce, displaying to the viewer a long-decay green pattern. The cascade structure of the screen gives more brightness and better purity than screens employing extended layers.

Onion-type screen

The onion-type screen (shown in detail in Fig. 5) has phosphor layer (30) adjacent the window (14), and a light-reflective metal layer (32) on the phosphor layer. The phosphor layer (30) consists essentially of built-up particles, one of which is shown in Fig. 6. Each particle includes a core (34) of a green-emitting medium-decay cathodoluminescent phosphor—such as silver-activated zinc cadmium sulfide; a nonluminescent spacer layer (36)—such as silica—thereon; and an outer skin (38) of a mixture of a blue-emitting medium-decay phosphor—such as silver-activated zinc sulfide—and a red-emitting medium-decay cathodoluminescent phosphor—such as yttrium europium oxysulfide. These built-up particles may also be made by the methods disclosed by Pritchard,¹ Kell,² or Messineo, et al.³ and may be comprised of phosphors with different emission characteristics. The phosphor layer (30) may be deposited by methods known in the art; for example, by settling.

In operating the tube, the beam (20, Fig. 1) scans the screen (22). At lower voltages (e.g., 5 kV), the outer skin (38, Fig. 6) luminesces, displaying to the viewer a medium-decay magenta pattern on the screen. At higher voltages (e.g., 15 kV), the cores (34) luminesce, displaying to the viewer a medium-decay green pattern. At intermediate voltages (e.g., 10 kV) both the cores (34) and the outer skins (38) luminesce, displaying to the viewer a medium-decay white pattern. The tube may be used in a multicolor display for a computer output, for an airport-traffic-control system, or for other information systems.

References

1. Pritchard, D. H., Patent No. 3,204,143
2. Kell, R. D., Patent No. 3,275,466
3. Messineo, P., et al., Patent No. 3,294,569

Reprint RE-17-6-20

Final manuscript received June 4, 1971

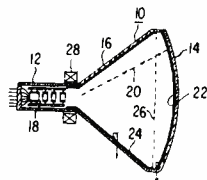


Fig. 1—Penetration-type cathode ray tube.

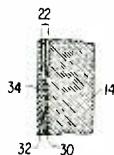


Fig. 2—Detail of cascade-type screen.



Fig. 3—Particles of the second phosphor layer for cascade-type screen.

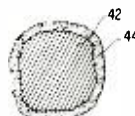


Fig. 4—Particles of the first phosphor layer for cascade-type screen.



Fig. 5—Detail of the onion-type screen.

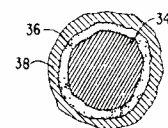


Fig. 6—Particles of the phosphor layer for onion-type screen.

Circuit simulation of bipolar integrated-circuit arrays

A. Feller
Advanced Technology Laboratories
Camden, N.J.



To meet the needs and requirements of equipment circuit designers, techniques were developed for simulating bipolar digital arrays. These techniques involve a series of large-signal bipolar models and two general-purpose circuit analysis programs capable of analyzing non-linear circuits in the time domain. The two programs are the ECAP and TRAC computer programs made operational on the RCA Spectra 70 computers. However, the large signal models are not constrained to these two programs, but in the appropriate form are applicable to other programs such as SCEPTRE, CIRCUS, NET I, and NET II.

The ability to characterize these complex digital circuits is useful in analyzing and designing bipolar circuits. Also, this ability is extremely valuable in understanding, if not solving, problems associated with interconnecting circuits. These interfacing problems include power supply distribution, special reference biasing circuits, coupling between signal lines, reflections, loading effects, noise effects, special interface circuits, and production tolerances and variations.

The key problem in simulating complex arrays is that of defining the values for the parameters for all the devices that form part of the complex array. Essentially the modeling technique to accommodate this problem uses the computer as a breadboard where the equipment designer combines his knowledge of the circuit, the particular performance parameter of interest, and the large-signal model to characterize the internal devices to a level of accuracy such that acceptable correlation exists between measured and computed results. At this point the developed model can then be used to provide computer data and/or information which is either difficult or impossible to measure.

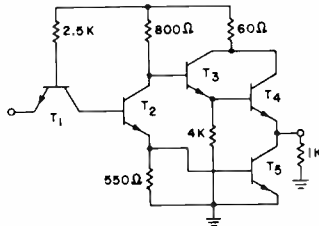


Fig. 1—TTL logic circuit analyzed.

The TTL circuit (Fig. 1) is one of six such circuits contained in a commercially available hex-inverter. The model used to represent this circuit using the ECAP program is shown in Fig. 2. To obtain the parameters for the various devices, the computer breadboarding technique was used to simulate the circuit driving a transmission line. The high level of correlation between measured and computed results, shown in Fig. 3, indicates that the devices have been simulated to a sufficient accuracy that the technique can be used to compute circuit characteristics that are not easily measured.

The TRAC program includes a standard charge-control model which was modified for bipolar devices by adding a resistor in series with either the collector or base circuit or both. Techniques were developed to obtain the needed model parameters in the laboratory. With TRAC, nonlinear components can be directly simulated, the models for various devices can be customized, and graphs of voltage vs. voltage-at-selected-points-in-the-circuit can be plotted in addition to the usual voltage-time graphs.

One typical circuit that was evaluated using the TRAC program was an experimental 4-input NOR emitter-coupled-logic circuit, shown in Fig. 4. The results of the analysis of this circuit is shown in Fig. 5.

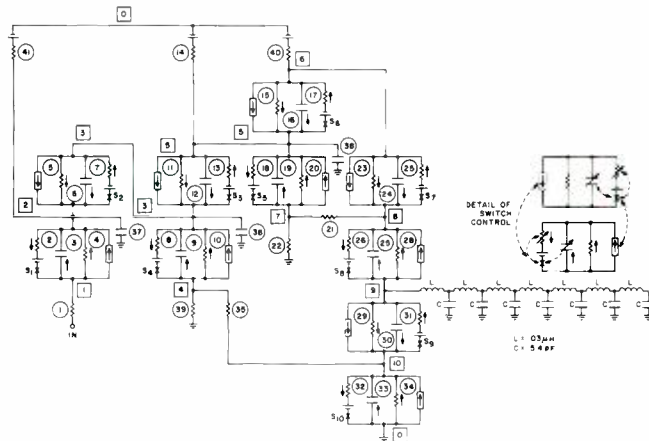


Fig. 2—Computer simulation model of TTL logic circuit.

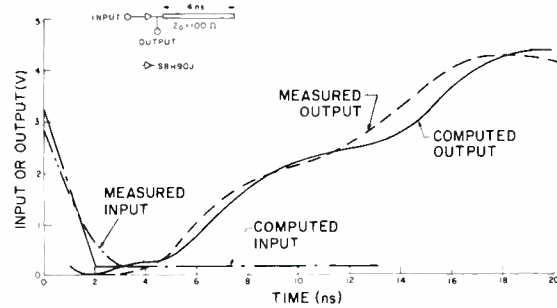


Fig. 3—Demonstration of correlation between computer simulation of TTL circuit driving a transmission line and measurements from actual circuit.

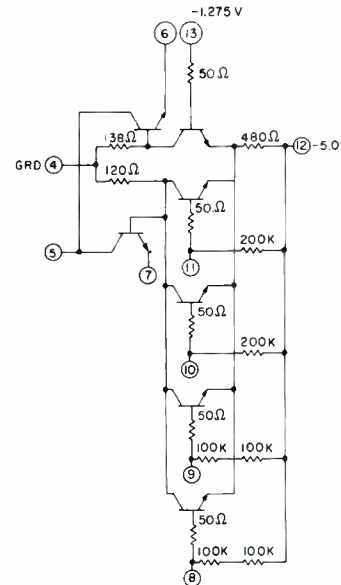


Fig. 4—Nanosecond emitter-coupled NOR logic circuit.

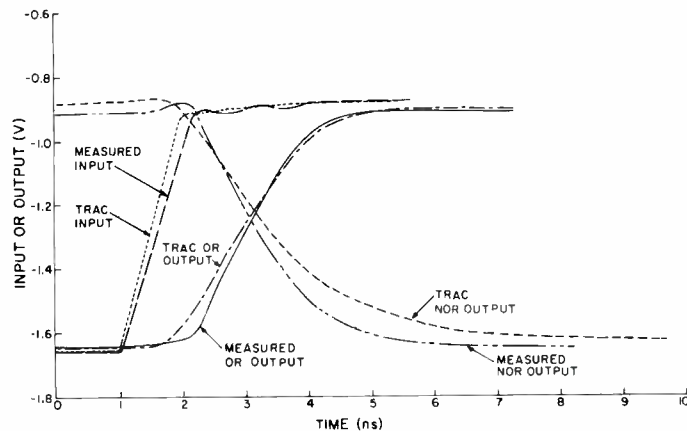


Fig. 5—Demonstration of correlation between computer simulation of NOR circuit and measurements from actual circuit.

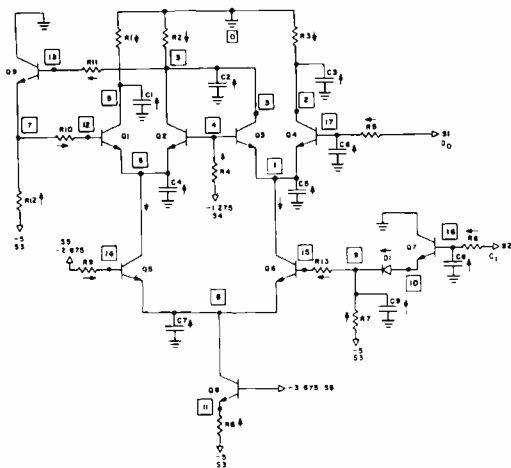


Fig. 6—Nanosecond ECL array storage element.

Also, the flip-flop circuit shown in Fig. 6 was simulated using TRAC. The same technique was used to obtain the parameters. Initial runs indicate delay times on the simulation within 15% of the measured delay times on the actual circuit.

Reprint RE-17-6-20

Final manuscript received September 19, 1971

Gigahertz-rate hundred-volt pulse generator

H. Kawamoto
Microwave Integrated Circuits
RCA Laboratories
Princeton, N.J.



A trapped plasma occurring in a high-efficiency microwave avalanche diode¹ induces a sharp, high pulse waveform^{2,3}— typically 0.5-ns wide and 100V in amplitude. The trapped plasma is a dense electron-hole plasma trapped in the high-resistivity n region of the pnn+ avalanche diode. A new device utilizing the trapped plasma is under development and is expected to process digital information at a gigahertz-rate. Such a device would be most useful as a driver in an optical data-communication system where hundred-volt, nanosecond pulses are needed for the laser modulator.

To demonstrate the capability of the trapped plasma devices, this paper reports related results for a pulse generator capable of producing a hundred volts using conventional high-efficiency microwave avalanche diodes. The performance of the new pulse generator is as follows:

Pulse amplitude:	125 V into a 50-Ω load
Repetition period:	840 ps (1.2 GHz)
Pulse width:	400 ps
Rise time:	100 ps
Fall time:	200 ps

The waveform of the pulse is shown in Fig. 1.

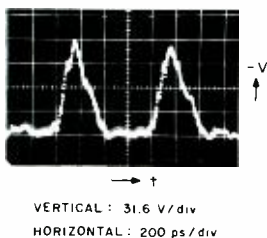


Fig. 1—Output signal from pulse generator.

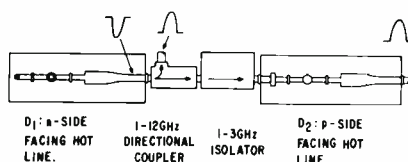


Fig. 3—Locking one pulse generator with another.

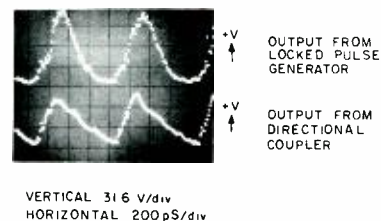


Fig. 4—Waveforms showing that one pulse generator locks another generator.

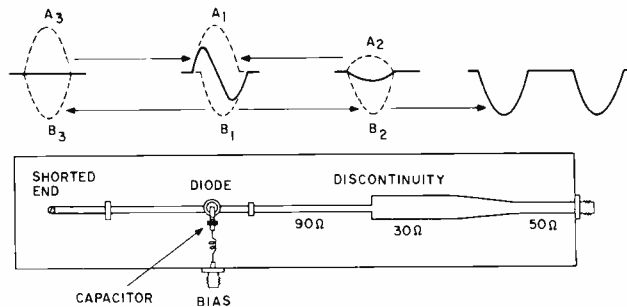


Fig. 2—Microstrip-line pulse-generator circuit.

Pulse generator

A pulse-generator circuit is illustrated in Fig. 2. A pnn+ silicon diode is placed in shunt with a microstrip line. The n+ side of the diode is facing the hot line. The microstrip line has a characteristic impedance of 90 ohms. One end of the 90 Ω line is short circuited; the other end is connected to a transmission line whose characteristic impedance is 30 Ω. The distance between the diode and the shorted end is approximately equal to the distance between the diode and the 90-to-30-Ω discontinuity point. The 30-Ω line is connected to a 50-Ω output line through a tapered-microstrip-line transformer.

The mechanism of operation is as follows: the diode operating in the high-efficiency mode generates a negative-going wave B₁ while receiving a positive-going wave A₁.^{2,3} Part of B₁ travels to the 90-to-30-Ω discontinuity point. The reflection coefficient at the discontinuity point is essentially frequency independent. The discontinuity partially transmits B₂ without changing its waveform or polarity. Thus, the pulse waveform is delivered to the output terminal. The discontinuity also reflects the rest of B₂ and reverses its sign, forming A₂ since the reflection coefficient is negative, i.e., $\rho = -0.5$.

It should be noted that a low-pass filter instead of the impedance discontinuity was previously used in the microwave signal generator;³ the low-pass filter passed only the fundamental component and rejected all the harmonics. Thus, only sinusoidal signals were delivered to the load in the microwave-generator circuit.

Part of the negative wave, B₁, generated at the diode travels toward the shorted end of the microstrip line. This shorted end reflects a positive-going wave, A₃. The positive waves A₂ and A₃ return to the diode at the same time since the round trip distance for A₂ is approximately equal to that for A₃. The combined waves (A₂ and A₃) trigger the diode again, and the diode generates the next cycle of B₁. The circuit is self-sustaining and keeps delivering a negative pulse train to the load. The time required in the return trip from the diode to the 90-to-30-Ω discontinuity is equal to a period from one pulse to the next.

Locking two pulse generators

An experiment has been performed in which one pulse generator (left hand side of Fig. 3) locks another pulse generator (right hand side of Fig. 3). The pulse generator on the right is the same as the one on the left, except that the shorted end is replaced by a tapered input line. Figure 4 shows that the output of the pulse generator on the right is locked with the output of the pulse generator on the left.

Conclusion

The high-efficiency avalanche diodes, previously used as microwave oscillators and amplifiers, have been demonstrated to generate

gigahertz-rate hundred-volt pulses. This pulse generator may be used as a timing-pulse source in a gigahertz-rate data processing system. Devices that utilize the trapped plasma provide high-power pulses. Such devices would find applications, such as a modulator for a laser or a millimeter-wave diode, in high-speed data communication systems.

Acknowledgment

The author thanks E. L. Allen, Jr. for his technical assistance, S. C. Liu and I. Martin for supplying the diodes, and K. K. N. Chang for his encouragement. He is thankful to W. L. Wilson and L. A. Stark of Cornell University for their suggestions on a measurement setup.

References

1. Prager, H. J., Chang, K. K. N., and Weisbrod, S., "High-Power High-Efficiency Silicon Avalanche Diodes at UHF and L-Band," *Proc. IEEE*, Vol. 55 (1967) p. 586.
2. Yanai, H., Torizuka, H., Yamada, N., and Ohkubo, K., "Experimental Analysis for the Large-Amplitude High-Efficiency Mode of Oscillation with Si Avalanche Diodes," *IEEE Trans. on Electron Devices*, Vol. ED-17 (Dec. 1970) p. 1067-1076.
3. Kawamoto, H., "Anti-Parallel Operation of Four High-Efficiency Avalanche Diodes," *1971 ISSCC Digest*, p. 178-179.
4. Levine, P. A., and Liu, S. C., "Tunable L-Band High-Power Avalanche-Diode Oscillator Circuit," *1969 ISSCC Digest*.

Reprint RE-17-6-20

Final manuscript received September 9, 1971

Binary light deflection system

Dr. J. A. Rajchman
Information Sciences
RCA Laboratories
Princeton, N.J.



A binary light deflection system is disclosed which directs an incident light beam in both x and y directions to any one of the many discrete positions in a utilization plane. A light beam from a source is directed through a number of identical deflection units arranged in series. The light beam emerging from a first deflection unit may have no deflection, a unit of x deflection, a unit of y deflection, or a unit of x deflection and a unit of y deflection. The first deflection unit is followed by a deflection-reducing lens, and a second identical deflection unit capable of imparting an additional amount of deflection to the received light beam. Additional lenses and deflection units produce additional amounts of deflection.

Each deflection unit includes an x -deflector and a y -deflector. Each deflector (as shown in Fig. 1) includes an electrically-controllable mirror (10) oriented at an angle β with respect to incident light beam (12) and a permanent reflector (14) oriented at an angle α with relation to reflector (10). The reflectors (10) and (14) are shown

on surfaces of a transparent solid wedge (16). The transparent wedge (16) is immersed in liquid (18) having the same index of refraction, and a low boiling point. The controllable reflector (10) consists of a transparent electrode through which an electric current can be passed to cause the formation of a film of vapor on the surface of the electrode. The vapor has an index of refraction differing greatly from that of liquid (18), so that it causes a total reflection of the incident light beam, on the face of the wedge.

In the operation of the individual deflector shown in Fig. 1, incident light (12) may pass through the surrounding liquid, through the wedge (16), and directly through the controllable reflector (10). On the other hand, if the controllable reflector (10) is activated, it reflects the incident light beam to the permanent reflector (14), and thence along a path which intersects the undeflected path at point P at an angle 2α with relation to the undeflected path.

An x - y deflection unit is shown in Fig. 2 to consist of two of the deflecting elements shown in Fig. 1 arranged in tandem with one wedge reversed and at right angles with the other, to successively provide a 2α unit of x -deflection followed by a 2α unit of y -deflection. The two deflectors are arranged so that the controllable reflector in the second or y -deflector is located to receive deflected and non-deflected beams from the first, or x -deflector. The light beam emerging from the deflecting unit of Fig. 2 may have any one of the four directions illustrated.

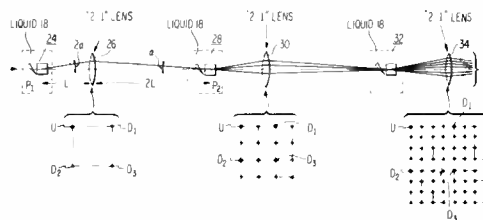


Fig. 3—Deflection system using three identical deflector units.

Fig. 3 is a deflection system including three identical deflector units—(24), (28), and (32)—arranged in series. The light beam incident to the first deflector unit emerges an undeflected path U, or one of three deflected paths D_1 , D_2 , D_3 , and passes through a lens (26), which converges the deflected beams to the controllable reflector of the x deflector in the second deflecting unit (28). The lens (26) is positioned a distance L from the first deflector (24) and a distance $2L$ from the second deflector (28). As a consequence, the deflected light beams arrive at the second deflecting unit (28) with an angle α , which is one-half the angle of deflection, 2α , imparted by the first deflecting unit (24).

The second deflecting unit (28) received a light beam having any one of four directions and either passes the received beam or imparts a 2α deflection in x and/or y directions to the received beam. Since the beam incident to the second deflector unit (28) may be at an angle α in the x and/or y directions, and since the second deflector unit (28) can cause a 2α deflection in the x and/or y directions, the beam emerging from the second deflector unit (28) is within a solid angle of $3\alpha \times 3\alpha$. The light beam at the second lens (30) may then have any one of the 16 positions shown in the diagram beneath the lens.

The lens (30) acts like lens (26) in converging the light beam to the third identical deflecting unit (32), from which the beam emerges in a solid angle of $3/2\alpha \times 3/2\alpha$ and may have any one of the 64 directions or positions shown in the diagram beneath the lens (34). Additional stages of deflection may be added to provide a still further binary increase in the number of output beam positions to which the light may be deflected. The asymptotic value of the emerging solid angle after passing through an indefinitely large number of deflection units is $4\alpha \times 4\alpha$. Therefore, there is always enough room in the lenses to accommodate the beam, no matter how many deflection units are cascaded. Each lens directs a beam to the following deflection unit with half the deflection angle of the beam received by the lens.

Reprint RE-17-6-20

Final manuscript received April 19, 1972

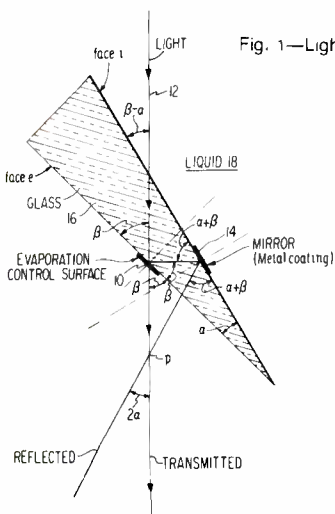


Fig. 1—Light deflector.

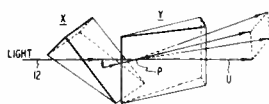


Fig. 2— x - y deflector.

High-power pin diode RF switch



D. H. Hurlburt
R. E. Cardinal
Research Laboratories
RCA Limited,
Montreal, Quebec

A high-power PIN diode SPDT RF switch for airborne applications has been developed. The switch design is unique in that bias is required for only one of the two switch positions. Hence this new solid-state switch can replace conventional electromechanical switches without rewiring.

Two separate versions of this switch have been constructed in microwave-integrated-circuit form:

- A 220 to 400 MHz (UHF) switch at 100 W CW
- A 950 to 1250 MHz (TACAN) switch at 4.5 kW peak (0.1% duty cycle)

The maximum v_{SWR} of these units is 1.5 and 1.3, respectively. The isolation is > 20 dB and the dissipative insertion losses are < 0.4 dB for both units.

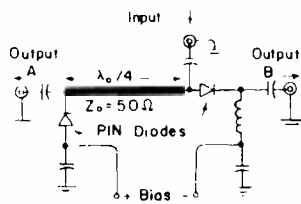


Fig. 1—Basic switch.

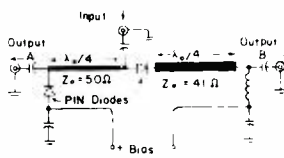


Fig. 2—Compensated switch.

Basic switch design

The basic switch design, shown in Fig. 1, incorporates both a series and shunt PIN diode. In the absence of applied bias, the series diode isolates output B and, for an ideal diode, all of the RF power is transmitted to output A. When bias voltage is applied, the shunt diode becomes an RF short circuit $\lambda_0/4$ from the input, and thus the line to output A presents an open circuit at the input at a frequency f_0 . Hence, in the ideal case, all of the RF power is transmitted to output B.

In the "diodes-on" mode, the v_{SWR} at the input is a function of the frequency as a result of the $\lambda_0/4$ length of line to the shunt diode. This situation can be improved considerably by the addition of another $\lambda_0/4$ length of line of a lower characteristic impedance, as shown in Fig. 2. By choosing $Z_0 = 41 \Omega$ for this additional length of line (assuming all other lines are 50Ω), the v_{SWR} at the input can be reduced to < 1.5 over an octave band, as compared to 1.8 max. without the compensation.

Switch construction

Two versions of this switch were constructed, and though each version has different frequency and RF power requirements, both require the operation of PIN diodes under high RF power with no applied reverse bias. It was shown that under such conditions the diodes will actually use a very small fraction of the RF signal to reverse bias themselves, providing there is no DC path enabling a reverse current to flow. Various PIN diodes were evaluated for operation under these conditions, and the Unitrode type UM-7008A was found to be acceptable providing it had an adequate heat sink. These diodes were found to be stable up to heat sink temperatures of 120°C ; beyond this point the diodes go into thermal runaway.

To eliminate DC paths around the diodes in the self-bias mode of operation, a special driver circuit was constructed. This driver allows operation of the switch from a 28V aircraft supply and has the following features:

- 1) Schmitt trigger for sensing the input bias level to insure adequate supply voltage for full operation of the diodes.
- 2) Complete isolation of the PIN diodes from the aircraft supply when the applied bias voltage is less than a preset level.
- 3) Constant current regulation to prevent aircraft supply noise from modulating the PIN diodes.

To achieve the low losses required in this application, an alumina substrate 0.075-inch thick was used for wider, and hence lower loss, microstrip lines. The substrates were coated on both sides with a vacuum deposited layer of chromium and copper to a thickness of $5 \mu\text{m}$. The RF circuitry was formed in the usual photographic and etching fashion. The resulting circuit and the backside of the substrate were then overplated with copper to a thickness of 0.001 inch. The losses of circuits formed in this fashion were found to be as low as those of 0.141 inch semi-rigid cable (0.06 to 0.08 dB/ λ_g).

In the UHF version, the series PIN diode was soldered directly across the series gap in the microstrip line. The shunt diode was soldered from the microstrip line to a plated "land" which was connected to the ground plane via a pair of chip capacitors. [100 pF, ATC-100, American Technical Ceramic Co.] This form of mounting provided minimum thermal impedance from the diode junction to the heat sink. Two series and two shunt diodes were necessary for the TACAN switch to provide the required isolation. In both series and shunt applications, the diodes were mounted a fraction of a wavelength apart and the series diodes were mounted in the same fashion as in the UHF version. The shunt diodes were soldered directly from the microstrip line to the shunt capacitors.

The addition of chip capacitors at the input and output connectors, and a simple RF filter completed the switch. The connections from the input and output terminals to the microstrip lines was formed by using 0.021×0.003 inch ribbon. These leads were fashioned into a small loop and the shape of the loop was altered to provide final "tuning" of individual circuits. The UHF and TACAN circuits are shown in Figs. 3 and 4, respectively. A preassembly view of the completed switch is shown in Fig. 5.

Acknowledgment

This project was sponsored jointly by WPAFB and the Department of Industry, Ottawa.

Reprint RE-17-6-20
Final manuscript received March 15, 1972



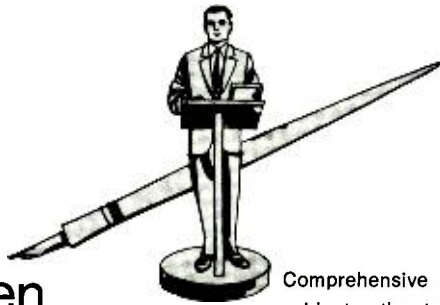
Fig. 3—UHF Switch.



Fig. 4—TACAN switch.



Fig. 5—Pre-assembly view.



Pen and Podium

Comprehensive subject-author index to Recent RCA technical papers

Both published papers and verbal presentations are indexed. To obtain a published paper, borrow the journal in which it appears from your library, or write or call the author for a reprint. For information on unpublished verbal presentations, write or call the author. (The author's RCA Division appears parenthetically after his name in the subject-index entry.) For additional assistance in locating RCA technical literature, contact: **RCA Staff Technical Publications, Bldg. 2-8, RCA, Camden, N.J. (Ext. PC-4018).**

This index is prepared from listings provided bimonthly by RCA Division Technical Publications Administrators and Editorial Representatives—who should be contacted concerning errors or omissions (see inside back cover).

Subject index categories are based upon the **Thesaurus of Engineering Terms, Engineers Joint Council, N.Y., 1st Ed., May 1964.**

Subject Index

Titles of papers are permuted where necessary to bring significant keyword(s) to the left for easier scanning. Authors' division appears parenthetically after his name.

SERIES 100 BASIC THEORY & METHODOLOGY

125 Physics

... electromagnetic field theory, quantum mechanics, basic particles, plasmas, solid state, optics, thermodynamics, solid mechanics, fluid mechanics, acoustics.

ELECTROMAGNETIC WAVES in plasma, Propagation of strong-field modulated—M. P. Bachynski, B. W. Gibbs (RCA Ltd, Mont.) *Canadian J. of Physics*, Vol. 49, No. 24, 12/15/71

ELECTROSTATIC FIELDS in a plasma by transverse electromagnetic waves, excitation of—M. P. Bachynski, B. W. Gibbs (RCA Ltd, Mont.) *Canadian J. of Physics*, Vol. 49, No. 24; 12/15/71

EXPONENTIAL ABSORPTION EDGES, Toward a unified theory of Urbach's rule and—D. Redfield, J. D. Dow (Labs. Pr) *Physical Review*, Vol. 5, No. 2, p. 594; 1/15/72

TURBULENT PLASMA: attenuation leading to saturation and cross polarization, Modified Born-back-scattering from—I. P. Shkarofsky (RCA Ltd, Mont.) *Radio Science*, Vol. 6, No. 8 & 9; 8/9/71

130 Mathematics

... basic & applied mathematical methods.

KORTEWEG—DE VRIES EQUATION FOR multiple collisions of solitons—R. Hirota (Labs. Pr) *Physical Review Letters*, Vol. 27, No. 18; p. 1192; 11/1/72

MISS DISTANCE ALGORITHMS & error sensitivities for encounters in the vertical plane—M. M. Levinson (ATL, Cam) *Navigation (J. of Inst. of Nav.) and IEEE Trans. on Aerospace & Electronic Systems*

135 Information Theory & Operations Research

... codes, modulation methods, signal processing, communication theory, game theory, queueing theory, computational linguistics, decision theory.

LANGUAGE identification, Automatic—J. R. Richards, W. F. Meeker (ATL, Cam) Rome Air Development Center, Griffiss AFB, N.Y.; 9/22/71

ADAPTIVE SPEECH RECOGNITION system—J. R. Richards (ATL, Cam) Rome Air Development Center Griffiss AFB, N.Y.; 9/22/71

160 Laboratory Techniques & Equipment

... experimental methods & equipment, lab facilities, testing, data measurement, spectroscopy, electron microscopy, dosimeters.

UNSHIELDED CAPACITOR PROBE TECHNIQUE for determining disk memory ceramic slider flying characteristics—G. R. Briggs, P. G. Herkart (Labs. Pr) *IEEE Trans. on Magnetics*, Vol. MAG-7, No. 3, p. 418; 9/71

MICROWAVE PROBE measurement techniques—R. G. Tipping (ATL, Cam) IEEE Solid State Conf., Philadelphia, Pa.; 2/16-18/71

170 Manufacturing & Fabrication

... production techniques for materials, devices & equipment.

BEAM LEAD BONDING to thick and thin films—W. J. Greig (SSD, Som) Greater NY Thin Film Chapter of the American Vacuum Soc., Princeton, N.J.; 10/71

BEAM LEAD BONDING to thick film conductors—K. R. Bube (Labs. Pr) Drexel University Philadelphia, Pa.; 2/15/72

BEAM LEAD PROCESSING of COS/MOS integrated circuits—L. A. Murray, B. W. Richards (SSD, Som) WESCON, San Francisco, Proc.; 8/71

CIRCUITS & PACKAGING for large scale military digital systems—J. A. Bauer (M&SR, Mrstn) IEEE Computer Society Packaging Committee, New York City; 1/20/72

COMPOSITE HERMETIC SEALS for COS/MOS beam leaded devices—H. Shoemaker, K. Strater, L. Murray (SSD, Som) *Electro-chemical Society Mtg.*, Cleveland, Ohio; 10/71

MICROCIRCUIT SCREEN PRINTER, Selecting a—R. H. Zeien (ATL, Cam) NEPCON 72 West 2/8/72 NEPCON 72 East Anaheim Calif. & New York; Proc. of NEPCON

RF SPUTTERING TECHNIQUES, Control of film properties by—J. L. Vossen (Labs. Pr) American Vacuum Society, New Mexico Chapter, Albuquerque, New Mexico, 1/19/72

SCREEN PRINTING for beam lead—H. Fenster, R. Zeien, W. Greig (ATL, Cam) 1971 Int'l Hybrid Microelectronics, Symp., Chicago, Ill.; 10/11/71

175 Reliability, Quality Control & Standardization

... value analysis, reliability analysis, standards for design & production.

INTEGRATED LOGISTICS SUPPORT Guide for defense systems, An appraisal of the new DoD—J. Hurley (M&SR, Mrstn) Chapter of the Society of Logistics Engineers, RCA ASD, Burlington, Mass.; 1/26/72

RELIABILITY—computer, calculation of device, circuit, equipment & system—D. R. Crosby (ATL, Cam) *IEEE Trans. on Reliability Special Issue*.

SILICON TECHNOLOGY, The quality of—A. Mayer (SSD, Som) *Solid State Technology*, 2/72

STANDARDS PROLIFERATION, Industry needs to take another look at—W. W. Thomas (ATL, Cam) Standards Engineers Soc., New York, N.Y., 10/4/71; Proc.

STATISTICAL SAMPLING?, What can you expect from—D. S. Wright (ASD, Burl) 2nd Annual Tech. Workshop on QC & Statistics—Princeton Univ., 12/4/71

180 Management & Business Operations

... organization, scheduling, marketing, personnel.

ENGINEERING/MARKETING interface, basic problems—R. G. Tipping (ATL, Cam) MBA Thesis, Fairleigh Dickinson Univ.

P requirements—Dr. J. Vollmer (ATL, Cam) AAAS and AIAA Joint Mtg., Philadelphia, Pa.; 12/28/71

PROJECT MANAGEMENT—An aerospace discipline going commercial—M. Buckley (M&SR, Mrstn) *IEEE. Univ. of Penn.*; 1/25/72

SERIES 200 MATERIALS, DEVICES, & COMPONENTS

205 Materials (electronic)

... preparation & properties of conductors, semiconductors, dielectrics, magnetic, electro-optical, recording, & electromagnetic materials.

CHALCOGENIDE SPINELS and alternative structures—H. von Philipsborn (Labs. Pr) *Zeitschrift fur Kristallographie*, Vol. 133, p. 464; 1971

COPPER WITH TRIETHENETETRAMINE in electroless plating baths, Spectrophotometric determination of—B. L. Goydich (Labs. Pr) *Mikrochimica Acta*, p. 675; 1971

GALLIUM PHOSPHIDE for luminescence investigations, Some problems in the preparation of—B. J. Curtis (Labs. Pr) Swiss Crystal Growth Soc., Zurich, Switzerland, 2/72

GRANULAR NICKEL FILMS, Effect of lattice expansion on the Curie temperature of—M. Rayl, P. J. Wojtowicz, M. S. Abrahams, R. L. Harvey (Labs. Pr) *Physics Letters*, Vol. 36A, No. 6, p. 447; 10/11/71

GRANULAR NICKEL FILMS, Ferromagnetism in—Y. Goldstein, J. I. Gittlemen (Labs. Pr) *Solid State Communications*, Vol. 9, p. 1197, 1971

IN-DOPED CdCr₂S₄, Magnetically formed surface high resistivity layer on—M. Toda (Labs. Pr) Meeting on Magnetic Semiconductors, Institute for Solid State Physics, Tokyo, Japan, 12/14/71

IRRADIATED SILICON, Influence of lithium dopant on the properties of—B. Goldstein (Labs. Pr) *Solar Cells* (Book), Section IV.2, pp. 291-301, 1971

LOW BIREFRINGENT ORTHOFERRITES for optical devices—R. B. Clover, Jr., C. Wentworth, S. Mroczkowski (Labs. Pr) *IEEE Trans. on Magnetics*, Vol. MAG-7, No. 3, p. 480; 9/71

LiNbO₃, Hologram storage and fixing mechanisms in—D. L. Staebler (Labs. Pr) Optical Sciences Center, University of Arizona, Tucson, Arizona, 1/17/72

MAGNETITE, Cathodoluminescence of—I. Balberg, J. I. Pankove (Labs. Pr) *Physical Review Letters*, Vol. 27, No. 18, p. 1371; 11/1/71

MIXED ZINC CADMIUM SULFIDE POLYCRYSTALLITES, Concentration dependence of Raman scattering from—J. Shamir, S. Larach (Labs. Pr) *Spectrochimica Acta*, Vol. 27A, p. 2105; 1971

210 Circuit Devices & Microcircuits

... electron tubes & solid-state devices (active & passive), integrated, array, & hybrid microcircuits, field-effect devices, resistors & capacitors, modular & printed circuits, circuit interconnection, waveguides & transmission lines.

BIPOLAR TRANSISTORS, GaAs vapor-grown—C. J. Nuese, J. J. Gannon, R. H. Dean, H. F. Gossenberger, R. E. Enstrom (Labs. Pr) *Solid-State Electronics*, Vol. 15, No. 1, p. 81, 1/72

COMPLEMENTARY MOS INVERTERS with composite gate insulators, Optimization of radiation resistance in—R. Feryszka, A. G. Holmes-Siedle, E. D. Smith, L. A. Murray (SSD, Som) IEEE Int'l Solid State Circuits Conf., Proc., Phila., Pa., 2/72

COMPLEMENTARY MOS, Sealed-junction beam-lead—B. W. Richards, L. A. Murray (SSD, Som) 1971 Int'l Hybrid Microelectronics Symp., Chicago, Illinois, 10/11/71

COMPLEMENTARY SYMMETRY MOS logic. Where can it be going?—A. J. Bosso (SSD, Som) *EDN/IEEE IC Seminar*, Washington, D.C., Boston, Mass., 8/3-5/71

DEVICES as circuit elements, Introduction to—K. K. N. Chang (Labs, Pr) *Microwave Symp.*, IEEE Lehigh Valley Section, Lehigh Univ., Bethlehem, Pa., 2/8/72

ECL, Dynamic testing of—M. I. Payne (SSD, Som) *IEEE Int'l Solid State Circuits Conf.*, Proc. Phila. Pa., 2/72

EMITTER DIFFUSION PARAMETERS on device characteristics, Effect of—P. J. Kannan (SSD, Som) *IEEE Int'l Electronic Devices Mtd.*, Washington, D. C., 10/71

GRANULAR METALS at low temperatures, Voltage-induced tunneling conduction in—P. Sheng, B. Abeles (Labs, Pr) *Physical Review Letters*, Vol. 28, No. 1, p. 34; 1/3/72

LINEAR IC's and their applications, A medley of—M. V. Hoover (SSD, Som) *EDN/IEEE IC Seminar*, Washington, D.C., Boston, Mass., 8/71

MEMORY MODULE, Beam lead COS/MOS—J. R. Oberman, N. H. Burton, L. A. Murray (SSD, Som) *IEEE Int'l State Circuits Conf.*, Phila., Pa., Proc., 2/72

MICROWAVE AMPLIFIER using an antiparallel avalanche-diode pair, High-power—H. Kawamoto (Labs, Pr) *IEEE Trans on Microwave Theory and Techniques*, Vol. MTT-19, No. 12 p. 911, 12/71

PIN diode, A high power—R. F. Switch, D. H. Hurlburt, R. E. Cardinal (Library, Canada) *Conf. Digest, Int'l Electrical Electronics Conf. & Exposition*, Toronto; 10/71

PNVp DIODES with improved CW power and efficiency, AM and FM noise performance of—S. G. Liu, J. J. Risko, P. A. Levine (Labs, Pr) 1972 *IEEE Int'l Solid-State Circuits Conf.*, Philadelphia, Pa., 2/16-18/72

POWER TRANSISTOR design considerations for better forward second breakdown characteristics—D. L. Franklin (SSD, Som) *IEEE-IGA Conf.*, Cleveland, Ohio, 10/71, *Record*

POWER TRANSISTORS, Thermal cycling ratings of—V. Lukach, L. Gallace, W. Williams (SSD, Som) 1972 *Annual Reliability & Maintainability Symp.*, San Francisco, Calif., 1/72

215 Circuit & Network Designs ... analog & digital functions in electronic equipment: amplifiers, filters, modulators, microwave circuits, A-D converters, encoders, oscillators, switches, masers, logic networks, timing & control functions, fluidic circuits.

AM RADIO applications, An IC for—L. Baar (SSD, Som) *IEEE Conf. on BTR*; 12/71

BIPOLAR TRANSISTOR MODEL for devices and circuit design—R. B. Schilling (SSD, Som)—*RCA Review*, 9/71

AVAILABLE MEMORY TECHNOLOGY, Review of—G. J. Wass (SSD, Som) *Control Engineering*; 1/72

COMMON-BASE VS. COMMON-EMITTER for 225- to 400-megahertz applications—Z. F. Chang, R. E. Horn (SSD, Som) *IEEE Int'l Electronic Devices Mtg.*, 10/71, Washington, D.C.

DIGITAL AUTO CLOCK using COS/MOS LSI technology—D. K. Morgan (SSD, Som) *IEEE Vehicular Technology Seminar*, 12/71

ELECTRONIC TIMING applications, Complementary MOS and liquid crystals—R. T. Griffin (SSD, Som) *Eurocon*; 10/71

INTERCONNECTION reflections—A. Feller (ATL, Cam) *Radiation Melbourne*, Melbourne, Florida.

LOW-POWER DIGITAL FREQUENCY SYNTHESIS application demonstrates unique COS/MOS performance characteristics—R. Funk (SSD, Som) *WESCON*, San Francisco, Calif.; 8/71; *Proc*

MICROWAVE LUMPED ELEMENTS from 1 to 12 GHz, Impedance measurements of—R. E. DeBrecht (Labs, Pr) *IEEE Trans on Microwave Theory and Techniques*, Vol. MTT-20, No. 1 p. 41, 1/72

MONOLITHIC MEMORY—users viewpoint—G. B. Herzog (Labs, Pr) 1972 *IEEE Int'l Solid-State Circuits Conf.*, Philadelphia, Pa., 2/16-18/72

PULSE GENERATOR, gigahertz-rate, hundred-volt—H. Kawamoto (Labs, Pr) 1972 *IEEE Int'l Solid-State Circuits Conf.*, Philadelphia, Pa., 2/16-18/72

SEVEN-STAGE BINARY COUNTER, Characteristics of a silicon-on-sapphire CMOS—W. Schneider, W. F. Gehweiler (Labs, Pr) 1972 *IEEE Int'l Solid-State Circuits Conf.*, Philadelphia, Pa., 2/16-18/72

SHIFT REGISTERS, Two-phase charge-coupled—W. F. Kosonocky, J. E. Carnes (Labs, Pr) 1972 *Int'l Solid State Circuits Conf.*, Philadelphia, Pa., 2/16-18/72

STEREO AMPLIFIER, An IC four-channel—L. Kaplan (SSD, Som) *Radio Electronics*; 10/71

TRAVELLING-WAVE AMPLIFIER using thin epitaxial GaAs layer—R. H. Dean, A. B. Dreeben, J. F. Kaminski, A. Triano (Labs, Pr) *Electronics Letters*, Vol. 6, No. 24; 11/5/71

225 Antennas & Propagation ... antenna design & performance, feeds & couplers, phased arrays, radomes & antenna structures, electromagnetic wave propagation, scatter, effects of noise & interference.

DUAL REFLECTOR ANTENNAS, Feed arrays for—L. I. Smilen (M&SR, Mrstn) Long Island Chapter, Group on Antennas & Propagation Polytechnic Inst. Farmingdale, N.Y., 12/9/71

JOSEPHSON-JUNCTION TRANSMISSION LINE, Wave propagation through a—R. Hirota (Labs, Pr) *J. of the Physical Society of Japan*, p. 279, 1972

240 Lasers, Electro-Optical & Optical Devices ... design & characteristics of lasers, components used with lasers, electro-optical systems, lenses, etc. (excludes: masers).

CO₂ LASERS—R. A. Crane (RCA Ltd, Mont) *RCA Corporate Laser Symp.*, Princeton, N.J.; 10/28/71

COMMUNICATIONS—A. Waksberg (RCA Ltd, Mont) *RCA Corporate Laser Symp.*, Princeton, N.J., 10/28/71

DETECTOR MOSAIC for ordnance flash location—I. Drukaroff, W. R. L. Thomas, H. Brkan (ATL, Cam) 1971 *Int'l IEEE Electron Devices Mtg.*, Washington, D. C., 10/12/71

ELECTROFAX LAYERS and speckles in reversal liquid development, Relationships between the physical properties of—E. C. Hutter (Labs, Pr) *Photographic Science and Engineering*, Vol. 15, No. 6, p. 456; 12/71

GaAIs CLOSE-CONFINEMENT LASER DIODES, Room temperature—R. B. Gill, T. Gonda, P. Nyual, A. Limm, R. Speers (SSD, Som) *Electro-optics Systems Design Conf.*, Proc., Anaheim, Calif.; 5/71

GaAs CLOSE CONFINEMENT LASER DIODES, Characteristics of—R. B. Gill, A. G. Zoundes (SSD, Som) *Electro-optics System Design Conf.*, New York, N.Y.; 9/71

GaAs INJECTION LASER DIODES, a new dimension for electronic systems—R. A. Felmlly (SSD, Som) *Optical Spectra*; 11/71

GaAs LASER DIODE ARRAY light sources, Moderate-power—A. Limm, P. Nyual, R. Gill, T. Gonda (SSD, Som) *Electro-optics Systems Design Conf.*, Proc., Anaheim, Calif.; 5/71

GaAs MILLIMETER WAVE avalanche diode noise—K. P. Weller (Labs, Pr) *Specialist Workshop on Compound Semiconductor Microwave Devices and Material Growth*, N.Y.; 2/16-18/72

LASER DIODES and arrays, High power LOC heterojunction—T. Gonda, H. Kressel, R. B. Gill, F. Z. Hawrylo (SSD, Som) *IEEE Int'l Electronic Devices Mtg.*, Washington, D.C.; 10/71

OPTICAL PATTERN RECOGNITION, Techniques for high-data-rate two dimensional—R. F. Croce, F. T. Burton (ATL, Cam) *RCA Review*, 12/71

OPTICAL WAVEGUIDE, Single crystal epitaxial ZnO on sapphire—J. M. Hammer, J. P. Witke, D. J. Channin, M. T. Duffy (Labs, Pr) *Topical Meeting on Integrated Optics-Guided Waves, Materials and Devices*, Las Vegas, Nevada, 2/7-10/72

OPTICAL WAVE PROPAGATION through random atmospheric turbulence (comments on) A theoretical study of—J. P. Lausade, A. Yanz, D. A. deWolf (Labs, Pr) *Radio Science*, Vol. 6, No. 10; p. 841, 10/71

SINGLE HETEROJUNCTION GaAIs CLOSE-CONFINEMENT LASERS from 250°K to 400°K—R. B. Gill, T. Gonda, R. R. Speers (SSD, Som) *IEEE Int'l Electronic Devices Mtg.*, Washington, D.C., 10/71

245 Displays ... equipment for the display of graphic, alphanumeric, & other data in communications, computer, military, & other systems, CRT devices, solid state displays, holographic displays, etc.

MOVING MAP display, Holographic multicolor—G. T. Burton, B. R. Clay (ATL, Cam) *NEREM*, Boston, Mass., 11/2-5/71 *NEREM Record*

250 Recording Components & Equipment ... disk, drum, film, holographic & assemblies for audio, image, & data systems.

HOLOGRAPHIC INFORMATION SYSTEMS, Promises and problems—J. A. Rajchman (Labs, Pr) *Workshop on Optical Communication Systems*, University of Maryland, College Park, Maryland; 1/27/72

LASER RECORDING system—D. Woywood (ATL, Cam) 1972 *Electro-Optics Int'l*, Brighton, England

MULTICHANNEL RECORDING synthetic gratings—S. L. Corsover (ATL, Cam) *Thesis*—Moore School of Electrical Engineering, Phila. Pa.; 8/16/71

SERIES 300 SYSTEMS, EQUIPMENT & APPLICATIONS

310 Spacecraft & Ground Support ... spacecraft & satellite design, launch vehicles, payloads, space missions, space navigation.

COMMUNICATIONS SATELLITE terminals, Commercial—A. Lovas (RCA Ltd, Mont) *RCA G&CS Satellite Communications Symp.*, Princeton, N.J., 11/11/71

DOMESTIC SATELLITE system, Canadian—D. Jung (RCA Ltd, Mont) *RCA G&CS Satellite Communications Symp.*, Princeton, N.J.; 11/11/71

320 Radar, Sonar, & Tracking Systems ... microwave, optical, & other systems for detection, acquisition, tracking, & position indication.

INSTRUMENTATION radar depot operations, RCA—W. Lustina (M&SR, Mrstn) *Society of Logistics Engineers*, Phila., Pa.; 1/19/72

325 Checkout, Maintenance, & User Support ... automatic test equipment, maintenance & repair methods, installation & user support.

DYNAMIC TESTING of ECL—M. I. Payne (SSD, Som) *IEEE Int'l Solid State Circuits Conf.*, Proc. Phila. Pa., 2/72

340 Communications Equipment & Systems ... industrial, military, commercial systems, telephony, telegraphy, & telemetry, (excludes: television & broadcast radio).

AMATEUR RADIO—a scientific hobby—J. Duffin (M&SR, Mrstn) *Moorestown High School*, Moorestown, N.J., 12/6/71

MM-WAVE COMMUNICATION system considerations—H. J. Moody (RCA Ltd, Mont) *RCA G&CS Satellite Communications Symp.*, Princeton, N.J.; 11/11/71

TRANSPONDER for 12- 15 GHz—T. A. Cagny (RCA Ltd, Mont) *Session on Satellites RCA G&CS Satellite Communications Symp.*, Princeton, N.J.; 11/11/71

360 Computer Equipment ... processors, memories, & peripherals.

COMPUTER MEMORIES—state of the art and challenges—J. A. Rajchman (Labs, Pr) *Scientific Staff Colloquium*, National Bureau of Standards, Washington, D.C.; 2/4/72

DIGITAL DISK memories—R. A. Shahbender (Labs, Pr) *Seminar*, Drexel University, Philadelphia, Pa.; 2/9/72

DIGITAL DISK memories—R. A. Shahbender (Labs, Pr) *Workshop of the Computer Elements Committee*, Phoenix, Arizona, January 16-19, 1972

HOLOGRAPHIC INFORMATION systems, Promises and problems in—J. A. Rajchman (Labs, Pr) *Workshop on Optical Communication Systems*, University of Maryland, College Park, Maryland; 1/27/72

LARGE-CORE STORAGE in perspective—J. G. Williams (Labs, Pr) *Computer Design*, Vol. 11, No. 1, p. 45, 1/72

Author Index

Subject numbers listed opposite each author's name indicates where complete citation to his paper may be found in the subject index. An author may have more than one paper for each subject category.

Advanced Technology Laboratories

Borkan, A., 240
Burton, G. T., 240, 245
Clay, B. R., 245
Corsover, S. L., 250
Croce, R. F., 240
Crosby, D. R., 175
Drukaroff, I., 240
Feller, A., 215
Fenster, H., 170
Greig, W., 170
Levinson, M. M., 130
Meeker, W. F., 135
Richards, J. R., 135
Thomas, W. R. L., 240
Thomas, W. W., 175
Tipping, R. G., 160, 180
Vollmer, J., 180
Woywood, D., 250
Zeien, R. H., 170

Aerospace Systems Division

Wright, D. S., 175

RCA Laboratories

Abeles, B., 210
Abrahams, M. S., 205
Balberg, I., 205
Briggs, G. R., 160

Bube, K. R., 170
Carnes, J. E., 215
Chang, K. K. N., 210
Channin, D. I., 240
Clover, R. B., 205
Curtis, B. J., 205
Dean, R. H., 210
DeBrecht, R. E., 21
de Wolf, D. A., 240
Dow, J. D., 125
Dreeben, H. B., 215
Duffy, M. T., 240
Enstrom, R. E., 210
Gannon, J. J., 210
Gehweiler, W. F., 215
Gittleman, J. I., 205
Goldstein, B., 205
Gossenberger, H. F., 210
Goydsh, B. L., 205
Hammer, J. M., 240
Harvey, R. L., 205
Herkart, R. G., 160
Herzog, G. B., 215, 360
Hirota, R., 130, 225
Hutter, E. C., 240
Kaminski, J. F., 215
Kawamoto, H., 210, 215
Kosonocky, W. F., 215
Larach, S., 205
Laussade, J. P., 240
Levine, P. A., 210
Liu, S. G., 210
Mroczkowski, S., 205
Nuese, C. J., 210
Pankove, J. I., 205
Rajchman, J. A., 250, 360
Rayl, M., 205
Redfield, D., 125
Fisko, J. J., 210

Schneider, W., 215
Shahbender, R. A., 360
Shamir, J., 205
Sheng, F., 210
Staebler, D. L., 205
Toda, M., 205
Triano, A., 215
von Philipsborn, H., 205
Vossen, J. L., 170
Welber, K. P., 240
Wentworth, C., 205
Williams, J. G., 360
Wittke, J. P., 240
Wojtowicz, P. J., 215
Yariz, A., 240

RCA Limited, Montreal

Bachynski, M. P., 125
Cagney, T. A., 340
Cardinal, R. E., 210
Crane, R. A., 240
Gibbs, B. W., 125
Hurlburt, D. H., 210
Jung, D., 310
Lovas, A., 310
Moody, H. J., 340
Shkarofsky, I. P., 125
Switch, R. F., 210
Waksberg, A., 240

Missile and Surface Radar Division

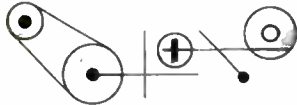
Bauer, J. A., 170
Buckley, M., 180
Duffin, J., 340
Hurley, J., 175
Lustina, W., 320
Smilen, L. I., 225

Solid State Division

Baar, L., 215
Bosso, A. J., 210
Burton, N. H., 210
Chang, Z. F., 215
Femly, R. A., 240
Feryszka, R., 210
Franklin, D. L., 210
Funk, R., 215
Gallace, L., 210
Gill, R. B., 240
Gonda, T., 240
Greig, W. J., 170
Fritfin, R. T., 215
Hawrylo, F. Z., 240
Holmes-Siedle, A. G., 210
Hoover, M. V., 210
Horn, R. E., 215
Kannam, P. J., 210
Kaplan, L., 215
Kressel, H., 240
Limm, A., 240
Lukach, V., 210
Mayer, A., 175, 205
Morgan, D. K., 215
Murray, L. A., 170, 210
Nywal, P., 240
Oberman, J. R., 210
Payne, M. I., 210, 325
Richards, B. W., 210
Schilling, R. B., 215
Shoemaker, H., 170
Smith, E. D., 210
Spears, R. R., 240
Strater, K., 170
Wass, G. J., 215
Williams, W., 210
Zourides, A. G., 240

Patents Granted

to RCA Engineers



As reported by RCA Domestic Patents, Princeton

Astro-Electronics Division

Radio Postal System Acknowledgment Apparatus—D. S. Bond (AED, Pr.) U.S. Pat. 3641432, February 8, 1972

Electromagnetic and Aviation Systems Division

Bowling Split Detector—W. A. Helbig, Sr., W. E. Woods (EASD, Van Nuys) U.S. Pat. 3637211, January 25, 1972

Logic Gate—E. B. Gamble (EASD, Van Nuys) U.S. Pat. 3641362, February 8, 1972

Logic Circuit Which Turns On and Off Rapidly—E. B. Gamble, R. H. Aires (EASD, Van Nuys) U.S. Pat. 3641368, February 8, 1972

Synchronization of Serial Memory—K. Katagi (EASD, Van Nuys) U.S. Pat. 3643220, February 15, 1972

Missile and Surface Radar Division

Target Acquisition Antenna—J. P. Grabowski, W. E. Powell (M&SR, Mrstn.) U.S. Pat. 3623094, November 23, 1971; Assigned to U. S. Government

Maximum Length Pulse Sequence Generators—E. C. Farnett, L. O. Upton (M&SR, Mrstn.) U.S. Pat. 3614400, January 10, 1972

Corporate-Network Printed Antenna System—O. M. Woodward (M&SR, Mrstn.) U.S. Pat. 3587110, January 24, 1972

Electronic Editing Apparatus—T. V. Bolger (M&SR, Mrstn.) U.S. Pat. 3646260, February 29, 1972

Capacitance Multiplication Network—W. Blumstein (M&SR, Mrstn.) U.S. Pat. 36424425, February, 1972

Wide Band Balun—O. M. Woodward (M&SR, Mrstn.) U.S. Pat. 3656071, April 11, 1972

Advanced Technology Laboratories

Low-Light Level Color Photography—K. K. C. Hudson, F. Shashoua (AT, Cam.) U.S. Pat. 3580151, May 25, 1971

Optical Compensating Filter with Selective Radial Absorption—K. Hudson (AT, Cam.) U.S. Pat. 3558208, January 26, 1971

Pulse-Method Circuit Element-Testing Method—N. R. Stewart, D. R. PreStar (AT, Cam.) U.S. Pat. 3643156, February 15, 1972

Bowling Pin Detector—E. Hutto, Jr., J. P. Mahoney (AT, Cam.) U.S. Pat. 3651328, March 21, 1972

Level Detector—G. J. Dusheck, Jr. (AT, Cam.) U.S. Pat. 3621308, November 16, 1971; Assigned to U. S. Government

Timing Logic—J. R. Barger (AT, Cam.) U.S. Pat. 3628156, December 14, 1971; Assigned to U. S. Government

Communications Systems Division

Temperature Compensated Crystal Oscillator—P. K. Mrozek (CS, Mdwind.) U.S. Pat. 3641461, February 8, 1972

Television Camera Utilizing a Parallel Striped Color Encoding Filter—R. A. Dischert (CS, Cam.) U.S. Pat. 3651250, March 21, 1972

Feedback Clipper—D. C. Herrman, L. J. Bazin (CS, Cam.) U.S. Pat. 3651339, March 21, 1972

Web Cartridge—B. L. Dickens, B. F. Melchioni, R. R. Werner (CS, Cam.) U.S. Pat. 3653608, April 4, 1972

Video Tape Recorder Synchronizing System—K. Louth (CS, Cam.) U.S. Pat. 3653989, April 4, 1972

Device to Keep a Capstan in Phase When Switching Modes—K. Louth, (CS, Cam.) U.S. Pat. 3654398, April 4, 1972

Commercial Systems

Automatic Beam Focusing System—H. Ball, (Indpls.) H. L. Peterson (CS, Burbank) U.S. Pat. 3647952, March 7, 1972

Solid-State Analog Cross-Point Matrix Having Bilateral Crosspoints—N. Hovagimyan, R. N. Van Delft (CSD, Cam.) U.S. Pat. 3639908, February 1, 1972

Beam Control System—D. J. Woywood (CSD, Cam.) U.S. Pat. 3646568, February 29, 1972

Computer Systems

Multi-Electrode Transducer Element—J. P. Watson (CS, Palm Beach Gardens) U.S. Pat. 3648279, March 7, 1972

Cable Harness Assembly Board and Method of Making the Same—F. H. Mosher, E. G. Jenney (CS, Palm Beach Gardens) U.S. Pat. 3653411, April 4, 1972

Motion Transfer Mechanism—F. A. Digilio (CS, Framingham) U.S. Pat. 3655126, April 11, 1972

Graphic Systems Division

Vector Generator—H. M. Scott, C. R. Corson (GSD, Dayton) U.S. Pat. 3638214, January 25, 1972

Variable Length Coding Method and Apparatus—J. P. Beltz (GSD, Dayton) U.S. Pat. 3643019, February 15, 1972

Laboratories

Color Correction of Prismatic Off-Axis Optical System—J. A. VanRaalte, W. J. Gorkiewicz (Labs., Pr.) U.S. Pat. 3637308, January 25, 1972

System and Filter for Encoding Color Images Onto Black and White Film—R. E. Flory, F. W. Spong (Labs., Pr.) U.S. Pat. 3637925, January 25, 1972

Compact, High-Power, High-Efficiency Silicon Avalanche Diode L-Band Oscillator—P. A. Levine, S. Liu (Labs., Pr.) U.S. Pat. 3638141, January 25, 1972

Ion Discharge Tube Employing Cathoretic Techniques—K. G. Hernqvist (Labs., Pr.) U.S. Pat. 3639804, February 1, 1972

Keyed Substrate Field Effect Transistor Frequency-Selective Circuits—T. Saeki (Labs., Tokyo) U.S. Pat. 3637935, January 25, 1972

Integrated Buffer Circuits for Coupling Low-Output Impedance Driver to High-Input Impedance Load—H. C. Lee (SSTC, Pr.) U.S. Pat. 3639787, February 1, 1972

- Selective Deposition of Metal**—R. D. Dis-
telano, E. A. James (Labs., Pr.) U. S. Pat.
3640765, February 8, 1972
- Method of Metalizing Semiconductor
Devices**—J. L. Vossen, Jr. (Labs., Pr.) U. S.
Pat. 3640811, February 8, 1972
- Method of Making Electrical Contacts on
the Surface of a Semiconductor Device**—J.
L. Vossen, Jr., J. H. Banfield (Labs., Pr.) U.
S. Pat. 3640812, February 8, 1972
- Adhesion of Nonconducting Materials**—R.
J. Ryan (Labs., Pr.) U. S. Pat. 3640853, Feb-
ruary 8, 1972
- Holographic Identification System**—D. L.
Greenaway, J. P. Russell (Labs., Zurich, Swit-
zerland) U. S. Pat. 3643216, February 15, 1972
- Ratio-Compensated Resistors for Inte-
grated Circuit**—A. G. F. Dingwall (SSTC, Pr.)
U. S. Pat. 3644802, February 22, 1972
- Image Storage System**—R. S. Silver, E.
Luedicke (Labs., Pr.) U. S. Pat. 3646390, Feb-
ruary 29, 1972
- Gyromagnetic Isolator Wherein Even Mode
Components Are Converted to Odd Mode
Components by Biased Ferrite**—C. P. Wen
(Labs., Pr.) U. S. Pat. 3646486, February 29,
1972
- Fabrication of Semiconductor Devices**—E.
J. Boleky, III and J. R. Burns (Labs., Pr.) U.
S. Pat. 3646666, March 7, 1972
- Method of Making High Area-Density Array
Photomasks Having Matching Registry**—F.
P. Heiman (Labs., Pr.) U. S. Pat. 3647438,
March 7, 1972
- Liquid Phase Double Epitaxial Process for
Manufacturing Light Emitting Gallium
Phosphide Devices**—I. Ladany (Labs., Pr.)
U. S. Pat. 3647579, March 7, 1972
- Color Encoding System Utilizing Two Filters
Alternately for Minimizing Effects of Image
Misregistration and Image Pickup Device
Lag**—W. J. Hannan (Labs., Pr.) U. S. Pat.
3647945, March 7, 1972
- Double Epitaxial Solution Regrowth
Process and Device Made Thereby**—F. Z.
Hawrylo (Labs., Pr.) U. S. Pat. 3649382, March
14, 1972
- Apparatus Permitting Reliable Selection of
Transmitted Television Message Infor-
mation**—J. J. Gibson (Labs., Pr.) U. S. Pat.
3649749, March 14, 1972
- Control Signal Generating Apparatus to
Permit Reliable Selection of Transmitted
Television Message Information**—J. J. Gib-
son (Labs., Pr.) U. S. Pat. 3649750, March 14,
1972
- Voltage Translation Circuit for MNOS Mem-
ory Array**—E. C. Ross (Labs., Pr.) U. S. Pat.
3649848, March 14, 1972
- High Power Semiconductor Device
Assembly**—K. K. N. Chang, H. J. Prager
(Labs., Pr.) U. S. Pat. 3649881, March 14, 1972
- Parametric Optical System**—A. H. Firester
(Labs., Pr.) U. S. Pat. 3629602, December 21,
1971; Assigned to U. S. Government
- High-Resolution Optical Upconverter**—A.
H. Firester (Labs., Pr.) U. S. Pat. 3629601,
December 21, 1971; Assigned to U. S. Govern-
ment
- Redundant, Speckle-Free Hologram
Recording Apparatus**—H. J. Gerritsen, W. J.
Hannan (Labs., Pr.) U. S. Pat. 3650595, March
21, 1972
- Liquid Crystal Light Valve Containing a Mix-
ture of Nematic and Cholesteric Materials
in Which the Light Scattering Effect is
Reduced When an Electric Field is Applied**
—G. H. Heilmeyer, J. E. Goldmacher (Labs.,
Pr.) U. S. Pat. 3650603, March 21, 1972
- Signal Translating Stage Providing Direct
Voltage Translation Independent of
Supplied Operating Potential**—A. L. Lim-
berg (Labs., Pr.) U. S. Pat. 3651347, March
21, 1972
- Gated Amplifier**—H. R. Beelitz (Labs., Pr.) U.
S. Pat. 3651421, March 21, 1972
- Information Storage System Employing
Optical Entry and Removal of Information**
—J. J. Amodei (Labs., Pr.) U. S. Pat. 3651488,
March 21, 1972
- Symmetrical Trough Waveguide Antenna
Array**—C. P. Wen (Labs., Princeton) U. S. Pat.
3653054, March 28, 1972
- Optical Upconverter**—A. H. Firester (Labs.,
Pr.) U. S. Pat. 3646358, February 29, 1972
- Microwave Hybrid Comprising Trough
Waveguide and Balanced Mixer Utilizing
Same**—C. P. Wen (Labs., Pr.) U. S. Pat.
3654556, April 4, 1972
- Waveguide Structure**—L. S. Napoli (Labs.,
Pr.) U. S. Pat. 3654572, April 4, 1972
- Alternating Voltage Excitation of Liquid
Crystal Display Matrix**—F. J. Marlowe, E. O.
Nester (Labs., Pr.) U. S. Pat. 3654606, April
4, 1972
- Four-Phase High Speed Counter**—U. Bhar-
ali (SSTC, Pr.) U. S. Pat. 3654441, April 4, 1971
- Liquid Crystal Display Assembly Having
Independent Contrast and Speed of Re-
sponse Controls**—G. H. Heilmeyer (Labs., Pr.)
U. S. Pat. 3655269, April 11, 1972
- Corona Generating Circuits for Elec-
trophotographic Printers Cooperatively
Operating with Television Receivers**—R. W.
Bruce, Jr. (Labs., Pr.) U. S. Pat. 3655912, April
11, 1972
- Charge Coupled Device**—Z. A. Weinberg
(Labs., Pr.) U. S. Pat. 3656011, April 11, 1972
- Semiconductor Device with Plurality of
Small Area Contacts**—L. S. Napoli, J. J.
Hughes (Labs., Pr.) U. S. Pat. 3656030, April
11, 1972
- Electrically and Optically Accessible
Memory**—J. A. Rajchman, W. F. Kosonocky
(Labs., Pr.) U. S. Pat. 3656121, April 11, 1972

Electronic Components

- Photographic Process for Preparing a
Screen Structure for a Cathode-Ray Tube**
—W. J. Maddox, M. R. Weingarten (EC, Lanc.)
U. S. Pat. 3636836, January 25, 1972
- Microwave Signal Delay Apparatus**—E. F.
Belohoubek (EC, Pr.) U. S. Pat. 3639802, Feb-
ruary 1, 1972; Assigned to U. S. Government
- Apparatus for Chemically Etching Surfaces**
—R. A. Alieman, W. N. Henry (EC, Lanc.) U.
S. Pat. 3640792, February 8, 1972
- Encapsulated Magnetic Memory Element**
—T. P. Fulton, H. DiLuca (EC, Needham
Hghs.) U. S. Pat. 3640767, February 8, 1972
- Microwave Delay Apparatus**—E. F.
Belohoubek (EC, Pr.) U. S. Pat. 3641388, Feb-
ruary 8, 1972; Assigned to U. S. Government
- Electron Beam Tube and Method of Adjust-
ing the Electrode Spacing of an Electron
Gun Therein**—M. K. Brown (EC, Lanc.) U. S.
Pat. 3643299, February 22, 1972
- Transferred Electron Amplifier**—B. S. Per-
lman, T. E. Walsh (EC, Pr.) U. S. Pat. 3644839,
February 22, 1972
- Apparatus for Measuring Light Transmis-
ion of a Semitransparent Membrane**—J.
B. Bucher (EC, Lanc.) U. S. Pat. 3645634, Feb-
ruary 29, 1972

- Microwave Limiter That Suppresses Lead-
ing Edge Spike of Radio Frequency Signal**
—W. W. Siekanowicz (EC, Pr.) U. S. Pat.
3648197, March 7, 1972
- Dark Fostepite Ceramic Composition**—H.
Notarius (EC, Hrsn.) U. S. Pat. 3649309, March
14, 1972
- Process for Coating Flatlike Surfaces**—B.
K. Smith (EC, Lanc.) U. S. Pat. 3652323, March
28, 1972
- Method of Fabricating a Porous Tungsten
Body for a Dispenser Cathode**—A. Month,
D. L. Thornburg (EC, Lanc.) U. S. Pat. 3653883,
April 4, 1972
- Color Kinescope Production with a Temp-
orary Mask**—R. W. Etter (EC, Lanc.) U. S. Pat.
3653901, April 4, 1972
- Slurry Process for Coating Particulate
Material Upon a Surface**—B. B. Bell, W. E.
Pederson (EC, Lanc.) U. S. Pat. 3653941, April
4, 1972

Solid State Division

- Operation of Field-Effect Transistor Cir-
cuits Having Substantial Distributed
Capacitance**—V. W. Chen, H. Amemiya (SSD,
Som.) U. S. Pat. 3638039, January 25, 1972
- Triggering Circuit for CRT Deflection System
Utilizing an SCR**—W. F. W. Dietz (SSD, Som.)
U. S. Pat. 3638067, January 25, 1972
- Hermetic High-Current Terminal for Elec-
tronic Devices**—W. L. Oates (SSD, Som.) U.
S. Pat. 3637917, January 25, 1972
- High Frequency Semiconductor Device**
—W. V. Fitzgerald, Jr. (SSD, Som.) U. S. Pat.
3641398, February 8, 1972
- Amplifier Using Bipolar and Field-Effect
Transistors**—S. A. Graf (SSD, Som.) U. S. Pat.
3644838, February 22, 1972
- Liquid Crystal Display Device**—R. I. Klein,
S. Caplan (SSD, Som.) U. S. Pat. 3647280,
March 7, 1972
- Fluid Cooled Apparatus for Testing Power
Semiconductor Devices**—D. R. Purdy, W. E.
Donnelly, (SSD, Som.) U. S. Pat. 3648167,
March 7, 1972
- Multi-Circuit Hybrid Module and Method for
Making**—D. M. Baugher, E. T. Hausman (SSD,
Som.) U. S. Pat. 3648116, March 7, 1972
- Reference Voltage Source**—S. A. Graf (SSD,
Som.) U. S. Pat. 3648153, March 7, 1972
- AC Line Operation of Monolithic Circuit**—J.
P. Keller, S. A. Graf (SSD, Som.) U. S. Pat.
3649887, March 14, 1972
- Apparatus for Increasing the Speed of
Series Connected Transistors**—A. G. F.
Dingwall (SSD, Som.) U. S. Pat. 3651342,
March 21, 1972
- Circuits for Driving Loads Such as Liquid
Crystal Displays**—R. A. Mao (SSD, Som.) U.
S. Pat. 3653745, April 4, 1972
- Counter**—G. D. Hanchett (SSD, Som.) U. S.
Pat. 3654440, April 4, 1972
- Static Charge Protective Packages for
Electron Devices**—T. W. Kosor (SSD, Som.)
U. S. Pat. 3653498, April 4, 1972

Consumer Electronics

- Brake Apparatus**—N. T. Mirkovic (CE,
Indpls.) U. S. Pat. 3638881, February 1, 1972
- Sample-And-Hold Circuit**—S. A. Steckler
(CE, Som.) U. S. Pat. 3641258, February 8,
1972
- Protection Circuit**—A. L. Limberg, S. A.
Steckler (CE, Som.) U. S. Pat. 3641361, Feb-
ruary 8, 1972

- Transistor Signal Translating Stage**—S. A.
Steckler (CE, Som.) U. S. Pat. 3641448, Feb-
ruary 8, 1972
- Semiconductor Mounting Structure**—R. C.
Owens (CE, Indpls.) U. S. Pat. 3641474, Feb-
ruary 8, 1972
- Toroidal Electromagnetic Deflection Yoke**
—W. R. Chiodo (CE, Indpls.) U. S. Pat.
3643192, February 15, 1972
- Sample-And-Hold Circuit**—A. L. Limberg
(CE, Som.) U. S. Pat. 3646362, February 29,
1972
- Control System**—L. A. Harwood (CE, Som.)
U. S. Pat. 3647940, March 7, 1972
- Kinescope Bias Arrangement to Provide
Both Constant Amplitude D. C. Restoration
Pulses and Arc Discharge Protection**—G.
E. Anderson (CE, Indpls.) U. S. Pat. 3647994,
March 7, 1972
- Remote Controlled Television Tuner Motor
Switching Circuit**—L. B. Juroff, L. M. Lunn
(CE, Indpls.) U. S. Pat. 3648135, March 7, 1972
- High Voltage Hold-Down Circuit**—R. K.
Waltner (CE, Indpls.) U. S. Pat. 3649901, March
14, 1972
- Electronically Tuned Ultra High Frequency
Television Tuner**—D. J. Carlson (CE, Indpls.)
U. S. Pat. 3649937, March 14, 1972
- Electrically Controlled Attenuation and
Phase Shift Circuitry**—A. L. Limberg (CE,
Som.) U. S. Pat. 3649847, March 14, 1972
- Electrical Circuit Providing Multiple V (Sub)
BE Bias Voltages**—A. L. Limberg (CE, Som.)
U. S. Pat. 3651346, March 21, 1972
- Electronically Tuned Ultra High Frequency
Television Tuner with Frequency Tracking
Tunable Resonant Circuits**—J. B. George,
S. E. Hilliker (CE, Indpls.) U. S. Pat. 3641409,
March 21, 1972
- Synchronous Detector Control**—E. J. Witt-
mann (CE, Som.) U. S. Pat. 3651418, March
21, 1972
- Dual Loop Receiver Tuning and Frequency
Tracking System**—L. J. Byers, J. M. Keeth
(CE, Indpls.) U. S. Pat. 3652938, March 28,
1972

Parts and Accessories

- Combined WHF-UHF Dipole Antenna Array**
—D. W. Peterson (P&A, Deptford) U. S. Pat.
3653056, March 28, 1972
- Antenna Rotator**—F. R. DiMeo, N. W. Burwell
(P&A, Deptford) U. S. Pat. 395505, July 27,
1971
- Collapsible Structure to Support Antenna
Elements**—F. R. DiMeo, N. W. Burwell (P&A,
Deptford) U. S. Pat. 3623117, November 1971
- Antenna (Design Pat.)**—F. R. DiMeo, N. W.
Burwell (P&A, Deptford) U. S. Pat. 222358,
October 19, 1971
- Antenna for Radio or Television Service
(Design Pat.)**—D. W. Peterson (P&A, Dept-
ford) U. S. Pat. 222359, October 19, 1971
- Stepper Drive Device**—F. R. DiMeo, N. W.
Burwell, J. D. Callaghan (P&A, Deptford) U.
S. Pat. 3501969, March 24, 1970
- UHF Television Antenna**—J. D. Callaghan
(P&A, Deptford) U. S. Pat. 3573832, April 6,
1971
- National Broadcasting
Company, Inc.**
- Color Phaser for Television Video Signals**
—R. J. Butler (NBC, New York) U. S. Pat.
3647965, March 7, 1972

Dates and Deadlines



As an industry leader, RCA must be well represented in major professional conferences . . . to display its skills and abilities to both commercial and government interests.

How can you and your manager, leader, or chief-engineer do this for RCA?

Plan ahead! Watch these columns every issue for advance notices of upcoming meetings and "calls for papers". Formulate plans at staff meetings—and select pertinent topics to represent you and your group professionally. Every engineer and scientist is urged to scan these columns; call attention of important meetings to your Technical Publications Administrator (TPA) or your manager. Always work closely with your TPA who can help with scheduling and supplement contacts between engineers and professional societies. Inform your TPA whenever you present or publish a paper. These professional accomplishments will be cited in the "Pen and Podium" section of the *RCA Engineer*, as reported by your TPA.

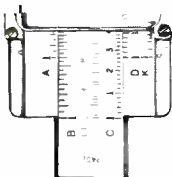
Calls for papers—be sure deadlines are met.

Date	Conference	Location	Sponsors	Deadline Date	Submit	To
SEPT. 24-27, 1972	Technical Ceramics—Control and Analysis	Bellevue Stratford Hotel, Philadelphia, Pa.	ACS	5/1/72 5/15/72 6/1/72	titles abst paper.	Basic Science Robert Ruh Metals and Ceramic Div Air Force Materials Lab Wright-Patterson Air Force Base, Ohio 45433 <i>Electronics</i> John C. Williams Room 1B-321 Bell Telephone Labs., Inc. 600 Mountain Avenue Murray Hill, NJ 07974 <i>Nuclear</i> Jack Belle Westinghouse Electric Corp. Betlis Atomic Power Lab. Box 79 West Mifflin, Pa. 15122
OCT 4-6, 1972	Ultrasonics Symposium	Statler Hilton Hotel, Boston, Mass.	G-SU	6/30/72	abst	L. P. Claiborne Texas Instr., Inc Dallas, Texas
OCT. 9-11, 1972	National Electronics Conference	Regency Hyatt House, Chicago, Illinois	Region IV et al	5/1/72	abst sum	Richard Horton Dept of EE, Iowa State Univ. Ames, Ia. 50010
NOV 1-3, 1972	Northeast Electronics Research & Engineering Meeting (NEREM)	Boston, Mass.	New England Sections	6/30/72	abst & ms	IEEE Boston Office 31 Channing St Newton, Mass. 02158
NOV 9-10, 1972	Canadian Communications & EHV Conference	Queen Elizabeth Hotel, Montreal, Quebec, Canada	Canadian Region, Montreal Section	6/15/72	sum	Dinkar Mukhedkar Ecole Polytechnique 2500 Marie Guyard Montreal 250, PQ, Canada
NOV 13-15, 1972	Conf. on Automatic Support Systems for Advanced Maintainability	Holiday Inn Phila., Pa.	G-AES Phila. Section	5/15/72	sum	Fred Liguori, Naval Air Engrg. Ctr., Phila., Penna 19112
NOV. 13-16, 1972	Fall Joint Computer Conference	Convention Ctr., Las Vegas, Nev.	S-C, AFIPS	4/3/72	ms	D. A. Meier, 1972 FCC Tech. Program, POB 835, Hawthorne, Calif. 90250
DEC. 6-8, 1972	Vehicular Technology Conference	Dallas, Texas	G-VT	6/30/72	sum	IEEE Headquarters 345 East 47th Street New York, NY 10017
JAN 28- FEB 2, 1973	IEEE Power Engineering Society Winter Meeting	Statler Hilton Hotel, New York, NY	S-PE	9/15/72	ms	J. W. Bean AEP Service Corp. 2 Broadway New York, NY 10004
SEPT. 16-20, 1973	Jt. Power Generation Technical Conference	Marriott Hotel New Orleans, Louisiana	S-PE ASME	5/4/73	ms	L. C. Grudmann New Orleans Public Service, Inc. 317 Baronne St. New Orleans, La 70160
SEPT. 18-21, 1973	Conference on High Voltage Direct Current Transmission	IEE, London, England	IEE, IEEE UKRI Section	5/26/72	syrr	IEE, 2 Savoy Place, London W. C. 2R OBL, England

Dates of upcoming meetings—plan ahead.

DATES AND DEADLINES

Date	Conference	Location	Sponsors	Program Chairman
JUNE 12-13, 1972	Chicago Spring Conf. on Broadcast & Television Receivers	Marriott Motor Hotel, Chicago, Illinois	G-BTR, Chicago Section	Richard Sjudges, Admiral Corp., 3800 Cortland St., Chicago, Illinois 60647
JUNE 12-15, 1972	Design Automation Workshop	Staller Hilton Hotel, Dallas, Texas	S-C, ACM, SHARE	H. Freitag, IBM Watson Res. Ctr., POB 218, Yorktown Heights, NY 10598
JUNE 14-16, 1972	1972 Summer Computer Simulation Conference	San Diego, Calif.	AIAA	American Institute of Aeronautics and Astronautics 1290 Avenue of the Americas New York, NY 10019
JUNE 14-16, 1972	AIAA/NABE Seminar—Orienting the Aerospace Industry to Changing Priorities	Los Angeles, Calif.	AIAA	American Institute of Aeronautics and Astronautics 1290 Avenue of the Americas New York, NY 10019
JUNE 18-23, 1972	Symposium on Fatigue at Elevated Temperatures	Univ. of Conn. Storrs, Ct. ASMMS	ASME, ASTM, ASMMS	J. J. Donohue, Mgr. The American Society of Mechanical Engineers United Engineering Center 345 E. 47th St. New York, NY 10017
JUNE 19-21, 1972	International Conference on Communications	Marriott Motor Hotel, Phila. Penna	S-Comm, Phila. Section	A. W. Weinrich, Applied Info Ind., 345 New Albany Rd., Moorestown, NJ 08057
JUNE 19-21, 1972	Int'l Symposium on Fault-Tolerant Computing	Marriott Hotel, Boston, Mass.	S-C, MIT	Gernot Metzger, Coord. Sci. Lab., Univ. of Ill., Urbana, Ill. 61801
JUNE 18-21, 1972	Temperatures (ASTM, ASME)	University of Connecticut Storrs, Ct.	ASME	The American Society of Mechanical Engineers United Engineering Center 345 E. 47th Street New York, NY 10017
JUNE 21-23, 1972	Joint Measurements Conference	Nat'l Bureau of Standards Boulder, Colo.	G-IM et al	P. K. Stein, Arizona State Univ., Tempe, Arizona 85281
JUNE 26-28, 1972	Applied Mechanics Conference	University of California, LaJolla, Ca.	ASME	The American Society of Mechanical Engineers United Engineering Center 345 E. 47th Street New York, NY 10017
JUNE 26-28, 1972	AIAA 5th Fluid and Plasma Dynamics Conference	Boston, Mass.	AIAA	American Institute of Aeronautics and Astronautics 1290 Avenue of the Americas New York, NY 10019
JUNE 26-29, 1972	Conference on Precision Electromagnetic Measurements	Nat'l Bureau of Standards Boulder, Colo.	G-IM, NBS, USNC/URSI	H. S. Boyne, Radio Bldg., Rm. 4075, NBS, Boulder, Colo. 80302
JUNE 27-30, 1972	International Data Processing Conference & Business Exposition	New York Hilton Hotel	DMPA	Data Processing Management Association 505 Busse Highway Park Ridge, Ill. 60068
JULY 4-6, 1972	Conference on Radio Receivers and Associated Systems	Univ. College of Swansea, South Wales	IERE, IEE, IEEE, UKRI Section	IERE, 8-9 Bedford Square, London W.C. 1B 3RG England
JULY 10-11, 1972	CASI/AIAA Meeting: Space—1972 Assessment	Ottawa, Canada	AIAA	American Institute of Aeronautics and Astronautics 1290 Avenue of the Americas New York, NY 10019
JULY 9-14, 1972	IEEE Power Engineering Society Summer Meeting	Fairmont Hotel, San Francisco Calif.	S-PE	W. R. Johnson, Pacific Gas & Elec. Co., 245 Market St., Rm. 1122, San Francisco, Calif. 94106
JULY 10-14, 1972	8th International Symposium on Rarefied Gas Dynamics	Stanford, Calif.	AIAA	American Institute of Aeronautics and Astronautics 1290 Avenue of the Americas New York, NY 10019
JULY 17-19, 1972	AIAA/SNAME/NAVY Advanced Marine Vehicles Meeting	Annapolis, Md	AIAA	American Institute of Aeronautics and Astronautics 1290 Avenue of the Americas New York, NY 10019
JULY 18-20, 1972	Int'l. Symposium on Electromagnetic Compatibility	Arlington Park Towers Hotel Arlington Heights, Illinois	G-EMC, Chicago Section	J. J. Krstansky, IIT Res Inst., 10 W. 35th St., Chicago, Ill. 60616
JULY 24-26, 1972	2nd Urban Technology Conference	San Francisco Civic Center	AICE, AIMMPE, ASME, CSG, IEEE, ICMA, NAC, NGC, NLC, NSPE, SAE, U.S. CM	Philip D. Schaub, AIAA Director of Communications 1290 Avenue of the Americas New York, NY 10019
JULY 24-27, 1972	Conference on Nuclear & Space Radiation Effects	Univ. of Washington Seattle, Wash.	G-NS	B. L. Gregory, Sandia Labs., POB 5800, Albuquerque, New Mexico 87115
JULY 25-27, 1972	Conference on Advances in Marine Navigational Aids	London, England	G-AES, IEEE, UKRI Section, IEE, IERE et al	IEE, Savoy Place, London W. C. 2R OBL, England
AUG. 7-9, 1972	AIAA 4th Aircraft Design, Flight Test, and Operations Meeting	Los Angeles, Calif.	AIAA	American Institute of Aeronautics and Astronautics 1290 Avenue of the Americas New York, NY 10019
AUG. 6-9, 1972	Heat Transfer Conf. (AIChE, ASME)	Brown Place Denver, Col.	ASME	The American Society of Mechanical Engineers United Engineering Center 345 E. 47th Street New York, NY 10017



Vollmer named General Manager, Palm Beach Division

Dr. James Vollmer has been appointed General Manager of the Palm Beach Division by Irving K. Kessler, Executive Vice President, Government and Commercial Systems.

Dr. Vollmer received the BS in General Science from Union College in 1945, the MA and PhD in Physics from Temple University in 1951 and 1956, respectively. In 1971, Dr. Vollmer graduated from Harvard University's Advanced Management Program. His research interests, publications, and patents cover a wide variety of fields, ranging from infrared properties of materials to plasma physics to quantum electronics. His professional experience includes—in order—five years of teaching at Temple University, eight years of supervising a research group at Honeywell and thirteen years of research supervision at RCA. Prior to his promotion, Dr. Vollmer was Director of the Advanced Technology Laboratories. Dr. Vollmer is a Fellow of the AAAS, a Fellow of the IEEE, and a member of the American Physical Society. His honors include membership in Phi Beta Kappa, Sigma Xi, Sigma Pi Sigma and Eta Kappa Nu. He is currently listed in *American Men of Science*, *Who's Who in the East*, and *Leaders in American Science*.

RCA receives contracts totaling \$102 million

The Service Company recently received U.S. Air Force contracts totaling \$102 million for operation and maintenance of the Distant Early Warning System (\$59.8 million) and the Ballistic Missile Early Warning System (\$42.5 million). Both are for fiscal years 1973 through 1975.

Degrees granted

- I. Dague, ATL, Camden PhD in EE, U. of P., 5/22/72
- L. Finn, CS, Cherry Hill Post Masters, EE, N.Y.U., 1/72
- J. Northrop, ITD, Lancaster MS, Applied Statistics, Villanova, 12/71



Paul Wright to head Advanced Technology Laboratories

Paul E. Wright has been appointed Director of Advanced Technology Laboratories by Dr. Harry Woll, Vice President of Government Engineering.

Mr. Wright received the BSME from California State Polytechnic College and the MSME from the University of Pennsylvania. He served in the U.S. Air Force from 1950 to 1954, and was an engineer with the State of California from 1954 to 1958. He joined RCA in 1958. Prior to his promotion, Mr. Wright was Manager of the Applied Physics and Mechanics Laboratory at ATL. As Director, Mr. Wright is responsible for

over 100 engineers and physicists charged with translating the recent advances of basic research into useful techniques and devices. Typical areas of effort are electro-optics, optics, lasers, millimeter waves, microwave physics, holography, sensors, microsonics, thermodynamics, pattern recognition, recording techniques, LSI hybrid techniques, and computer technology. Mr. Wright is a Registered Professional Engineer in New Jersey. He is a member of the National Society of Professional Engineers, the New Jersey Society of Professional Engineers, the ASME and the IEEE.

Licensed engineers

When you receive a professional license, send your name, PE number (and state in which registered), RCA division, location, and telephone number to: RCA Engineer, Bldg. 2-8, RCA, Camden, N.J. As new inputs are received they will be published.

Aerospace Systems Division

M. D. Brazet, ASD, Burlington, Mass. PE-25738; Massachusetts

Global Communications Inc.

S. L. Latargia, GlobCom, New York, PE-19151; New Jersey

Communication Systems Division

J. W. Seymour, GCS, Phoenix, Arizona, PE-8340; Arizona; PE-14609; New Jersey; PE 012479 E; Pennsylvania

RCA Review, March 1972

Volume 33, Number 1

Contents

Special Issue on optical storage and display media

Foreword	Juan J. Amodei
Holographic Information Storage	E. G. Ramberg
Materials for Magneto-Optic Memories	R. W. Cohen R. S. Mezrich
Holographic Recording in Lithium Niobate	J. J. Amodei D. L. Staebler
Optical and Holographic Storage Properties of Transition Metal Doped Lithium Niobate	W. Phillips J. J. Amodei D. L. Staebler
Phase Holograms in Dichromated Gelatin	D. Meyerhofer
Redundant Holograms	A. H. Firester E. C. Fox T. Gayeski W. J. Hannan M. Lurie
Wavelength Dependent Distortion in Fraunhofer Holograms and Applications to RCA Holotape	R. A. Bartolini D. Karlsons M. Lurie
Recording Considerations for RCA Holotape	R. A. Bartolini J. Bordogna D. Karlsons
Thermoplastic Media for Holographic Recording	T. L. Credelle F. W. Spang
Recyclable Holographic Storage Media	J. Bordogna S. A. Keneman J. J. Amodei
Erase-Mode Recording Characteristics of Photochromic CaF ₂ , SrTiO ₃ and CaTiO ₃ Crystals	R. C. Duncan, Jr.
High Contrast, High Sensitivity Cathodochromic Sodalite for Storage and Display Applications	R. W. Faughnan I. Shidlovsky
Liquid Crystals for Electro-Optical Application	J. A. Castellano

The RCA Review is published quarterly. Copies are available in all RCA libraries. Subscription rates are as follows (rates are discounted 20% for RCA employees)

	DOMESTIC	FOREIGN
1-year	\$6.00	\$6.40
2-year	10.50	11.30
3-year	13.50	14.70

Promotions

Solid State Division

J. Litus, Jr. from Assoc. Engr., Product Devel. to Leader Technical Staff (D. R. Carley, Somerville)

D. Baugher from Leader Technical Staff to Manager Application Engineering Power Transistors (C. R. Turner, Somerville)

R. Denning from Leader Technical Staff to Manager Design Engineering Power Transistors (C. R. Turner, Somerville)

Entertainment Tube Division

W. J. Harrington from Mgr., Production Engineering Color Picture Tube to Mgr. Manufacturing Process and Equipment Engineering (S. S. Stefanski, Lancaster)

Industrial Tube Division

R. L. Rodgers, Engr., Product Development to Engineering Ldr., Product Development (E. D. Savoye, Lancaster)

RCA Service Company

W. C. Clair from Sys. Service Engr. to Ldr., Sys. Service Engineers (G. L. Beden, Proj. Support Operations, Camden)

Astro-Electronics Division

R. D. Smith from Engrg. Scientist Technical Staff to Mgr. Software Development Engrg. (A. Aukstikalnis, Hightstown)

Electromagnetic and Aviation Systems Division

W. J. Davis from Staff Engrg. Scientist, Government Engineering Dept. to Mgr., Data Processing Engrg. (R. H. Aires, Van Nuys)

Staff announcements

Robert W. Sarnoff, Chairman of the Board and Chief Executive Officer, announced the assignment of **Charles R. Denny**, Executive Vice President, Washington. **Samuel E. Ewing** will be on special assignment to the Washington office until his retirement August 1.

Anthony L. Conrad, President, has announced that **Irving K. Kessler**, Executive Vice President, Government and Commercial Systems, will assume responsibility for the Palm Beach Gardens, Florida, facility.

Palm Beach Division

Irving K. Kessler, Executive Vice President, Government and Commercial Systems, has announced the appointment of **James Vollmer** as General Manager, RCA Palm Beach Division.

Electronic Components

John B. Farese, Executive Vice President, Electronic Components, has appointed **Fred M. Bauer** Division Vice President, Finance.

Entertainment Tube Division

Matthew M. Bell, Manager, Equipment Engineering, Circleville Plant, Manufacturing, has announced the following appointments: **Frederick L. Armstrong**, Engineering Leader, Equipment Engineering; **Braudice B. LeMay**, Engineering Leader, Development Engineering; **Richard W. Marshall**, Engineering Leader, Control Equipment.

Charles T. Lattimer, Manager, Product Engineering, Circleville Plant Manufacturing has announced the organization of Product Engineering as follows: **Richard N. Haigh**, Manager, Funnel Engineering; **James Millar**, Manager, Mold Design and Development; **Robert K. Schneider**, Manager, Mix and Melt Engineering; **Alan M. Trax**, Manager, Panel Engineering.

Industrial Tube Division

Ralph E. Simon, Manager, Electro-Optics Products Operations, has announced his organization as follows: **Charles W. Biral** continues as Manager, Camera Tube Operation; **Clarence A. Groah** continues as Manager, Electro-Optics Products Administration; **Robert C. Pontz** is appointed Manager, Photo Tube and Solid State Opto-Electronics Operation; **Eugene D. Savoye** continues as Manager, Advanced Technology; and **James A. Zollman** is appointed Manager, Image and Display Tube Operation.

Robert C. Pontz, Manager, Phototube and Solid State Opto-Electronics Operation, announces his organization as follows: **Richard Glicksman**, Manager, Solid State Opto-Electronics; **Stanley Katz**, Engineering Leader, Product Development (Opto-Electronics); **Andrew G. Zourides**, Engineering Leader, Product Development (Opto-Electronics); **Harold R. Krall**, Manager, Electro-Optics Systems; **Thomas T. Lewis**, Engineering Leader, Product Development (Phototube Applications); **Dennis E. Persyk**, Engineering Leader, Product Development (Phototubes); **Robert C. Pontz**, Acting Manager, Adept and Phasor Development; **Kenneth A. Thomas**, Manager, Photo Tube Manufacturing.

James A. Zollman, Manager, Image and Display Tube Operation, has announced his organization as follows: **Robert W. Fitts**, Manager, Image Tube Manufacturing and Production Engineering; **Fred A. Helvy**, Manager, Image and Display Tube Design Engineering; **Wayne E. Rohland**, Manager, Display Tube Manufacturing and Production Engineering; and **James A. Zollman**, Acting Manager, Image and Display Tube Applications.

Eugene D. Savoy, Manager, Advanced, has appointed **Robert L. Rodgers** Engineering Leader, Product Development (Silicon Technology).

RCA Institutes, Inc.

John W. Wentworth, Director, Operations, has announced his organization as follows: **Marshall M. Carpenter, Jr.**, Director, Professional Educational Services; **James D. Daras**, Director, Custom Education; **Murray R. Dick**, Director, Studio School; **Lester Dittersdorf**, Director, Home Study School and

Marketing; **John J. McCoid**, Manager, Industrial Relations; **F. Robert Michael**, Director, Educational Projects Development; **Lewis W. Snow**, Director, RCA Technical Institute; **N. Michael Terzian**, Director, Resident School; and **Thomas J. Wheeler**, Treasurer and Controller.

Government and Commercial Systems

Irving K. Kessler, Executive Vice President of Government and Commercial Systems announced the appointment of **Max M. Tall**, Director, Government Product Assurance.

Aerospace Systems Division

John R. McAllister, Division Vice President and General Manager, Aerospace Systems Division, has appointed **George A. Earle, Jr.**, Director, Marketing.

Astro-Electronics Division

C. S. Constantino, Division Vice President and General Manager, has announced the appointment of **Philip J. Martin** as Director, Marketing and Advanced Planning.

Communications Systems Division

James M. Osborne, Division Vice President, Government Communications Systems, has announced the appointment of **Francis H. Stelter, Jr.**, as Director, Marketing.

Electromagnetic and Aviation Systems Division

Frederick H. Krantz, Division Vice President and General Manager, has appointed **Carl J. Cassidy** as Director, Government Marketing.

John P. Mollema, Manager, Marketing, Aviation Equipment Department, has announced the appointment of **John K. Nims** as Manager, Marketing Planning and Services and **Curtis H. Roberts** as Manager, Domestic General Aviation Sales, for RCA's Aviation Equipment Department.

Research and Engineering

Jerome Kurshan, Manager, Marketing, has announced the appointment of **William J. Dennehy** as Manager, Market Development.

Laboratories

George D. Cody, Director of the Physical Electronics Research Laboratory, has announced the following appointments: **Juan J. Amodei**, Head of Quantum Electronic Research, and **Rabah Shahbender**, Head of Applied Electronics Research.

Solid State Division

William C. Hittinger, Vice President and General Manager of Solid State Division, has announced the following appointments: **Ralph S. Hartz** as Manager, Packaged Circuit Functions and **A. F. Liersch** as Manager, Market Research and Planning.

RCA Service Company

Joseph F. Murray, Division Vice President, Government Services has announced the appointment of **John J. Connors** as Division Vice President of Government Services Marketing.

Awards

Missile and Surface Radar Division

The following engineers received technical excellence awards for their performance during the fourth quarter of 1971. They were cited for their contributions as follows:

S. Batterman defined and documented the requirements and design of the SPY-1 control programs for AEGIS. He developed the computer program and system functional interrelationships for SPY-1, defined and documented the allocation of computer program functions to subprograms, provided both technical direction and system consultation for several design teams, and served as coordinator and major contributor for both the EDM-1 SPY-1 control computer program performance and design requirement specifications.

A. G. Chressanthis is cited for his work, on the small ship study for the SPY-1 of AEGIS. The study presented a simplified, low-cost, smaller version of the present SPY-1 signal processor to facilitate emplacement aboard a presently available ship. Mr. Chressanthis, the key individual in the signal processing area, considered all conceptual and implementation aspects of the signal processor in arriving at a smaller processor which retained most of the basic characteristics of the present signal processor.

R. L. Stegall developed the system concept and configuration of the digital instrumentation radar. This represents the first successful attempt at configuring an instrumentation radar which will sell at a comparatively low cost, yet satisfy the needs of many of the test ranges. This proposed design fills out the lower end of our range instrumentation product line, and shows promise of production similar to the FPS-16 radar. A contract for several systems is expected about mid 1972.

O. M. Woodward conceived, developed, modified, and proved the design of an antenna type which is to be used on the Viking Mars Lander Program. As a type, it will be used to satisfy two antenna requirements: One at 400 MHz and the other at 2200 MHz. This design is a major improvement over the proposal concepts in terms of cost, performance, weight, reliability, and commonality.

O. M. Woodward also was selected as the 1971 Annual Technical Excellence Award for his outstanding performance throughout the year.

Aerospace Systems Division

Richard J. Murray won Second Prize in the exploded view competition of the Ninth Annual Technical Art Exhibit, sponsored by Boston's Museum of Science and the Technical Art Group of the Society for Technical Communication. The exhibit encompasses a broad range of industrial, scientific, medical and other technically oriented artwork and photography.

In addition to participating in the Exhibit and Awards Banquet, Mr. Murray will be invited to display his artwork at the 11th

International Technical Communications Conference of the Society for Technical Communication to be held in Houston in 1973.

J. B. Fuller was selected as Engineer of the Month for January 1972 for his outstanding performance during integration and test of the PDR and in field support and successful flight testing of the system on a B-52G aircraft.

The team of **H. L. Fischer, R. E. Hartwell, L. M. Hill, V. G. Hillard, B. W. Jackson, E. G. Lauginger, R. A. Lindley, A. G. Olsson, and A. G. Vallance** received the technical excellence team award for January 1972. The Automated Test System for Jet Engine Accessories (ATSJEA) developed by this team is the world's first automatic mechanical-hydraulic tester for jet engine accessories. The system was designed so that a total of forty stands can eventually be driven by the same central computer, plus four more mini-computers. This accomplishment has placed RCA in an excellent position for growth in the non-electronic test area.

George J. Lamonakis of System Design Support was selected as Engineer of the Month for February 1972. Mr. Lamonakis designed and built a shock facility to provide 1000-g, 6-ms, half-sine capability to support ASD's special sensor product line, and to continue to provide shock capability for other product lines (typically 15g, 11ms).

The team of **Donald F. Dion, John J. Klein, Hugo Logemanf, Jr., George S. Pearce, and George J. Sandorfi** from Radiation Systems Engineering received the technical excellence team award for February 1972. The team successfully modified and rebuilt the high-resolution 2-inch RBV camera on a quick-reaction program. Verification of the circuits and layouts on boards to be improved had to be accomplished with minimum interference to tests underway.

The team of **R. N. Piscatelli** from System Programming and **A. C. Spear** from System Engineering received the technical excellence team award for March 1972. This team developed a fully operable design-automation printed-circuit-board system within 12 months. All milestones were met or exceeded with trial EQUATE and Model 215 boards processed in December.

Larry B. Blundell of Radiation Systems Engineering was selected as Engineer of the Month for May 1972. His work on the design of a phase-lock-loop for a critical system resulted in equipment which met the specification during bench tests and performed well in the field.

The team of **E. M. Fisher, A. H. Frim, H. C. Hale, J. Harrison, E. M. O'Brien, A. G. Olsson, R. C. Plaisted, J. Salvato, F. A. Schwedner, J. A. Shay, and E. M. Sutphin** from Automatic Test Equipment Engineering received the technical excellence team award for May 1972. Within three months after contract award, the RCA Data Bus System group (under **R. J. Monis**) designed, fabricated, tested and shipped a complete operational Data Bus System to the NASA Manned Spacecraft Center for subsequent integration in the Space Shuttle program.

Communication Systems Division

Donald A. McClure of Communications Equipment Engineering, Government Communication Systems, is the recipient of the first technical excellence award of 1972. He is being recognized for his outstanding performance as the lead transmitter engineer on the Coherent Synthetic Aperture Radar (CSAR) Program. Mr. McClure made a significant contribution to the successful proposal, providing the design descriptions of the VHF and HF transmitters, and costing the design effort. Subsequent to the program award, he was responsible for the initial development of the VHF transmitter, and designed, breadboarded, and proved out the HF transmitter.

Electromagnetic and Aviation Systems Division

Two EASD engineers recently received "Engineering Merit Awards" from the San Fernando Valley Engineers' Council. The Council consists of sixteen technical societies representing more than 4,000 engineers; it recognized only 11 individuals for merit awards in 1972.



Fred Krantz, Division Vice President and General Manager, EASD, with Maureen Schmidt and George Lucchi at awards ceremony.

George Lucchi, Manager, Aviation Equipment Engineering, was honored for "Significant Contributions to Engineering a Better Tomorrow Through Technology in the Field of Flight Safety and Navigation."

Mr. Lucchi is recognized as a leader in general avionics. He holds five patents which have advanced the state of the art in weather radar, distance measuring equipment, and air traffic control transponders. He has been a key element in expanding RCA's commercial avionics from a single product to a wide spectrum of aviation equipment.

Maureen R. Schmidt, Senior Member, Engineering Design and Development Staff, assigned to Data Terminals Engineering, was honored for "achievements in software engineering and for significant contributions to the community in conservation and human ecology."

Mrs. Schmidt is recognized as an engineer who combines a high degree of technical professionalism with an active involvement in community affairs. Her memberships in many groups result in her enthusiastic participation in efforts to improve the environment as well as to simulate interest and activity in preserving our cultural heritage.

Professional activities

Corporate Engineering Services

A. R. Trudel was elected to the Board of Directors of the American National Standards Institute.

RCA Laboratories

S. F. Dierk has been appointed to the American National Standards Institute subcommittee (Z-39-SC/32) dealing with technical report numbering.

Government and Commercial Systems

Nicholas Pensiero was named to the New Jersey State Chamber of Commerce Public Relations Advisory Committee.

Electromagnetic and Aviation Systems Division

M. E. Collins was elected as a Fellow of the American Society for Quality Control. His citation reads: "In recognition of professional services rendered to the national defense program and for significant contributions to the quality control profession as a whole." Mr. Collins is presently a member of the Work Elements Committee of the national ASQC. He is also a member of the Executive Advisory Board and past-chairman of the Los Angeles Section of ASQC.

Astro-Electronics Division

Bert Sheffield was elected a Director of the Board of Eta Kappa Nu Association, the national electrical engineering honor society. Mr. Sheffield was named to a two-year term on the Board, which directs the activities of some 125 honor society chapters at colleges and universities throughout the United States. Founded in 1904, the society has a membership of more than 50,000 graduate electrical engineers.

Three attorneys admitted to practice

Herbert Jacobson and **William J. Michals**—both members of the Patent Department—have recently passed the New Jersey Bar Examination and were sworn on May 17, 1972 to practice before the New Jersey Supreme Court and the U.S. District Court for the District of New Jersey. **Marvin N. Benn**—also a member of the Patent Department—has passed both the Illinois State Bar and Washington, D.C., Bar examinations and admitted to practice law in May 1972.

Mr. Jacobson received the Juris Doctor degree from the Brooklyn Law School in 1965 and the Master of Laws degree in Trade Regulation from the New York University Graduate School of Law in 1970. Mr. Jacobson is also a member of the New York Bar and admitted to practice before the Supreme Court of the United States. He received the

BSEE from the University of Rhode Island in 1961. He joined the RCA Patent Staff in January, 1971.

Mr. Benn received the Juris Doctor degree from the University of Illinois in June 1971, the Masters in Engineering administration from Southern Methodist University, and the BSEE from the University of Illinois in 1966. He joined the RCA Patent Staff in September 1971.

In addition, **Dennis H. Irlbeck**, having been admitted to practice before the United States Patent Office and to membership in the New Jersey State Bar, has been appointed to the position of Patent Counsel.

Patents and Licensing holds annual meeting

The Annual Patents and Licensing Meeting was held at the Host Corral, Lancaster, Pa., on January 18-21. This meeting provided a forum for informal discussions of both departmental and interdepartmental problems related to Patents Operations, Domestic Licensing, and International Licensing. A new addition to this year's program was the discussion of a topic which had been formulated by each department. Each topic was first discussed by small groups having representation from each department. The conclusions were then presented by the chairman to a combined meeting of all participants.

Benjamin Abeles, Richard Williams, and J. Guy Woodward named Fellows of RCA Laboratories.

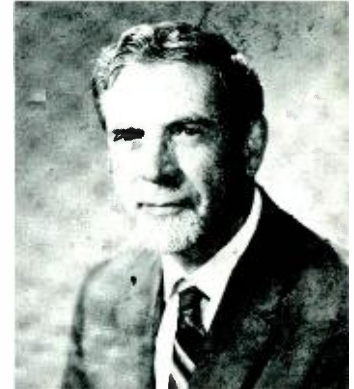
Dr. Benjamin Abeles, Dr. Richard Williams and **Dr. J. Guy Woodward** have been named Fellows of the Technical Staff of RCA Laboratories in Princeton, N.J. The Fellow designation is comparable to the same title used in universities and technical societies. It is given by RCA in recognition of a record of sustained technical contributions in the past and in anticipation of continued technical contributions in the future.



Dr. Abeles has done distinguished research in the fields of galvanomagnetic effects, thermoelectricity, microwave phonons, and superconductivity. A graduate of the University of London in 1944, he received a Master's degree from Charles University in Prague in 1949 and the PhD in Physics from Hebrew University in Jerusalem in 1956. Since joining RCA Laboratories as a trainee in 1956, he has received three RCA Laboratories Achievement Awards. And in 1963, he received the Corporation's highest technical honor, the David Sarnoff Award in Science. He is a Fellow of the American Physical Society and a member of the executive committee of the Division of Solid State Physics.



Dr. Williams has performed outstanding research on the electrical properties of insulators, internal photoemission, solid surfaces, high electric fields in solids, liquid crystals and electrons on the surface of liquid helium. He was graduated from Miami University (Ohio) in 1950 and received the PhD in Physical Chemistry from Harvard in 1954. He joined RCA Laboratories in 1958 and has since received two RCA Laboratories Achievement Awards and a David Sarnoff Award in Science. In 1969, he was a Fulbright Lecturer in the Escola de Engenharia, São Carlos, Brazil. Dr. Williams is a member of Phi Beta Kappa and a Fellow of the American Physical Society.



Dr. Woodward has distinguished himself in research on stereophonic sound reproduction, phonographic and magnetic tape recording, high resolution magnetic recording heads, and in the improvement of the quality and information storage capacity of disk recording systems. He was graduated from North Central College in 1936. He received the MS from Michigan State College in 1939 and the PhD in Physics from Ohio State in 1942. Dr. Woodward was recently installed as President of the Audio Engineering Society, and in 1968 received the Society's Emile Berliner Award. He is a Fellow of the Acoustical Society of America, the IEEE, and the Audio Engineering Society.

Woolley is TPA for Palm Beach Division

Phil Woolley has been appointed Technical Publications Administrator for the Palm Beach Division, Palm Beach Gardens, Fla. In this capacity, Mr. Woolley is responsible for the review and approval of technical papers; for coordinating the technical reporting program; and for promoting the preparation of papers for the *RCA Engineer* and other journals, both internal and external.



Mr. Woolley received the BS in Naval Science and the BSEE, both from Duke University. He joined the RCA Specialized Trainee program and in 1948 was assigned to Components Engineering in the Tube Division, Camden, N.J. In 1951, he joined the Resident Engineering Activity in Bloomington (Home Instruments). In 1952, he transferred to RCA in Cambridge. There he assisted in establishing a Resident Engineering function to support the design of record changer mechanisms and hi-fi, stereo, radio and tape instruments. In 1960 he moved to EDP in Palm Beach as a member of the Technical Staff. He is presently Manager of Packaging and Power Systems.

O'Donnell is EdRep for Industry Systems



J. J. O'Donnell has been appointed Editorial Representative for Industry Systems, Aerospace Systems Division, Marlboro, Mass. Mr. O'Donnell is responsible for planning and processing articles for the *RCA Engineer* and for supporting the Corporate-wide technical papers and reports program.

Mr. O'Donnell received the BSEE from Villanova University in 1949. From 1949 to 1955, he worked in the field of Pilotless aircraft development. He joined the RCA's Electronic Products Division in 1955 in the Components Group of Standards Engineering. In 1960, Mr. O'Donnell joined the Electronic Data Processing Division where had responsibilities for design and development on the 301, 601, 3301 Systems. At the start of the Spectra Systems, Mr. O'Donnell was assigned as Manager of Packaging, Power Supply, and Standards Engineering. In 1971, he was appointed as Manager, Technical Services for Industry Systems.

Rearick is TPA for Parts and Accessories

Charles C. Rearick has been appointed Technical Publications Administrator for RCA Parts and Accessories, Deptford, N.J. In this capacity, Mr. Rearick is responsible for the review and approval of technical papers; for coordinating the technical reporting program; and for promoting the preparation of papers for the *RCA Engineer* and other journals, both internal and external.



Mr. Rearick joined RCA in 1956, having graduated that year from the University of Maine with the BSEE. He completed the engineering training program and then served two years of military service as an army lieutenant. He returned to the Home Instrument Division engineering labs at Cherry Hill, where he became responsible for the acoustical and audio performance of the TV product line. After one year with the M&SR Division, he transferred to the Camden plant where he participated in various audio, digital signal processing and magnetic recording projects. In 1969 he transferred to his present position as the engineer responsible for the design and approval of the Parts and Accessories Division's New Product Marketing activity. This activity is responsible for the investigation of all potential commercial product ideas not presently being developed or marketed by any other branch or division of RCA. He received his MS in Engineering for Graduate Work in Electrical Engineering from the University of Pennsylvania in 1969.

RCA Engineer binders available

Wire-rod-type, brown, simulated-leather binders are available for binding back issues of the *RCA Engineer*. The binders are $9\frac{1}{4} \times 12 \times 3\frac{1}{4}$ and will hold about 10 issues each. The magazines are held in place by wire rods (supplied) that run along the center fold of the magazine and snap in place (no need to punch holes or otherwise mutilate the issue). These binders may be ordered directly for two-week delivery as follows: Order by stock number and description exactly as below: make check or money order payable directly to the vendor, and specify method of shipment:

Binder, rod type, 358-34,
price \$3.92 each.

Order from:

Mr. Schaffer, A. Pomerantz & Co.
1525 Chestnut St., Philadelphia, Pa.
Phone: 215 LO-86116

DiMauro and Silverstein are new EdReps for Solid State Division

Joseph DiMauro and Seymour Silverstein have been appointed Editorial Representatives for the Solid State Division. Editorial Representatives are responsible for planning and processing articles for the *RCA Engineer*, and for supporting the corporate-wide technical papers and reports program. Mr. DiMauro will represent the Mountaintop plant and Mr. Silverstein will cover the Power Transistor operation in Somerville.



Mr. DiMauro received the BME from the Polytechnic Institute of Brooklyn and the MBA from Wilkes College. He joined Electronic Components as an Equipment Development Design Engineer at the Harrison plant. He later transferred to Somerville where he was a Manufacturing Engineer and an Engineering Writing Specialist. He joined Mountaintop as a Manufacturing Engineer, advancing to Engineering Leader and then to his present position of Manager, Quality Assurance. Mr. DiMauro is a licensed Professional Engineer in Pennsylvania and New Jersey.



Mr. Silverstein received the BSME from City College of New York in 1951 and the BSEE from the same college in 1956. He received the MS in Management Science from Stevens Institute of Technology in 1965. Mr. Silverstein joined RCA in 1951 as a Trainee. He joined the Semiconductor Division in 1952 and was assigned to the Development Shop in Harrison. He later transferred to Somerville, where he has developed, refined, and optimized device processes prior to their transfer to the factory. Mr. Silverstein transferred to the Semiconductor Model Shop in 1959, where he gained extensive knowledge in the pilot production devices. He was promoted in 1961 to Design Engineer and was assigned to the Industrial Design group of the Semiconductor Division. Mr. Silverstein is now a senior member of the technical staff in Power Transistor Design. In 1969, he was the recipient of an RCA Achievement Award for his work in developing the Versawatt plastic transistor package. Mr. Silverstein holds one patent on processes for semiconductor devices.

Index to RCA Engineer Volume 17

This index covers Vol. 17-1 (June-July 1971), 17-2 (Aug.-Sept. 1971), 17-3 (Oct.-Nov. 1971), 17-4 (Dec. 1971-Jan. 1972), 16-5 (Feb.-Mar. 1971), and the present issue, 17 (April-May 1971). Since *RCA Engineer* articles are also available as reprints, the reprint number (PE-000) is noted throughout. *RCA Engineer* papers are also indexed along with all other papers written by the RCA technical staff in the annual *Index to RCA Technical Papers*.

Subject Index

Titles of papers are permuted where necessary to bring significant keyword(s) to the left for easier scanning. Authors' division appears parenthetically after his name.

SERIES 100 BASIC THEORY & METHODOLOGY

110 Earth & Space Sciences

... geology, geodesy, meteorology, atmospheric physics, astronomy, outer space environment, etc.

OPTICAL PROPERTIES of Water in Situ, Measuring—Dr. L. E. Mertens, W. H. Manning, Jr. (Sv.Co. Fla) 17-2 RCA Reprint Booklet. *RCA Optics*, PE 535

125 Physics

... electromagnetic field theory, quantum mechanics, basic particles, plasmas, solid-state, optics, thermo-dynamics, solid mechanics, fluid mechanics, motion, acoustics, etc.

see also 105 CHEMISTRY
205 MATERIALS (ELECTRONIC)
270 MATERIALS
(Mechanical)

OPTICS AND ELECTRON OPTICS as Competitive and Complementary Technologies—Dr. E. G. Ramberg (Labs, Pr) 17-2 RCA Reprint Booklet. *RCA Optics*, PE 535, PE 539

130 Mathematics

... basic & applied mathematical methods
see also 140 CIRCUIT & NETWORK
THEORY
370 COMPUTER PROGRAMS
(SCIENTIFIC)

MONTE CARLO TECHNIQUES for use in Upper Atmosphere Problems—R. R. McKinley, S. M. Siskind, Dr. G. K. Bienkowski (AED, Pr) 17-5 RCA Reprint RE-17-5-4

150 Environmental & Human Factors

... influence of physical environment and/or human users on engineering design; life support in hostile environments

HUMAN ROLE in Command and Control Systems of the 70's, The—B. Patrusky (CSD, Camden) 17-1 RCA Reprint Booklet Government Engineering, PE 532

160 Laboratory Techniques & Equipment

... experimental methods & equipment, lab facilities, testing, data measurement, spectroscopy, electron microscopy, dosimeters.

TRIBOELECTRIC MEASUREMENTS, Procedure for Making—E. C. Giaino, Jr. (Labs, Pr) 17-1 RCA Reprint PE 523

170 Manufacturing & Fabrication

... production techniques for materials, devices, & equipment
see also 175 RELIABILITY, QUALITY CONTROL, & STANDARDIZATION

CENTRAL COMPUTER SYSTEM a Manufacturing Cost Saver—S. V. Cianfrone (CS, PBG) 17-4 RCA Reprint RE-17-4-6

CHIP COLLECTION, Drilling—M. Novick (AED, Pr) 17-2 RCA Reprint Booklet. *Government Engineering*, PE 532

DETERMINING MANPOWER for Inprocess Inspection by use of Queuing Theory—J. Davin (CE, In) 17-4 RCA Reprint RE-17-4-11

HYBRID PACKAGING for High Performance—H. Fenster (SSD, Som) 17-4 RCA Reprint RE 17-4-16

JOINING OPERATION for Ceramic Circuits—State of the Art—E. R. Skaw (CE, In) 17-1 RCA Reprint RE 17-1-9

PACKAGING CONCEPTS for Beam-Lead Devices—A. S. Rose, W. D. Bailey, H. Fenster, W. J. Greig (SSD, Som) 17-3 RCA Reprint RE-17-3-15

PHOTOMASK RESOLUTION, Optical and Mechanical Limits of—H. Hook (Labs, Pr) 17-6 RCA Reprint 17-6-17

PRINTING INKS, Rheological Properties of—Y. H. Wang (CE, In) 17-1 RCA Reprint 17-1-8

THERMAL RESISTANCE of Integrated Circuits, New Techniques for Measuring—J. P. Lintz (CS, PBG) 17-5 RCA Reprint 17-5-22

175 Reliability, Quality Control, & Standardization

... value analysis, reliability analysis, standards for design & production, etc.
170 MANUFACTURING & FABRICATION
325 CHECKOUT, MAINTENANCE, & USER SUPPORT

METRICATION—C. P. Kocher (R&E, Camden) 17-5 RCA Reprint RE-17-5-6

RELIABILITY Engineering, Trends in—V. Lukach (SSD, Som) 17-4 RCA Reprint 17-4-3

SUBMITTING TO UL for Safety—D. K. Obenland, F. E. Korzekwa (CE, In) 17-4 RCA Reprint RE-17-4-9

180 Management & Business Operations

... organization, scheduling, marketing, personnel

BUSINESS AND LONG RANGE PLANS, Basic Time-Sharing Programs for—R. R. Lorentzen (EC, Hr) 17-4 RCA Reprint RE 17-4-22

DESIGN ENGINEERING All the Way—J. L. Hathaway (NBC, NY) 17-5 RCA Reprint RE-17-5-10

ENGINEERING ETHICS and the Consumer—Dr. James Hillier (R&E, Pr) 17-4 RCA Reprint RE 17-4-23

INSIDE ROMANIA, 1970—Dr. J. I. Pankove (Labs, Pr) 17-1 RCA Reprint PE 527

INVENTOR and His Patent Attorney "Why Didn't You Ask Me?"—J. D. Lazar (P&L, Pr) 17-1 RCA Reprint PE 524

LABORATORIES RCA LTD—A Profile—R. F. Holtz (Labs, Zurich) 17-2 RCA Reprint Booklet. *RCA Optics*, PE 535

PROFESSIONAL SOCIETIES, The Engineer and—I. M. Seideman (AED, Pr) 17-3 RCA Reprint RE 17-3-21

RCA Part V—The Years 1966-1971—Dr. J. Hillier (R&E, Pr) 17-1 RCA Reprint Booklet. *Five Historical Views*, PE-534

RCA SHAREHOLDERS—1971, Address to—R. W. Jarrico (Corp., NY) 17-1 RCA Reprint RE 17-1-2E

READERSHIP SURVEY, Fourth RCA Engineer—P. C. Farbro (Corp., NY) 17-2 RCA Reprint RE 17-2-17

RESEARCH CONFERENCE, MIT-RCA—W. O. Hadjock (R&E, Camden) 17-1 RCA Reprint PE-544

RESEARCH, The Five Hats of—J. Hillier (R&E, Pr) 17-6 RCA Reprint 17-6-18

SOCIETY? Engineers: What Can You do for—Dr. G. H. Brown (P&L, Pr) 17-1 RCA Reprint Booklet. *Government Engineering* PE-532, PE 525

SOLID-STATE TECHNOLOGY CENTER—Purpose and Plans—R. Engelbrecht (SSD, Som) 17-3 RCA Reprint RE 17-3-18

SOLID STATE: Where It's Been and Where It's Headed—W. C. Hittinger (SSD, Som) 17-2 RCA Reprint PE 549

SERIES 200 MATERIALS, DEVICES, & COMPONENTS

205 Materials (Electronic)

... preparation & properties of conductors; semiconductors; magnetic, electro-optical, recording, & electro-magnetic materials
see also 270 MATERIALS
(MECHANICAL)
105 CHEMISTRY
125 PHYSICS
160 LABORATORY TECHNIQUES & EQUIPMENT
170 MANUFACTURING & FABRICATION

INSULATING FILMS, Breakdown Measurements of—Dr. J. E. Carnes, Dr. M. T. Duffy, Dr. C. W. Mueller (SSD, Som) 17-3 RCA Reprint PE 537

MATERIALS AND PROCESSES LABORATORY—Dr. J. A. Amick (SSD, Som) 17-3 RCA Reprint RE 17-3-11

PHOTOCHROMIC AND CATHODOCHROMIC Recording Materials, Inorganic—R. C. Duncan, Jr., Dr. B. W. Faughnan, Dr. W. Phillips (Labs, Pr) 17-2 RCA Reprint Booklet. *RCA Optics*, PE 535, PE 538

SINGLE CRYSTALS and Thin Films, Preparation of—B. Curtis, J. Kane, H. Lehmann, H. von Philipsborn, R. Widmir (RCA Ltd, Zurich) 17-3 RCA Reprint 17-3-19

210 Circuit Devices & Microcircuits

... electron tubes & solid-state devices (active & passive); integrated, array, & hybrid microcircuits; molecular circuits; resistors & capacitors; modular & printed circuits; circuit interconnection; waveguides & transmission lines; etc.
see also 220 ENERGY & POWER SOURCES
205 MATERIALS (ELECTRONIC)
225 ANTENNAS & PROPAGATION
215 CIRCUIT & NETWORK DESIGNS

BEAM-LEAD COS/MOS Integrated Circuit—L. A. Murray, B. W. Richards (SSD, Som) 17-3 RCA Reprint RE 17-3-8

CAPACITORS for Ceramic Integrated Circuits—J. H. Shelby (CE, In) 17-1 RCA Reprint RE 17-1-10

CERAMIC CIRCUIT PRODUCTION, The Use of Small Computers for—C. A. Brombaugh, M. Oakes, J. W. Stephens, L. L. Tretter (CE, In) 17-1 RCA Reprint RE-17-1-6

CERAMIC INTEGRATED CIRCUIT Development—R. D. Snyder, J. W. Stephens (CE, In) 17-1 RCA Reprint RE-17-1-5

COMPUTER MICROELECTRONICS Resident Facility—D. E. Kowalik (CS, PBG) 17-3 RCA Reprint 17-3-2

COS/MOS IC's Offer 25-ns Speed and Direct Interfacing with Saturated Logic, New Low-Voltage—R. E. Funk (SSD, Som) 17-1 RCA Reprint RE 530

ECL DEVICES, Measuring Input Impedance of—R. Au (CS, PBG) 17-4 RCA Reprint RE 17-4-24

FLIP-CHIP SEMICONDUCTOR DEVICES for Hybrid Circuits—B. A. Hegarty (CE, In) 17-1 RCA Reprint RE 17-1-11

LAMINATED OVERLAY POWER TRANSISTORS, High-Voltage—R. Amantea, H. Becke, P. Bothner, J. White (SSD, Som) 17-4 RCA Reprint RE 17-4-2

PIEZOCERAMIC DEVICE Application—P. Nelson (EASD, Van Nuys) 17-2 RCA Reprint Booklet. *Government Engineering* PE 532.

PIN DIODE RF Switch, High Power—D. H. Hurlburt, R. E. Cardinal (RCA Ltd., Mont.) 17-6 RCA Reprint RE 17-6-20

P-MOS TECHNOLOGY for Quick Turn-around Custom LSI—T. R. Mayhew, K. R. Keller, H. Borkan (SSD, Som) 17-4 RCA Reprint RE 17-4-19

POWER TRANSISTORS, Development of Low- and medium-frequency—J. Gaylord, J. Olmstead, Dr. A. Blicher (SSD, Som) 17-3 RCA Reprint RE 17-3-14

PULSE GENERATOR, Gigahertz-Rate Hundred-Volt—K. Kawamoto (Labs, Pr) 17-6 RCA Reprint 17-6-20

RADIATION-RESISTANT COS/MOS Devices—L. A. Murray, Dr. J. M. Smith (SSD, Som) 17-4 RCA Reprint RE 17-4-14

SCHOTTKY BARRIER DEVICES—R. T. Seils (CS, PBG) 17-4 RCA Reprint RE 17-4-10

SCREEN-PRINTED RESISTORS, The Advantages of—T. R. Allington (CE, In) 17-1 RCA Reprint RE 17-1-7

SEMICONDUCTOR IC Technology—H. S. Miller (SSD, Som) 17-3 RCA Reprint RE 17-3-13

SILICON-ON-SAPPHIRE, The Ultimate MOS Technology—E. J. Boleky, Dr. P. A. Crossley, J. E. Meyer, S. G. Policastro, Dr. W. C. Schneider (SSD, Som) 17-3 RCA Reprint RE 17-3-5

THYRISTOR Horizontal Deflection and High-Voltage Circuits—G. Forster (RCA Ltd, Zurich) 17-3 RCA Reprint RE 17-3-19

"VAPODEP"—(EC, Harsn) *RCA Application Note*, L. A. Jacobus, R. H. Brader (SSD, Som) 17-3 RCA Reprint RE 17-3-10

VIDEO AMPLIFIER, Hybrid Microelectric—L. J. Thorpe (CSD, Camden) 17-5 RCA Reprint RE 17-5-18

215 Circuit & Network Designs

... analog & digital functions in electronic equipment; amplifiers, filters, modulators, microwave circuits, A-D converters, encoders, oscillators, switches; logic & switching networks; masers & microwave circuits; timing & control functions; fluidic circuits.

see also: 210 CIRCUIT DEVICES & MICROCIRCUITS
225 ANTENNAS & PROPAGATION
220 ENERGY & POWER SOURCES
140 CIRCUIT & NETWORK THEORY

BIPOLAR/MOS INTERFACE CIRCUIT Design and Technology—H. Beelitz, N. Dirick (SSD, Som) 17-3 RCA Reprint RE 17-3-12

CMOS CUSTOM ARRAYS, Computer-Generated Low-Cost—A. Feller, A. M. Smith, R. Noto, P. W. Ramondetta, R. L. Pryor, J. N. Greenhouse (ATL, Camden) 17-3 RCA Reprint RE 17-3-4

COS/MOS MEMORY ARRAY Design—A. Dingwall, J. Jorgensen, J. Oberman, G. Waas (SSD, Som) 17-3 RCA Reprint RE 17-3-17

COS/MOS MEMORY SYSTEM Design, Low-Power—J. R. Oberman, G. J. Waas (SSD, Som) 17-4 RCA Reprint RE 17-4-1

FLUORESCENT INVERTER, Single-Transistor Regulated—J. C. Sondermeyer (SSD, Som) 17-4 RCA Reprint RE 17-4-24

FREQUENCY COMPARATOR—F. C. Easter (EASD, Van Nuys) 17-5 RCA Reprint RE 17-5-22

INTERPHONE AMPLIFIER, New High Impedance—J. L. Hathaway (NBC, NY) 17-1 RCA Reprint RE 17-1-16

MONOLITHIC APPLICATIONS—Divisional Interface—R. H. Bergman, F. Borgini, L. Dillon, Jr., G. E. Skorup (SSD, Som) 17-4 RCA Reprint RE 17-4-18

PHOTO ALARM Does Double Duty, Simple—J. F. Kingsbury (Labs, Pr) 17-1 RCA Reprint RE 17-1-21

SEMICONDUCTOR ARRAYS FOR Mass Memories—N. D. Reddy, Dr. W. Bosenberg, N. Burton, I. Kalish, L. Pope (SSD, Som) 17-3 RCA Reprint RE 17-3-22

UNIJUNCTION OSCILLATORS With a Bootstrap T_{FL} Output, Classical—R. A. Mancini, G. H. Fairfax (CS, PBG) 17-1 RCA Reprint RE 17-1-21

240 Lasers, Electro-optical, & Optical Devices

... design & characteristics of lasers; components used with lasers in electro-optical systems, lenses, (excludes: masers).

see also: 205 MATERIALS (ELECTRONIC)
210 CIRCUIT DEVICES & MICROCIRCUITS
215 CIRCUIT & NETWORK DESIGNS
125 PHYSICS
245 DISPLAYS

CLOSE-CONFINEMENT LASER DIODES, High-Power GaAs—T. Gonda, R. B. Gill (SSD, Som) 17-2 RCA Reprint RE 17-2-5

COLOR PHOTOGRAPHY, Low-Light-Level—E. Hutto, Jr. (ATL, Camden) 17-2 RCA Reprint Booklet, *RCA Optics* PE 535

FACSIMILE SYSTEM Using the LR 70 Laser Scanner, High Speed—L. W. Dobbins (CSD, Camden) 17-6 RCA Reprint RE 17-6-22

HOLOGRAPHIC Information Storage and Retrieval—Dr. R. S. Mezrich (Labs, Pr) 17-1 RCA Reprint PE 526

HOLOGRAPHIC RECORDING IN Crystals—Dr. J. J. Amodei, Dr. W. Phillips, Dr. D. L. Staebler (Labs, Pr) 17-2 RCA Reprint Booklet, *RCA Optics*, PE 535, PE 540

IMAGE REPRODUCER (LBIR), Laser Beam—S. M. Ravner (AED, Pr) 17-2 RCA Reprint Booklet, *RCA Optics*, PE 535, PE 543

LASER BEAM IMAGE REPRODUCER, Third-Generation—S. Ravner (AED, Pr) 17-6 RCA Reprint RE 17-6-15

LASER SYMPOSIUM, Corporate—H. Sobol (Labs, Pr) 17-5 RCA Reprint RE 17-5-21

LIGHT DEFLECTION System, Binary—J. A. Rajchman (Labs, Pr) 17-6 RCA Reprint RE 17-6-20

OPTICAL SIGHT, LCRU—M. Levene (ATL, Camden) 17-3 RCA Reprint RE 17-3-19

OPTICS AND ELECTRON As Competitive and Complementary Technologies—Dr. E. G. Ramberg (Labs, Pr) 17-2 RCA Reprint Booklet, *RCA Optics*, PE 535, PE 539

SILICON MOSAIC TARGET—Blending Semiconductor and Camera Tube Technologies—A. D. Cope (EC, Lanc) 17-4 RCA Reprint RE 17-4-5

245 Displays

... equipment for the display of graphic, alphanumeric, & other data in communications, computer, military, & other systems; CRT devices, solid state displays, holographic displays, etc. (excludes: television)

see also: 205 MATERIALS (ELECTRONIC)
345 TELEVISION & BROADCAST SYSTEMS

ALEPHECHON STORAGE TUBE, Display System Using the—F. J. Marlowe, F. Wendt, C. Wine (Labs, Pr) 17-6 RCA Reprint RE 17-6-12

CATHODOCHROMIC IMAGE DISPLAY Applications—Dr. I. Gorog (Labs, Pr) 17-2 RCA Reprint Booklet, *RCA Optics*, PE 535, PE 541

COLOR DECODING PROJECTOR For Low-Light-Level Color Photography—Dr. L. J. Nicastro, E. Hutto, Jr. (ATL, Camden) 17-2 RCA Reprint Booklet, *RCA Optics*, PE 535

CRT, High Resolution—O. Choi, C. J. Widder (EC, Lanc) 17-6 RCA Reprint RE 17-6-14

CRT PHOTO TYPESETTING SYSTEM, Hardware Software Tradeoffs for a—S. Raciti (GS, Dayton) 17-6 RCA Reprint RE 17-6-21

CRT TESTER, Precision—E. D. Simshauser (GS, Dayton) 17-6 RCA Reprint RE 17-6-13

DIGITAL READOUTS—P. Farina (SSD, Som) 17-6 RCA Reprint RE 17-6-3

ELECTROPHOTOGRAPHY—H. Kress (RCA Ltd, Zurich) 17-3 RCA Reprint RE 17-3-19

FACSIMILE PRINTING Using Liquid Crystal Arrays—J. Tufts, DL. Matthies, (Labs, Pr) 17-6 RCA Reprint RE 17-6-1

HOLOGRAPHIC Audio/Video Storage & Display—R. Norwalt, P. Nelson (EASD, Van Nuys) 17-6 RCA Reprint RE 17-6-7

IDEOGRAPHIC COMPOSING MACHINE—W. F. Heagerty (CE, In) 17-2 RCA Reprint Booklet, *RCA Optics*, PE 535

IMAGE ENHANCEMENT, Digital and Optical Techniques for—P. C. Murray, W. W. Lee (AED, Pr) 17-6 RCA Reprint RE 17-6-16

LIQUID CRYSTAL DYNAMIC SCATTERING, Application of—H. C. Schindler (SSD, Som) 17-6 RCA Reprint RE 17-6-2

MULTI-COLOR DISPLAYS, Penetration-Type Cathode-Ray Tube for—D. D. Shaffer (EC, Lanc) 17-6 RCA Reprint RE 17-6-20

NUMITRON Applications—F. Feyder (SSD, Som) 17-6 RCA Reprint RE 17-6-5

NUMITRONS, Design and Constructions of—R. Reichert (SSD, Som) 17-6 RCA Reprint RE 17-6-4

STORAGE TUBES for Computer Displays—F. J. Marlowe (Labs, Pr) 17-6 RCA Reprint RE 17-6-11

VECTOR GENERATION, A Technique for Constant Rate Digital—W. Poppen, J. Lyon (EASD, Van Nuys) 17-6 RCA Reprint RE 17-6-8

VISIBLE-LIGHT-EMITTING DIODES—C. J. Nuese, H. Kressel, I. Ladany (Labs, Pr) 17-6 RCA Reprint RE 17-6-10

250 Recording Components & Equipment

... tape, disk, drum, film, holographic, & other assemblies for audio, image, & data systems; magnetic tape, tape heads, pickup devices, etc.

see also: 340 COMMUNICATIONS EQUIPMENT & SYSTEMS
360 COMPUTER EQUIPMENT
345 TELEVISION & BROADCAST SYSTEMS

DIGITAL DISK MEMORIES—Dr. R. Shahbender, Dr. J. G. Woodward (Labs, Pr) 17-5 RCA Reprint RE 17-5-1

DRUM MEMORIES, EASD—J. M. Chambers, G. Bircsak, J. K. Mathews (EASD, Van Nuys) 17-5 RCA Reprint RE 17-5-17

HOLOGRAPHIC Audio/Video Storage & Display—R. Norwalt, P. Nelson (EASD, Van Nuys) 17-6 RCA Reprint RE 17-6-7

MAGNETIC RECORDING, Advanced Digital—G. V. Jacoby (CS, Marl) 17-5 RCA Reprint RE 17-5-14

MATERIAL TRANSFER RECORDING—M. L. Levene, Dr. R. D. Scott, B. W. Siryj (ATL, Camden) 17-2 RCA Reprint Booklet *RCA Optics*, PE 535

SIGNAL DETECTION in Digital Magnetic Recording Stores—Dr. A. A. Guida (Labs, Pr) 17-5 RCA Reprint RE 17-5-2

270 Materials (Mechanical)

... preparation & properties of structural, adhesive, protective, hydraulic & lubricant materials

see also: 205 MATERIALS (ELECTRONIC)
125 PHYSICS
160 LABORATORY TECHNIQUES & EQUIPMENT

MAGNETIC MATERIALS for Disks—Dr. E. F. Hockings (Labs, Pr) 17-5 RCA Reprint RE 17-5-5

275 Mechanical, Structural, & Hydraulic Components

... bearings, beams, servo's, valves, etc.

see also: 270 MATERIALS (MECHANICAL)

DIGITAL DISK SLIDERS, Aerodynamics of—Dr. G. R. Briggs, J. Guaracini, P. G. Herkart (Labs, Pr) 17-5 RCA Reprint RE 17-5-7

HYSTERESIS MOTORS and New Damping Techniques, Hunting in—S. P. Clurman (CSD, Camden) 17-3 RCA Reprint PE 533

PAPER FEED SYSTEM for a High-Speed Printer—D. Janz (CS, Marl) 17-5 RCA Reprint RE 17-5-13

STEPPER-MOTOR Film Drive—F. R. Goldammer (Labs, Pr) 17-5 RCA Reprint RE 17-5-9

280 Thermal Components & Equipment

... heating & cooling components & equipment; thermal measurement devices; heat sinks & thermal protection designs; etc.

LOUVER SYSTEM, Frictionless Bimetal-Actuated—R. J. Williams (AED, Pr) 17-5 RCA Reprint RE 17-5-8

PHASE-CHANGE HEAT-TRANSFER Techniques—B. Shelpuk (AED, Pr) 17-2 RCA Reprint Booklet, *Government Engineering*, PE 532

SERIES 300 SYSTEMS, EQUIPMENT & APPLICATIONS

310 Spacecraft & Ground Support

... spacecraft & satellite design, launch vehicles, payloads, space missions, space navigation.

see also: 110 EARTH & SPACE SCIENCES
325 CHECKOUT, MAINTENANCE, & USER SUPPORT
150 ENVIRONMENTAL & HUMAN FACTORS
320 RADAR, SONAR, & TRACKING SYSTEMS

CELESTIAL NAVIGATION, The New—Inexpensive Position Fixes by Satellite—J. E. Board (AED, Pr) 17-5 RCA Reprint RE 17-5-12

ITOS-1 (TIROS-M), Design and Orbital Performance of—A. Schnapl (AED, Pr) 17-1 RCA Reprint Booklet, *Government Engineering*, PE 532, PE 542

315 Military Weapons & Logistics

... missiles, command & control, etc.
see also 325 CHECKOUT, MAINTENANCE & USER SUPPORT
340 COMMUNICATIONS EQUIPMENT & SYSTEMS
320 RADAR, SONAR, & TRACKING SYSTEMS

COMMAND AND CONTROL SYSTEMS of the 70's, The Human Role in—B. Patrusky (CSD, Camden) 17-1 RCA Reprint Booklet, *Government Engineering*, PE 532

325 Checkout, Maintenance, & User Support

... automatic test equipment, maintenance & repair methods, installation & user support, etc.
see also 175 RELIABILITY, QUALITY CONTROL & STANDARDIZATION

EQUIPMENT TESTER, Automatic Communications—F. Plifferling, D. H. Williamson (Corp Mrstn) 17-5 RCA Reprint RE 17-5-19

TEST-DATA ACQUISITION AND PROCESSING, RUDI: Computer-Controlled—B. Mangolds (EC, Hr) 17-1 RCA Reprint Booklet, *Government Engineering*, PE 532

Author Index

Subject listed opposite each author's name indicates where complete citation to his paper may be found in the subject index. An author may have more than one paper for each subject category.

Astro-Electronics Division

Blenkowski, G. D., 130
Board, J. E., 310
Kingsbury, J. F., 215
Lee, W. W., 245
McKinley, R. R., 130
Murray, P. C., 245
Novick, M., 170
Ravner, S. M., 240
Schnapf, A., 310
Seideman, I. M., 180
Sheipuk, B., 280
Siskind, S. M., 130
Williams, R. J., 280

Communications Systems Division

Clurman, S. P., 205
Dobbins, L. W., 240
Mackiw, G. E., 340
Patrusky, B., 150, 315
Sass, E. J., 340
Thorpe, L. J., 210, 215
Tyree, B. E., 340
Williamson, D. H., 325

Computer Systems

Fairfax, G. H., 215
Janz, D., 275
Lintz, J. P., 170
Mancini, R. A., 215
Singleton, R. S., 370

Consumer Electronics

Allington, T. R., 210
Brombaugh, C. A., 210
Heagerty, W. F., 245
Hegarty, B. A., 210
Hong, S. O., 365
Lockhart, R. K., 345
Oakes, M., 210
Shelby, J. H., 210
Skaw, E. R., 170
Snyder, R. D., 210
Stephens, J. W., 210
Tretter, L., 210
Wang, Y. H., 170
Young, S. P., 365

340 Communications Equipment & Systems

... industrial, military, & commercial systems; telephony, telegraphy, & telemetry (excluding: television & broadcast radio).
see also: 345 TELEVISION & BROADCAST SYSTEMS
250 RECORDING COMPONENTS & EQUIPMENT
225 ANTENNAS & PROPAGATION
135 INFORMATION THEORY & OPERATIONS RESEARCH

COMMUNICATION NETWORK, Simulation for a Circuit and Message Switch—K. Weir, P. Boehn (CSD, Camden) 17-4 RCA Reprint RE 17-4-24

MULTIPLE PSK SIGNALS Through a Hard Limiter, Error Rate of—B. E. Tyree, J. Bailey (CSD, Camden) 17-5 RCA Reprint RE 17-5-16

NEW PRODUCTS Engineering in Consumer Electronics—R. K. Lockhart (CF, In) 17-5 RCA Reprint RE 17-5-11

SPEECH BANDWIDTH COMPRESSION BY Analytic Rooting—E. J. Sass, G. E. Mackiw (CSD, Camden) 17-2 RCA Reprint Booklet, *Government Engineering*, PE 532

VIDEOVOICE—S. N. Friedman (Glob-Com, NY) 17-2 RCA Reprint PE 545

Electromagnetic and Aviation Systems Division

Bircsak, G., 250
Chambers, J. M., 250
Easter, F. C., 215
Goodman, S. A., 365
Lyon, J., 245
Nelson, P., 210, 245, 250
Norwalt, R., 245, 250
Poppen, W., 245

Electronic Components

Choi, O., 245
Gill, R. B., 240
Gonda, T., 240
Kleppinger, R. E., 370
Mangolds, B., 325
Shaffer, D. D., 245
Widder, C. J., 245

Global Communications Inc.

Friedman, S. N., 340

Graphics Systems

Raciti, S., 245
Simshauser, E. D., 245

Government and Communications Systems Staff

Plifferling, F., 325

NBC

Hathaway, J. L., 180, 215

Patents and Licensing

Brown, G. H., 180
Lazar, J. D., 180

Research and Engineering

Hadlock, W. O., 180
Hillier, J., 180
Kocher, C. P., 175
Phillips, J. C., 395
Strobl, F. J., 395

365 Computer Programming & Applications

... languages, software systems, & general applications (excluding: specific programs for scientific use)
see also: 370 COMPUTER PROGRAMS (SCIENTIFIC)
360 COMPUTER EQUIPMENT

ALSIM—Microprogram Simulator—S. O. Hong, S. P. Young (CS, Marl) 17-1 RCA Reprint RE 17-1-3

DATA MANAGEMENT System, Peripheral—S. A. Goodman (EASD, Van Nuys) 17-5 RCA Reprint RE 17-5-15

QUEUE FORMATION in Computer Systems, Assessment of—A. S. Merriam (ATL, Camden) 17-1 RCA Reprint Booklet, *Government Engineering*

370 Computer Programs (Scientific)

... specific programs & techniques for scientific use; computation, simulation, computer aided design, etc.; (entries in this category generally consist of program documentation, listings, use instructions, decks, or tapes)
see also 365 COMPUTER PROGRAMMING & APPLICATIONS

AUTOMATED DESIGN OPERATIONS: A Profile—J. P. Le Gault (CS, PBG) 17-4 RCA Reprint RE 17-4-4

RCA Laboratories

Amodei, J. J., 240
Briggs, G. R., 160
Faughnan, B. W., 205
Gialmo, E. C., 160
Goldammer, F. R., 275
Gorog, I., 245
Guarnacini, J., 275
Guida, A. A., 250
Herkart, P. G., 275
Hockings, E. F., 215
Holtz, R. G., 180
Hook, H., 170
Kawamoto, K., 215
Kressel, H., 245
Ladany, I., 245
Mariowe, R. J., 245
Mathews, J. K., 250
Matthies, D. L., 245
Mezrich, R. S., 240
Pankove, J. I., 180
Phillips, W., 205, 240
Rajchman, J. A., 240
Ramberg, E. G., 125, 240
Shahbender, R., 250
Sobol, H., 240
Staebler, D. L., 240
Tults, J., 245
Wendt, F., 245
Wine, C., 245
Woodward, J. G., 250

RCA Limited

Cardinal, R. E., 210
Curtis, B., 205
Forster, G., 210
Hurlburt, D. H., 210
Kane, J., 205
Kiess, H., 245
Lehmann, H., 205
von Philipsborn, H., 205
Widmir, R., 205

Solid State Division

Amick, J. A., 205
Bailey, J., 340
Bailey, W. D., 170
Beelitz, H., 215
Blücher, A., 210
Boteky, E. J., 210
Bosenberg, W., 215
Brader, R. H., 210
Burton, N., 210
Cames, J. E., 205
Crossley, P. A., 210
Dawson, R. H., 210
Dingwall, A., 215

BUSINESS AND LONG RANGE PLANS, Basic Time-Sharing Programs for—R. R. Lorentzen (EC, Hr) 17-4 RCA Reprint RE 17-4-22

DESIGN AUTOMATION—Promise and Practice—E. P. Helpert, Dr. J. C. Miller, D. G. Ressler (SSD, Som) 17-3 RCA Reprint RE 17-3-9

DIGITAL SIMULATION as a Design Tool—C. B. David, Dr. J. C. Miller, Dr. L. M. Rosenberg (SSD, Som) 17-4 RCA Reprint RE 17-4-13

PRODUCT ANALYSIS Using a Time-Sharing Computer—R. E. Kleppinger (EC, Hr) 17-1 RCA Reprint RE 17-1-19

SIMULTANEOUS NONLINEAR EQUATIONS, Computer Solution of General Sets of—R. S. Singleton (CS, PBG) 17-5 RCA Reprint RE 17-5-3

380 Graphic Arts & Documentation

... printing, photography, & typesetting, writing, editing, & publishing; information storage, retrieval, & library science; reprography & micro-storage
see also 365 COMPUTER PROGRAMMING & APPLICATIONS

TYPESETTING Than Setting Type, There's More to—P. E. Justus (GS, Dayton) 17-4 RCA Reprint RE 17-4-7

Ditrick, N., 215
Duffy, M. T., 210
Dumin, D. J., 205
Engelbrecht, R., 180
Farina, P., 245
Fenster, H., 170
Feyder, F., 245
Funk, R. E., 210
Gaylord, J., 210
Greig, W., 170
Helpert, E. P., 370
Jacobus, L. A., 210
Jacoby, G. V., 250
Jorgenson, J., 215
Kallish, I., 215
Kowalek, D. E., 210
Lukach, V., 175
Meyer, J. E., 210
Miller, H. S., 210
Miller, J. C., 370
Mueller, C. W., 205
Murray, L. A., 210
Oberman, J. R., 215
Olmstead, J., 210
Policastro, S. G., 210
Pope, L., 215
Reddy, N. D., 215
Reichert, R., 245
Ressler, D. G., 370
Richards, B. W., 210
Rose, A. S., 170
Schindler, H. C., 245
Schneider, W. C., 210
Waas, G. J., 215

Corporate Staff

Fabro, P. C., 180
Samoff, R. W., 180

Advanced Technology Laboratories

Feller, A., 215
Greenhouse, J. N., 215
Hutto, E., 240, 245
Levene, M. L., 240
Merriam, A. S., 365
Nicastro, L. J., 245
Noto, R., 215
Pryor, R. L., 215
Ramondetta, P. W., 215
Scott, R. D., 250
Sirry, B. W., 250
Smith, A. M., 215

Service Company

Manning, W. H., 110
Mertens, L. E., 110

Editorial Representatives

The Editorial Representative in your group is the one you should contact in scheduling technical papers and announcements of your professional activities.

Government and Commercial Systems

Aerospace Systems Division

M. H. AKILLIAN* Engineering, Burlington, Mass.
J. J. O'DONNELL* Industry Systems Burlington, Mass.

Electromagnetic and Aviation Systems Division

C. S. METCHETTE* Engineering, Van Nuys, Calif.
J. McDONOUGH* Engineering, Van Nuys, Calif.

Astro-Electronics Division

I. M. SEIDEMAN* Engineering, Princeton, N.J.
S. WEISBERGER* Advanced Development and Research, Princeton, N.J.

Missile & Surface Radar Division

T. G. GREENE* Engineering, Moorestown, N.J.

Government Engineering

M. G. PIETZ* Advanced Technology Laboratories, Camden, N.J.
J. E. FRIEDMAN* Advanced Technology Laboratories, Camden, N.J.
J. L. KRAGER* Central Engineering, Camden, N.J.

Government Plans and Systems Development

E. J. PODELL* Engineering Information and Communications Camden, N.J.

Communications Systems Division

Commercial Systems

A. H. LIND* Chairman, Editorial Board, Camden, N.J.
N. C. COLBY* Mobile Communications Engineering, Meadow Lands, Pa.
R. N. HURST* Studio, Recording, & Scientific Equip. Engineering, Camden, N.J.
R. E. WINN* Broadcast Transmitter & Antenna Eng., Gibbsboro, N.J.

Government Communications Systems

A. LIGUORI* Engineering, Camden, N.J.

Palm Beach Division

P. M. WOOLEY* Palm Beach Product Laboratory, Palm Beach Gardens, Fla.

Research and Engineering

Laboratories

C. W. SALL* Research, Princeton, N.J.
I. H. KALISH* Solid State Technology Center, Somerville, N.J.
M. R. SHERMAN* Solid State Technology Center, Somerville, N.J.

Electronic Components

Entertainment Tube Division

J. KOFF* Receiving Tube Operations, Woodbridge, N.J.
J. H. LIPSCOMBE* Television Picture Tube Operations, Maricn, Ind.
E. K. MADENFORD* Television Picture Tube Operations, Lancaster, Pa.

Industrial Tube Division

J. M. FORMAN* Industrial Tube Operations, Lancaster, Pa.
H. J. WOLKSTEIN* Microwave Tube Operations, Harrison, N.J.

Solid State Division

E. M. McELWEE* Chairman, Editorial Board, Somerville, N.J.
J. DIMAURO* Solid State Division, Mountaintop, Pa.
S. SILVERSTEIN* Power Transistors, Somerville, N.J.
E. M. TROY* Integrated Circuits, Somerville, N.J.
J. D. YOUNG* Solid State Division, Findlay, Ohio

Consumer Electronics

C. HOYT* Chairman, Editorial Board, Indianapolis, Ind.
R. BUTH* Engineering, Indianapolis, Ind.
R. C. GRAHAM* Radio Engineering, Indianapolis, Ind.
F. HOLT* Advanced Development, Indianapolis, Ind.
E. JANSON* Black and White TV Engineering, Indianapolis, Ind.
W. LIEDERBACH* Ceramic Circuits Engineering, Rockville, Ind.
J. STARK* Color TV Engineering, Indianapolis, Ind.
P. HUANG* Engineering, RCA Taiwan Ltd., Taipei, Taiwan

Services

RCA Service Company

M. G. GANDER* Consumer Products Administration, Cherry Hill, N.J.
W. W. COOK* Consumer Products Service Dept., Cherry Hill, N.J.
R. M. DOMBROSKY* Technical Support, Cherry Hill, N.J.
R. P. LAMB* Missile Test Project, Cape Kennedy, Fla.

Parts and Accessories

C. C. REARICK* Product Development Engineering, Deptford, N.J.

RCA Global Communications, Inc.

W. S. LEIS* RCA Global Communications, Inc., New York, N.Y.
J. D. SELLERS* RCA Alaska Communications, Inc., Anchorage, Alaska

National Broadcasting Company, Inc.

W. A. HOWARD* Staff Eng., New York, N.Y.
M. L. WHITEHURST* Record Eng., Indianapolis, Ind.

RCA Records

RCA International Division

C. A. PASSAVANT* New York, N.Y.

RCA Ltd.

W. A. CHISHOLM* Research & Eng., Montreal, Canada

Patents and Licensing

J. EPSTEIN* Staff Services, Princeton, N.J.

*Technical Publication Administrators listed above are responsible for review and approval of papers and presentations.

RCA Engineer

A TECHNICAL JOURNAL PUBLISHED BY CORPORATE ENGINEERING SERVICES
"BY AND FOR THE RCA ENGINEER"

FORM NO. RE-17-6

Printed in U.S.A.